Tundra rivers of the last glacial

van Huissteden, J.

1990

TUNDRA RIVERS OF THE LAST GLACIAL: SEDIMENTATION AND GEOMORPHOLOGICAL PROCESSES DURING THE MIDDLE PLENIGLACIAL IN TWENTE, EASTERN NETHERLANDS.

Jacobus van Huissteden

VRIJE UNIVERSITEIT TE AMSTERDAM

TUNDRA RIVERS OF THE LAST GLACIAL: SEDIMENTATION AND GEOMORPHOLOGICAL PROCESSES DURING THE MIDDLE PLENIGLACIAL IN TWENTE, EASTERN NETHERLANDS.

ACADEMISCH PROEFSCHRIFT

ter verkrijging van de graad van doctor aan
de Vrije Universiteit te Amsterdam,
op gezag van de rector magnificus
dr. C. Datema,
hoogleraar aan de faculteit der letteren,
in het openbaar te verdedigen
ten overstaan van de promotiecommissie
van de faculteit der aardwetenschappen
op donderdag 7 juni 1990 te 14.00 uur
in het hoofdgebouw van de universiteit, De Boelelaan 1105

door

Jacobus van Huissteden

geboren te Utrecht

Centrale Huisdrukkerij van de Vrije Universiteit

1990

Promotor : prof. dr. J. Vandenberghe
Copromotor : prof. dr. T. van der Hammen
Referent : prof. dr. G.C. Maarleveld

Aan mijn vader
Aan Bram

Vermenigvuldigd door de Centrale Huisdrukkerij van de Vrije Universiteit.

Adres van de auteur:

J. van Huissteden,
Instituut voor Aardwetenschappen, Vrije Universiteit,
De Boelelaan 1085,
Postbus 7161,
1007 MC Amsterdam.

Contents.

Acknowledgements.

This study has been financed by the Netherlands Organization for Scientific Research (N.W.O., project number 751.358.005). Besides on financial support, this research project depended on the contributions of many people. I wish to express my gratitude to anyone who has supported me in one way or another.

My promotor, Prof. Dr. J. Vandenberghe is thanked for his support (not only with respect to scientific matters) and constructive discussions of the results. My co-promotor, Prof. Dr. T. van der Hammen, also taught me respect for previous achievements of science. My colleague Dr. E.Th. Ran is credited for her thorough palaeobotanical research and kind cooperation. Prof. Dr. Roeleveld and Dr. B. van Geel are acknowledged for their role in the initiation of the research project and discussions of the results during its progress. Prof. Dr. G.C. Maarleveld is thanked for reviewing the manuscript.

Prof. Dr. Mook and his staff at the Centre for Isotope Research in Groningen are credited for the radiometric datings and comments on the dating results. Dr. A. van der Wijk is thanked for his explanations on Uranium-Thorium dating. Dr. L. Krook is credited for his contributions to the sediment-petrological research, and for correcting the English text. Drs. W. Elzenga introduced me to the electron microscope study of sand grains. I owe much to Drs. Th. B. Roep, Dr. J. Schwan, Drs. L van der Valk and Dr. C. Kasse for their valuable suggestions with regard to the sedimentological part of the project. Dr. Y. Baumfalk and Dr. W. ten Kate contributed by discussing some of the statistical methods with me. Ing. M. Konert, Mrs. M.J. Boone and Mr. R. van Elsas prepared the numerous grainsize and heavy mineral analyses. The use of the computer for data storage and analysis has been of vital importance. Martin Konert and my friend Bram Grimm have guided my first steps on this path.

The numerous borings have been made by Drs. M. de Bakker, Drs. R. Middelburg, Drs. P.J. Thomas, Drs. C.A. Peeters, Drs. A. Spaanderman, Drs. H.J.M. Meuffels, Drs. A. Bak, Drs. T.B. van der Werf, Drs. P.E. van Olst, Drs. C.E. Mak, Drs. E. Wassenaar, Drs. M. Diederiks and Mr. M. van der Sande, as part of their graduation fieldwork. They all contributed to an amiable atmosphere during the field campaigns. Mr. T.C.M. Spierings and Mr. D.M. van Harlingen handled the hydraulic coring equipment in the field, technical assistance has been given by Mr. Th.A. Hamer and his colleagues. Mr. H. Sion and the photography department of the Biology Faculty prepared the illustrations. The cooperation of the site staff of Rijkswaterstaat and building contractor Dirk Verstoep B.V. has been indispensable for the study of the Hengelo A1 exposure. The landowners in the municipalities of Denekamp, Losser and Weerselo are thanked for their permission to enter their property. The staff of museum 'Natura Docet' and Mr. and Mrs. Benneker in De Lutte are acknowledged for their hospitality.

The staff of the Rijks Geologische Dienst has contributed in many ways. Prof. Dr. W.H. Zagwijn, Drs. G.H.J. Ruegg, Mr. J. de Jong, Drs. P. Cleveringa and Mr J.G. Zandstra are acknowledged for their permission to study reports and analysis results from interesting sites which I could not visit. Also Dr. E.A. van de Meene and Mr. C. den Otter are thanked for their support. The research department of the Waterleiding Maatschappij 'Overijssel' is acknowledged for providing a large number of penetration cone soundings.

Finally (but not in the last place), I wish to express my gratitude to José, Joyce, Renske and Elwin. They had to endure an always too busy husband and father, but still managed to return their support for this uncertain enterprise. My mother is thanked for the many hours she watched the children while I was working at home.

Summary.

During the Last Glacial (Weichselian) the relief of the Dutch sand regions has been levelled by erosion of higher parts of the landscape, and sedimentation in basins and valleys. The deposits in the lower parts of the landscape have recorded the Weichselian climatic and geomorphological history. A large part of this sediment sequence (the Twente Formation) consists of a series of sand, silt, and peat beds of Middle Pleniglacial age (ca. 60,000 - 26,000 years B.P.), known as the 'Mekkelhorst Member'. These sediments have been deposited by rivers and wind in a lowland tundra landscape. The dynamics of this depositional environment is the subject of this thesis. The study area has been the Dinkel valley and Hengelo basin (Twente region, Eastern Netherlands), the type region of the Twente Formation. Here Weichselian age deposits may reach a thickness of more than 25 m in glacial basins of Saalian age.

The large number of borings in the Dinkel valley made on behalf of this study, allows a refinement of the subdivision of the Twente Formation with respect to the deposits of Pleniglacial age. The Pleniglacial age units as used in this study are: the Dinkel Member (fluvial and aeolian deposits of Early Pleniglacial age), the Mekkelhorst Member (mainly fluvial deposits, Middle Pleniglacial age), the Beverborg Member (introduced in this study, Late Pleniglacial age; combines genetically related fluvial and aeolian deposits, formerly included in other units), and the Lutterzand Member s.s. (aeolian deposits of Late Pleniglacial age). The Mekkelhorst Member consists of the above-mentioned characteristic sand/silt/peat sequence (the Tilligte beds), and laterally equivalent fluvial and aeolian sands (Puntbeek sands).

The subdivision is supported by heavy mineral analysis. This has shown the presence of mineralogical differences between Twente Formation units, which can be attributed to changes in environmental conditions and sediment sources. Starting during the Early Pleniglacial freshly eroded, unweathered material has been transported into the basins, mainly derived from glacial sediments of the Drente Formation. Another sediment source during the Middle Pleniglacial has been loess, added from outside the basins.

Stratigraphical analysis of borehole data and penetration cone soundings has been crucial. This has been accomplished with help of a core description database which contains modules for lithologic classification, graphical output, and statistical facilities. Detailed stratigraphical analysis has been focussed on the Mekkelhorst Member. It proves that fine-grained beds within this unit rarely can be traced over more than a few hundred meters in the borehole sections. Even in detailed sections very rapid lateral variation occurs, caused by lateral facies changes, erosive truncation and cryoturbation. Three erosion levels occur within the Mekkelhorst Member. The first (I) overlies the basal clay beds of the Tilligte beds, which appear to be older than 50,000 B.P. It is associated with a shift in drainage direction in the northern Dinkel valley. The second erosion level (II) is dated at ca. 38,000 B.P., and is associated with fluvial incision. The third erosion level (III) is dated between 34,000 and 32,000 B.P. and is generally a rather flat hiatus.

Erosion level II also can be traced within the Hengelo basin. In the exposures it is associated with periglacial phenomena (ice wedge casts, large cryoturbations) which point to temporary presence and degradation of permafrost. The ice wedge casts occur in silty material only. This indicates mean annual temperatures between -4.5° C and -6° at that time (approximately 40,000 - 39,000 B.P.). The ensuing permafrost degrada-

tion has led to the development of thaw lakes, of which the deposits have been found in an exposure near Hengelo. The fluvial erosion is probably somewhat older than the permafrost degradation.

The exposures also reveal the importance of floodbasin environments in the Tilligte beds, while channel deposits are of relatively minor extent. Many sand beds prove to be crevasse splay and levee deposits which interrupt silt and peat deposition in lacustrine or semi-terrestrial floodbasin environments. Delta-like foresets of the crevasse splays point to deposition in shallow lakes. Lateral migration of channels has been restricted, while vertical accretion dominates.

Grainsize analysis, carried out with the help of multivariate statistics, confirms the dominance of overbank environments. Most sands in the borehole sections do not differ from crevasse splay sands found in the exposures. Many grainsize distributions, especially those of the silts, show evidence of an aeolian component in the sediment. The presence of an aeolian component has been confirmed by quartz grain surface characteristics, studied with the help of the electron microscope. In general aeolian processes appear to have been influential during the Middle Pleniglacial, but preservation of aeolian deposits has been restricted by fluvial reworking. Middle Pleniglacial sands of possible (fluvio-)aeolian origin occur mainly on the eastern margin of the Dinkel valley upstream of Denekamp. This indicates predominantly (north-) westerly wind directions during the Middle Pleniglacial.

A lithofacies classification for the borehole logs has been developed. The occurrence of different lithofacies types shows variations throughout the Dinkel area: deposits with many peat layers in an isolated tributary basin (Tilligte basin), clay rich deposits at the base of the Tilligte beds, deposits dominated by relatively coarse channel sands in the Dinkel valley upstream of Denekamp. In the eastern part of the valley sands dominate completely (Puntbeek sands), indicating an easterly course of the erstwhile main river.

Markov chain analysis of the lithofacies sequences shows that the Tilligte beds consist of a non-random, but disordered sequence, influenced by the interference of several depositional processes. The most important sequence appears to be a coarsening upward sequence starting with peat, going to silt or clay, and ending with sands. This sequence has been attributed to crevasse splay propagation and channel belt avulsions in floodbasin environments. Most of the Tilligte beds has been deposited by an anastomosing river system with well developed floodbasins and extensive crevasse splays. In the Dinkel valley upstream of Denekamp meandering rivers with more lateral channel migration may have occurred. The Puntbeek sands consist partly of meandering or braided channel deposits, partly of fluvio-aeolian deposits along the valley margins.

Analysis of radiocarbon datings shows a decreasing sedimentation rate in the Dinkel valley during the Middle Pleniglacial. Datings from other areas in Belgium, the Netherlands, and northwest Germany have been used to study the distribution of dateable material in time. Special attention has been paid to the statistical significance of the number of datings per time interval. A significant maximum in the amount of radiocarbon datings on peat occurs between 42,000 and 40,000 B.P., followed by a minimum between 39,000 and 37,000 B.P. The minimum is attributed to decreased floodplain stability, caused by erosion and permafrost thaw associated with erosion level II. The peat formation maximum may have been caused by flood plain stabilization associated with drier climatic conditions.

The general environmental conditions in the Netherlands during the Middle Pleniglacial have been comparable to those in present-day

western Alaska, and north-European tundra lowlands. During the entire Middle Pleniglacial tundra and shrub tundra environments have been maintained in the Twente area. Combination of sedimentological with palaeobotanical data (Ran, 1990) shows that on a local scale the vegetation is dominated by the floodbasin development. Climatic variations during the Middle Pleniglacial did not induce large changes on this general pattern in the Netherlands. Evidence for a distinct cold phase is present in the shape of ice wedge development around 39,000 B.P. Further periglacial phenomena (frost cracks, cryoturbations) indicate that a cold climate generally persisted throughout the Middle Pleniglacial (mean annual temperature below -1°). Palaeohydrological variations recorded in the fluvial sequence are: possible high river discharges before ca. 50,000 B.P., associated with the basal clays of the Tilligte beds; low discharges between 42 and 39,000 B.P. followed by high discharge associated with erosion level II (38,000 B.P.). Probably the amount of winter precipitation has been most influential on the discharge variations.

Combination of the palaeobotanical data and the data from this study, and comparison with continuous palaeobotanical sequences from France (Ran, 1990), allows to refine the chronostratigraphic subdivision of the Middle Pleniglacial. The proposed sequence consists of: the Lattrop Interval (approximately 60,000 - 50,000 B.P., humid/cool climate), the Moershoofd Interstadial complex (approximately 50,000-40,000 B.P., humid, with warmer oscillations), the Hasselo Stadial (approximately 40,000 - 38,000 B.P., cold and dry), the Hengelo Interstadial (approximately 38,000 - 36,000 B.P., humid/warmer), the Huneborg Interval (approximately 36,000 - 32,000 B.P., probably relatively cold and dry) and the Denekamp Interstadial complex (approximately 32,000 - 26,000 B.P., humid/warmer oscillations).

Samenvatting.

Tijdens de laatste ijstijd (Weichselien) is het reliëf van de Nederlandse zandgebieden afgevlakt door erosie van de hogere delen van het landschap en sedimentatie in bekkens en dalen. In de afzettingen in de lagere delen van het landschap is de geschiedenis van klimaat en landschap tijdens het Weichselien vastgelegd. Een groot deel van dit sedimentpakket (de Twente Formatie) bestaat uit zand, leem en veenlagen van Midden Pleniglaciale ouderdom (ca. 60.000 - 26.000 jaar B.P.), bekend onder de naam 'Mekkelhorst Member'. Deze sedimenten zijn door rivieren en wind afgezet in een laagland toendra landschap. De dynamiek van dit afzettingsmilieu is het onderwerp van dit proefschrift. Het studiegebied is de Dinkel vallei en het bekken van Hengelo (Twente, Overijssel), het typegebied van de Twente Formatie. Hier kunnen afzettingen van Weichselien ouderdom dikten bereiken van meer dan 25 m in glaciale bekkens daterend uit het Saalien.

Het grote aantal boringen dat in de Dinkel vallei gezet is ten behoeve van deze studie, heeft geleid tot een verfijning van de onderverdeling van de Twente Formatie met betrekking tot de afzettingen van Pleniglaciale ouderdom. De eenheden van Pleniglaciale ouderdom, zoals gebruikt in deze studie, zijn: de Dinkel Member (fluviatiele en aeolische afzettingen, Vroeg Pleniglaciale ouderdom), de Mekkelhorst Member (voornamelijk rivierafzettingen, Midden Pleniglaciale ouderdom), de Beverborg Member (in deze studie geïntroduceerd, Laat Pleniglaciale ouderdom; combineert genetisch verwante fluviatiele en aeolische afzettingen die voorheen in andere eenheden opgenomen waren), en de Lutterzand Member s.s. (aeolische afzettingen van Laat Pleniglaciale ouderdom). De Mekkelhorst member bestaat uit bovengenoemde karakteristieke zand/leem/veen sequentie (Tilligte lagen), en lateraal equivalente fluviatiele en aeolische zanden (Puntbeek zanden).

De onderverdeling is onderbouwd met behulp van zware mineralen analyse. Hiermee is aangetoond dat er mineralogische verschillen bestaan tussen de eenheden binnen de Twente Formatie, toegeschreven aan veranderingen in milieu-condities en sedimentbronnen. Vanaf het Vroeg Pleniglaciaal wordt vers geërodeerd, onverweerd materiaal aangevoerd in de bekkens, voornamelijk afkomstig uit glaciale afzettingen van de Drente Formatie. Een andere sedimentbron tijdens het Midden Pleniglaciaal is löss, afkomstig van buiten de bekkens.

Stratigrafische analyse van een grote hoeveelheid boorgegevens en conussonderingen is van cruciaal belang geweest. Dit is bereikt met behulp van een boringen database, die opties bevat voor lithologische klassificatie, grafische uitvoer en statistische faciliteiten. Gedetailleerde stratigrafische analyse is vooral gericht op de Mekkelhorst Member. Het blijkt dat fijnkorrelige lagen in deze eenheid zelden over meer dan een paar honderd meter vervolgd kunnen worden in de boorsecties. Zelfs in gedetailleerde secties treedt zeer snelle laterale variatie op, veroorzaakt door laterale facies wisselingen, erosieve afsnijding en cryoturbatie. Drie erosienivo's zijn in de Mekkelhorst Member aangetroffen. Het eerste (I) ligt op de basale kleilagen van de Tilligte lagen, die waarschijnlijk ouder zijn dan 50.000 B.P. Het gaat samen met een verschuiving in de afvoerrichting in het noordelijke Dinkeldal. Het tweede erosienivo (II) is gedateerd op ca. 38.000 B.P., en vertoont fluviatiele insnijding. Het derde erosienivo (III) is gedateerd tussen 34.000 en 32.000 B.P., en is over het algemeen een vrij vlak hiaat.

Erosienivo II kan ook binnen het Hengelo bekken vervolgd worden. In de ontsluitingen gaat het samen met periglaciale verschijnselen (ijswiggen, grote cryoturbaties), die wijzen op tijdelijke aanwezigheid en

degradatie van permafrost. De ijswiggen komen alleen in lemig materiaal voor, wat aantoont dat de gemiddelde jaartemperatuur in die tijd (ca. 40.000 - 39.000 B.P.) tussen -4.5° C en -6° heeft gelegen. De erop volgende permafrost degradatie heeft geleid tot de vorming van dooimeren, waarvan de afzettingen gevonden zijn in een ontsluiting bij Hengelo. Het erosienivo is waarschijnlijk iets ouder dan de permafrost degradatie.

De ontsluitingen onthullen eveneens het belang van rivierkom-milieus in de Tilligte lagen, terwijl geulafzettingen een relatief geringe verbreiding hebben. Veel zandlagen blijken crevasse splay en oeverwalafzettingen te zijn, die de afzetting van leem en veen in lacustriene of semi-terrestrische kom-milieus onderbreken. Delta-achtige gelaagdheid in de crevasse splays wijst op afzetting in ondiepe meren. Laterale migratie van geulen is beperkt geweest, terwijl vertikale opvulling overheerst.

De korrelgrootte-analyse, uitgevoerd met behulp van multivariate statistiek, bevestigt de overheersing van riviervlakte-milieu's buiten de geulen. De meeste zanden in de boorsecties verschillen niet van de crevasse splay zanden in de ontsluitingen. Veel korrelgrootte-verdelingen, vooral die van de lemen, wijzen op een duidelijke aeolische component in het sediment. De aanwezigheid van een aeolische component is bevestigd door oppervlaktekenmerken van kwartskorrels, die bestudeerd zijn met behulp van de elektronen-microscoop. In het algemeen lijken aeolische processen een belangrijke invloed te hebben gehad gedurende het Midden Pleniglaciaal, maar fluviatiele omwerking heeft het bewaard blijven van aeolische afzettingen beperkt. Midden-Pleniglaciale zanden van mogelijk (fluvio-) aeolische oorsprong komen vooral voor aan de oostelijke rand van het dal bovenstrooms van Denekamp. Dit wijst op voornamelijk (noord)westelijke windrichtingen tijdens het Midden-Pleniglaciaal.

Voor de lagen in de boorbeschrijvingen is een lithofacies klassifikatie ontwikkeld. De verspreiding van de verschillende lithofacies klassen vertoont variaties in het Dinkel gebied: afzettingen met veel veenlagen in een geïsoleerd zijdal (Tilligte bekken), kleirijke afzettingen aan de basis van de Tilligte lagen, afzettingen gedomineerd door relatief grove geulsedimenten in de Dinkel vallei bovenstrooms van Denekamp. In de oostelijke delen van de vallei overheersen zanden geheel (de Puntbeek zanden), wat wijst op een oostelijke loop van de toenmalige hoofdrivier.

Markov keten analyse van de lithofacies opeenvolgingen toont aan, dat de Tilligte lagen uit een niet toevallige, maar weinig geordende opeenvolging bestaat, beïnvloed door een samenspel van verschillende afzettingsprocessen. De meest belangrijke opeenvolging blijkt een naar boven toe grover wordende opeenvolging te zijn, beginnend met veen, gaande naar silt of klei, en eindigend met zanden. Deze opeenvolging wordt toegeschreven aan crevasse splay uitbreiding en stroomgordel avulsies in rivierkom-milieus.

Het grootste deel van de Tilligte lagen is afgezet door een anastosomerend riviersysteem met goed ontwikkelde kommen en uitgebreide crevasse splays. In het Dinkeldal bovenstrooms van Denekamp kunnen meanderende rivieren met meer laterale verplaatsing van geulen zijn voorgekomen. De Puntbeek zanden bestaan deels uit meanderende of vlechtende geulafzettingen, gedeeltelijk uit fluvio-aeolische afzettingen langs de dalranden.

Analyse van ^{14}C dateringen toont een afnemende sedimentatiesnelheid aan gedurende het Midden-Pleniglaciaal in de Dinkel vallei. Dateringen uit andere gebieden in België, Nederland en noordwest Duitsland zijn gebruikt om de verdeling van de dateerbaar materiaal in de tijd te

bestuderen. Speciale aandacht is besteed aan de statistische significantie van het aantal dateringen per tijdsinterval. Een significant maximum in de dateringen op veen ligt tussen 42.000 en 40.000 B.P., gevolgd door een minimum tussen 39.000 en 37.000 B.P. Het minimum is toegeschreven aan afname van de stabiliteit van de riviervlakte door erosie en opdooien van de permafrost, samengaand met het ontstaan van erosienivo II. Het veenvormings-maximum kan veroorzaakt zijn door stabilisatie van de riviervlakten geassocieerd met een droger klimaat.

De algemene milieu-omstandigheden in Nederland tijdens het Midden Pleniglaciaal zijn vergelijkbaar geweest met die in de huidige toendra laaglanden van westelijk Alaska en noordelijk Europa. Gedurende het hele Midden Pleniglaciaal hebben zich in Twente toendra en struiktoendra milieus gehandhaafd. Combinatie van sedimentologische en palaeobotanische gegevens (Ran, 1990) toont aan dat op een lokale schaal de vegetatie overheerst wordt door de ontwikkeling van de rivierkommen. Klimaatsvariaties gedurende het Midden Pleniglaciaal hebben niet geleid tot sterke veranderingen van dit algemene beeld. Aanwijzingen voor een duidelijke koude fase zijn aanwezig in de vorm ijswig-ontwikkeling rond 39.000 B.P. Verdere periglaciale verschijnselen (vorstspleten, cryoturbaties) wijzen erop dat over het algemeen het Midden-Pleniglaciale klimaat koud bleef (gemiddelde jaartemperatuur beneden -1°). Palaeohydrologische veranderingen vastgelegd in de fluviatiele opeenvolging zijn: mogelijke hoge rivierafvoeren vóór 50.000 B.P., samengaand met afzetting van de basale kleilagen van de Tilligte lagen; lage afvoeren tussen 42.000 en 39.000 B.P.; hoge afvoer in samenhang met erosienivo II (38.000 B.P.). Waarschijnlijk is vooral de hoeveelheid winterneerslag van invloed geweest op de afvoer veranderingen.

Combinatie van de palaeobotanische gegevens en de gegevens uit deze studie, en vergelijking met ononderbroken palaeobotanische sequenties uit Frankrijk (Ran, 1990) maakt het mogelijk de tijdstratigrafische onderverdeling van het Midden Pleniglaciaal te verfijnen. De voorgestelde opeenvolging bestaat uit: het Lattrop Interval (ca. 60.000-50.000 B.P., vochtig/koud klimaat), het Moershoofd Interstadiaal complex (ca. 50.000 - 40.000 B.P., vochtig, met warmere oscillaties), het Hasselo Stadiaal (ca. 40.0000 - 38.000 B.P., koud en droog), het Hengelo Interstadiaal (ca. 38.000-36.000 B.P., vochtig/warmer), het Huneborg Interval (ca. 36.000-32.000 B.P., waarschijnlijk relatief koud en droog), en het Denekamp Interstadiaal complex (ca. 32.000-26.000 B.P., vochtige/warmere oscillaties).

I. Introduction.

I.1. Background and aim of this study.

Periglacial erosion and sedimentation processes during the last glaciation have been an important agent in re-shaping the glacial landforms dating from the Saalian glacial time in the Netherlands and northwest Germany. The subdued relief of these areas contrasts with the much stronger relief which exists in areas affected by the ice cap of the last glaciation (Weichselian). Levelling of the relief of the Saalian landforms occurred by both erosion and deposition in depressions of the glacial landscape (Maarleveld, 1960). The resulting valley and basin fills contain valuable information on climate and landscape development during the last glaciation.

Therefore the periglacial valley development during the last glaciation has attracted attention among Quaternary geologists and geomorphologists. Especially the Weichselian Pleniglacial has been a time of prominent valley aggradation (Van der Hammen, 1957; Van der Hammen & Wijmstra, 1971; De Gans, 1981; Vandenberghe et al., 1984; Vandenberghe, 1985). These valley and basin fills consist of sand, clay, silt and peat layers, for which an aeolian and fluvial origin is assumed. In the Netherlands the term 'fluvio-periglacial' is used for this type of deposits. Most authors agree that during the Late Pleniglacial sandy braided rivers and aeolian sand deposition prevailed (e.g. Van der Hammen & Wijmstra, 1971; De Gans, 1981; Vandenberghe et al., 1984; Van Huissteden et al., 1986a, 1986b). With respect to the Middle Pleniglacial deposits knowledge is more fragmentary. The intercalations of sand, silt and peat beds represent a marshy alluvial plain environment. Aeolian intercalations also may be found (e.g. Van der Hammen & Wijmstra, 1971; Vandenberghe, 1985).

Of course similar environments also did occur at earlier glacial times in the Netherlands, as the descriptions of e.g. the Kedichem Formation testify (Doppert et al., 1975; Vandenberghe et al, 1985; Kasse, 1988; Vandenberghe & Kasse, 1989). A study of deposits dating from the last glacial therefore, also might contribute to knowledge of similar older deposits which are less easily sampled for study.

Knowledge about the Pleniglacial deposits is of economical importance also. Deposits dating from the last ice age may attain considerable thickness, up to 25 m or more (Van Huissteden et al., 1986a). This is especially the case in glacial basins of Saalian age. The fine grained beds may pose foundation problems, as is demonstrated by the use of pile foundations in several locations. They also provide shallow aquitards, relevant for groundwater pollutant movement. In such cases knowledge of sediment body geometry and lateral facies variations is important. Geometrical parameters of sediment bodies, such as interconnectedness and shape of sand bodies, are closely related to the sedimentary environment (Collinson, 1978; Bridge & Leeder, 1979).

Due to their position in the landscape, natural exposures in these sediments are very rare. Older studies of these sediments mainly relied on scarce man-made exposure data and a few deeper boreholes. This is the cause of many uncertainties in the knowledge on these deposits. Unresolved questions pertain to the interpretation of the sedimentary environments, the strati-

graphical relations within the basin fills, the interpretation of palaeobotanical data, and the link of geomorphical and sedimentary processes with the climatic changes of the Last Glacial.

In recent years the prospects for studying these sediments has been greatly improved through the development of hydraulic and hand drilling equipment which can take undisturbed cores of sandy sediments lying below the water table. With the hand drilling equipment depths of 10 m can be reached during a few hours, so a large number of boreholes can be made in a field season at low costs. The development of penetration cone sounding adds valuable information (Waterleiding Maatschappij 'Overijssel', 1985). This means that data can be gathered at a much higher density and in a shorter time than before. An indispensable improvement is the easy access to computer facilities which enables handling of the large amount of field data, necessary for a detailed three-dimensional study of alluvial sediments. The use of computers in storing the data also allows more rigorous statistical analysis than was possible hitherto. Also new developments in analytical techniques, especially dating techniques, palaeobotanical analysis and sedimentary petrology, may prove to be promising. Next, the amount of data on present-day periglacial environments has been greatly extended. Especially important in this respect are advances in the hydrology of the periglacial zone (Clark, 1988). Recent progress in fluvial sedimentology and palaeo-hydrology further improves the interpretation of the fluvial deposits (Miall, 1978a; Gregory, 1983). From other parts of Western Europe, more continuous records of the climatic history of the Last Glacial have been gathered (Woillard & Mook, 1982; De Beaulieu & Reille, 1984a,b).

To benefit from these new developments a joint research project has been set up by the Palynology and Palaeo/Actuoecology section of the Hugo de Vries Laboratorium of the University of Amsterdam and the section of Quaternary Geology/Lowland studies of the Earth Sciences Faculty of the Free University. The project has been financially supported by the Netherlands Organisation for Scientific Research (NWO). Attention is focussed on the Middle Pleniglacial deposits. This thesis concentrates on the sedimentological and geomorphological aspects. The palaeoecological aspects are described by Ran (1990).

As study area for this research project the Dinkel valley in the Twente region in the Eastern Netherlands has been chosen. In the Twente region many of the type sites of the chrono- and lithostratigraphy of the last glacial are located (Van der Vlerk & Florschütz, 1950; Van der Hammen & Wijmstra, 1971; Zagwijn, 1974). The Dinkel valley has been the subject of extensive study by Van der Hammen & Wijmstra (1971). A nearly complete sedimentary sequence from the last glacial is present. The Middle Pleniglacial deposits are over 10 m thick in some parts of the valley (Van Huissteden et al., 1986a). The present study aims to obtain insight into the geomorphical and sedimentary processes which operated in the Dinkel valley during the Middle Pleniglacial. It is attempted to achieve this through chrono- and lithostratigraphical, sedimentological, and sediment-petrographical analysis of the Middle Pleniglacial deposits. The integration with the results of the palaeobotanical study by Ran (1990) enables a more comprehensive understanding of the environmental conditions at that time.

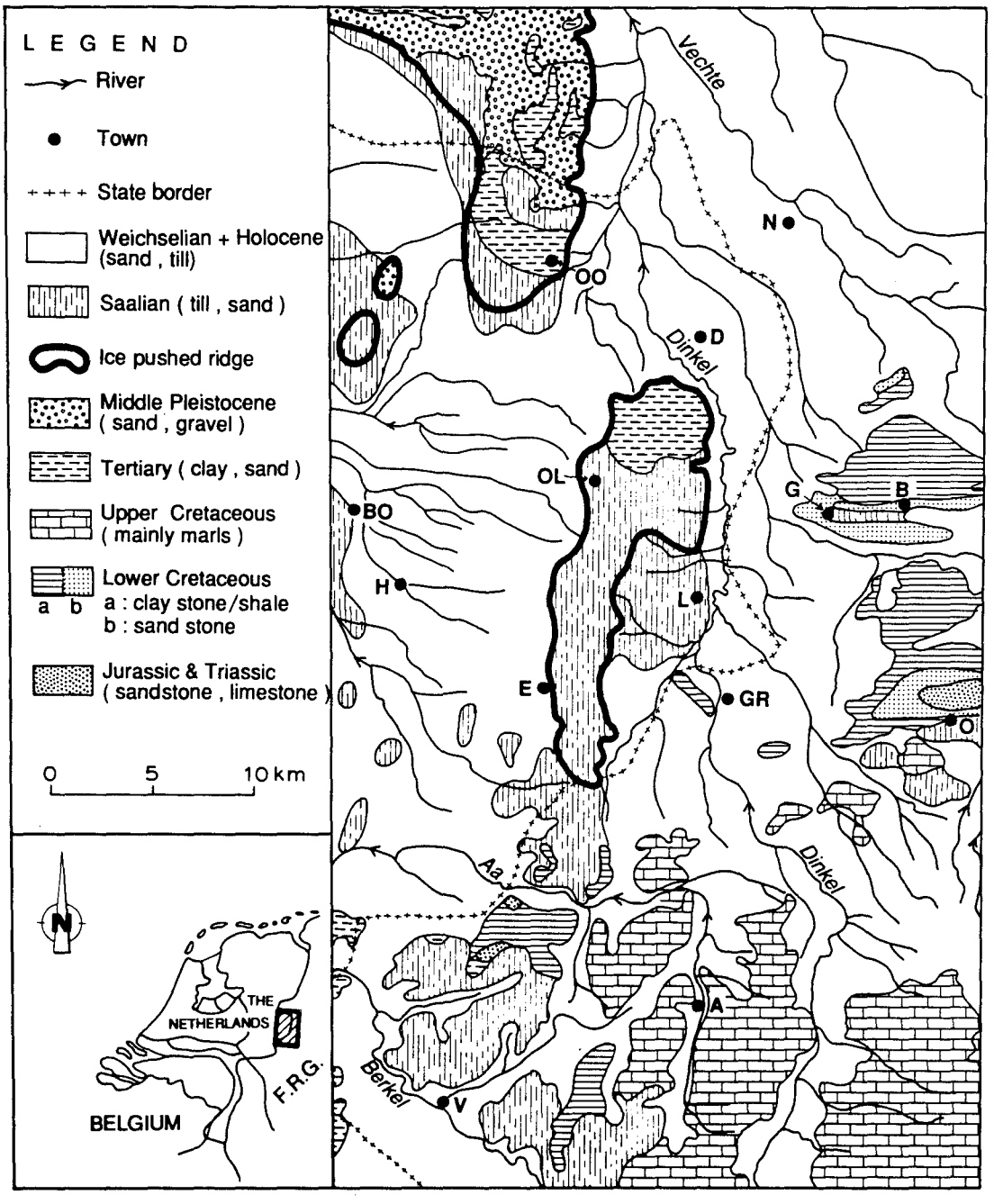

Figure I.1. River courses and global geology of the Dinkel drainage basin, compiled from Geologische Overzichtskaarten van Nederland (Zagwijn & Van Staalduinen, eds., 1975) and Geologische Übersichtskarte 1:200.000 Blatt Lingen (Bundesanstalt für Geowissenschaften und Rohstoffe, 1984). Ice pushed ridges include Lower Tertiary clays and sands, and Middle Pleistocene fluvial sands. OO: Ootmarsum; N: Nordhorn; D: Denekamp; OL: Oldenzaal; B: Bentheim; G: Gildehaus; O: Ochtrup; GR: Gronau; L: Losser; E: Enschede; H: Hengelo; BO: Borne; A: Ahaus; V: Vreden.

I.2. Outline of the geomorphology and geology of the Dinkel valley.

The Dinkel river has its source area near the village of Holtwick in NW Germany (fig. I.1). The river partly flows on Dutch ter-

ritory, in the municipalities of Losser and Denekamp. North of Nordhorn in Germany it has its confluence with the Vechte river. The present-day river is small and sinuous. The bankfull discharge equals approximately 45 m^3/sec, the drainage area amounts ca. 618 km^2.

In the Dutch part of the river course the floodplain elevation drops from ca 35 to ca 20 m. The floodplain gradient amounts 0.8 m/km upstream of the town of Denekamp, and diminishes to 0.6 m/km downstream of Denekamp. Upstream of Denekamp the present river flows on a well defined floodplain with oxbow lakes and point bar swale and ridge patterns. The Holocene floodplain is bordered by slightly higher terrain, on the 1 : 50,000 scale geomorphological map of the Netherlands (Kleinsman et al., 1978) described as 'coversand plain'. Van Huissteden et al (1986a) have distinguished two floodplain levels of Late Pleistocene age in this terrain. These terraces are covered by aeolian sand sheets and low dunes ('coversands') of Late Pleistocene age (Van der Hammen & Wijmstra, 1971). Dune formation connected with coversand deposition has led to blocking and diversion of river courses during the Late Glacial (Van der Hammen, 1951). Downstream of Denekamp the limits of the recent floodplain are less distinct. Here the recent alluvium merely spreads out on low-lying areas of the pre-existing Upper Pleistocene surface. The original floodplain morphology has been strongly modified by recent agricultural land improvement operations in this area.

Before entering Dutch territory the river flows over horizontal or gently folded strata of Mesozoic age (fig. I.1), locally covered by till or glaciofluvial sediments of Saalian age (Boigk et al., 1960). The Mesozoic strata include shales, claystones, sandstone and limestone. In the studied reach of the valley two E-W striking anticlinal structures occur, the Losser anticline and the Bentheim anticline (Aelmans, 1974). These fold structures are traversed by NNW-SSE trending faults (Kemper, 1968). Mesozoic outcrops border the valley on the eastern side as far north as the Isterberg, south of Nordhorn. Lower Cretaceous sandstones (Bentheim and Gildehaus sandstones) have formed steep cuesta ridges with an east-west trend, starting at the eastern side of the valley. Generally, however, the relief is subdued on the eastern valley sides, as most of this area is underlain by shales.

The Cretaceous is discordantly overlain by Tertiary clay and glauconitic sands. The top of the Mesozoic strata steeply dips to the NW in the study area (Waterleiding Maatschappij 'Overijssel', 1985). The formations of Tertiary age which occur in the area are the Landen Formation (marine sands and clay, Paleocene age), Dongen Formation (marine sands and clay, Eocene age), Rupel Formation (marine clay, Oligocene) and the Breda Formation (marine sands, Miocene) (Letsch & Sissing, 1983). Fluvial deposits of Early and Middle Pleistocene age (Harderwijk and Enschede Formations) overly the Tertiary formations. These consist of coarse sand with gravel (Doppert et al., 1975). The Enschede Formation is the most widespread, the Harderwijk Formation occurs only in the northern part of the area.

Both the Tertiary and Lower/Middle Pleistocene formations are exposed in hill ridges on the western side of the valley. These ridges (fig. I.2) originated as push moraines during the Rehburg stage of the Saalian glaciation. The ridges reach heights up to 80 m. Besides the ridges deep glacial basins have been formed.

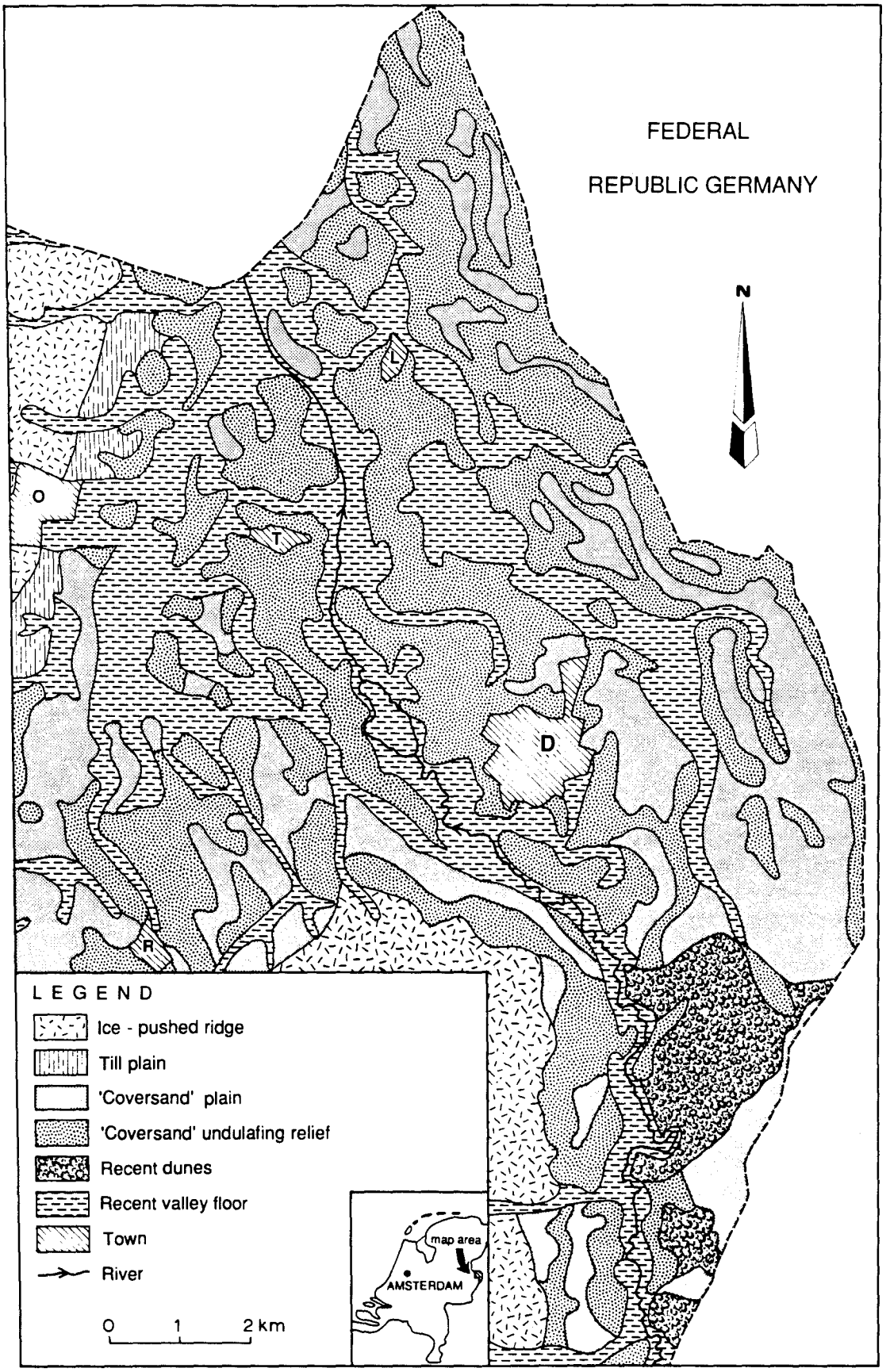

Figure I.2. Geomorphology of the northern part of the Dinkel valley, after Geomorfologische Kaart van Nederland 1:50,000 (Kleinsman et al., 1977). O: Ootmarsum; L: Lattrop; T: Tilligte; D: Denekamp; R: Rossum.

The main basin in the study area is the Nordhorn basin. Its base is found locally more than 75 m below the present surface (Jelgersma & Breeuwer, 1975; Van den Berg & Beets, 1987). Overriding of the ice-pushed ridges led to the formation of a gap between the ice-pushed ridges of Ootmarsum and Oldenzaal, in this study designated as the Tilligte basin. South of this gap another depression was formed largely by subglacial meltwater erosion, the Hengelo basin (Van den Berg & Beets, 1987). In a later phase of the Saalian glaciation the ice-pushed ridge system in the Twente region has been overridden by a rapid advance of the ice. This advance converted the ridges into drumlin-like features, by plastering thick till mantles against the sides and southern ends of the ridges (Van den Berg & Beets, 1987). During the retreat of the ice sheet the glacial basins have been filled in by glacio-fluvial and glacio-lacustrine sediments (Aelmans, 1974; Waterleiding Maatschappij 'Overijssel' N.V., 1985).

During the Eemian and Weichselian more than 25 m of fluvial and aeolian sediments have been deposited in the glacial basins (Van der Hammen & Wijmstra, 1971). The stratigraphy of the basin and valley fill will be treated extensively in section III. The present-day floodplain has been shaped by a fluvial incision phase during the Late Glacial (Van der Hammen & Wijmstra, 1971).

I.3. Present knowledge of the Middle Pleniglacial environmental conditions and deposits in the Netherlands.

The fine grained deposits of Middle Pleniglacial age are usually rich in botanical remains which allow palaeo-environmental reconstructions of this part of the last ice age in the Netherlands. It is not surprising therefore that most literature on Middle Pleniglacial deposits concerns palaeobotanical studies (e.g. Van der Vlerk & Florschütz, 1950, Van der Hammen, 1951, Zagwijn, 1961, 1974; Kolstrup & Wijmstra, 1977, Teunissen & Teunissen-van Oorschot, 1974, Brinkkemper et al., 1987). Other studies pertain to sediment deformations caused by soil freezing which may provide diagnostic palaeoclimatic data (e.g. Maarleveld, 1976; Vandenberghe, 1983a,b). Data on sedimentary structures are relatively rare. Publications which pay considerable attention to sedimentological aspects are those by Ruegg (1975, 1981). Some general studies concerning specific sites or regions also pay attention to depositional environments of the Middle Pleniglacial deposits (e.g. Van der Hammen & Wijmstra, 1971; De Gans, 1981; Van Huissteden et al., 1986a, b).

A few publications give clues to a synoptic description of the Middle Pleniglacial fluvial environment and palaeohydrology. Van der Hammen (1957) mentions the cold and wet character of the 'Inter-Pleniglacial' climate in contrast to the very cold and dry conditions during the Late and Early Pleniglacial. Paepe (1972) presents a curve indicating an exponential increase in river channel width-depth ratio from Eemian time up to the Late Pleniglacial, unfortunately based on an incomplete set of data. This increase is attributed to the climatic evolution during the Last Glacial. Van Huissteden et al. (1986a,b) suggest the presence of meandering rivers during the Middle Pleniglacial, based on the abundance of fine grained overbank deposits. Zagwijn (1974) and Van der Hammen & Wijmstra (1971) describe Middle Pleniglacial peat and silt beds in the Twente region. The fact that these beds could be traced over large distances, led the latter authors

to the conclusion that such beds did represent a change in sedimentation of more than local significance, in this case a change towards a warmer climate. The sand beds between the interstadial beds in this model represent 'niveo-fluvial' deposits, pointing to colder climatic circumstances (Van der Hammen et al., 1967; Maarleveld, 1976). De Gans (1981) interprets the humic loam layers in the Middle Pleniglacial deposits of the Drentsche Aa valley as thermokarst lake deposits. Aeolian sedimentation also has been reported. The aeolian sediment occurs either as addition of reworked loessic material deposited in lacustrine or floodplain environments (Paepe, 1972; Bisschops, 1973; Vandenberghe, 1985), aeolian sand (Van der Hammen et al., 1967), or sandy loess (Vandenberghe & Krook, 1981). In general the fluvial component dominates in the valleys and basins, while aeolian activity influenced interfluvial sites (Vandenberghe, 1985).

Uncertainties exist with respect to the presence or absence of permafrost during the Middle Pleniglacial. In general the climate of the Middle Pleniglacial is considered to be warmer than that of the Early and Late Pleniglacial (Van der Hammen, 1957; Van der Hammen et al., 1967; Maarleveld, 1976). From the Late and Early Pleniglacial times permafrost indications in the shape of ice wedge casts are abundant (Maarleveld, 1976; Vandenberghe & Krook, 1981; Vandenberghe, 1985). Maarleveld (1976) presents indications of a colder episode around 42 ka. The interpretation of Middle Pleniglacial silts as thermokarst lake deposits described by De Gans (1981) implies at least discontinuous permafrost. Vandenberghe (1985) did not find indications for the presence of permafrost during this period in the southern part of the Netherlands.

Combination of the palaeo-environmental data into a historical sequence offers severe difficulties in the fluvial environment sketched above, due to problems of age determination. Warmer phases (Denekamp, Hengelo and Moershoofd Interstadials) are derived from palaeobotanical and stratigraphical data (Van der Hammen et al., 1967; Van der Hammen, 1971; Zagwijn, 1974; see table I.1). These three interstadials, together with the intervening cold stadials, comprise the Middle Pleniglacial. Recently new interstadial names have been published for the time range older than 40 ka (Vandenberghe, 1985; Behre & Lade, 1986; see table I.1). Most of the climatic oscillations are not of a large magnitude, and are palaeobotanically recorded as changes between shrub tundra and tundra vegetations (Zagwijn, 1974; Kolstrup & Wijmstra, 1977).

Van der Hammen et al. (1967) indicate mean july temperatures ranging mostly between 5° and 10° during the Middle Pleniglacial. Between ca. 40 and 43 ka temperatures slightly lower than 5° are assumed. Kolstrup & Wijmstra (1977) found evidence for higher temperatures (up to 15°) during the Hengelo Interstadial and around 50 ka (Moershoofd Interstadial). These higher temperatures seem to be incompatible with the treeless character of the landscape at that time. Kolstrup & Wijmstra (1977) assume that wind action has been a factor limiting tree growth.

Name	Age estimate	First publication
LATE GLACIAL:		
Allerød	11.3-11.9 ka	Hartz & Milthers, 1901; Jessen, 1935; Iversen, 1942; for the Netherlands: Van der Hammen, 1951, 1957; Van der Hammen & Vogel, 1966; Van Geel et al., 1989.
Bølling	12-12.4 ka	
PLENIGLACIAL:		
Denekamp	29-32 ka	Van der Hammen et al., 1967; Vogel & Van der Hammen, 1967; Van der Hammen, 1971.
Hengelo	37-39 ka	Van der Hammen et al., 1967; Zagwijn, 1974.
Moershoofd	43-50 ka	Van der Hammen et al., 1967; Zagwijn & Paepe, 1968.
Riel	ca. 50-55 ka	Vandenberghe, 1985.
Glinde	> Moershoofd	Behre & Lade, 1986.
Oerel	> Moershoofd	
EARLY GLACIAL:		
Keller		Menke, 1976.
Odderade	> ca 58 ka	Averdieck, 1967.
Brørup	> ca 58 ka	Andersen, De Vries & Zagwijn, 1960.
Amersfoort	> ca 58 ka	Zagwijn, 1961.

Table I.1. Interstadial names, published in the Netherlands and NW Germany (partly after Van der Hammen, 1971).

II. Characteristics of periglacial river deposits.

II.1. The periglacial zone - its definition and diversity.

The adjective 'periglacial' is widely used to refer to areas which show the geomorphical effects of a rigorous cold climate. Originally, the term 'periglacial' was introduced by Lozinsky (1909, cited by Karte, 1979) to designate the climate and climatically controlled weathering processes in areas bordering the Pleistocene ice sheets. Gradually the meaning of the word 'periglacial' has been extended to its present meaning.

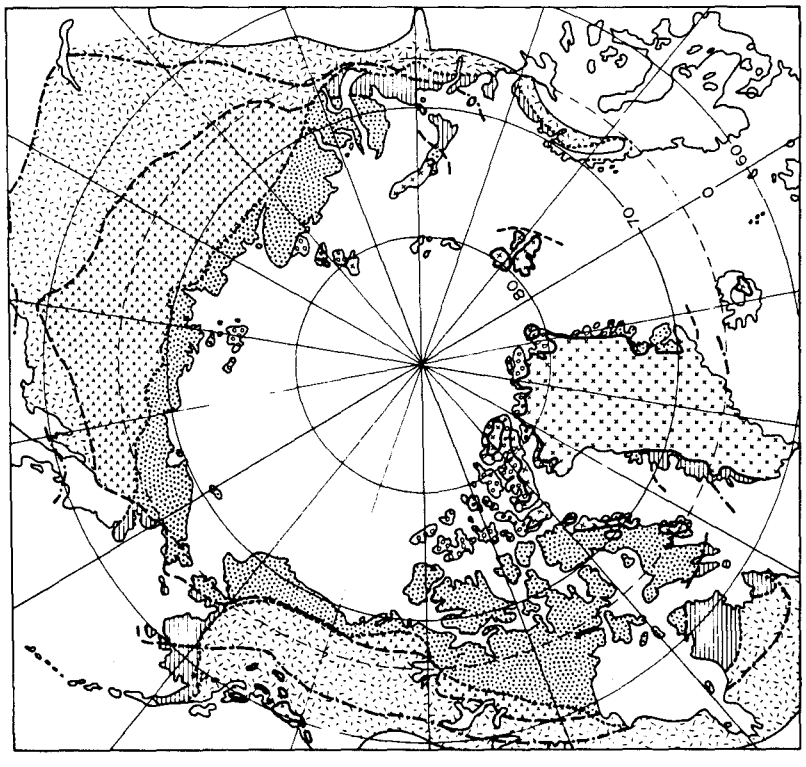

Figure II.1. Regional subdivision of the present periglacial zone, after Karte (1979).

General reference works on the subject stress the difficulties in finding criteria to delimit the periglacial zone geographically (e.g. Péwé, 1969; French, 1976; Washburn, 1979). Tricart (1970) and Karte (1979) stress the importance of a geomorphological highly active frost climate as a characteristic of the periglacial zone. Climatic parameters also may be used for

delimitation. For instance, French (1976) includes all areas with a mean annual temperature below +3° in the periglacial zone. Washburn (1979), however, emphasizes the arbitrary nature of such quantitative parameters. Also vegetation boundaries, e.g. the northern forest border, may be inefficient, as periglacial phenomena are known to occur widespread throughout northern forests in continental North America and Asia (e.g. Washburn, 1979). Karte (1979) delimits the periglacial zone using morphological phenomena as diagnostic criteria. According to Karte & Liedtke (1981) the boundaries of the periglacial zone have to be defined in different ways, varying from region to region, depending on the continentality of the climate.

The periglacial zone exhibits a wide variety in climates, vegetation types and permafrost distribution. For comparison of the palaeo-environment with modern analogues the subdivisions which can be made within the periglacial zone itself are interesting. A useful regional subdivision (fig. II.1) of the present northern periglacial zone has been developed by Karte (1979). Important variations are due to latitudinal and longitudinal variations of the climate. Next, local relief plays an important role in the kind of processes which dominate. Each of the regions distinguished by Karte in the periglacial zone is characterized by a typical set of geomorphological features, ground ice conditions, vegetation and climatic parameters. Important members of this subdivision are the typical polar tundra areas with continuous permafrost and a shrub- or grass-tundra vegetation, the sparsely vegetated polar frost debris zone, oceanic areas with a shrub- or grass-tundra vegetation but without continuous permafrost, and forested continental areas with continuous permafrost.

II.2. Terminology related to periglacial fluvial deposits in the Netherlands.

In the Netherlands the term 'fluvio-periglacial' is used as an adjective for flowing water deposits of the periglacial environment. A definition, given in geological map descriptions of the Dutch Geological Survey reads: 'Sediments deposited by flowing water under periglacial conditions. The water may be rain water, snowmelt water or soil water originating from the active layer; the sediment is of local origin (translation by the author; see e.g. Ter Wee, 1979). Ruegg (1975) stresses the ephemeral character of the depositional process. In the definition above several widely differing elements have been combined.

Some questions with regard to this definition remain. First, the 'local' element is very ambiguous. It is unclear to what extent periglacial fluvial deposits in smaller valleys with nearby sediment sources (e.g. the Dinkel valley) differ from those in larger valleys (e.g. the Vechte or Meuse), besides probably a scale factor. The structures and lithologies found in fluvio-periglacial deposits may occur in any fluvial deposit. Second, the influence of the source of the flowing water on the resulting deposits is unclear. Third, it is hardly known how the fluvial sedimentary environment is influenced by periglacial conditions, as will be shown below.

Another frequently used adjective for periglacial running water deposits is 'niveo-fluviatile' (Van der Hammen, 1971; Kolstrup, 1980) or 'niveo-fluvial' (Edelman & Steur, 1951; Van

der Hammen, 1957). Van der Hammen (1951) uses 'snow meltwater deposits' which has a similar meaning. These terms refer to mainly sandy deposits in smaller valleys. Again, the strong reference to a specific water source is a disadvantage of these terms. In many (sub)arctic watersheds summer rainfall runoff is equally important as snowmelt runoff (Church, 1977). De Ploey (1972) and Mücher & De Ploey (1977) have shown the importance of slope erosion by rainwater runoff in former periglacial environments. It will be difficult to judge to what extent snowmelt runoff has been important in the formation of a specific deposit.

Several studies have shown that periglacial valley fill deposits in the Netherlands are highly variable in aspect and genesis (Van der Hammen & Wijmstra, 1971; Zagwijn, 1974; De Gans, 1981; Vandenberghe, 1985; Van Huissteden & Vandenberghe, 1988). As will be shown below the existence of a specific periglacial fluvial facies is unlikely, and consequently there is no need for a special terminology related to periglacial valley fills. Common adjectives such as 'fluvial', 'lacustrine', 'aeolian' or 'colluvial' suffice well for major subdivisions.

II.3. Indications for a periglacial or (sub)arctic environment in river deposits.

As mentioned above, the periglacial environment is highly variable, with climates ranging from oceanic to highly continental, and vegetation types ranging from densely forested to desert. Next, fluvial processes are only partly related to climate. A large number of dependent and independent variables, acting over different time scales, exert their influence on the fluvial system (Schumm, 1977). History and geology of the drainage basin are important independent variables next to climate. Vegetation and the discharge distribution throughout the year are the most obvious climate-dependent variables. It will be clear that periglacial rivers must be as variable in their characteristics as the periglacial zone itself.

From a search of generally available literature (mainly North-American sources) a list of fluvial processes and features, related to cold climate has been compiled here. Their diagnostic value with respect to a periglacial environment, as well as their possible preservation in ancient deposits varies. These features may be grouped as follows:

1. Periglacial deformation phenomena on sediments exposed to frost activity;
2. The effect of low water temperature on sediment transport, settling and erosion;
3. The effect of growth, presence and decay of a winter ice cover on the river;
4. The effects of icings;
5. The effect of frozen bank material on bank stability and erosion;
6. Discharge regime;
7. Sediment yield.
8. Channel morphology.

II.3.1. Periglacial phenomena.

Different types of fissure structures (frost fissures, ice wedge casts), involutions and pingo or palsa scars may be found on

surfaces which once have been subjected to periglacial climatic conditions. It will not be attempted here to give an overview of the abundant literature on these subjects. Reviews on fissure structures and ice wedge casts are given for example by Dylik & Maarleveld (1967), Washburn (1979) and Harry & Gozdzik (1988). A recent review on cryoturbatic involutions is that of Vandenberghe (1988). Other frost effects in soils are described by Van Vliet-Lanoë (1985). Pingos, palsas and related forms have been reviewed by Pissart (1988), De Gans (1988) and Seppälä (1988). Zagwijn & Paepe (1968), Maarleveld (1976) and Vandenberghe (1983a) present an overview of periglacial phenomena which are known from Twente Formation deposits in the Netherlands.

If correctly identified, they are good indicators of a periglacial setting of the fluvial deposits (Black, 1969b, 1976). The main restriction is that these phenomena are all post-sedimentary deformations and may not be caused by conditions at the time of formation of the fluvial host material. Also the cryogenic origin of deformation phenomena has to be established (Butrym et al., 1964). Deformations due to waterlogging of sediment (loadcasting, desiccation cracking) are very common in any fluvial deposit and may resemble features of cryogenic origin (Reineck & Singh, 1975; French, 1986).

On active alluvial plains periglacial deformation phenomena are likely to occur in overbank environments, or more rarely on channel bars. As many periglacial features require specific formative conditions, they may be used for palaeo-environmental or palaeo-temperature interpretation (Williams, 1975; Maarleveld, 1976; Black, 1976). This will be more extensively discussed in subsequent sections.

II.3.2. Water temperature effects.

Low water temperatures will have some effect on sediment erosion and transport, as fluid viscosity increases with decreasing temperature. Viscosity in turn controls settling velocity, especially of clay and silt-size particles. At 0° fall velocity is approximately one-half that of 20°. As a consequence, suspended sediment transport is influenced. First, the suspension load of a cold river will be coarser on the average, as is demonstrated by Bridge (1981). Second, the vertical distribution of suspension material is influenced, and the amount of suspended material increases. This holds especially for the finest fractions (Lane et al., 1949; Colby & Scott, 1965). Also bed material discharge might increase. Reports on this increase of bed material discharge are conflicting, however (Hubbell & Al-Shaikh Ali, 1961).

Low water temperatures are not typical of arctic rivers and occur in rivers of the temperate zone as well. By contrast, in lowland tundra drainage basins where the slow passage of water through sod mats and shallow ponds result in rapid warming by the sun, river water temperatures may reach levels up to 20° C (Craig & McCart, 1975). Hence it will be difficult, if not impossible, to separate grainsize effects due to low water temperature from other processes which influence grainsize.

II.3.3. The effects of river ice.

An ice cover is not restricted to rivers of the periglacial zone. Within the periglacial zone its effects are more prominent only. Presence of an ice cover may lead to marked changes in the velocity distribution within the river channel, accompanied by bed scouring (Tsang & Szucs, 1972). Floating ice during growth or decay of an ice cover exerts several marked effects.

With conditions of rapid freezing and turbulent water, anchor ice forms on protruding weeds or stones on the river bottom. Anchor ice might enclose bottom sediment (Michel, 1972; Gilfilian et al., 1972). The same holds for bottomfast ice in shallow channels. It may be the major source of coarse ice-rafted debris. This debris may be deposited in overbank environments during spring breakup floods.

Spring breakup is usually accompanied by high water stages due to snowmelt. Breakup at a certain locality along a river is the time when river ice starts moving downstream in spring. A sequence of processes leads to the clearing of the ice cover from the river (Michel, 1972; Mackay & Løken, 1974). First, meltwater starts running above the ice, preferably along the channel edges. The first meltwater does not carry a heavy sediment load yet, but the sediment concentration rises as soon as the ground surface on drainage basin slopes starts thawing (Walker, 1967). Mass wasting from river banks can deposit substantial amounts of bank material on the ice in this stage (Washburn, 1979). As the river stage continues rising the ice cover breaks. Considerable amounts of water-transported sediment may be deposited on ice which is still frozen to river bed or banks, contributing to ice rafted sediment (Walker, 1967). Moving ice also may be an agent in riverbank erosion (Walker et al., 1987). Scouring of bar surfaces by moving ice masses is a common feature (Dionne, 1987). It may produce scoured grooves and ice-shove ridges (Church, 1988). As the rate of ice movement increases formation of ice jams may occur at upstream ends of reaches where the ice cover is still intact, or at channel constrictions. When such a jam gives way to the pressure of impounded water tremendous forces are released (Michel, 1972).

In small lowland rivers ice jams tend to be of lesser importance (Antonov et al., 1972). The presence of snow plugs and bottomfast ice in smaller lowland and wetland channels has similar effects, by promoting overland diversion of river channel flow (Marsh & Woo, 1981; Clark, 1988; Woo, 1988; Woo & DiCenzo, 1989). During the first stages of snowmelt, wetland channels even can be entirely inactive (Woo & DiCenzo, 1989).

With respect to the preservation of scours created by moving river ice, comments are rare. Besides by ice, scour grooves also may be produced by other floating objects, e.g. trees. Anomalous cobble-sized fragments in fine-grained floodplain sediments may have been ice-rafted. Ice rafting is not a specific periglacial feature, it may occur in temperate zone rivers as well. High flood levels and overland flow diversions caused by ice or snow blockage of channels will promote deposition of relatively coarse bed material in floodplain environments, and more frequent channel diversions or avulsions. The latter in turn may lead to higher channel deposit densities (Bridge & Leeder, 1979).

II.3.4. Icings.

Icings are a special form of river ice. They consist of thick ice masses, formed by successive freezing water extruded to the surface by seepage (Washburn, 1979). Under natural conditions icings are formed by spring seepage, or by river water breaking through the ice cover during freeze-up. The last process especially occurs in shallow rivers, when hydrostatic pressures develop as downward freezing ice reaches the river bottom (French, 1976). River icings may contain large volumes of ice. A single icing in an Alaskan river valley was over 10 m thick, more than 1 km wide and 2 km long (Ferrians et al., 1969). Icings may contain several percentages of the annual runoff volume, and contribute to river discharge long after spring snowmelt (Kane & Slaughter, 1972).

According to Black (1969b), preservation of fossil forms created by icings will be unlikely. However, the ice masses can divert streamflow outside channels (Froehlich & Słupik, 1982), on the other hand bank sections are protected from erosion (Clark, 1988). The effects on channel diversion may influence overbank deposition and channel deposit density in ancient deposits, as noted in the previous paragraph.

II.3.5. Bank stability.

Freezing of unconsolidated river bank and bed material raises its shear strength (Cooper & Hollingshead, 1973). Blocks and lumps of non-cohesive sediments which would otherwise not survive any fluvial transport might indicate the erstwhile presence of ice-cemented frozen banks, if preserved in channel deposits.

River banks in permafrost areas often display a special form of bank undercutting in spring: the formation of thermal-erosional niches. The river water melts the ice in the lower part of the frozen bank and carries away the sediment, resulting in deep undercutting the overlying frozen bank material. Subsequently, river bank failure may occur, preferably along ice wedges and frost fissures (Walker and Arnborg, 1966; Walker et al., 1987; Bryant, 1982). Thermo-erosional niches only rarely can be recognized in ancient deposits (e.g. Vandenberghe et al., 1974; Kolstrup, 1985). Niching also may occur, however, in river banks composed of layers of cohesive and non-cohesive sediments without presence of permafrost (Thorne & Lewin, 1979).

Reports on the effect of frozen bank and bed material on channel geomorphology and mobility are conflicting (Clark, 1988). Church (1974) stresses the importance of thermo-erosional niching, which favours lateral erosion. Exposure of ground ice in river banks also leads to rapid erosion of river banks (Church, 1977). Other authors stress that frozen banks may inhibit lateral channel migration (Cooper & Hollingshead, 1973; Slaughter & Collins, 1981). Scott (1978) concluded from a study of river reaches in northern Alaska that the presence of permafrost does not exert a strong negative influence on bed and bank erosion. The effects vary from site to site, with composition of bank material as the principal variable. The impeding influence of permafrost on erosion is most effective with cohesive bank material which shows lower thaw rates. Also the thermal input is an important factor which depends on (micro)climate and discharge regime. An additional factor which affects river banks is

nivation resulting from local accumulations of snow (Miles, 1976).

II.3.6. Discharge distribution.

The discharge distribution throughout the year for arctic rivers is very characteristic. Streamflow is reduced or ceases during winter, while in spring large amounts of stored water are released by snowmelt in the drainage basin (Mackay & Løken, 1974). Infiltration into the still frozen ground is restricted, although not absent (Marsh, 1988; Clark, 1988). Most of the meltwater thus contributes to overland flow (Kane & Hinzman, 1988; Clark, 1988). The main effect of arctic river discharge regimes is a concentration of river discharge in a relatively short time of the year. For instance, in the Colville river on the Alaskan North Slope, discharge is concentrated in 40 % of the year (Arnborg et al., 1966). Concentration of discharge can be expected to occur in regions where snow cover persists for longer than one month in 50 % of the years (Church, 1988). For many rivers, the nival flood is the major sediment transporting event (Church, 1988). Magnitude of spring breakup floods depends strongly on weather conditions (Michel, 1972; Church, 1988). With slow melting of the snow in the drainage basin discharge increase will be less prominent. Usually, however, rainstorms accompany snowmelt and augment discharge. Ice jams further raise flood height. Areas with a nival flood regime are by no means restricted to the arctic. At present the countries surrounding the North Sea are just outside the climatologically defined nival region (Church, 1988).

Superposed on this general pattern are modifications by local climate and other drainage basin characteristics. In tundra regions the total runoff is on average 60-70 % of the precipitation. In forested regions, evapotranspiration takes a larger part of the precipitation. Vegetation characteristics influence response time of the rivers (McCann et al., 1972; Church, 1974). The presence or absence of permafrost also is an important factor. Groundwater contribution is low in continuous permafrost areas, but may increase to 40 % in the discontinuous permafrost zone (Mackay & Løken, 1974). The presence of permafrost at shallow depth promotes quick response of rivers to snowmelt and storm events (McCann et al., 1972; Slaughter et al., 1983). Diurnal discharge variations by snowmelt processes are reported frequently from smaller streams.

Church (1974) distinguishes four types of discharge regimes: the subarctic nival regime, the arctic nival regime, the proglacial regime and the muskeg regime. The subarctic and arctic nival discharge regimes are characterized by the presence of a pronounced spring flood and generally low flow throughout the summer, with exception of rainstorm floods. In high arctic watersheds underlain by continuous permafrost groundwater discharge is virtually absent and rivers are dry in winter. Because of generally lower summer rainfall in the high arctic, the spring flood usually dominates. In the subarctic river basins groundwater contributes to the river discharge, and summer rainstorms may produce flood peaks of higher magnitude than the spring flood. Proglacial rivers derive much of their discharge from ablation of glacier ice which continues to rise throughout the summer. Long

persisting snow drifts in the drainage basin may have a similar effect (Church, 1988).

The muskeg discharge regime which deserves special attention in the context of this study, occurs in poorly drained basins, wetland areas and lowland tundra areas with many standing water bodies. High water retention of thick grass- or shrub-tundra sod mats plays an important role. With this type of discharge regime response of the river to either rainstorms or spring snowmelt is very slow. Flood peaks are lower and reaction times are longer. However, Woo (1988) has demonstrated that the examples of muskeg regime rivers cited by Church (1974) are not representative. In any case the spring snowmelt flood in wetland areas is more pronounced and more rapid than stated by Church (1988), due to low infiltration rate of the frozen wetlands and channel blockage by snow and ice (Woo, 1988).

Pronounced snowmelt flooding means that arctic river channels need to have a higher capacity than other rivers with comparable yearly discharge quantity and drainage basin. This will be expressed in a relative difference of channel dimensions: width, depth, meander wavelength, and channel gradient (Schumm, 1977). An example is given by Vandenberghe (1987). Other evidence of arctic types of discharge regimes will be difficult to find in ancient deposits. Bryant (1982, 1983) describes differences between present-day arctic nival and proglacial rivers. Van Huissteden & Vandenberghe (1988) use a combination of sedimentary structures and palaeobotanical data as evidence of presence/absence of a pronounced nival regime.

II.3.7. Sediment yield.

It is generally accepted that slope processes are intensified in periglacial environments, although quantitative data which allow comparison with other climatic zones are rare. Many descriptions concern processes which are more or less specific to the periglacial zone, e.g. gelifluction. Reviews are given by French (1976), Washburn (1979) and Lewkowicz (1988). The relative importance of the different types of process is generally unknown. For this study mass wasting processes which occur in low relief areas are most important.

Rapid mass movement processes which may occur in low relief areas are usually related to the presence of permafrost with ground ice, and its degradation by thermal erosion. These include active layer flowing and gliding and ground-ice slumps (French, 1976; Lewkowicz, 1988). The latter process is often induced when ice-rich permafrost is exposed by other erosion processes (Lewkowicz, 1987).

Slow mass wasting processes are frost creep, gelifluction and slopewash. Frost creep is not confined to the periglacial zone, it probably reaches its highest movement rate in the subarctic and higher middle latitudes, as it depends on freeze-thaw alternations (Washburn, 1979; Lewkowicz, 1988). Gelifluction is the most well known process which occurs specifically in periglacial environments. It may occur on slopes as gentle as 1° (St-Onge, 1965). According to Washburn (1979), factors which influence gelifluction rate are: soil moisture, vegetation cover, slope gradient and soil grain-size distribution. Soil moisture is most important; a well developed vegetation cover tends to retard the process. Especially materials with a high silt content are

sensitive. Gelifluction processes are most effective in climates with sufficient precipitation and mean annual temperatures below 0° (Karte, 1979).

Slopewash in periglacial areas has not received much attention until recently. Liedtke (1983) attributes the levelling of the older morainic landscape in northwestern Germany mainly to 'abluation' (periglacial slopewash) during the Weichselian, and states that solifluction played only a minor role since the widespread gravelly-sandy substratum of these areas is less sensitive to solifluction.

The rate of slopewash will vary throughout the periglacial zone, depending on vegetation, material and slope hydrology. Vegetation differs widely in aspect and ground cover in the arctic; ground cover values range between 5% ground cover and fully covered (Tedrow, 1977; Edlund, 1987). Data concerning sediment yield in relation to vegetation mainly have been obtained from (semi-)arid and temperate climates (e.g. Langbein & Schumm, 1958), and suggest highest sediment yields in semi-arid areas with desert-shrub vegetation. The situation may be different in arctic areas with presence of frozen ground and snow-cover. French (1976) states that the concentration of most precipitation and runoff in a short time of the year, and the presence of a permafrost table which prevents penetration of runoff into the ground, enhances rill and sheetwash erosion in areas of sparse vegetation. Overland flow during snowmelt carries considerable amounts of sediment (McCann et al., 1972; Wilkinson & Bunting, 1975). The latter studies pertain to sparsely vegetated areas, underlain by permafrost. Lewkowicz et al. (1978) measured an erosion rate of 10.04 $gm^{-2}y^{-1}$ on a 5° slope with 60-80 % vegetation cover on silty colluvium on Banks Island, Canada. This value is low, compared with data from different climatic zones given by Walling & Webb (1983). From measurements on low angle slopes in the tundra-polar desert transition on Banks Island, Lewkowicz (1983) reports weight losses of 0.3 - 5.8 $gm^{-2}y^{-1}$ by suspended sediment transport. The values are higher near snowbanks than on interfluvial sites. These denudation rates are among the lowest in the world. Lewkowicz suggests, that the values will be higher in polar desert areas and lower in tundra regions. French & Lewkowicz (1981) conclude that slopewash is not a major geomorphic agent in periglacial areas, and that other mass wasting processes, notably gelifluction, dominate.

In many areas of the periglacial zone, aeolian deposition of either loess or aeolian sand is of widespread occurrence (e.g. Seppälä, 1972; Péwé, 1975; Pissart et al., 1977). The aeolian material also contributes to the sediment yield of arctic drainage basins, by deposition on the alluvial plain. However, most of this aeolian material is usually reworked from the alluvial plain itself (Péwé, 1975; Bryant, 1982; Good & Bryant, 1985), although other sources, e.g. fluvioglacial sediments may be important locally (Pissart et al., 1977; Seppälä, 1971, 1972). The aeolian activity may lead to mixing or interfingering of aeolian and fluvial deposits, especially in overbank environments (Good & Bryant, 1985).

An important conclusion is that high sediment delivery to arctic rivers is certainly not a general rule. On the contrary, low values are of general occurrence throughout the periglacial zone. Much depends on other drainage basin characteristics than

climate, such as relief, soil characteristics and presence of glaciers.

II.3.8. River channel morphology.

It is often assumed that rivers in periglacial regions tend to develop braided channels of large width-depth ratio. French (1976) for instance states that the braided channel is the most common occurring type in periglacial regions. Partly this may be caused by the widespread occurrence of proglacial streams with high sediment discharge and a strong tendency to braiding. Nevertheless, topographical maps and airphoto collections of periglacial regions display all types of rivers, from straight to sinuous and single-channel to multi-channel, as is common in other morphogenetic regions as well. Many examples of periglacial single-channel and sinuous rives are known from literature (e.g. Walker, 1973; Church, 1977; Forbes, 1983; Bryant, 1982).

Obviously there is no river channel morphology which can be considered as typical of the periglacial zone. General morphogenetical conditions vary throughout the periglacial zone, and in many cases local factors, such as drainage basin relief, will override these general conditions. This does not exclude, however, the possibility that sub-regions of the periglacial zone may show a tendency towards a specific channel pattern, as the examples of French (1976) show.

II.3.9. Conclusion.

The literature cited above shows that river deposits in the periglacial environment do not differ substantially from those of other regions. Major river characteristics, such as morphology, discharge regime and sediment load are very diverse within the periglacial zone. There is no indication for the existence of anything like a zonal type of river deposit in this respect.

The most certain indications of a periglacial setting of river deposits are small scale sedimentary structures, most of which are likely to be very rare. These include features like ice-rafted debris, ice-scour phenomena, thermo-erosional niches in preserved bank sections, and lumps of non-cohesive sediments which were apparently frozen during transport. Periglacial phenomena are good indicators if it can be shown that these are contemporaneous with the deposit considered.

Also a gradual difference in architecture of the deposits may be found, although this is not of strong diagnostic value. High spring discharges combined with the chance of channel blockage by ice or snow, tend to promote channel diversions and overbank deposition which may lead to higher channel deposit densities. In the more arid periglacial environments interfingering with aeolian deposits may occur.

III. Stratigraphical framework.

III.1. Chronostratigraphical classification of continental non-glacial deposits from the last glaciation.

Although this study focusses on a specific part of the last glacial time, a discussion of the entire stratigraphy of the deposits of that period is useful. Many data have been gathered which add to refinement of this stratigraphy, and a description of the Middle Pleniglacial deposits cannot be given without considering the stratigraphical relations to the overlying and underlying units.

It has become customary to classify deposits dating from the Last Glaciation in the Netherlands under the name 'Weichselian' (Zagwijn, 1961, 1975). Previously, Van der Vlerk & Florschütz (1950, 1953) and Van der Hammen (1951, 1971) used 'Tubantian' (derived from the Roman name for the Twente region) for the deposits dating from the Last Glacial in the Netherlands, as correlation with the type region of the Weichselian was not sufficiently well established at that time. The definition of the Weichselian (or -more correct - Vistulian) stage is based on sequences in the glaciated area during the Last Glacial (Bowen, 1978). The type region is the Lower Vistula area in Poland (INQUA Stratigraphic Commission, 1981). In large parts of Western Europe glacial deposits are absent, and other continental depositional environments dominated. Stratigraphical relations therefore differ from those in the glaciated areas. It is stratigraphically more correct to use a separate chronostratigraphical division in the periglacial areas of the Last Glacial which could be a good reason to rehabilitate 'Tubantian' as a chronostratigraphical stage name for the Last Glaciation outside the West-European glaciated areas. For the sake of continuity of stratigraphical nomenclature, 'Weichselian' however will be maintained here. The chronostratigraphical lower boundary of the last glaciation is placed at the start of the first cold oscillation after the climatic optimum of the Eemian (Zagwijn, 1961; INQUA Stratigraphic Commission, 1981, 1984). The type locality for the Eemian / Weichselian transition is located in the Eem valley, where the Weichselian continental deposits overlie Eemian age marine deposits (Zagwijn, 1961).

The Weichselian is commonly subdivided in three substages. In the Netherlands, the subdivision Early Glacial - Pleniglacial - Late Glacial is commonly used since the publication by Van der Hammen et al. (1967). Based on uranium-thorium dating on peat of several continental records in Europe, the age of the Early Glacial/Pleniglacial boundary appears to be somewhat earlier than 70 ka (Van der Wijk 1987). Van der Hammen et al. (1967), Woillard & Mook (1982) and Vandenberghe (1985) correlate this boundary with the stage 4/5 boundary in the $\delta^{18}O$ record in deep-sea cores after Emiliani (1955) and Hays et al. (1976). The boundary of the Pleniglacial-Late Glacial transition is placed at 13 ka, after Van der Hammen et al. (1967).

The Pleniglacial is subdivided into Early Pleniglacial, Middle Pleniglacial (or Inter Pleniglacial, Van der Hammen, 1957), and Late Pleniglacial (Van der Hammen et al., 1967; Van der Hammen, 1971). Van der Hammen et al. (1967), Vandenberghe (1985) and Woillard & Mook (1982) correlate the Early Pleniglacial with stage 4, the Middle Pleniglacial with stage 3, and the Late

Pleniglacial with stage 2 in the $\delta^{18}O$ record of the deep-sea cores (fig. III.1).

A further subdivision of the Weichselian has been based on stadial-interstadial cycles which receive the rank of chronozones (Bowen, 1978). Interstadials which have been recognized in the Netherlands and NW Germany are shown in table I.1. Especially for the older levels (> 40 ka) the age relations are uncertain, due to inherent uncertainties of radiocarbon datings in this time range. Therefore the Moershoofd Interstadial is often designated as the 'Moershoofd Complex', as it may contain several oscillations (Kolstrup & Wijmstra, 1977).

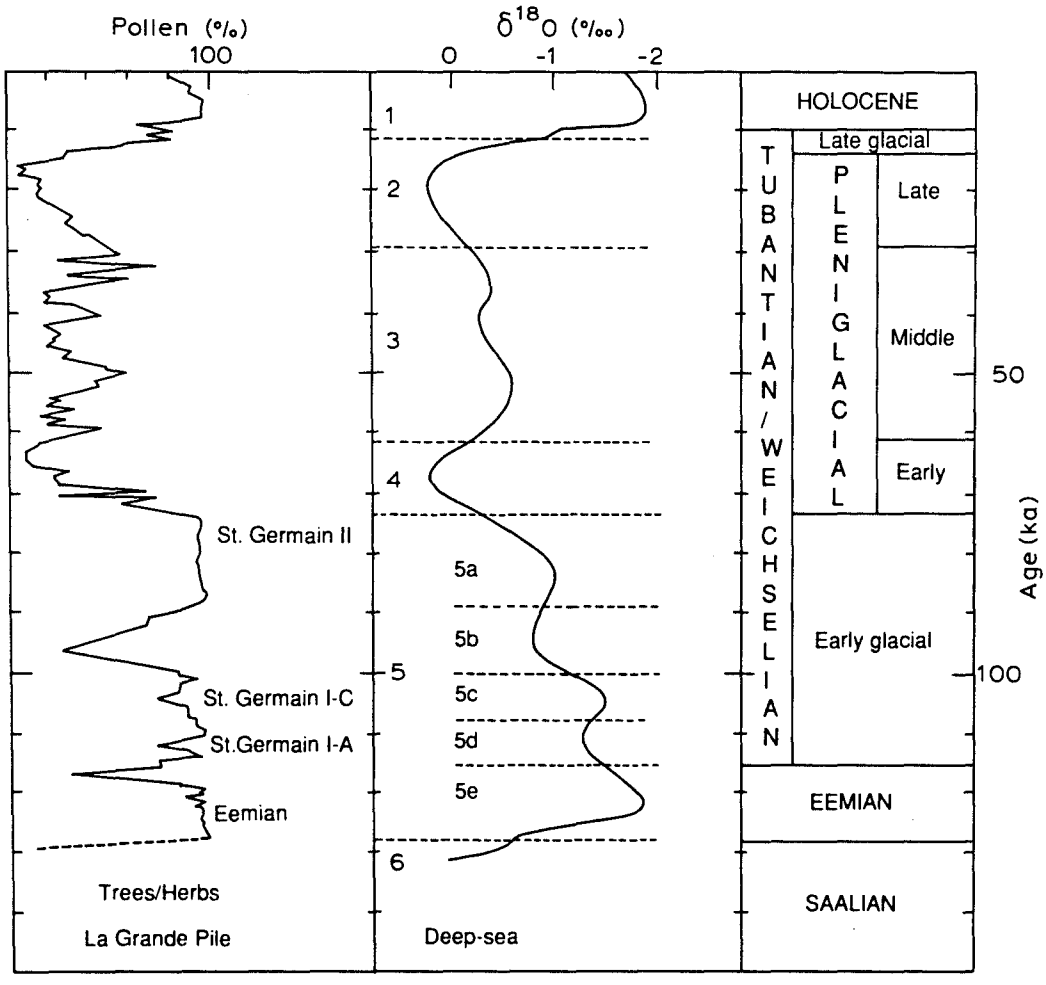

Figure III.1. Correlation of Weichselian (Tubantian) chronostratigraphy in the Netherlands with continuous arboreal pollen curve from La Grande Pile site (A) and oxygen isotope stages in deep-sea cores (B). Curves after a compilation by Van der Wijk (1987); A: after Mook & Woillard (1981); B: after Emiliani (1955), stage boundaries after Hayes et al. (1976).

III.2. Lithostratigraphy.

III.2.1 The Twente Formation and its relation to other units.

The continental deposits of Weichselian age are classified in the Netherlands into two formations, the Kreftenheye and Twente Formations (Doppert et al., 1975). In Northwest Germany these deposits are known as 'Talsande' (Boigk et al., 1960). The Twente

Formation as a lithostratigraphical unit has been formally introduced by Zagwijn (1961). It is a complex unit consisting of sediments of various origin. Aeolian sands, loess, meltwater deposits, slope deposits, fluvioperiglacial deposits, peat and lake deposits are included (Van der Hammen et al., 1967; Doppert et al., 1975). The sediments are of 'local' origin (Doppert et al., 1975). In practice the adjective 'local' is used to distinguish these deposits from contemporaneous fluvial deposits of the Rhine and Meuse (the Kreftenheye Formation).

The Asten Formation which underlies the Twente Formation in valleys and basins, consists of peat and fluvial deposits of Eemian age. Where the Asten Formation mainly consists of fluvial deposits, this formation, and the basal unit of the Twente Formation locally may be difficult to distinguish from each other. In the study area, the Twente Formation is often overlain by the Singraven Formation. The Singraven Formation consists of peat, clay and sand beds of fluvial origin, mainly of Holocene age (Van der Hammen & Wijmstra, 1971; Doppert et al., 1975). These deposits are usually rich in organic matter. Deposition of this type of sediment already started during the Late Glacial (Van der Hammen & Wijmstra, 1971). Doppert et al. (1975) include both Late Glacial and Holocene fluvial sediments in the Singraven Formation. Other formations which may overlie the Twente Formation are the Kootwijk Formation (aeolian sands) and Griendtsveen Formation (peat).

III.2.2. Subdivision of the Twente Formation as used in this study.

The classic subdivision of the Twente Formation has been developed by Van der Hammen (1971) and is based on the valley fill of the Dinkel river. The main lines of the existing stratigraphy are confirmed by the field data in this study (fig. III.2). The greatly extended amount of data, combined with recent literature on comparable sequences in other regions, allows some further refinements of the lithostratigraphy established by Van der Hammen (1971):

- The Beuningen gravel bed is a well recognizable stratigraphical level, with a very widespread occurrence in Belgium, the Netherlands and Northwest Germany, separating sediments with different aspects (par. III.3.3.4,5). It is considered therefore as an excellent marker horizon for distinction between major units.
- In the Dinkel valley, fluvial sands of considerable thickness have been found between the Mekkelhorst Member and the Beuningen gravel bed. These sands underlie the 'Older Coversand I' or interfinger with these, especially where the sequence between the Mekkelhorst Member and the Beuningen gravel bed is thick. The fluvial sands differ in many lithological aspects from those of the underlying Mekkelhorst Member. The transition is usually a sharply defined erosional transition, with striking differences in grain size, organic matter content, mineralogy and colour (par. III.3.3.3,4). Previously these fluvial sands have not been recognized as a separate entity.

The essential adjustment of the existing stratigraphy is the introduction of a new member (Beverborg Member) which incorporates the fluvial sands between the Mekkelhorst Member and the Beuningen gravel bed, and the 'Older Coversands I'. At least in the Twente region this Beverborg Member is a distinct lithostra-

tigraphical unit. The upper and lower boundaries of this unit conform to well established stratigraphical markers (Beuningen gravel bed, abovementioned erosional base of the fluvial sands, truncating the Mekkelhorst Member). The Mekkelhorst Member is consists of the typical sand/silt/peat sequence of Middle Pleniglacial age which is found in the Dinkel valley and many other locations. The Lutterzand Member as defined here (Lutterzand Member sensu stricto hereafter) is restricted to the Older Coversand II of Van der Hammen (1971).

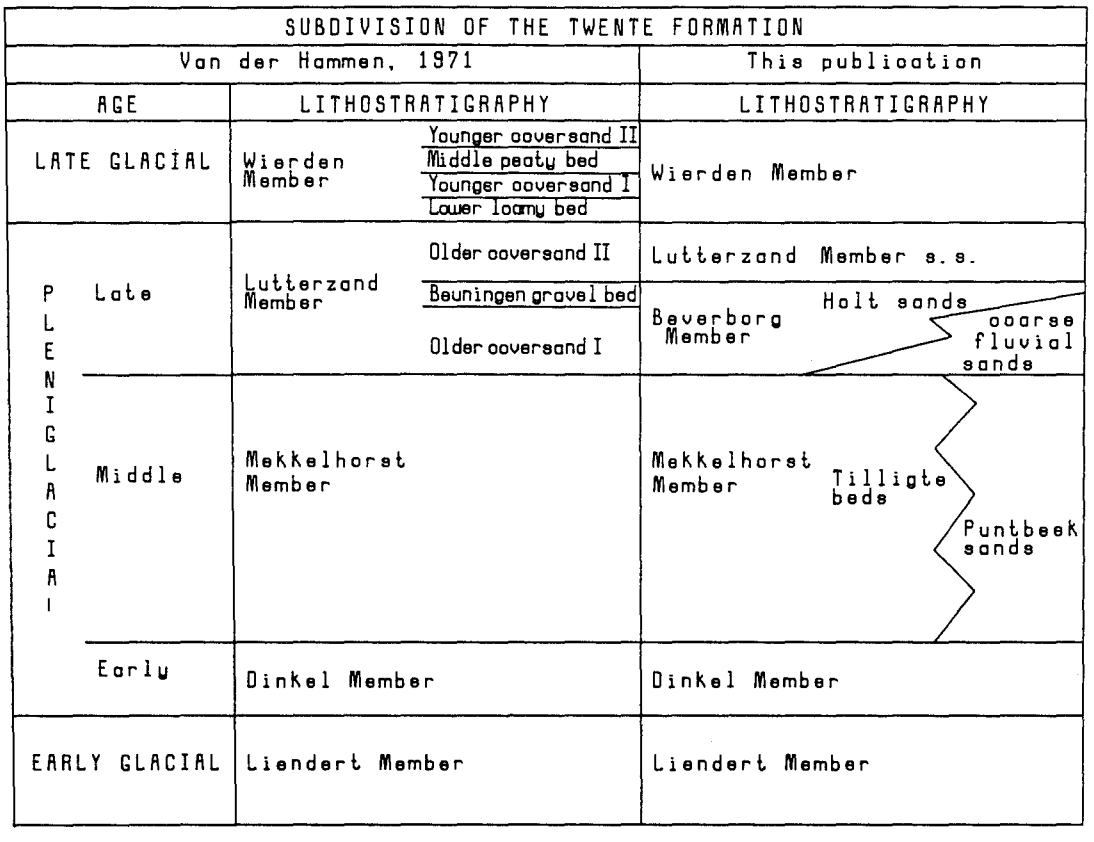

Figure III.2. Subdivision of the Twente Formation as used in this study, compared with the original subdivision by Van der Hammen (1971).

III.3. Description of lithostratigraphical units.

III.3.1. Substratum.

Close to the ice-pushed ridges (e.g. in the Tilligte section), the substratum consists of Tertiary clay, gravelly sand of the Enschede Formation, or till of the Drente Formation. In the basins between the ridges the Late Quaternary fill is underlain by fluvio-glacial sand and glacio-lacustrine silts of the Drente Formation (Waterleiding Maatschappij 'Overijssel' N.V., 1985). These sediments rarely have been reached in the borings. Their main characteristic is the high lime content. On the eastern valley side Lower Cretaceous shale has been found.

III.3.2. Asten Formation.

In the Dinkel valley this formation mainly consists of sand, clay and peat beds. The Asten Formation is of Eemian age (Doppert et al., 1975). The peat beds are the most conspicuous elements. These are usually thick beds of Sphagnum peat. All sediments of the formation frequently contain wood fragments. Vivianite concretions also have been found. Where thick peat beds are lacking in the Asten Formation the distinction between the Asten Formation and the overlying Twente Formation is more difficult. Near the base of the Asten Formation coarse fluvial sands occur in some deeper borings (Van Huissteden et al., 1986a). This may point to a fluvial incision phase at the end of the Saalian or the start of the Eemian. Fluvial incision of this age also has been reported by De Gans (1981).

Most of the Asten Formation sands contain relatively high percentages of tourmaline and metamorphic minerals, compared with most Twente Formation sediments. In general, the sediments are non-calcareous, but lime-rich sediments also occur. This probably depends on the amount of freshly reworked substratum sediment.

III.3.3. Twente Formation.

III.3.3.1. Liendert Member.

This unit has been defined by Van der Hammen (1971). Its type site is De Liendert, near Amersfoort, of which a description is given by Zagwijn & Paepe (1968). It consists of sand, clay, silt and peat beds. The clay and silt beds prove to reach considerable thickness in the Dinkel valley, more than 1 m is not uncommon. The thicker silt and clay beds occur near the base of the member in the Nordhorn basin. These may be of lacustrine origin. Peat beds are generally thinner than those of the Asten Formation and contain less wood. In general, the Liendert Member is at most weakly calcareous. Towards the top sand beds and lime content usually increase. Heavy mineral spectra from the Liendert Member do not differ significantly from those of the Asten Formation (par. V.1). The Liendert Member is of Early Weichselian age (Zagwijn, 1961; Van der Hammen, 1971).

There is no conclusive evidence for an important fluvial incision phase at the Eemian/Weichselian transition, such as reported from the Flemish Valley by De Moor (1983). The top of the Asten Formation has been preserved, as Late Eemian pollen assemblages have been found in the analyzed cores (Van Huissteden et al., 1986a; Van Geel, pers. comm.). The transition between the Asten and Twente Formations involves mainly a decrease in peat deposition. In one boring (Noord Deurningen, fig. III.3) it consists of a transition of peat towards lacustrine clay.

III.3.3.2. Dinkel Member.

This unit has been defined and described first by Van der Hammen (1971). The more abundant borehole data in this study allow to describe its stratigraphical relationships more precisely. According to Wijmstra et al. (1971), the Dinkel Member consists of coversand-type sediments with intercalations of coarser material. The sands lack organic matter. The definition is mainly based on the Mekkelhorst boring (op. cit., page 68). Here, the

Dinkel Member reaches a thickness of 9.4 m. The Dinkel Member has been deposited during the Early Pleniglacial.

From the present data, this thickness proves to be an anomalous situation. Borings and penetration cone soundings - also in the immediate neighbourhood of the Mekkelhorst boring - indicate that the zone which correlates best with this Dinkel Member may be up to 5 m thick. Thickness in many borings and penetration cone soundings proves to be considerably less (figs. III.3, IV.3-6). In these borings, levels which are comparable to the upper part of the Dinkel Member in the Mekkelhorst boring contain silt and peat beds which are a downward continuation of the typical Middle Pleniglacial silt/peat/sand sequence (Tilligte beds, see below). This strongly suggests that the upper part of the Dinkel Member in the Mekkelhorst boring is a lateral, sandier equivalent of the lower part of the Tilligte beds. A study of the description and lacquer peels of the Mekkelhorst boring shows that indeed the upper part of the sediments ascribed to the Dinkel Member contain vegetal remains which is a characteristic property of the Tilligte beds. This would reduce the thickness of the Dinkel Member in this boring to 6 m which compares better with values found elsewhere.

In most borings the Dinkel Member consists of a zone of strongly calcareous fine to coarse sand. In penetration cone soundings it usually appears as a well defined zone of low friction ratio values (par. IV.1.2). Clearly defined silt or clay beds are absent, as well as organic matter. Often the sand is silty, with distinct thin bedding not unlikely that of the coversands deposited during the Late Pleniglacial (Van der Hammen, 1971). Also current ripple cross lamination is found. In some borings the Dinkel Member is very thin or practically absent. In these cases only a rather thin gravelly zone occurs at the top of the Liendert Member (e.g. boring Scholtenhave, fig. III.3). In one boring (Dorpermeien) very coarse, gravelly sands with clay and peat lumps have been found. These probably correlate with the above-mentioned coarse zone in other borings. In the Lattroperstraat boring (fig. III.3) the silty sands have been found on top of the coarse gravelly zone. With respect to the underlying deposits the heavy mineral spectra show a decrease in the amount of tourmaline and metamorphic minerals, and an increase of the hornblende percentage (par. V.1). Especially the log of boring Venweg (fig. III.3) may provide a parastratotype for the Dinkel Member.

In the Netherlands a fluvial incision phase has been recorded, dating from the transition between Early Glacial and Pleniglacial (Vandenberghe et al., 1984; Vandenberghe, 1981, 1985) or from the transition from Early to Middle Pleniglacial (De Gans, 1981). The coarse sands at the base of the Dinkel Member suggest a fluvial incision in the Dinkel basin also, at the start of, or during the Early Pleniglacial. Often a gravel bed is found which truncates ice wedge casts of Early Pleniglacial age (Steinsohle 1; Zagwijn & Paepe, 1968, or Gilze gravel, Vandenberghe, 1985). At the Amersfoort site described by Zagwijn & Paepe (1968) the Steinsohle 1 is overlain by Lower Pleniglacial coversand-type sediments. The coarse base of the Dinkel Member probably correlates with the Steinsohle 1, while the overlying coversand-type sediments of the Dinkel Member correlate with those overlying the Steinsohle 1 of Zagwijn & Paepe (1968). On basin slopes the stratigraphical equivalent of the Dinkel Member is usually a

gravel bed correlative with the Steinsohle 1 or Gilze gravel (e.g. De Poppe exposure, par. VIII.3.1).

III.3.3.3. Mekkelhorst Member.

The Mekkelhorst Member conforms to the original definition of the Mekkelhorst Member described by Van der Hammen (1971). See, however, the previous paragraph with respect to its lower boundary. The top is marked by a generally erosional transition towards the Beverborg Member. In some cases, sands which previously have been attributed to the top of the Mekkelhorst Member (e.g. 'upper sands' of the Mekkelhorst Member in the Lutterzand exposure, sands above 4.4 m in the Mekkelhorst boring) should be correlated with the Beverborg Member based on lithological characteristics (par. III.3.3.4). The age of the Mekkelhorst Member is Middle Pleniglacial, ranging from at least 55 ka to ca. 26 ka as indicated by radiocarbon datings. Two sub-units which are lateral equivalents of each other, can be distinguished within the Mekkelhorst Member. These are the Tilligte beds and the Puntbeek sands. The Tilligte beds represent the Middle Pleniglacial sand/silt/peat facies which is found in many locations (Van der Hammen et al., 1967; Zagwijn & Paepe, 1968; Zagwijn, 1961, 1974; De Gans, 1981; Vandenberghe, 1985). The Puntbeek sands consist entirely of sands which show similar lithological characteristics as the sands in the Tilligte beds.

The Mekkelhorst boring, described by Wijmstra et al. (1971) is the stratotype of the Mekkelhorst Member. The Mekkelhorst Member is represented by the tract between 4.4 and 10.6 m in this boring. Other sections and borings presented in section IV of this study are suggested as para-stratotypes (par. III.3.3.3.1).

III.3.3.3.1. Tilligte beds.

The Tilligte beds have been described earlier by Van Huissteden et al (1986a), Van Huissteden & Vandenberghe (1988) and Vandenberghe & Van Huissteden (1989); in the latter publications as 'Tilligte Member'. On behalf of continuity of stratigraphical nomenclature, it is preferred to maintain 'Mekkelhorst Member' as formal name for these beds. Type sections for the Tilligte beds are the borehole sections near the village of Tilligte, the Tilligte section and the Laarhuis-Rammelbeek section (par. IV.2.1, 2). The Tilligte beds are characterized by the presence of organic matter, clay, silt, gyttja and peat layers, intercalated with fine and medium (rarely coarse) sands. The heavy mineral spectra are similar to those of the Dinkel Member, with generally high percentages of hornblende. The colour of sands without organic matter is usually rather dark, with a distinct greenish component. With exception of the peat beds the Tilligte

Figure III.3 (next page). Core logs of deeper borings (location of borings see fig. IV.1). Top: boring number and location name. Depth relative to surface. Characters next to columns and connecting lines between columns show stratigraphical correlation. S = Singraven Formation; C-L = Twente Formation; C = Wierden Member + Lutterzand Member s.s.; B = Beverborg Member; T = Mekkelhorst Member, Tilligte beds; D = Dinkel Member; L = Liendert Member; A = Asten Formation; DR = Drente Formation.

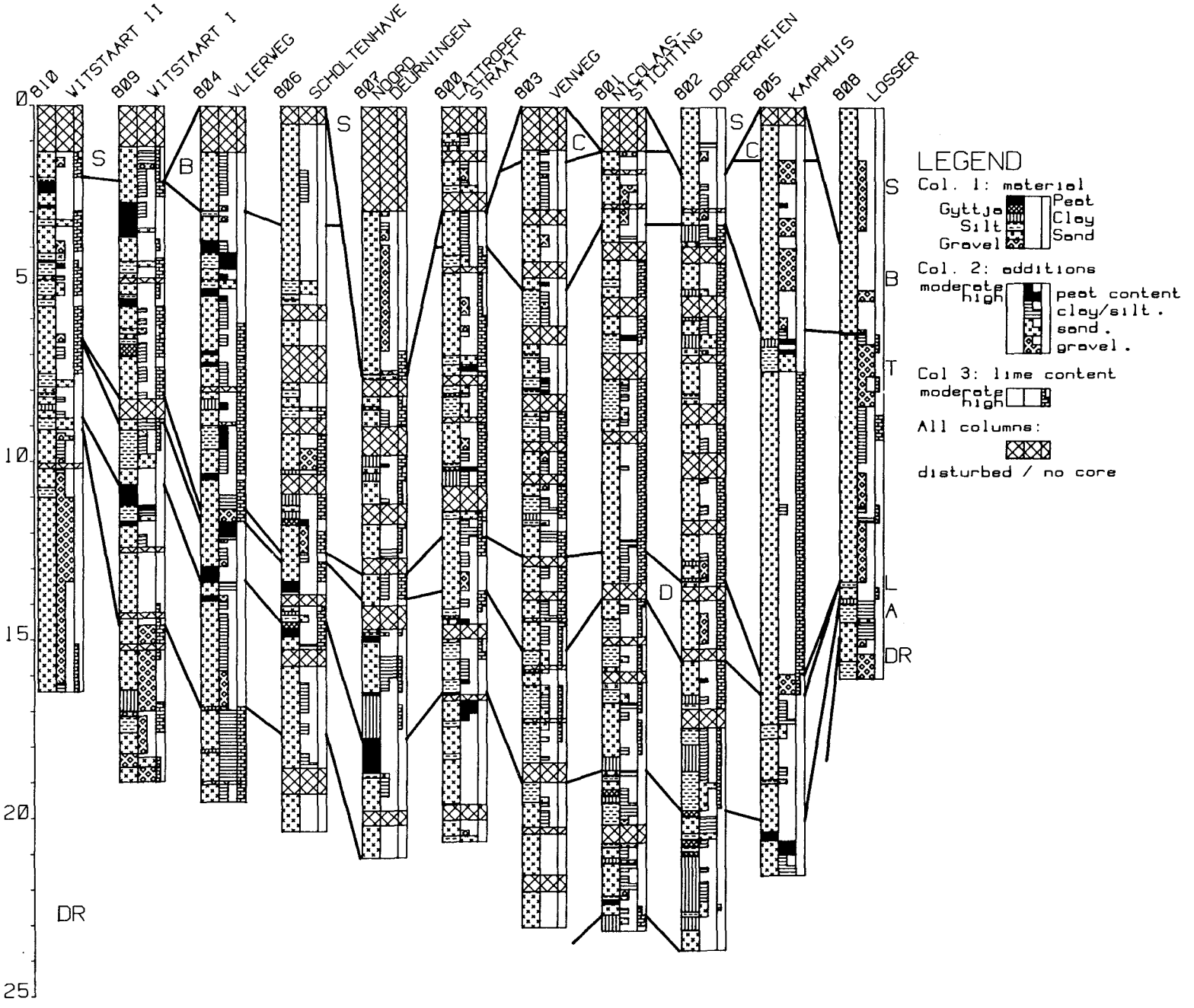
B10 WITSTAART II
B09 WITSTAART I
B04 VLIERWEG
B06 SCHOLTENHAVE
B07 NOORD DEURNINGEN
B00 LATTROPER STRAAT
B03 VENWEG
B01 NICOLAAS-STICHTING
B02 DORPERMEIEN
B05 KAMPHUIS
B08 LOSSER
0
5
10
15
20
25
DR
S
B
S
C
S
C
D
S
B
T
L
A
DR
LEGEND
Col. 1: material
Gyttja
Silt
Gravel
Peat
Clay
Sand
Col. 2: additions
moderate
high
peat content
clay/silt .
sand .
gravel .
Col 3: lime content
moderate
high
All columns:
disturbed / no core

beds are usually strongly calcareous, especially in the lower part of the unit. Nevertheless, limeless clastic beds also may occur.

The top of the Tilligte beds is marked by a usually erosional transition to the overlying unit (either the Beverborg Member or the Singraven Formation). The lower boundary is placed at the appearance of the first bed containing organic matter, or the first silt/clay bed, above the Dinkel Member.

North of Denekamp a complex of thicker and more continuous silt and clay beds is found near the base of the Tilligte beds which is referred to as the 'basal clays'. Further detailed subdivision of the Tilligte beds is not feasible, as most beds are of local significance only (Vandenberghe & Van Huissteden, 1989).

III.3.3.3.2. Puntbeek sands.

A Middle Pleniglacial facies without silt and peat beds also occurs in the Dinkel valley, as a lateral equivalent of the Tilligte beds. It consists of an alternating sequence of coarse and finer, often silty sands. These sands occur in the eastern part of the Dinkel valley and on the western valley margin south of Denekamp. Type sections are the Lattrop-Denekamp and Beverborg sections and the De Poppe exposure (par. IV.2.3,4). Apart from the absence of silt beds and organic matter the sands show the same characteristics as the Tilligte beds: lime-rich, greenish-gray colours, and similar mineralogy (par. V.1). These deposits are also genetically related to the Tilligte beds. This sand facies of the Mekkelhorst Member will be referred to as the Puntbeek sands.

III.3.3.4. Beverborg Member.

The Beverborg Member comprises the former 'Older Coversands I' and 'Beuningen complex' or Beuningen gravel bed' of the Lutterzand Member, as defined by Van der Hammen (1971). Furthermore, coarse fluvial sands are included which overly the Mekkelhorst Member and interfinger with the 'Older Coversands I'.

The reasons why these units are combined here into the Beverborg Member, are their strong lithological contrast with the underlying Mekkelhorst Member, and their apparent genetical relation expressed by lateral interfingering. The base of the Beverborg Member is marked by a sharp, generally erosional transition to the Tilligte beds, with a very striking change in colour, organic matter content, lime content and grainsize. The Beuningen gravel bed is located at the top of the Beverborg Member (fig. III.2). It often shows a gradational transition to the usually underlying Older Coversand I or Holt sands which is an argument in favour of inclusion within the new unit. The Beuningen gravel bed is a very distinct stratigraphical marker occurring throughout the Netherlands, Northwest Germany and Belgium (e.g. Van der Hammen et al., 1967; Zagwijn & Paepe, 1968; Van der Hammen, 1971; Vandenberghe & Gullentops, 1977; Kolstrup, 1980; Vandenberghe, 1985; Meyer, 1986).

Interfingering of the Older Coversands I with coarse fluvial sands has been demonstrated in an exposure along the Dutch-German border (Holt exposure, Van Huissteden et al. 1986a; Vandenberghe & Van Huissteden, 1988, fig. III.4). Also in the nearby Lutter-

zand exposure gradual transitions of coarse fluvial sands towards Older Coversands I occur, and lenses of coarse sands are found within the Older Coversand I. The same facies relations occur in the Dinkel canal section (Wijmstra & De Vin, 1971). A borehole section (Beverborg section, par. IV.2.4) demonstrates the correlation between the Holt sequences and the sequence in below the Older Coversand II in the Lutterzand section.

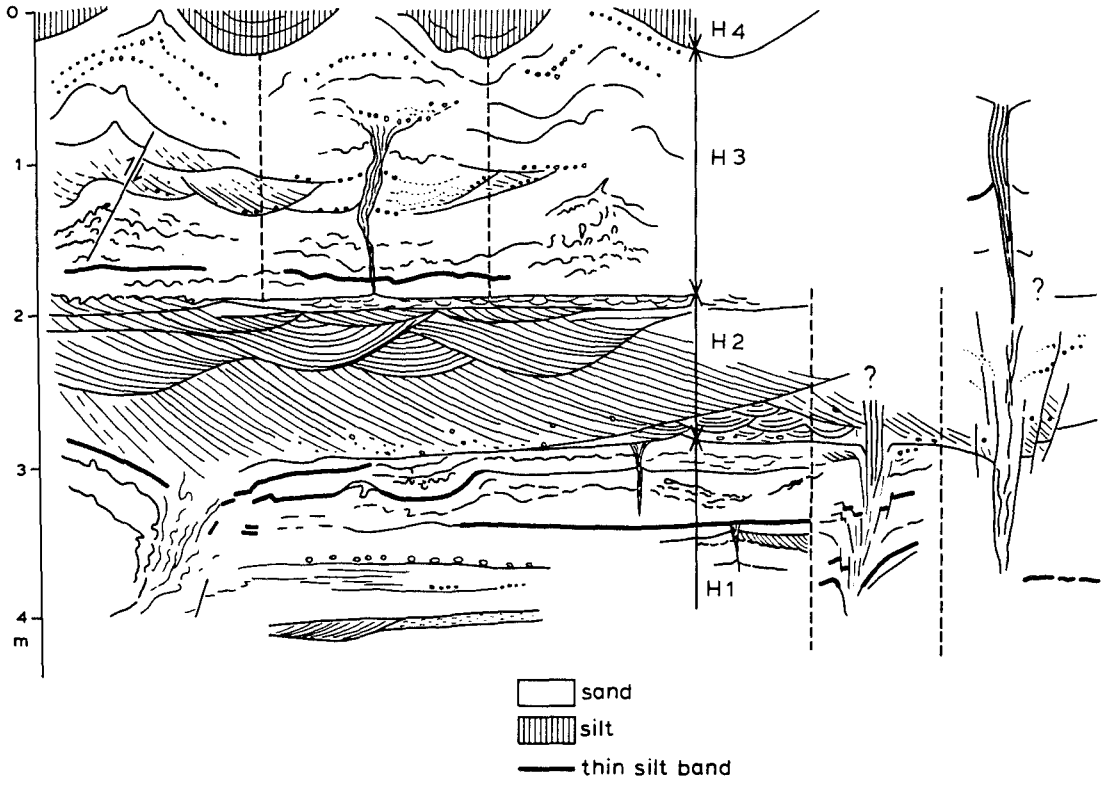

Figure III.4. Composite section showing stratigraphy and sedimentary structures of the Holt sand pit (location see fig. IV.1.).

Van Huissteden et al. (1986a) have argued for a Late Pleniglacial age for the Beverborg Member. In all sections this unit overlies the Mekkelhorst Member which has been radiocarbon dated with ages up to 27 ka (par. IV.2-4). Age estimates for the Beuningen gravel bed range between 14 and 19 ka (Kolstrup, 1980; De Gans, 1981). The abundant occurrence of ice-wedge casts throughout this unit points to a correlation with the Weichselian cold maximum in the Netherlands. Previously, coarse fluvial sands at the base of the Lutterzand exposure which are lithologically similar to the coarse fluvial sands in the Beverborg Member, have been assigned a Middle Pleniglacial age and have been correlated with the Mekkelhorst Member (Wijmstra & Schreve-Brinkman, 1971). This has been based on a palynological dating of an intercalated sandy silt bed. The palynological dating is contradicted by radiocarbon datings in the Beverborg section (par. IV.3.4; Van Huissteden et al., 1986a), and also lithological similarity points to correlation of these sands with the Beverborg Member.

General characteristics of the Beverborg Member are: absence of organic matter; fine to coarse sand; silt beds are rare. Frost fissures and ice-wedge casts which may be of the syngenetic type occur throughout the member. The colour of the sand is not greenish, and lighter than that of the Tilligte beds. The sand is

almost always limeless. The heavy mineral spectra show a decrease of hornblende, accompanied by an increase in garnet with respect to the underlying deposits (par. V.1).

The Older Coversand I (or Holt sands, Van Huissteden et al., 1986a) are fine, usually silty sands in which thin gravel strings may occur. Compared to the typical 'coversands' of the Lutterzand Member s.s. (Older Coversand II), the Holt sands are often markedly ill sorted, as a consequence of more frequent fluvial reworking. Often the Holt sands show a typical pattern of subvertical joints, described by Vink & Sevink (1971) as 'vertical platy structure'. Immediately below the Beuningen gravel bed the sediments are usually strongly cryoturbated (Van Huissteden et al., 1986a). Also traces of soil development may be found in this case (Beuningen soil, Vink & Sevink, 1971).

The coarse fluvial sands (or 'Beverborg sands', Van Huissteden et al., 1986a) are usually rich in gravel in upstream locations south of Denekamp. They exhibit sedimentary structures pointing to a fluvial channel origin, such as crossbedding, and various kinds of ripple cross-lamination. Vandenberghe & Van Huissteden (1988) have shown the strong genetical relation between the coarse fluvial sands and the Holt sands. The Holt sands are interpreted as an overbank facies of the river which deposited the coarse sands. In this overbank environment aeolian sedimentation alternates with surficial fluvial reworking by overbank flooding. Also Wijmstra et al. (1971) note the presence of a 'niveo-fluviatile' component in the Older Coversand I.

The Beuningen gravel bed may be composed of several gravel strings. In that case the lower strings usually have been influenced by cryoturbatic deformations, while the uppermost string always truncates the cryoturbations. In the Lutterzand section the gravel strings grade into shallow, gravel-rich channel fills (Wijmstra & Schreve-Brinkman, 1971).

The Beverborg-Gildehaus section (fig. III.5), combined with the nearby Lutterzand exposure (Wijmstra & Schreve-Brinkman, 1971) and the Holt exposure (Van Huissteden et al., 1986a; Vandenberghe & Van Huissteden, 1988; fig. III.4) serve as type localities for the Beverborg Member.

The Beverborg Member varies strongly in thickness; for instance at the location of the Holt exposure, the sequence is at least 5 m thick, while in the Tilligte basin it is often considerably less (< 2 m). Interfingering of coarse fluvial sands and Older coversand I-type sands occurs where the Beverborg Member is thick and well developed. The classical sequence of 'Older Coversands I' overlying the coarse fluvial sands is more common in locations where the Beverborg Member is thin. In the Hengelo basin, comparable sediments are almost absent (Zagwijn, 1974; par. VI.2.1).

Figure III.5 (next page). Facies distribution within the Beverborg Member, in a valley cross section south of Denekamp. See fig. IV.1 for location. Arrows indicate locations of borings, depth relative to Dutch O.D. Squares = sands dominantly coarser than ca. 210 µm by field estimate (coarse fluvial sands); dots = finer sands (Holt sands or Older Coversand I); broken lines = strongly silty sands (Holt sands). M = disturbed soil, S = Singraven Formation, C = Wierden + Lutterzand Member s.s. ('coversands'), T = Tilligte beds.

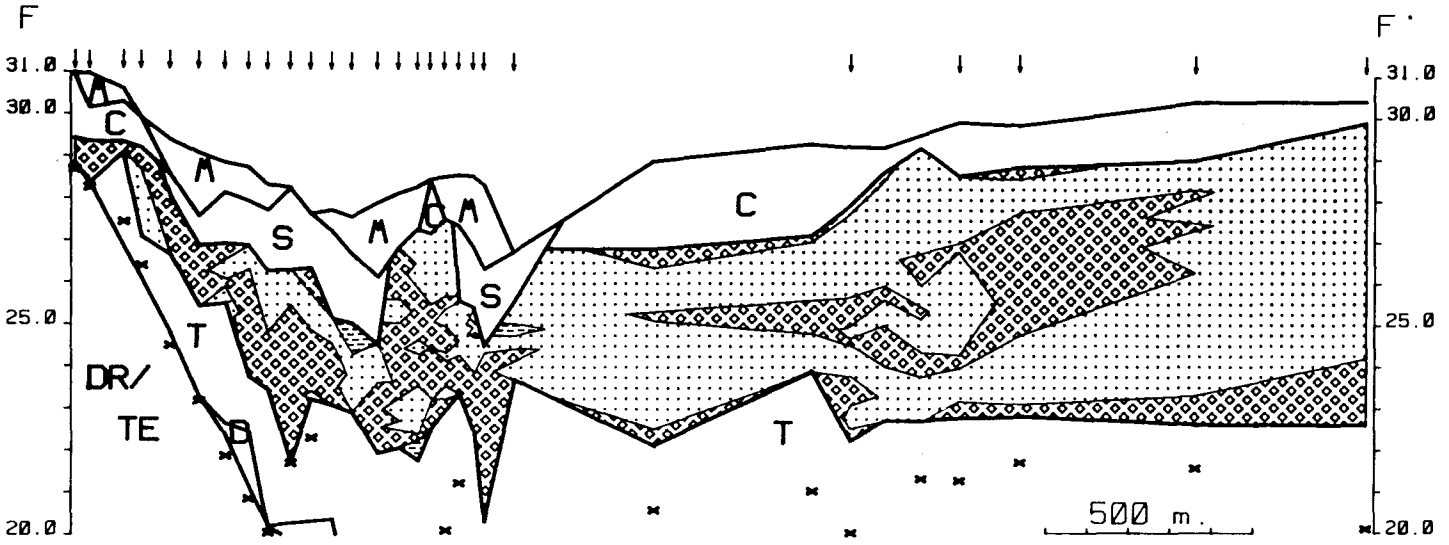
F
F'
31.0
30.0
25.0
20.0
C
M
S
T
DR/
TE
500 m.

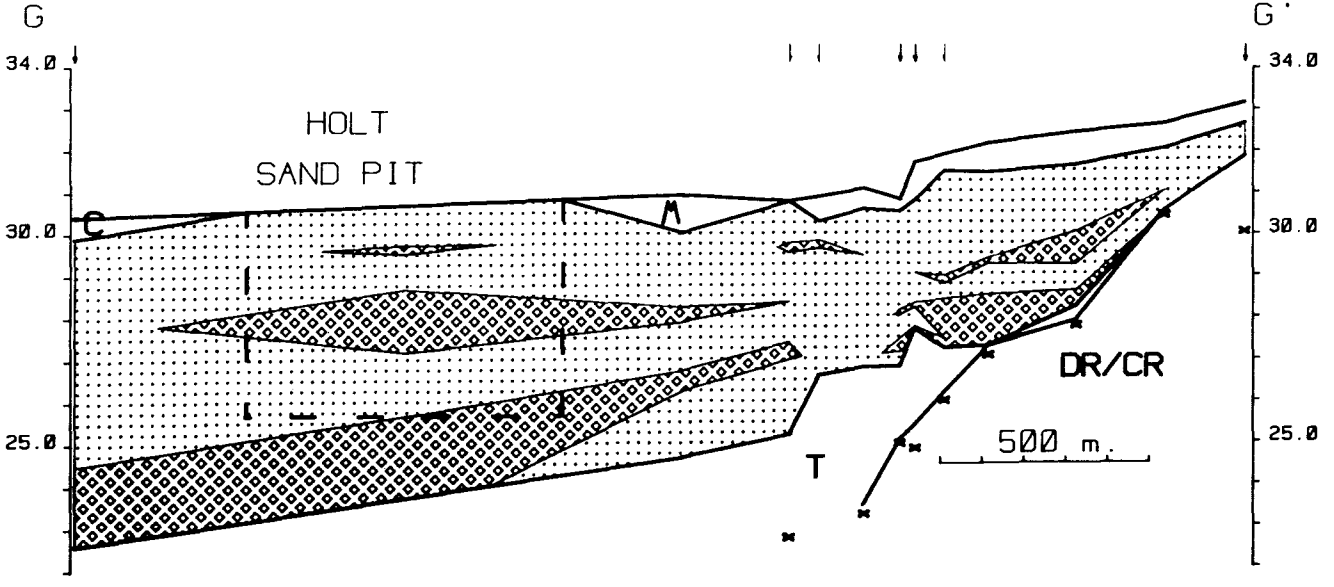
G
G'
34.0
30.0
25.0
HOLT
SAND PIT
C
M
T
DR/CR
500 m.

The transition from Mekkelhorst towards Beverborg Member is a transition between entirely different types of river deposit (Van Huissteden & Vandenberghe, 1988). The Mekkelhorst Member has been deposited by low width/depth ratio channels on a marshy alluvial plain while the Beverborg Member represents braided river and fluvio-aeolian deposits. The transition itself is accompanied by erosion of older Mekkelhorst Member deposits in most localities, although deep fluvial incision has been absent. Most likely, the erosion has been accomplished by avulsive channel belt displacements which have accompanied the change in river morphology. At the top of the Beverborg Member two distinct topographical levels occur which are interpreted as terrace levels. On the higher terrace the coversand-type sediments are thickest, beneath the lowest terrace fluvial sediments dominate. Both levels do not differ much in age as the higher level probably represents an overbank environment of the river on the lower level.

III.3.3.5. Lutterzand Member sensu stricto.

In this study the 'Lutterzand Member' is restricted to the 'Older Coversands II' of Van der Hammen (1971), and will be designated as Lutterzand Member sensu stricto. The Lutterzand Member in the original definition by Van der Hammen (1971) is referred to as 'Lutterzand Member sensu lato'. The Lutterzand section is the type section of this unit. The Lutterzand Member s.s. overlies the Beverborg Member (fig. III.2). In the Lutterzand section it is either exposed at the surface, or overlain by younger aeolian sands (Wierden Member). The age of the Lutterzand Member s.s. is Late Pleniglacial.

The Older Coversand II is a lithologically distinct unit which consists of horizontally bedded fine to medium sands. Lenses of very fine gravel also may be found. It occurs as a more or less continuous cover of variable thickness on the other units. The Older Coversand II and stratigraphical equivalents are of widespread occurrence in Northwest Europe (Schwan, 1988a). The top surface displays a very gentle undulating relief, locally more marked ridges may occur. Generally it is agreed that these sands are of aeolian origin, structures pointing to running water are rare. Schwan (1988b) describes in detail the sedimentary structures and genesis. In the Lutterzand section which is situated along the valley axis, climbing current ripple lamination has been found locally, indicating reworking by water. Outside the basin, where the substratum occurs at shallow depth, the Lutterzand Member s.s. and the Wierden Member are usually the only significant representatives of the Twente Formation.

III.3.3.6. Wierden Member.

The Wierden Member has been defined by Van der Hammen (1971). Type sites are in the surroundings of Wierden and the Usseler Veen (Van der Hammen, 1971; Van Geel et al., 1989). The Wierden Member consists of aeolian sands. These are generally coarser, with a lower silt content, than those of the Lutterzand Member s.s. The Wierden Member is of Late Glacial age (Van der Hammen, 1971; Koster, 1982). Peat and silt beds, dating from the Bølling and Allerød Interstadials occur locally (Van der Hammen, 1971). Fluvial sediments of Late Glacial age also have been included in the Wierden Member (Van der Hammen & Wijmstra, 1971). Alterna-

tively, these sediments may be included in the Singraven Formation (see below). The distribution of the Wierden Member is patchy. It occurs as low, gently sloping dune-like forms throughout the valley. The dunes locally have dammed earlier river channel courses (Van der Hammen, 1951).

III.3.4. Singraven Formation.

The Singraven Formation consists of fluvial channel and floodbasin deposits: sand, silt, clay, gyttja and peat. The unit has been introduced by Van der Hammen (1971). Type site is the Singraven estate near Denekamp. The Singraven Formation occurs either as fluvial incision fills or as surficial clay and fen peat covers in low-lying areas. The preceding fluvial incision phase is of Late Glacial age (Van der Hammen & Wijmstra, 1971). This fluvial incision phase is of widespread occurrence in the Netherlands and western Europe (e.g. De Gans, 1981; Vandenberghe et al., 1984, 1987; Starkel, 1983). Several radiocarbon datings (par. IV.2.3.2) bracket the age of the maximum incision in this area between ca. 11.5 ka and 12.3 ka. The Singraven Formation sediment is usually rich in organic matter and may contain wood. Peat, gyttja and clay beds are common. Sand is often coarse with gravel concentrates. Locally, the sand mainly consists of reworked aeolian sands. Due to the high amount of organic matter the sands often have a 'dirty' appearance, but especially the larger incision fills contain clean sands. Usually the sediment is free of lime, but lime-rich material may occur due to reworking of older lime-rich units. Van der Hammen (1971) confines the Singraven Formation to the Holocene; Doppert et al. (1975) also include Late Glacial sediments into the formation. In this study the latter practice has been followed, as the fluvial sediments of Late Glacial and Holocene age may be difficult to distinguish from each other. The base of the Singraven Formation represents the (renewed) appearance of significant fluvial activity in the shape of a meandering river system.

III.3.5. Kootwijk and Griendtsveen Formations.

The Kootwijk Formation represents younger dune sands, mostly of Late Holocene age (Doppert et al., 1975; Koster, 1982). This unit occurs in the Dinkel valley mainly upstream of Denekamp (e.g. Lutterzand area). It is not found in the borehole sections.

Older maps (Van der Hammen & Bakker, 1971) indicate the former presence of large swampy areas, mainly on the higher terrace associated with the Beverborg Member. These areas are known locally under the name of 'veld'. In these areas, Holocene peat deposits of the Griendtsveen Formation (Doppert et al., 1975) did occur. According to Van der Hammen & Bakker (1971), most of the peat has disappeared by peat digging.

IV. Litho- and chronostratigraphical analysis of the Dinkel valley.

IV.1. Data collection and processing.

IV.1.1. Combination of field data into sections.

To depict the variability within the Middle Pleniglacial deposits of the Dinkel valley, synoptic cross-valley sections and more detailed borehole grids and sections have been made (fig. IV.1). The borings have been carried out with a hand auger above the water table, and below the water table with small diameter (ø 5 cm) corers, combined with light-weight pvc casing. With this equipment depths up to 11 m. have been reached. At selected sites cored borings with hydraulic equipment (ø 10 cm) have been made to depths up to 24 m. Additional data have been obtained from penetration cone soundings, made on behalf of hydrological reconnaissance (Waterleiding Maatschappij 'Overijssel' N.V., 1985).

The core descriptions of the borings have been stored in a core description database, developed at the Free University Institute of Earth Sciences (Konert & Van Huissteden, 1987). This database features graphic output of both single borehole columns and borehole sections. During the last year of fieldwork the database has been implemented on a portable microcomputer which allowed more rapid evaluation of the sections in the course of the fieldwork. This resulted in a better adaptation of the field activities to stratigraphical problems encountered in the field.

Further computer processing of borehole descriptions and penetration cone soundings has been accomplished with the help of a borehole description database written by the author. The program package facilitates highlighting of different lithological aspects of the borehole sections. Representation of the penetration cone soundings within the sections is accomplished by converting sounding graphs (or geophysical well logs) into boring columns by binning of the values into classes. Program functions are:

- Query operations in the core description data base which include the vertical (sequential) relations between layers in a boring;
- Construction and printing of borehole sections which show the query results;
- Compilation of data from the query results for statistical applications or contour plotting;
- An interface with a drawing program for the final construction of borehole sections;
- Interpolation of penetration cone sounding/ log graphs with unequal sampling interval;
- Zonation of penetration cone soundings/logs;
- Merging of soundings/logs with borings in a section;
- Cross-correlation of segments of sounding/log graphs, enabling stretch or shrink of one segment versus the other;
- Printing of sounding/log graphs.

Necessarily, the high amount of detail in the core descriptions has to be summarized to draw the sections. For the sake of legibility, lithological detail only has been shown for the Middle Pleniglacial deposits (Tilligte beds and Puntbeek sands)

which are the main subject of this study. Simplification of the core description detail within the Middle Pleniglacial deposits has been carried out by classification of the layers. The lithological categories shown in the sections within the Middle

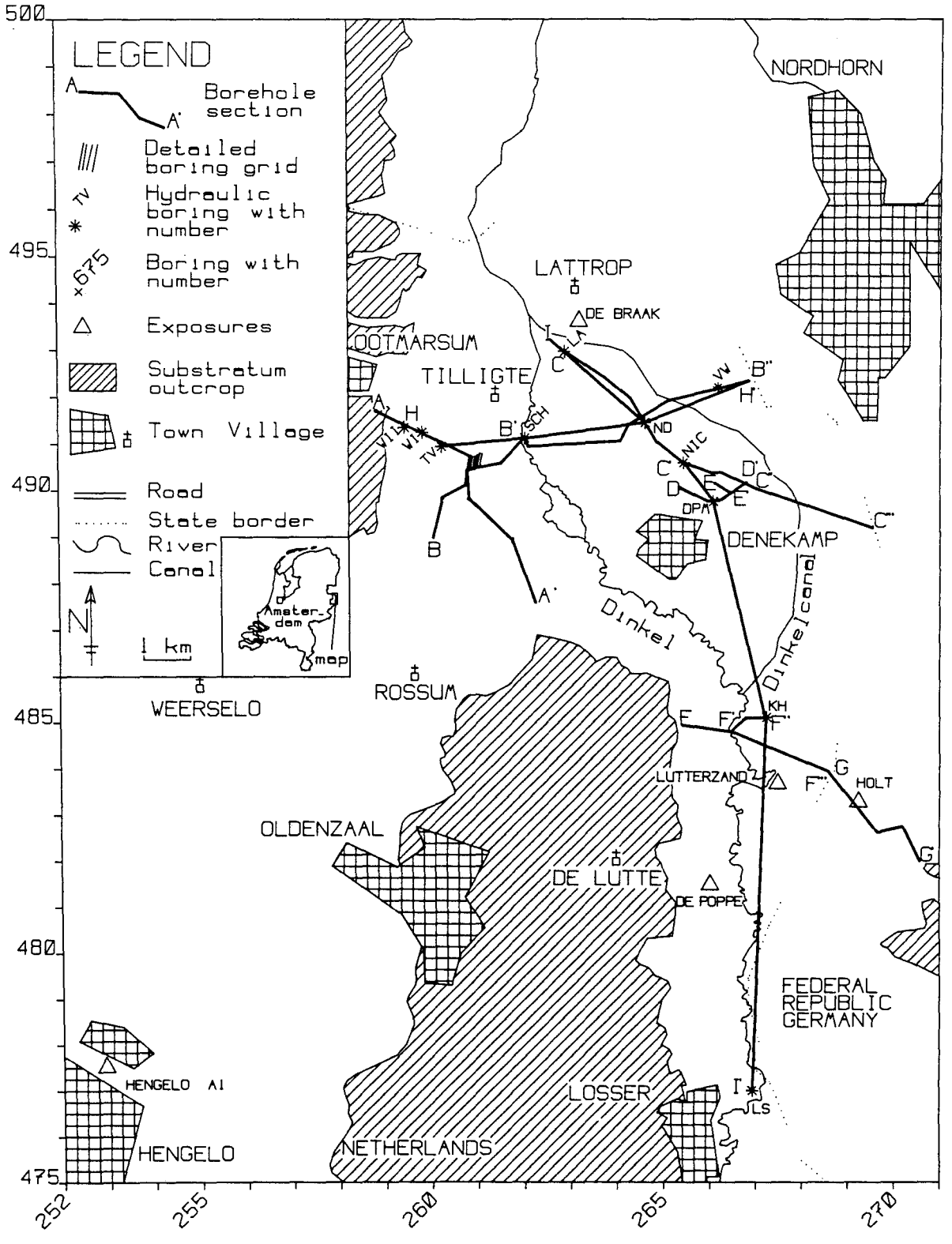

Figure IV.1. Location of borehole sections and exposures. Coordinates according to Dutch topographical maps.

Pleniglacial deposits, match with the lithofacies classes developed in par. VIII.1, based on sedimentary structures and sediment analysis. This has been achieved with the help of the query option of the program package described above. The descriptions of the lithofacies types can be translated into sets of query rules. These sets of query rules are non-overlapping (not allowed to produce layers which fall into more than one category). This is tested by treating different sets of query rules in one program run, followed by construction of a 'confusion matrix' which indicates the percentage of overlap of categories.

A short description of the relevant lithological categories (par. VIII.1) is repeated here:

A. Channel sands (medium to coarse, silt-free sands, gravel);
B. Overbank sands (fine or slightly silty sands);
C. Sand-silt intergrades (very silty/humic sand, sandy silt);
D. Floodbasin silt;
E. Floodbasin clay;
F. Peat;
G. Gyttja;
H. Intraclast beds of reworked, fragmented silt, clay or peat.

The output of the query option can be used directly as input for the graphics functions. A further step in summarization of the borehole data consists of generalization. Layers less than 10 cm thickness have been drawn separately only in cases of very distinct lithology.

The penetration cone soundings (Dutch static penetrometer tests made with electrical continuous registering equipment) have been obtained as graphs on paper. Both the cone resistance (C) and the local friction (W) have been recorded. A third graph represents the friction ratio which is the quotient of cone resistance and local friction expressed as a percentage (W/C x 100%). For computer processing, the graphs have been digitized using a digitizer table. To reduce the amount of data, only the friction ratio curve has been digitized, as this proved a fairly adequate indication for lithology in this case (Waterleiding Maatschappij 'Overijssel' N.V., 1985). Digitizing proves to be most accurate, when all minima, maxima and inflection points on the curve are digitized, instead of using fixed interval or stream mode digitizing. Afterwards, the graphs have been resampled by using linear interpolation with an interpolation distance of 5 cm.

Exact correlation of penetration cone data with the lithological categories in the core descriptions is not possible. Comparison of borings and soundings at approximately the same location yields indications on representative friction ratio values for the different lithological categories (fig. IV.2). Even in such a situation some discrepancies arise, due to short distance lithological variation. Also data from literature has been used (Sanglerat, 1972; Waterleiding Maatschappij 'Overijssel' N.V., 1985).

The friction ratio values have been classified as indicated in table IV.1. The sounding graphs cannot be converted, using these values, without any pre-processing. To avoid an undesirable large amount of thin 'layers' caused by small-scale lithological variation and instrument noise, the significant changes in the sounding graphs have to be selected beforehand by a zonation of the sounding graph. An automatic, nonparametric zonation algorithm described by Griffiths (1982), has been used. Essentially, this

algorithm searches for runs of persistent change in the log values (= unidirectional slope of the log graph). The location of the maximum slope in such a run is determined to serve as a zone boundary, as it most likely represents the location of a significant lithological boundary. Next, the log values in the run on either side of the boundary are reassigned to the values of the data points at either ends of the run. The minimum run length which is considered to be a 'persistent event' in the log graph can be determined by the user, and will depend on the bed thickness of interest. For the sections, a minimum bed thickness of 20 cm. proves to suffice. From impersistent runs the log value mean is determined, and assigned to all points in the run.

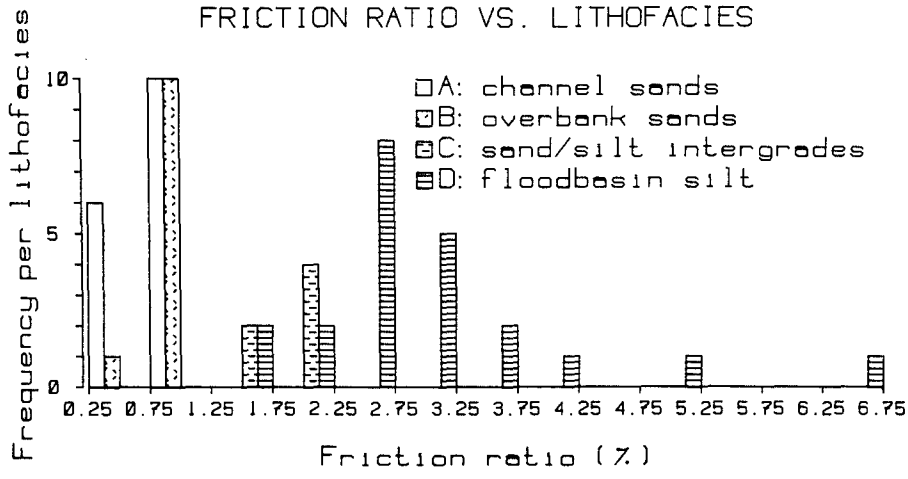

Figure IV.2. Comparison between lithofacies classes (see section VIII) in boring 661 and friction ratio values of a penetration cone sounding at the same location. Boring 661 is located in borehole section Lattrop-Denekamp (fig. IV.13).

Value range	Lithology
0.0 - 1.0	coarser sands, e.g. category A in the borings
1.0 - 1.5	finer sands, e.g. category B
1.5 - 2.0	sand-silt intergrades, e.g. category C,H
2.0 - 3.0	silt, silty clay e.g. category D,E
> 3.0	clay, gyttja, peat, e.g. category E,F,G

Table IV.1. Correlation between friction ratio values of penetration cone soundings and lithology.

Variations on this algorithm can be obtained by considering slope minima in persistent runs as lithologically significant as well. Furthermore, most long impersistent runs prove to be zones with low friction ratios which are the sands. Simply calculating the mean value over such a run would obliterate any distinction between coarser and finer sands. Therefore it has been attempted to subdivide the impersistent runs further using the 'generalized difference' measure of Webster (1973).

In summary, the following steps have been undertaken to combine the logs with the borings into sections:

1. Digitizing and re-interpolation of the friction ratio graphs;

2. Zonation of the graphs;
3. Binning of the zone values into value classes;
4. Drawing of sections in which both the soundings and borings are represented as lithological columns.

IV.1.2. Computer assisted stratigraphical correlation.

The penetration cone soundings lend themselves well to experiments with computer-assisted numerical procedures to search for matching segments. In view of the scope of this study, the automated matching approach is restricted to the relatively simple method of cross-correlation computation between segments at different lags (Davis, 1986). Prior to correlation, the soundings have been segmented using the algorithm of Griffiths (1982), in this case with a run length of 60 cm. To account for thickness variations of units, the computer program which has been developed for calculating the correlation values is capable of stretching or shrinking segments relative to each other. Based on suggestions of Shaw & Cubitt (1978), the program output consists of a contour map of correlation values with along the x and y axis stretch/shrink factor and lag respectively. The contours immediately show the best combinations of lag and stretch/shrink factors. In many cases, different combinations will be found which give high cross-correlation values. Geological considerations have to be taken into account to select the best possible stratigraphical correlation.

Bed-to-bed correlation within the Middle Pleniglacial sediments is not feasible by this method. The borehole sections show that at this level of stratigraphical detail, truncation, thickness changes, and lateral facies changes occur at distances much shorter than the distance between the penetration cone soundings. A more profitable approach proves to be the lateral tracing of units of two meters or more thickness. This has been applied to the Dinkel Member. In the sounding graphs this unit can be distinguished as a 1-4 m thick zone of consistently low friction ratio values. In most cases visual correlation of the Dinkel Member is easy. Problems arise with highly irregular graphs, containing many small spikes which obscure a possible correlation, and with locations where fine-grained beds are less well developed in the over- or underlying units (Tilligte beds and Liendert Member). Application of cross-correlation computation provided in most of these cases an acceptable criterion to determine the unit boundaries.

Illustrations of the correlation procedure are given in fig. IV.3 and 4. Fig. IV.3 shows an area just north of Denekamp. Several graphs in this area provide examples of common correlation problems. Graph 94 is a strongly 'spiky' graph, very close to the location of boring Dorpermeien (DPM in fig. IV.1). From this boring it appears that many of the spikes are caused by clay and peat intraclasts, embedded in a matrix of coarse sand. The zone which most likely represents the Dinkel Member, is found at an unusual low position in sounding 94, compared with other

Figure IV.3 (next page). Correlation of the Mekkelhorst Member, Dinkel Member and Liendert Member between penetration cone soundings in an area north of Denekamp. Penetration cone sounding 94 is situated at approximately the same location as hydraulic boring Dorpermeien (location: see fig. IV.1).

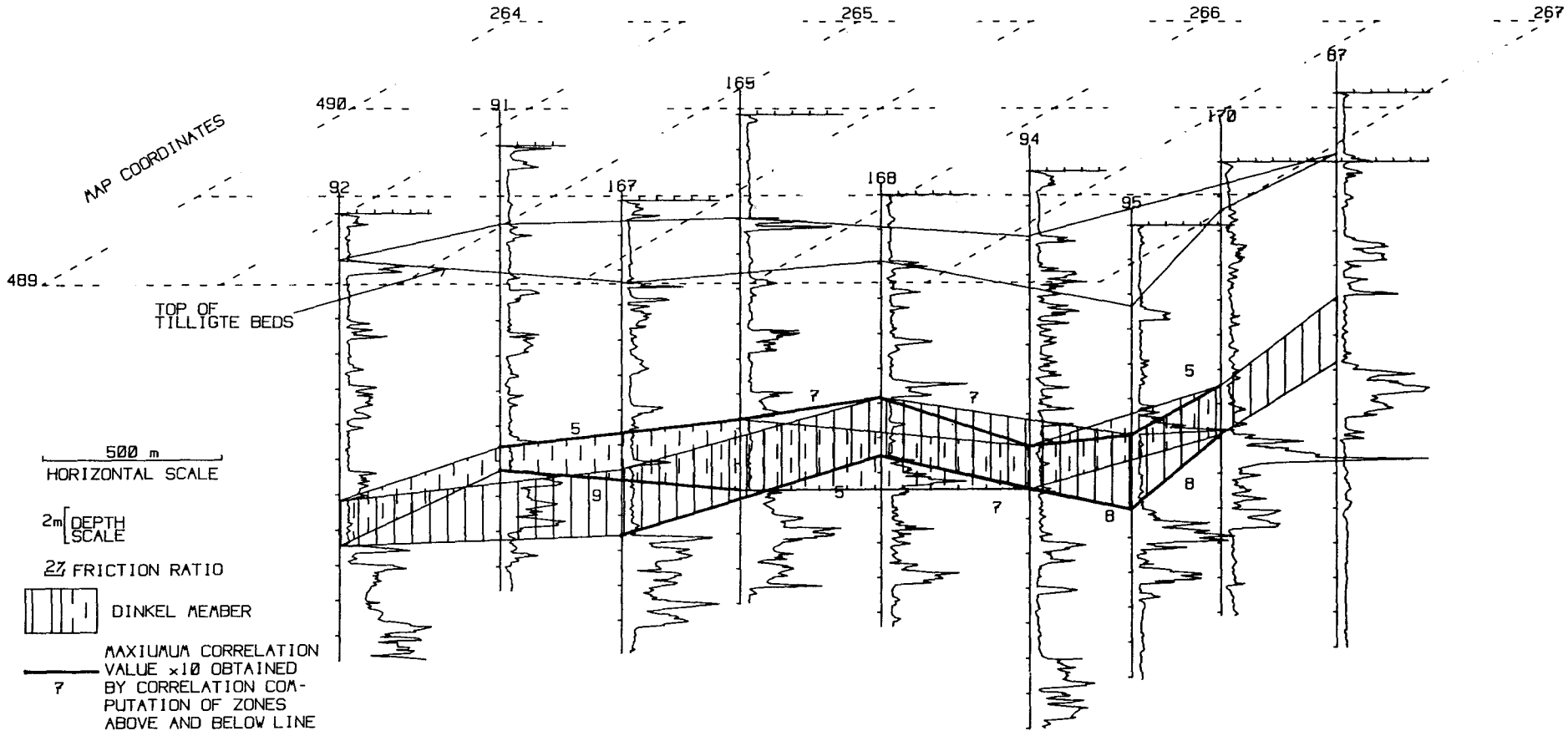
264
265
266
267
490
489
91
92
165
167
168
94
95
170
97
MAP COORDINATES
TOP OF TILLIGTE BEDS
500 m
HORIZONTAL SCALE
2m DEPTH SCALE
2% FRICTION RATIO
DINKEL MEMBER
MAXIUMUM CORRELATION VALUE x10 OBTAINED BY CORRELATION COMPUTATION OF ZONES ABOVE AND BELOW LINE
7

nearby soundings. The visually inferred Dinkel Member in sounding 168 occurs at an unusual high position.

Fig. IV.4 shows in detail the zonation and computed correlations between sounding 168 and 94. Segment 2-4 in 168 represent the Tilligte beds. Correlation with segment 5 and 6 of 94 yields as highest correlation value r = 0.4. Based on visual correlation, zone 5 in 168 and 7 and 8 in 94 may represent the Dinkel Member. This is confirmed by high r values between these zones (0.7-0.9). However, the highest value is obtained by correlation of 168/5 with 94/7 alone. Matching the zone which represents the Dinkel Member in sounding 95 (fig. IV.3, thick lines) with 94/7 also yields high r values. Therefore, correlation of only 94/7 with the Dinkel Member is most probable. This is confirmed by the data of boring Dorpermeien.

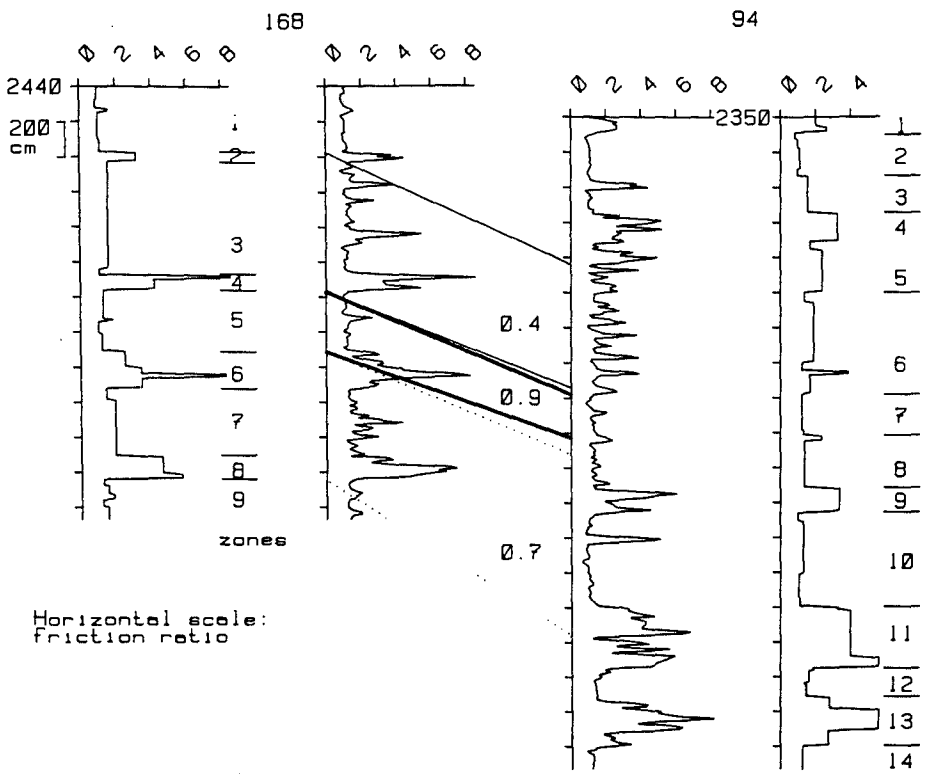

Figure IV.4. An example of cross-correlation between segments of two penetration cone soundings, showing zonation of the soundings (extreme left and right) and computed cross-correlation values (middle). See fig. IV.3 for the location of the soundings.

Next, correlation values of zones 168/6-8 with zones 94/9-13 have been computed, to test correlation between units underlying the Dinkel Member. Several combinations of lags and stretch / shrink factors yield r values of 0.7. One such combination has been indicated in fig. IV.4 (dotted lines). It suggests correlation of 168/6-8 (Liendert Member and/or Asten Formation) with 94/8-11. However, the resulting strong slope of the fine-grained beds in this case is not very likely, considering the floodbasin environment in which these beds should have been deposited. The other high correlation values suggest correlation of zone 168/7-8 with 94/8-9 only which suggests a deep erosional truncation of the equivalent of zone 168/6-8 in sounding 94. This agrees with the extremely coarse facies of the Dinkel Member in boring Dorpermeien.

Graph 170 provides correlation problems due to ill development of the silts in the Tilligte beds. In graph 91, the inferred Dinkel Member is unusually thin (fig. IV.3). In these cases, correlation values have been computed for zones above and below the problematic boundaries (thick lines in fig. IV.3). The results of correlation computation largely confirm the initial visual interpretation. In graph 170, the zone which most likely represents the Dinkel Member has been stretched and shifted downward somewhat, based on the computed correlation. The results show considerable thickness variations of the Dinkel Member, and the presence of local relief variations in the order of 8 m at its base.

As Schwarzacher (1975) points out, statistical matching does not necessarily mean true stratigraphical correlation. Geological judgement is necessary, to decide whether a match between two segments is valid as a stratigraphical correlation which means that both segments belong to the same stratigraphical unit. This is demonstrated also by the examples above. The range of possible correlations is restricted by knowledge of the sedimentary environment and stratigraphy. For instance, in the Tilligte beds and Liendert Member strong inclinations of fine-grained beds are unlikely. On the other hand, the computed matches in the lower part of sounding 94 agree well with the local presence of a deep channel incision at the base of the Dinkel Member. This shows that computed matches indeed may assist stratigraphical correlation, in cases where visual correlation of graphs is ambiguous.

IV.2. Two synoptic sections of the Upper Pleistocene basin fill.

From the deeper borings in this study and the cone penetration soundings an east-west and a north-south section of the basin fill have been constructed, to display the thickness variations of the main lithostratigraphical units described in par. III.3 (figs. IV.5,6; location in fig. IV.1).

The base of the Upper Pleistocene basin fill shows in the N-S section a pronounced step slightly south of Denekamp. This is the transition from the Dinkel valley towards the deep glacial basin of Nordhorn. It is also the location of important facies transitions and thickness variations within the overlying units. In the E-W section (located north of Denekamp) the base of the Upper Pleistocene units gently dips towards the east.

The Asten Formation is well developed within the basin. Both thick peat deposits and fluvial deposits are present. In the valley part of the section it is markedly thinner. The Liendert Member of the Twente Formation is found both in the basin and the valley. In the basin, however, it may be somewhat thinner on the average than the Asten Formation. Thick lacustrine clays within the Liendert Member are probably confined to the basin.

The Pleniglacial deposits occupy most of the post-Saalian basin fill. The base of the Dinkel Member marks a fluvial down-cutting phase. This unit is thin throughout most of the basin. It thickens towards the east, where it occurs in a mainly aeolian facies. The thickest Dinkel Member deposits appear to occur above the step which separates the basin and the valley. It is also the approximate location of the Mekkelhorst boring described by Wijmstra et al. (1971). Possibly an alluvial fan-like situation existed here during the Early Pleniglacial at the entrance of the deeper basin. For part of the basin the basal surface of the

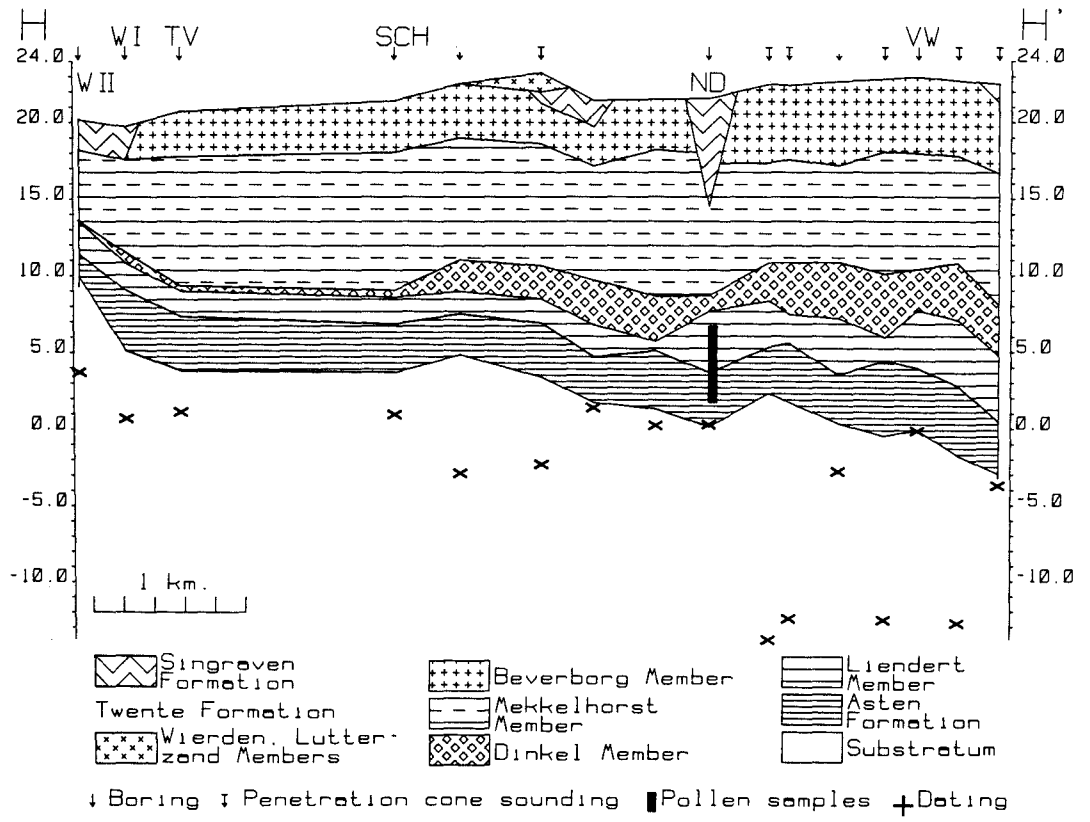

Figure IV.5. West - east section of the Upper Pleistocene valley fill north of Denekamp. Location see fig. IV.1. WI, WII: hydraulic borings Witstaartweg I and II, TV: boring Tilligte Vlierweg; SCH: boring Scholtenhave; ND: boring Noord Deurningen; VW: boring Venweg (fig. III.3).

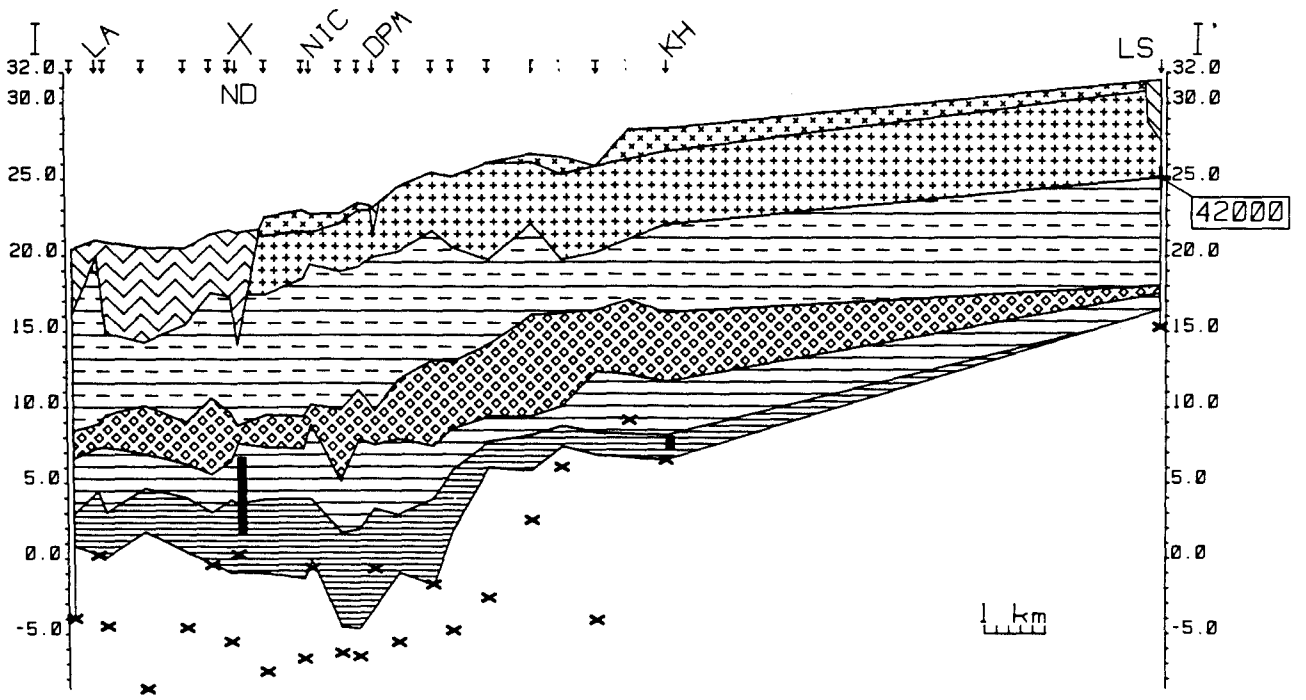

Figure IV.6. North - South section of the Upper Pleistocene valley fill. Location see fig. IV.1, legend see fig. IV.5. LA: boring Lattrop; NIC: boring Nicolaasstichting; DPM: boring Dorpermeien; KH: boring Kamphuis; LS: boring Losser (fig. III.3).

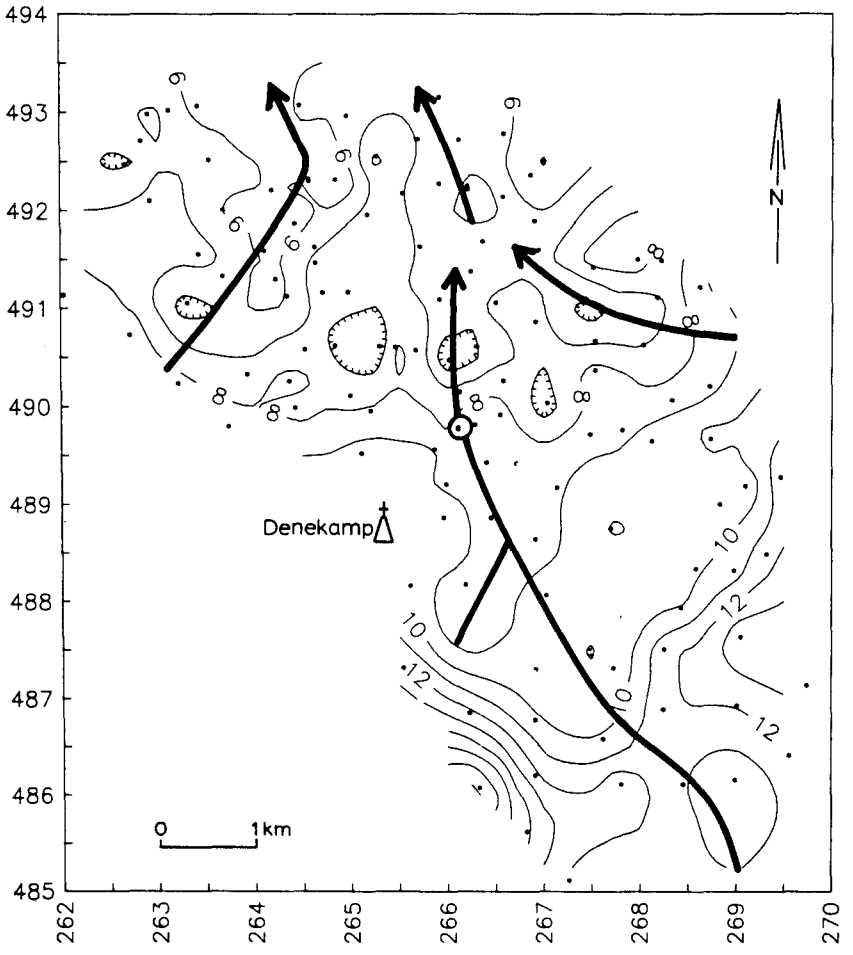

Figure IV.7. Contour lines of the top of the Liendert Member, with indication of palaeo-drainage pattern associated with the Early Pleniglacial fluvial incision phase. Circle: location of boring Dorpermeien.

Dinkel Member can be reconstructed (fig. IV.7; par. IV.1.2). It represents an erosion surface, shaped during the Early Pleniglacial fluvial incision phase. A palaeo-drainage pattern can be reconstructed from the contour lines. The drainage line entering the basin from the main valley runs across the site of boring Dorpermeien, where an extremely coarse channel facies of the Dinkel Member is found (par. IV.4.2). Another prominent feature is the step at the entrance of the basin south of Denekamp.

The Mekkelhorst Member (Tilligte beds and Puntbeek sands) is the most characteristic and also the thickest unit (up to 10 m) of the Pleniglacial sequence, especially in the basin north of Denekamp. The Beverborg Member is second in thickness (up to 6 m). Its thickness diminishes towards the basin centre, and the unit reaches its greatest thickness in the valley upstream of the basin. Clearly, the Pleniglacial has been the time during which most of the basin fill has been deposited. Average deposition rates for the Middle Pleniglacial Tilligte beds range between 0.16 and 0.35 mm/year in the areas crossed by the west-east section of fig. IV.5 (par. IX.3). In the Dinkel valley south of Denekamp, estimated average deposition rates for the Beverborg Member are locally at least 0.46 mm/year, but in the basin downstream (especially the Tilligte basin) it may be less than 0.23 mm/year locally. The Late Pleniglacial sedimentation rate

may have been somewhat higher, and in any case it is much more irregularly distributed. Possibly the Beverborg Member rivers have been incapable to distribute the larger amount of sediment, delivered along the main valley, throughout the entire basin.

After deposition of the Beverborg Member, the fluvial aggradation of the basin has come to an end. During the remaining part of the Tubantian, aeolian deposition (Lutterzand and Wierden Members) and fluvial erosion dominate. Thick deposits of the Singraven Formation occur only locally as incision fills, and do not represent widespread fluvial aggradation.

IV.3. Cross-valley sections of the Middle Pleniglacial deposits.

Below, a stratigraphical evaluation of each section will be given. Because this study is focussed on the Middle Pleniglacial deposits, only the lithological detail of the Tilligte beds and Puntbeek sands is shown in the sections.

The stratigraphical evaluation also includes a discussion of the radiocarbon datings. In par. IX.2.1 more attention will be paid to the evaluation criteria for the radiocarbon datings. Datings on peat, checked by an extract dating, are considered below as the most reliable dating results which can be obtained from this type of sedimentary environment. By propagation from these 'fixed points' an estimation of possible errors for other datings can be obtained. Appendix I contains a list of the radiocarbon datings used in this study and their possible error sources.

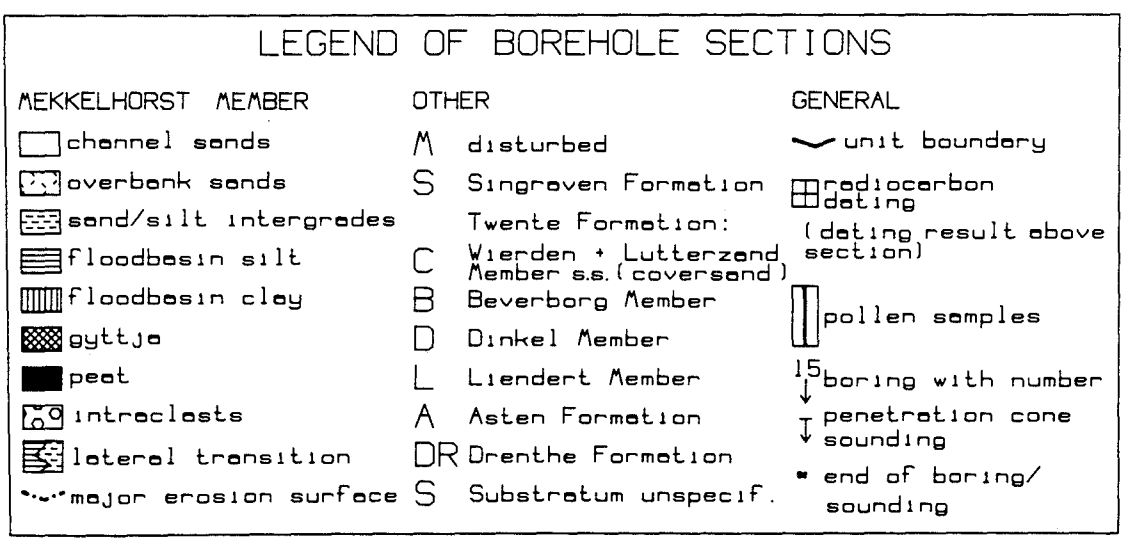

Figure IV.8. Legend of borehole sections. Lithological detail is shown only for the Middle Pleniglacial deposits (Mekkelhorst Member).

IV.3.1. The Tilligte section.

IV.3.1.1. Lithostratigraphy.

The Tilligte section (fig. IV.9) already has been discussed by Van Huissteden et al. (1986a). The section is situated close to the drainage divide between the Hengelo basin and the Dinkel valley, and runs from the ice-pushed ridge near Ootmarsum towards the ridge of De Lutte-Oldenzaal (fig. IV.1). At present more

radiocarbon datings are available from the large number of peat beds in this section. Two hydraulic borings have been added to the section.

The substratum mainly consists of calcareous clayey or silty till of the Drente Formation. Also fluvio-glacial sediment of the Drente Formation has been found, consisting of glauconiferous coarse sand near the ice-pushed ridge and finer sand and silt near the basin centre (Van Huissteden et al., 1986a). The base of the Asten Formation consists of rather coarse sand with gravel, while near the top peat and silt beds occur. The Liendert Member is comparatively thin, and dominated by peat and silt beds. The Dinkel Member occurs as a thin gravel-rich zone, at most 0.7 m thick.

Within the Tilligte beds a twofold subdivision can be made. In the western part peat beds are very abundant, and coarser sands are less common. Strikingly, peat beds are abundant also close to the ice-pushed ridge and not only in the centre of the basin; also with respect to nearby tributary valleys from the ice-pushed ridge the section occupies a drainage divide position. The peat beds are dipping rather strongly towards the basin centre (approximately 2 m/km) which might indicate the combined influence of floodplain gradient and compaction. In the eastern part the amount of peat beds strongly diminishes, and the thickness of sand beds increases.

A further stratigraphical differentiation within the Tilligte beds can be made by tracing the base of coarser sand units and other erosion phenomena within the section. In this way three erosion levels, occurring in most borings, could be outlined. This does not mean, however, that these levels present the only erosion features in the section. Erosion phenomena occur at various levels throughout the sections. The erosion levels indicated below are only those features which show a wider lateral extent and which represent clear hiatuses in many locations. They have been marked by dotted lines in fig. IV.9. In several locations the erosion has cut through older beds and is associated with channel deposits of coarse sand. The erosion levels can be traced between these channels by thinner coarse beds and intraclast levels. In such cases beds with large age differences occur closely above each other (par. IV.4.1). The erosion levels have been numbered I, II and III. The most well defined erosion level is level II. Especially in the centre of the section, it is associated with coarse channel fills of varying thickness. Erosion level III is situated higher in the section. In the western part it merges with the erosion at the top of the Tilligte beds. Level I which is the oldest, is found in the central part of the section. This is suggested by the coarse sand at the base of the borings in this reach, at a level where in boring Vlierweg silt and clay beds occur. As most borings do not reach sufficiently deep, this level cannot be traced with certainty here, but it has been found also in other sections.

Figure IV.9 (next page). Tilligte section. Location: see fig. IV.1. Legend: see fig. IV.8. WI, WII: hydraulic borings Witstaartweg I and II, TV: boring Tilligte Vlierweg. X: crossing with Laarhuis-Rammelbeek section (fig. IV.10).

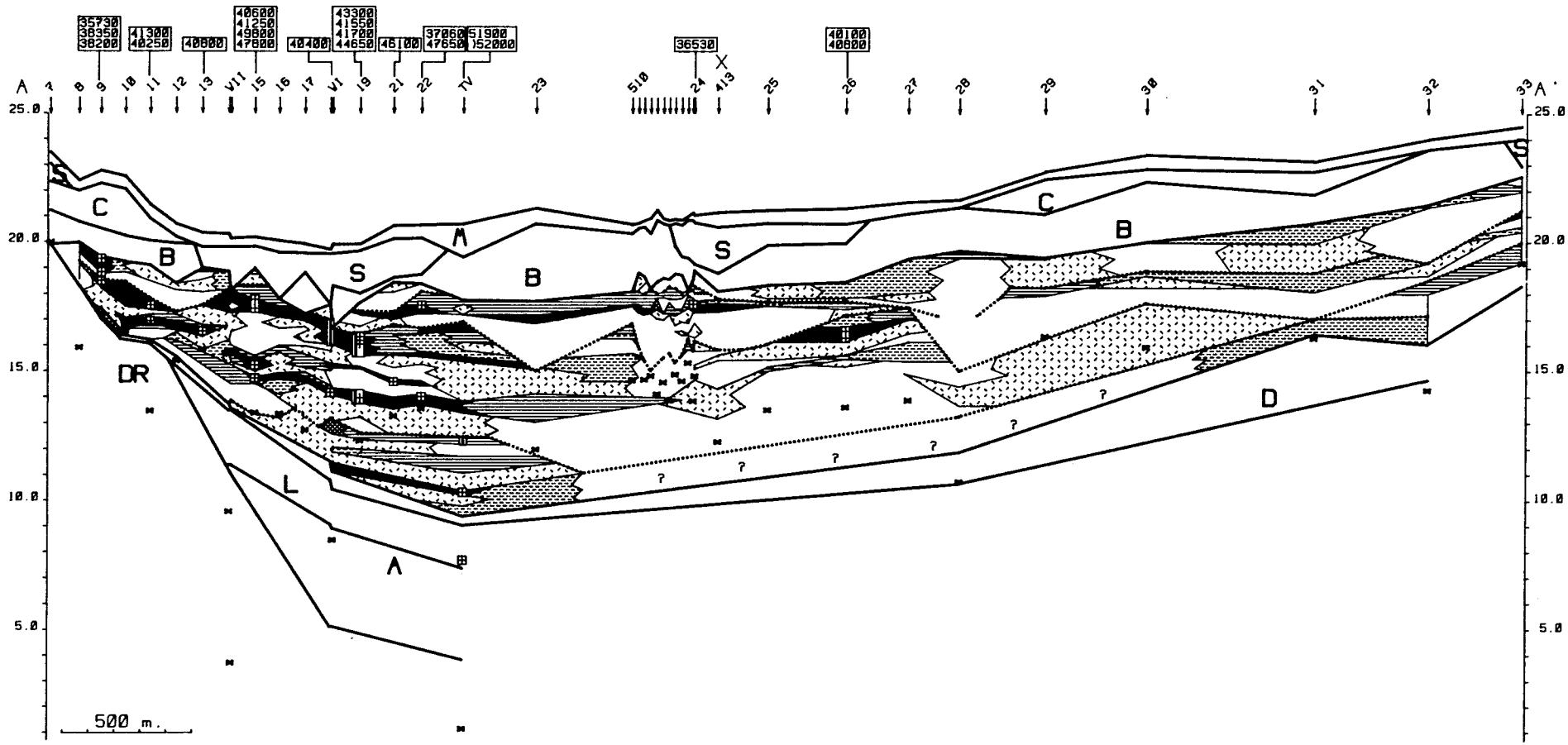
A
A'
25.0
20.0
15.0
10.0
5.0
S
C
B
M
DR
L
A
D
500 m.

The Beverborg Member is thin in the western part of the section. In the centre and eastern part of the basin, it becomes somewhat thicker. Coversands of the Lutterzand and Wierden Members are mainly restricted to the eastern and extreme western parts of the section. Singraven Formation sediments are represented by shallow incision fills which mainly consist of clay and peat, with coarse sand at the base.

IV.3.1.2. Chronostratigraphy.

Appendix I shows the datings in this section. Datings which can be considered as reliable 'fixed points' (dating on peat, of which extract and residue datings match) occur in boring 11, 13, 15, 24 and 26. Also datings in boring 19A (20 m east of boring 19, Brinkkemper et al., 1987) belong to this category. Significant deviations between extract and residue datings occur with the topmost dating of boring 9. This topmost dating, and possibly the other two closely below it therefore might be somewhat too young. Also the topmost dating in boring 15 shows a rather strong deviation between residue and extract dating, but the age of ca. 40 ka fits well with the datings in borings 11 and 19. Seemingly, stratigraphical reversal occurs with the topmost datings of boring 19A and the lowermost datings of boring 15, but a normal stratigraphical order fits in the 90 % probability ranges indicated by the standard deviations.

Further marked deviations from the framework determined by the datings above are rare. In boring Witstaart I a dating of 40.4 ka has been obtained from a peat bed which shows considerably older datings (ca. 44-50 ka) in nearby borings. Sample contamination during sampling might have occurred. Boring TV (Tilligte Vlierweg) produced two very old datings. The upper one gives an age around 52 ka which is not in contradiction with the lowermost dated peat levels (46-47 ka) from the other borings. This finite age might be an artefact, but other datings from comparable levels in other sections also frequently yield finite ages in this range. Moreover, it is supported by the presence of the Early Pleniglacial erosion level between the two datings.

The abundance of datings in the western part of the section leads to a further chronostratigraphical differentiation. The dating results show the presence of several peat/silt complexes within the Tilligte beds, each of which has been deposited within a rather narrow range of ages, and can be delineated as lithological entities as well. Between each complex ages differ significantly, while within each of these complexes age differentiation is rather poor. Age of top and bottom of such a complex does not differ more than a few thousand years. In the older complexes most of these age differences are masked by the standard error of the radiocarbon datings. The peat/silt complexes also may incorporate interfingering sand beds. This grouping of peat and silt beds by age is a local phenomenon, restricted to this relatively small area of the valley. In other sections these age groups cannot be traced.

The youngest of the peat/silt complexes is younger than ca. 32 ka. This is based on the results of the detailed grid area, and will be discussed below. The Tilligte section itself does not provide datable material in this range. In most of the Tilligte section, and also the other borehole sections, it has been

removed by erosion. It is found as sandy silt beds eastward of boring 26 in the Tilligte section.

The second of these complexes yields ages between 38 and 35 ka. The datings of boring 22 and 24 show ages around 37 and 36.5 ka for peat beds at its base, but the results of the detailed grid area show that this age may be slightly older. This complex is found between boring 19 and 26 as an approximately 1 m thick silt unit with peat and gyttja beds at its base.

The third peat/silt complex is considerably thicker, up to 2 m. Typically, ages between 40 and 42 ka are obtained from this complex. It contains the thickest peat beds of the section and includes interfingering sand beds in its western part. With exception of local erosion, it is found throughout the western part of the section, up to boring 26.

A fourth complex has ages estimated between ca. 44 and 50 ka. The uncertainty arises from the large standard deviations in this age range. In the western part of the section, it is found between boring 11 and 24, where it appears as two peat levels separated by sand beds. Older peat and silt beds cannot be grouped because of the lack of datings.

The erosion levels can be dated with the help of the ages of the silt/peat complexes. Generally the situation in the extreme western part of the section can be characterized as dominant peat/silt/sand sedimentation, interrupted at certain short time intervals by erosion. The oldest erosion level predates the 46 ka peat/silt complex, thus having an age over 47 ka at least. The second erosion level postdates the 40-42 ka complex. It has an age between 38 and 40 ka. The third level postdates the 35-38 ka complex, and is probably older than at least 32 ka, based on the detailed grid area (par. IV.4.1.2).

Besides this age differentiation, the datings show an overall decrease in net sedimentation rate (par. IX.3), especially after ca. 40 ka. There is no indication for drainage from the Hengelo basin towards the Dinkel valley, as assumed by Zagwijn (1974). The datings in this section exclude this possibility, as most of the dated beds are situated on a higher level than beds of comparable age in the southern part of the Hengelo basin.

IV.3.2. The Laarhuis-Rammelbeek section.

IV.3.2.1. Lithostratigraphy.

This section runs from a point just north of the drainage divide between the Hengelo basin and the Dinkel valley, towards the Rammelbeek at the Dutch-German border north of Denekamp, close to the present drainage divide with the Vechte river valley (fig. IV.1). The starting point of the section (the Laarhuis site) is the location of a small exposure which is the type site for the Middle Pleniglacial Denekamp Interstadial (Kolstrup & Wijmstra, 1977). The first six borings of this section are located approximately 150 m to the west of this exposure. The section crosses the Tilligte section at boring 24 and 413. The section is split up into two parts, BB' and B'B'' (figs. IV.10 and 11). The fist part has an approximate SW-NE orientation, following the axis of the Tilligte basin, the second part has a WSW-ENE orientation, roughly perpendicular to the present stream direction in the Dinkel valley north of Denekamp. In the second part the

borehole data have been supplemented with penetration cone soundings.

In the eastern part of the section the penetration cone soundings show evidence of Drente Formation sediments with generally intermediate friction ratio values. The Asten Formation is found in the three hydraulic borings incorporated in this section. It consists of sands with relatively thin peat beds at the top (boring Scholtenhave), sands overlain by a thick peat bed with wood (boring Noord Deurningen) or silt and sand beds (boring Venweg). The Asten Formation is overlain by clay, sand and peat of the Liendert Member of the Twente Formation. Thick, probably lacustrine clay beds mainly occur in the lower part of the Liendert Member.

From the start of the section up to boring Noord Deurningen, the Dinkel Member mainly consists of a rather thin gravelly zone. In section B'B'' it becomes thicker towards the east. In boring Venweg the Dinkel Member consists of nearly 4 m. of silty sands with a distinct thin bedding. All the older valley fill units are dipping very gently to the east. This tendency becomes stronger eastward from boring Venweg. It probably indicates the transition towards the Vechte valley.

The Tilligte beds are represented by the same peat-rich facies in the extreme SW part of the section, as is found in the western part of the Tilligte section. This changes quickly to a more sandy/silty facies south of the area where the Tilligte and Laarhuis-Rammelbeek sections cross. This points to the presence of a major drainage line in this area, roughly parallel to the section. From boring 24 up to boring Scholtenhave, the peat-rich facies returns again. Eastward from boring Scholtenhave, peat beds are less common. Silt beds are still abundant, however.

In this area also well-developed clay or clayey silt beds are found near the base of the Tilligte beds. This typical, well recognizable complex of fairly continuous beds will be denoted below as the basal clays. The most striking attribute of the basal clays is the generally higher clay content, compared with the overlying fine-grained beds.

The same erosion levels as found in the Tilligte section also can be traced within the Tilligte beds in this section. Level I is better developed in this section than in the Tilligte section. Level III is only identified in the southern part of the section.

The Beverborg Member increases in thickness in eastern direction. Coversand-like silty sands are well developed in this part of the section. In most of the section, however, coarse sands dominate in the Beverborg Member. Locally, coversands belonging to the Lutterzand and Wierden Members occur. The Singraven Formation consists of a number of incision fills, sometimes overlain by Wierden Member aeolian sands of the Twente Formation. A very deep incision, filled with coarse, gravelly sand is found at boring Noord Deurningen in B'B''. The other shallower incision fills contain varying amounts of silt, clay, gyttja and woody fen peat, besides sand beds.

Figure IV.10 (next page). Southwestern part of Laarhuis-Rammelbeek section. Location: see fig. IV.1. Legend: see fig. IV.8. SCH: boring Scholtenhave. X: crossing with Tilligte section (fig. IV.9).

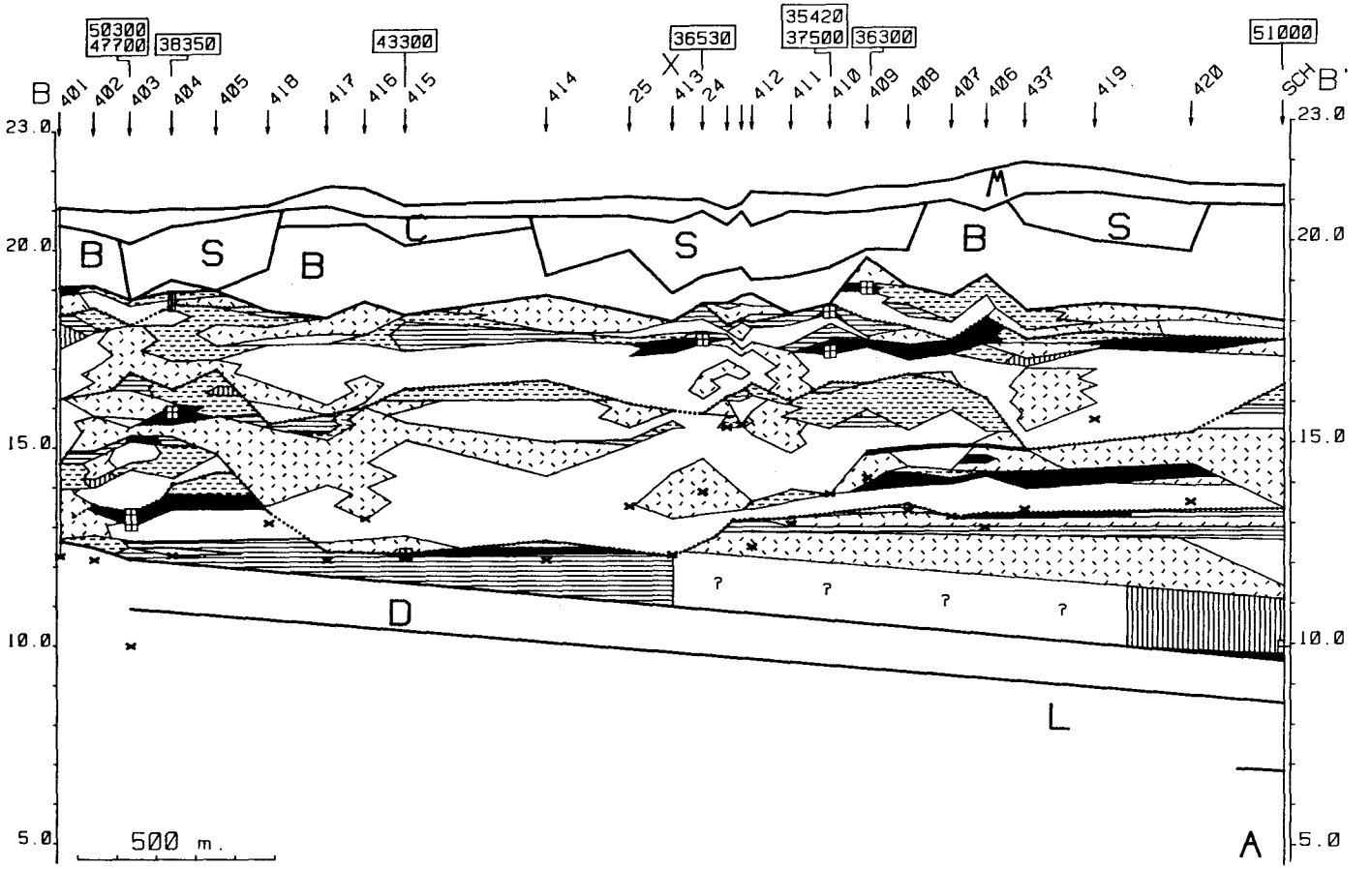
50300
47700
38350
43300
36530
35420
37500
36300
51000
B
401
402
403
404
405
418
417
416
415
414
25
413
24
412
411
410
409
408
407
406
437
419
420
SCH
B'
23.0
20.0
15.0
10.0
5.0
M
B
S
B
C
S
B
S
D
L
?
?
?
?
500 m.
A

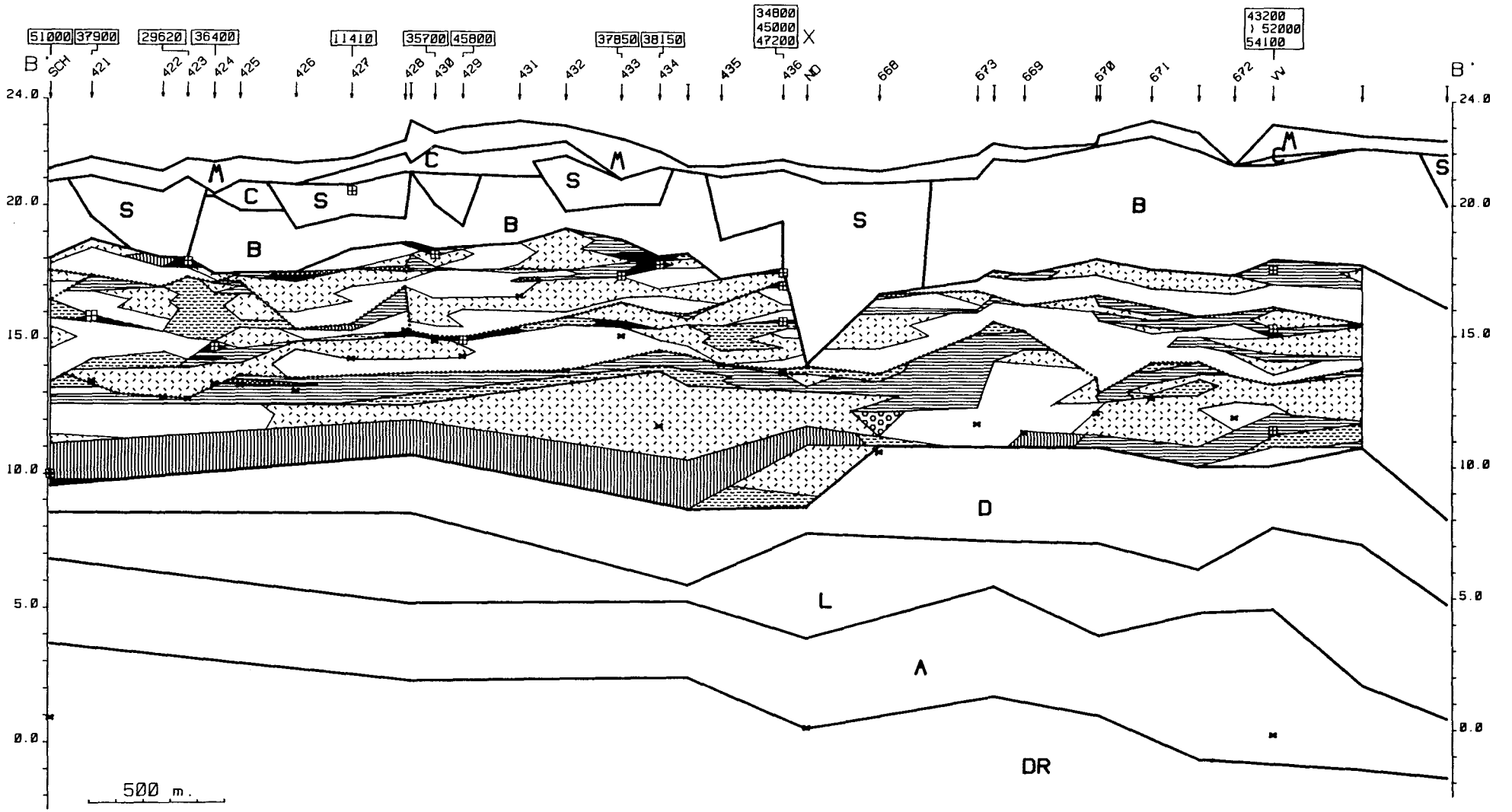
B
SCH
421
422
423
424
425
426
427
428
430
429
431
432
433
434
435
436
ND
668
673
669
670
671
672
W
B'
51000
37900
29620
36400
11410
35700
45800
37850
38150
34800
45000
47200
43200
52000
54100
24.0
20.0
15.0
10.0
5.0
0.0
S
M
C
B
D
L
A
DR
500 m.

Figure IV.11 (previous page). Northeastern part of Laarhuis-Rammelbeek section. Location: see fig. IV.1. Legend: see fig. IV.8. SCH: boring Scholtenhave; ND: boring Noord Deurningen; VW: boring Venweg. X: crossing with Lattrop-Denekamp section (fig. IV.12).

IV.3.2.2. Chronostratigraphy.

Because of the smaller number of peat beds, less radiocarbon datings are available for this section (Appendix I). Only a few extract datings have been obtained because of the generally small sample sizes. For the first part of the section (BB') comparisons can be made with the Tilligte section for an evaluation of these datings. The thin peat/silt bed at the top of the Tilligte beds in the first part of the section can be correlated with the Denekamp Interstadial peat bed found in the Laarhuis exposure. Datings on this peat bed have been published by Kolstrup & Wijmstra (1977). The age is between 30100 ±300 (GrN 4348, base of peat) and 29300 ±300 (GrN 4349, top of peat).

The datings in boring 403, 404 and 410 are confirmed by ages on comparable peat beds in the Tilligte section. The unusual old extract of the lowermost dating in boring 410 (Appendix I) might point to the presence of reworked extractable organic matter in this peat. A peat bed near the base of the Tilligte beds in boring 415 yields an age of ca. 43 ka. As the datings from boring 403 indicate, an age over 47 ka should be expected; probably the sample has been contaminated. The age of 36.3 ka from boring 409 points to presence of reworked organic matter in the sample, as datings on lower levels in nearby borings indicate. In boring Scholtenhave a thin humic clay/gyttja bed near the base of the Tilligte beds has been dated at ca. 51 ka. This fits well with a dating of ca. 52 ka from a comparable depth in the Tilligte section. Uranium-Thorium datings (Van der Wijk, 1987; par. IX.1) from the same boring do not contradict this radiocarbon dating.

Clear deviations from the Tilligte section stratigraphy occur in the borings 421, 422 and 424. The extract datings in boring 423 and 424 point to contamination, and the dating of 36.4 ka in boring 424 is evidently too young. Also the dating in boring 421 (37.9 ka) might be too young, an age of at least 39 ka is more likely.

The datings in boring 429, 430, 433 and 434 are consistent with each other, and with the Tilligte section stratigraphy. The topmost dating of ca 34.8 ka in boring 436 is probably somewhat too young, as datings on the same level in boring 433 and 434 are older, ca. 38 ka. The lowest dating of ca. 47 ka corresponds well with that in 429. Boring 427 yields a dating of 11.4 ka on woody peat below a coversand layer, it indicates the presence of a Late Glacial fluvial incision.

The last sequence of datings originates from boring Venweg on the eastern end of the section. The dating of 43 ka at the topmost bed is derived from humic silt, and might contain reworked organic matter. The second dating yields an infinite age (> 52 ka). However, its extract dating is finite, indicating an age of ca 45 ka. This suits well with ages of 46-47 ka obtained from peat beds on the same depth level in other borings. Probably the high residue age is caused by the presence of reworked organic matter. The age of 54 ka of the lowermost dating is not unlikely, considering its position close above the Dinkel Member.

IV.3.3. The Lattrop-Denekamp section.

IV.3.3.1. Lithostratigraphy.

The Lattrop-Denekamp section (figs. IV.12-14) is situated approximately parallel to the present drainage of the area, (fig. IV.1). North of Denekamp it takes a more eastern direction. In this area it is situated close to the Dinkel Canal section, described by Wijmstra & De Vin (1971). Near this former exposure the distance between the boreholes has been shortened to allow a more detailed study. Also two other detailed sections have been made in that area (par. IV.4.2).

The substratum (Drente Formation) has been reached in boring Nicolaasstichting. Its top consists of calcareous sandy clay at this location. The penetration cone soundings frequently show beds with high friction ratio values in the surrounding area, indicating the presence of fine grained glacio-lacustrine deposits. However, throughout most of the section friction ratio values in the substratum are low.

The lower part of the Asten Formation consists of sandy deposits, at the top fine grained beds and peat are prominent. In boring Lattroperstraat it consists largely of sand. In boring Nicolaasstichting silt, clay and gyttja beds are found, containing vivianite nodules near the base of the formation. The Liendert Member of the Twente Formation shows the same facies distribution as in the previous section. In all three deep borings, fine-grained beds, probably of a lacustrine origin, occur at the base. Near the top also sand and peat beds are found. The Dinkel Member mainly consists of silty sands. The borings and penetration cone soundings indicate varying thickness. In boring Lattroperstraat the silty sands are underlain by coarse gravelly sand.

In the northwestern part of the section the Tilligte beds show their characteristic silt-rich facies. The basal clays of the Tilligte beds are especially well developed as thick clay and silt beds in this part of the section. In the eastern part of the section the lateral transition from the Tilligte beds towards the Puntbeek sands is situated. Going from west to east, peat beds disappear first, silt beds become generally sandier and appear to finger out against increasingly thicker sand beds. Lithological tracing of the silt beds clearly shows that the Puntbeek sands have been deposited contemporaneously with most of the silt-peat facies. In this part of the section the Puntbeek sands probably postdate the basal clays. The Puntbeek sands mark the main drainage line of the valley (par. VIII.2.1).

The erosion levels found in the previous sections can be traced in this section as well. Especially level I is well developed, marking the top of the basal clays in the northern part of the section. Level II apparently has formed a deep incision in the central part of the section and merges with level I. This has been deduced mainly from a anomalous series of datings. Level III could not be identified with certainty, only

Figure IV.12 (next page). Northwestern part of Lattrop-Denekamp section. Location: see fig. IV.1. Legend: see fig. IV.8. LA: boring Lattroperstraat; ND: boring Noord Deurningen; NIC: boring Nicolaasstichting. X: crossing with Laarhuis-Rammelbeek section (fig. IV. 11).

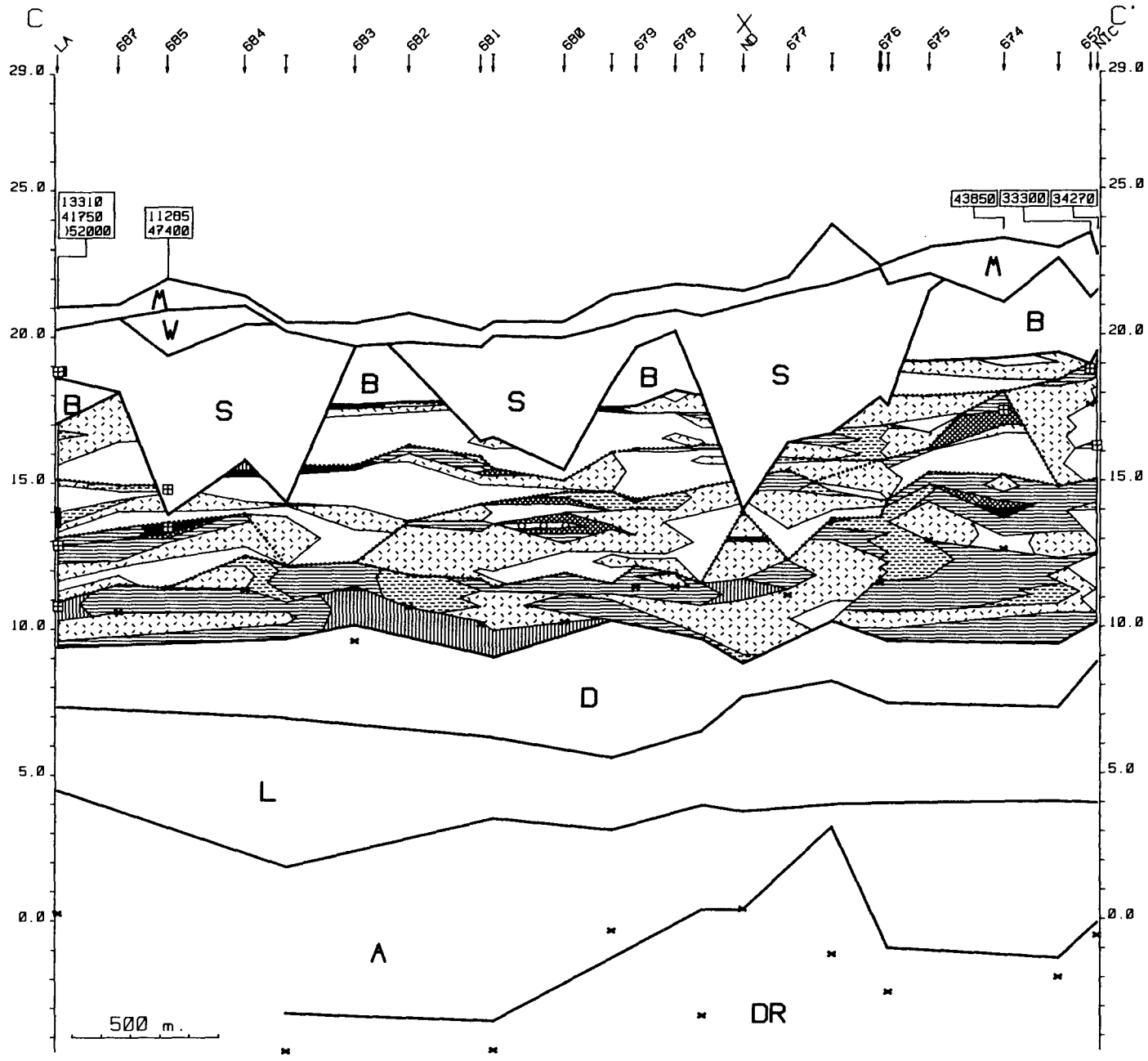
C
C'
LA
687
685
684
683
682
681
680
679
678
ND
677
676
675
674
652
MTC
29.0
25.0
20.0
15.0
10.0
5.0
0.0
13310
41750
52000
11285
47400
43850
33300
34270
M
W
B
S
D
L
A
DR
500 m.

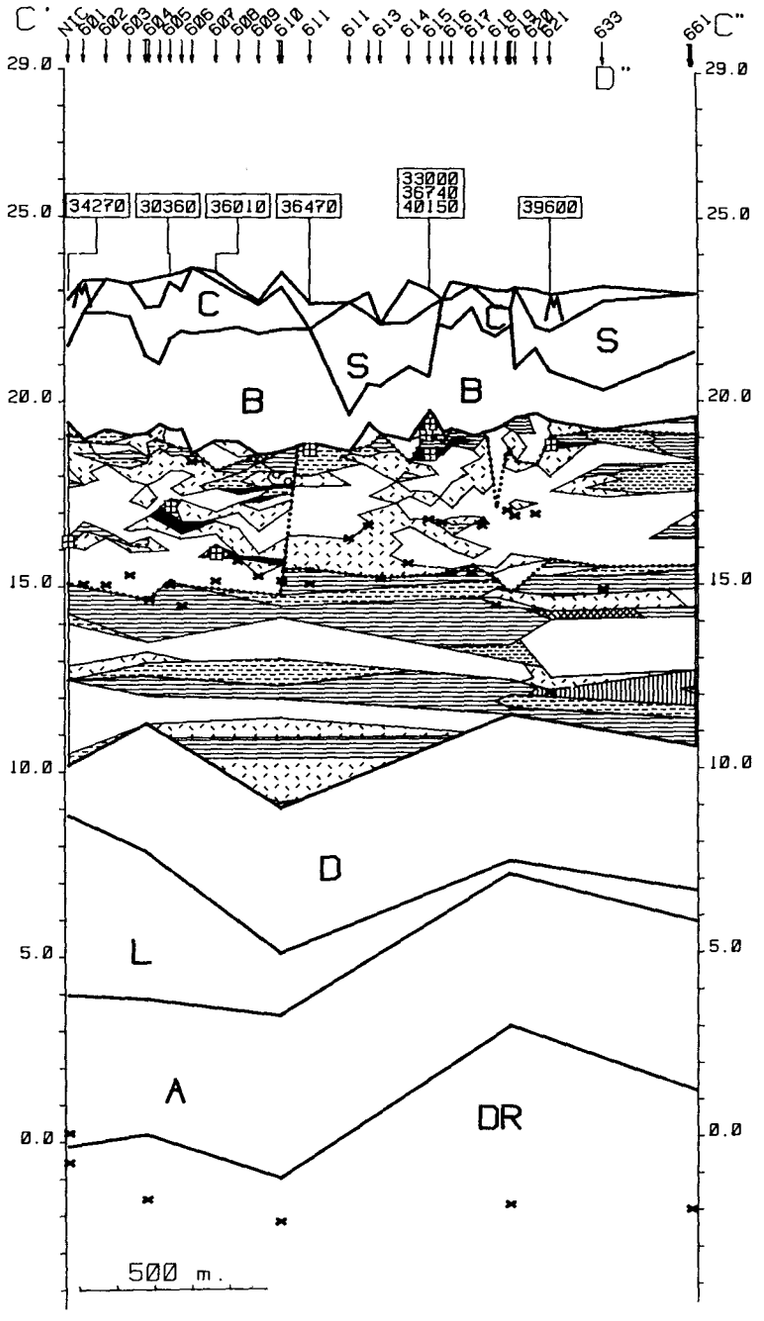
C'
NIC
601
602
603
604
605
606
607
608
609
610
611
611
613
614
615
616
617
618
619
620
621
633
D"
661
C"
29.0
25.0
20.0
15.0
10.0
5.0
0.0
34270
30360
36010
36470
33000
36740
40150
39600
M
C
S
B
D
L
A
DR
500 m.

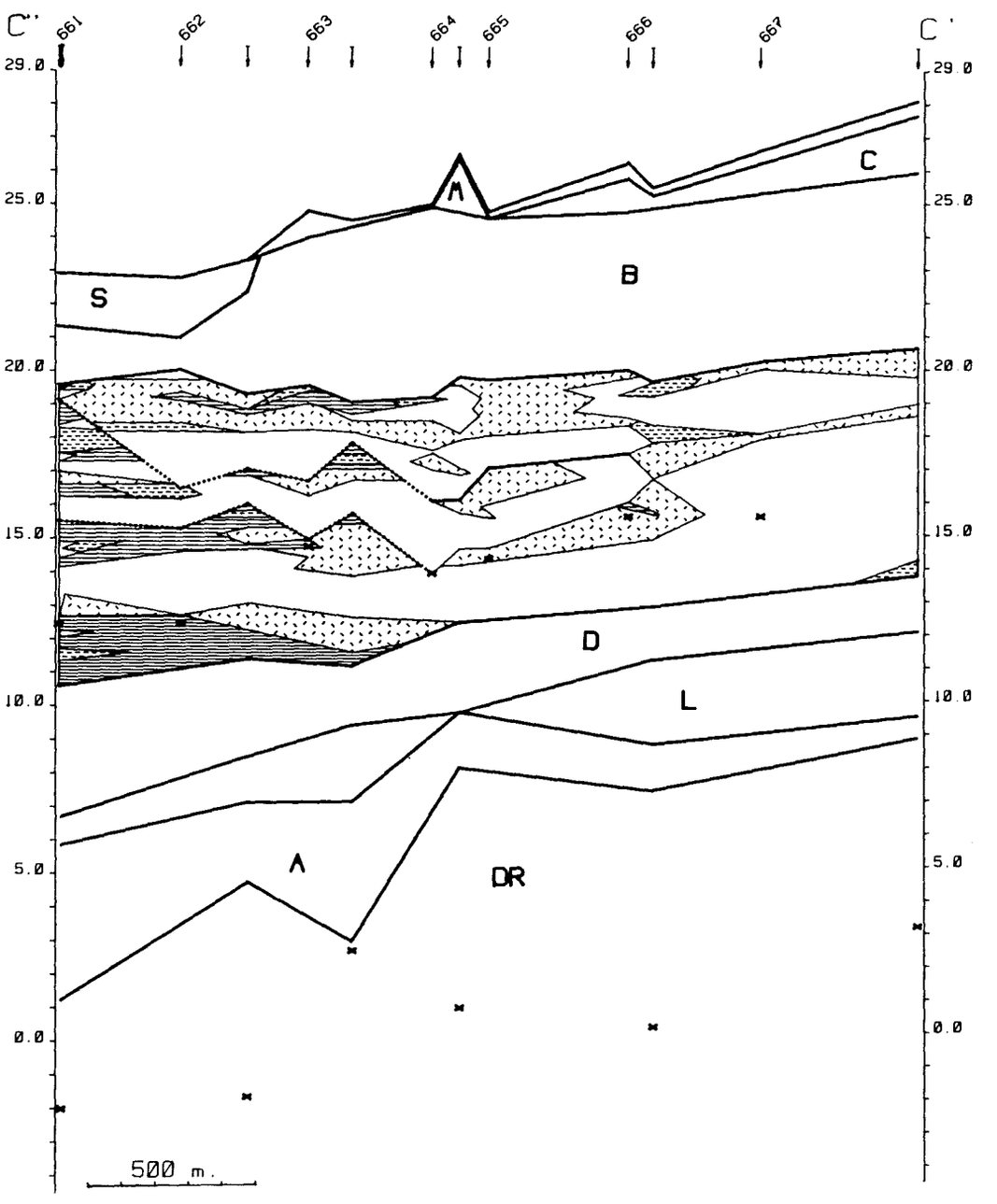
C"
661
662
663
664
665
666
667
C'
29.0
25.0
20.0
15.0
10.0
5.0
0.0
M
C
S
B
D
L
A
DR
500 m.

Figure IV.13 (previous page, left). Central part of Lattrop-Denekamp section. Location: see fig. IV.1. Legend: see fig. IV.8. NIC: boring Nicolaasstichting.

Figure IV.14. (previous page, right). Eastern part of Lattrop-Denekamp section. Location: see fig. IV.1. Legend: see fig. IV.8.

in the central part of the section there are indications for its presence. In the sandy facies in the easternmost part of the section the location of the erosion levels is uncertain.

The Beverborg Member and Lutterzand Member s.s. are ill represented in the northwestern part of the section. In the eastern part the Beverborg Member reaches a thickness of up to 5.5 m. In the northwestern part of the section deep fluvial incisions filled with Holocene/Late Glacial sediment of the Singraven Formation occur. The incision fills mainly contain coarse sand, alternating with peat, gyttja and silt beds.

IV.3.3.2. Chronostratigraphy.

Two datings indicating Late Glacial ages have been obtained from boring Lattroperstraat and boring 685 in the northern part of the section. The first dating, obtained from a humic silt bed slightly below 19 m +O.D., yielded an age of 13.3 ka (without alkali treatment). Accelerator datings on seeds from this bed performed by the radiocarbon laboratory of the Uppsala university provided ages of 12885 ±185 and 12315 ±125 (Ua 924, 925). The second Late Glacial age (11285 ±25, GrN 13403, checked by extract dating) originates from a peat bed in boring 685, at a much lower level (ca. 15 m +O.D.). It is not certain whether the peat is reworked or occurs in situ. The difference in elevation between this sample and the previous one is caused by fluvial incision during the Late Glacial. It illustrates the depth to which these incisions reach: at least 4 m at this location.

Middle Pleniglacial datings which are confirmed by extract datings, and can be used as reference points for comparison of other datings, are the datings in boring Lattroperstraat (41.75 ka age), 674, 607 and 621 (Appendix I). The first three of these are derived from gyttja's, and may show a somewhat too high age. The lowermost dating of boring Lattroperstraat yields an age over 52 ka. As it overlies the Dinkel Member, this infinite age does not contradict a Middle Pleniglacial age for the dated peat/clay bed. Deviations which point to erroneous dating results occur in boring 685 (lowest dating) and 605. The dating of 53.6 ka in boring 685 is too old, as the same bed yields a much younger age in boring Lattroperstraat. The extract and residue age of boring 605 differ significantly from each other and from datings on similar levels in nearby borings (607, Nicolaasstichting).

The datings in boring 652 to 607 (section C'C'', fig. IV.13) are consistently younger as datings on the same levels elsewhere. Especially the dating of 36.01 ka in boring 607 which is confirmed by an extract dating, indicates that these younger ages must be considered as reliable. It is further confirmed by a similar age on the same depth level in boring Nicolaasstichting. In boring 611, 615 and 621 older ages are found again at a considerably higher level. The ages in boring 615 and 621 are most likely correct.

The deviating ages in boring 652-607 most likely point to the presence of a fluvial incision fill. The age of the incision corresponds to that of erosion level II from the previous sections. Its base can be traced along the top of a thick silt bed at approximately 15 m +O.D. The eastern and western borders of this incision are lithologically less clear. The datings indicate that these borders are located near boring 674 and 611.

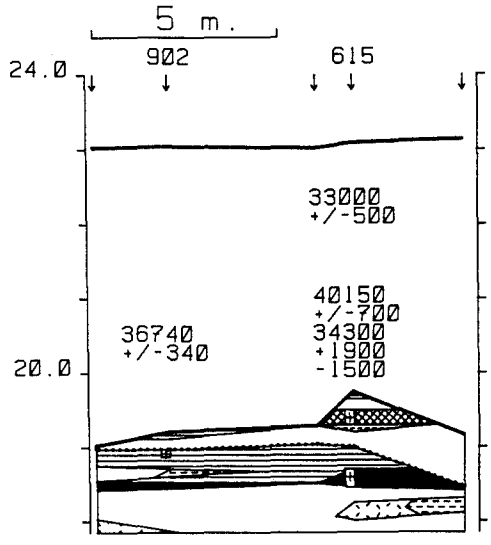

Figure IV.15. Detail of the top of the Tilligte beds near boring 615 (Lattrop-Denekamp section, fig. IV.13), with radiocarbon dating results. Short distance lateral changes are related to erosion phenomena and possibly cryogenic disturbance. Legend: see fig. IV.8.

Erosion level II can be traced towards boring 615, where three datings, located closely above each other, yield strongly differing ages. Near boring 615 several additional borings have been made to collect additional material for pollen analysis and radiocarbon dating. This short section may serve to illustrate the chronological complexity and extremely short distance lithological variation of the Middle Pleniglacial deposits (fig. IV.15).

The lowermost dating (40.15 ka) shows a significantly younger extract dating. However, correlation with boring 621 indicates that the residue age is reliable. The peat is overlain by silt, the top of which is dated as 36.7 ka in a boring 5 m to the east which is to be regarded as a minimum age. An obvious erosional hiatus is present immediately above the silt. Locally, the erosion has cut through the underlying silt and peat bed. The topmost dating in 615 yields a dating of 33 ka on a gyttja bed. The erosional hiatus represents erosion level II and possibly III as well. Strikingly, the youngest gyttja/silt bed could not be found in three of the five borings, not even in a boring 1 m west from 615. This patchy distribution may be the effect of cryoturbation, and irregular erosion associated with the base of the Beverborg Member.

Boring 615 and 621 are situated closely to the Dinkel Canal sections described by Wijmstra and De Vin (1971), where beds of Denekamp Interstadial age have been exposed. Therefore it is rather surprising, that no datings in the age range of the Denekamp Interstadial (30-32 ka) could be obtained. Only the

topmost dating of 615 approximates this age range. As shown above the erosion associated with the base of the Beverborg Member could be the main cause of this lack of 'Denekamp Interstadial' datings.

IV.3.4. The Beverborg section.

The Beverborg section (fig. IV.16) has been described earlier by Van Huissteden et al. (1986a). It is situated south of Denekamp (fig. IV.1), upstream of the region where the wide glacial basin grades into the narrower southern Dinkel valley. More recently the section has been extended towards the eastern valley edge. The section is situated close to the Lutterzand exposure described by Wijmstra & Schreve-Brinkman (1971), and crosses the Holt sand pit described by Van Huissteden et al. (1986a) and Vandenberghe & Van Huissteden (1988). Because of terrain accessibility restrictions, the section has been split into two separate parts on Dutch territory, and a third part on German territory (fig. IV.1). One hydraulic boring (boring Kamphuis) is incorporated in this section.

The substratum has been reached in the western and eastern parts of the section. It consists of till with high amounts of Tertiary clay (western part) or Cretaceous shale fragments (eastern part). The Asten Formation is found in boring Kamphuis and consists of sand with wood fragments, gyttja and peat. The pollen content of the organic deposits points to a lacustrine environment (Van Geel et al., 1986), associated with a river floodplain. In the Liendert Member the typically lacustrine facies, found in the Nordhorn basin downstream, is lacking. It mainly consists of sand with two intercalated silt beds. The Dinkel Member is coarse and rich in gravel. Other borings on the valley sides show the presence of a gravel bed, correlative with the Dinkel Member, between the substratum and deposits of the Mekkelhorst Member.

Because of the thickness of the overlying sediments only the top levels of the Middle Pleniglacial deposits could be reached in most borings. On the extreme western side of the valley silty sand is found which represents the Puntbeek sands. An exposure in a similar position shows sedimentary structures which indicate a wet aeolian to shallow fluvial environment for this type of material (par. VIII.3.1). In the western part of the section fragmentary silt and peat beds have been found, and therefore these deposits represent the Tilligte beds. Near the present valley centre thicker and more continuous silt beds occur. The sands of the Tilligte beds in this upstream location are coarser and contain more gravel than in the basin downstream. West of the Dinkel river a gradual lateral change to the Puntbeek sands occurs, similar to the facies change in the eastern part of the previous section. The Puntbeek sands prove to continue up to the extreme eastern valley edge, without a return to the more characteristic silt/peat beds of the Mekkelhorst Member. Towards the eastern valley edge only the proportion of somewhat finer, siltier sands increases. These finer sands probably represent the same depositional environment as is found on the extreme western

Figure IV.16 (next page). The Beverborg-Gildehaus sections. Location: see fig. IV.1. Legend: see fig. IV.8. KH: boring Kamphuis.

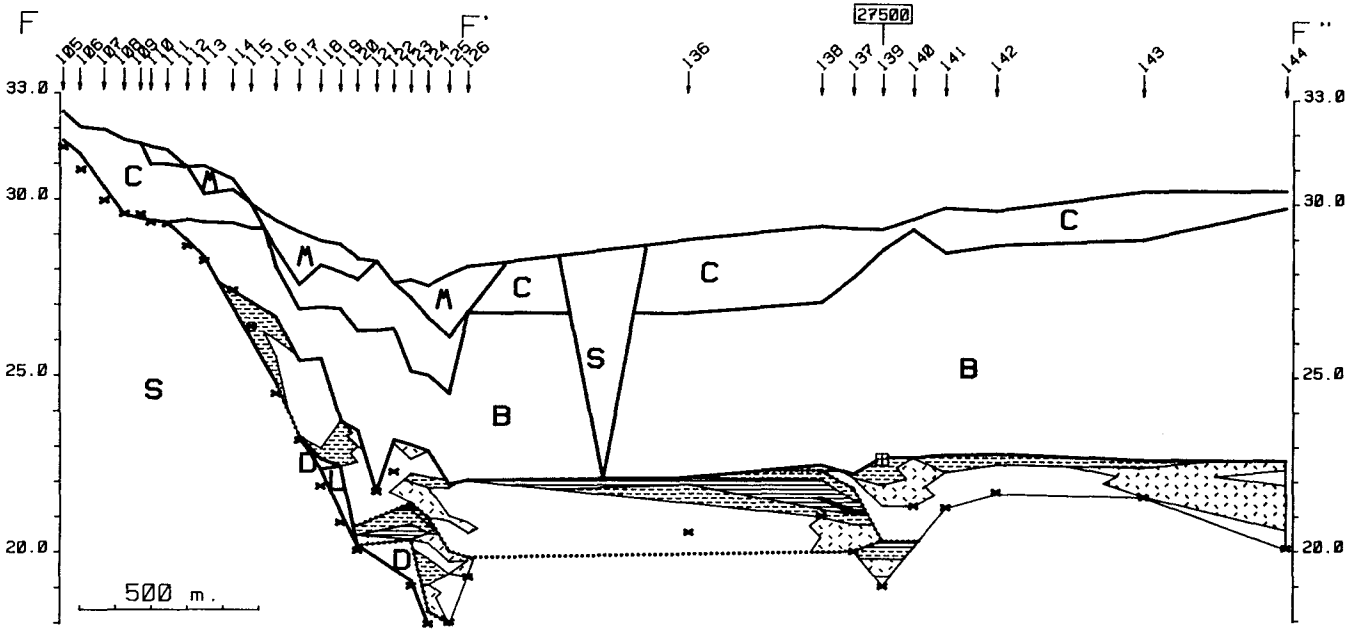
F
F'
F''
27500
105 106 107 108 109 110 111 112 113 114 115 116 117 118 119 120 121 122 123 124 125 126
136
138 137 139 140 141 142
143
144
33.0
30.0
25.0
20.0
C
M
S
B
D
500 m.

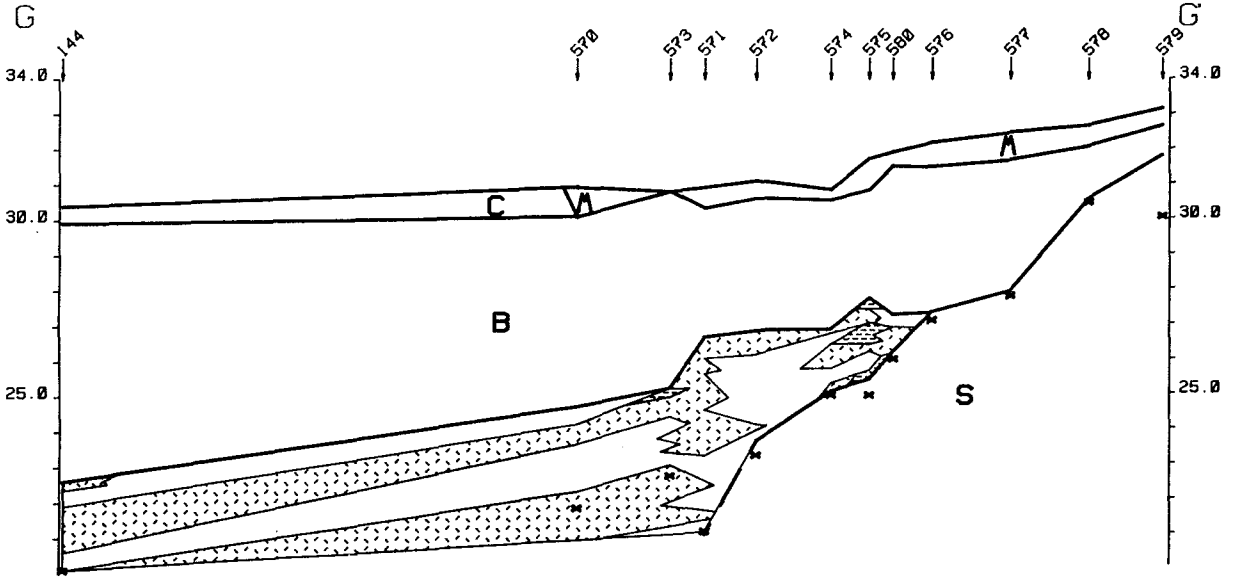
G
G'
144
570 573 571 572 574 575 580 576 577 578 579
34.0
30.0
25.0
C
M
B
S

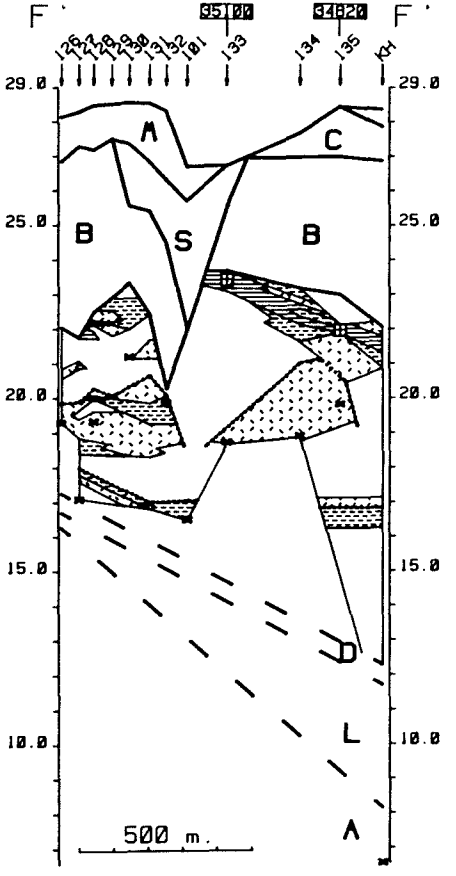
F'
F'
35100
34820
125 122 128 129 130 131 132 101 133 134 135 KH
29.0
25.0
20.0
15.0
10.0
M
C
B
S
B
D
L
A
500 m.

side of the valley. However, it occupies a larger area on the eastern valley side as is shown by section GG'.

The location of erosion levels, as found in the previous sections, is uncertain here. Only in the western part of the section possible erosion surfaces can be traced lithologically. A sandy silt bed around 17 m, in several borings overlain by coarse sands, probably marks the location of erosion level I. Higher in the section, a complex of thinner silt beds and fine sands occur, erosively overlain by coarser sands at approximately 20 m. It may correlate with erosion level II downstream. Erosion level III could be identified with more certainty; it overlies the thick silt beds in the centre of the valley.

Also the fluvial sands in the Beverborg Member are coarser than average. The Beverborg Member is very thick in this section, compared with the downstream sections. Especially in the western part of the section the erosion at the base of the Beverborg Member is very well developed. The top of the Beverborg Member shows a marked step in the eastern part of the section (at boring 139) which is masked at the terrain surface by thicker Lutterzand Member (s.s.) deposits west of this step. A similar step is visible in the western part of the section. These steps represent terrace levels associated with the Beverborg Member (par. III.3.3.4).

Boring 133 and 135 yielded datings of ca 35 ka on peaty intercalations in a silt bed between 21 and 23 m. Both datings are confirmed by an extract dating. This silt can be traced towards the east in boring 139, where it is truncated by erosion (erosion level III). The erosion level is overlain by humic silt, dated in boring 139 at 27.5 ka. Although this sample could not be subjected to alkali extraction and the figure of 27.5 ka can be regarded as a minimum date only, strong contamination at this depth is not very likely.

The datings from the Beverborg section and the previous sections clearly prove that the sands of the Beverborg Member are entirely of Late Pleniglacial age. Also the sequence found below the Lutterzand Member s.s. in the Lutterzand exposure should be placed within the Beverborg Member on lithostratigraphical grounds. However, a sandy silt bed in this part of the Lutterzand sequence has been provisionally dated as Middle Pleniglacial by Wijmstra & Schreve-Brinkman (1971) on palynological grounds. By comparison with the Beverborg section it proves that this silt is located at a considerably higher level than the dated Middle Pleniglacial beds in the Beverborg section. This silt bed therefore may be considerably younger than 27 ka.

IV.4. Detailed grid areas.

IV.4.1. The detailed grid area south of Tilligte.

IV.4.1.1. Lithostratigraphy.

At the location of the crossing between the Tilligte and the Laarhuis-Rammelbeek section, an area has been studied in detail with borings located on a grid with a minimum borehole distance of 30 m (fig. IV.17, 18, 19), to obtain a detailed three-dimensional view of the facies variations within the Tilligte beds. Especially a silt/peat/gyttja complex, occurring at a depth of 17-19 m above O.D. has been the object of study.

Due to intensive levelling of the area during reallotment operations, the stratigraphy of the units covering the Tilligte beds has been disturbed locally. In summary, the Tilligte beds are covered here by up to 2 m. of gravelly sand from the Beverborg Member, erosively overlain by the Singraven Formation. The Singraven Formation incisions locally reach the top of the Tilligte beds. From the originally present Lutterzand Member s.s. only traces could be found.

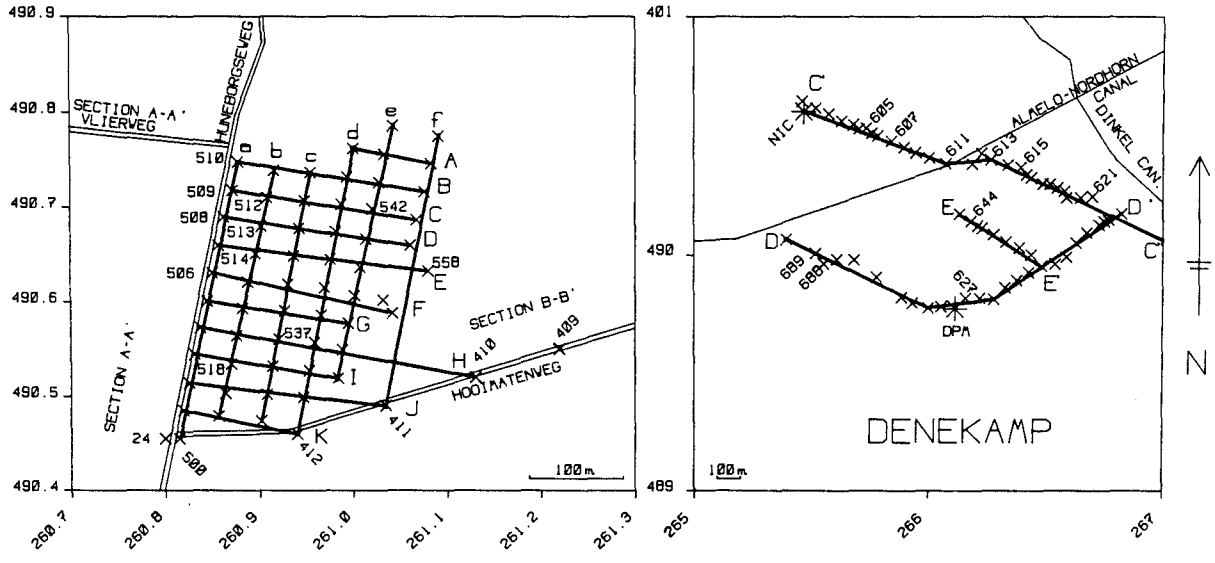

Figure IV.17. The detailed grid area south of Tilligte (right) and north of Denekamp (left), with location of the sections. Location and legend: see fig. IV.1.

Within the sampled part of the Tilligte beds two major erosion surfaces can be identified which can be correlated with the upper two erosion levels in the Tilligte and Laarhuis-Rammelbeek sections. With these levels as principal boundaries, the Tilligte beds in this area can be subdivided into four units (fig. IV.18).

The lowermost unit (DT1) is overlain by erosion level II. It mainly consists of interfingering silt and sand beds. The sands are in general rather fine and strongly calcareous. The second unit (DT2) consists of 1-2 m of mostly medium to coarse sand, with some finer intercalations. The sand is not calcareous. DT2 is overlain by a complex of silt, peat and gyttja beds (unit DT3). DT3 is overlain by erosion level III. Unit DT4 consists of intercalated sand and silt beds.

The elevation of the erosion surface II strongly varies and shows evidence of channel development. Erosion level III shows less relief. The main indication for a considerable hiatus associated with erosion level III is shown by the radiocarbon datings, and frequent smaller-scale erosion phenomena at the top of DT3.

Figure IV.18 (next page). North-south sections of the detailed grid area south of Tilligte. Legend: see fig. IV.8; location: see fig. IV.17.

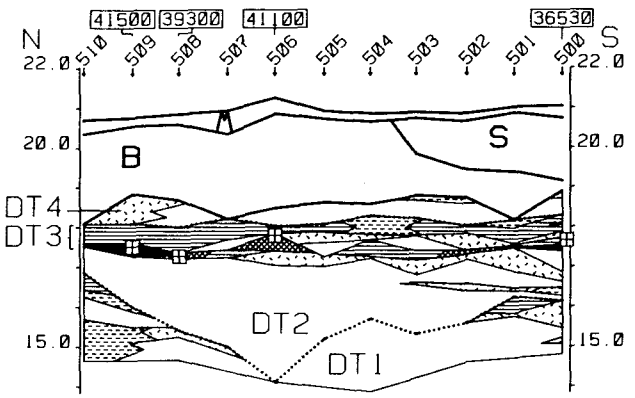

50 m. Section a

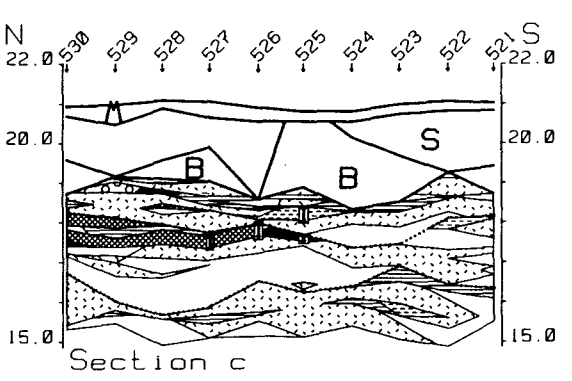

Section c

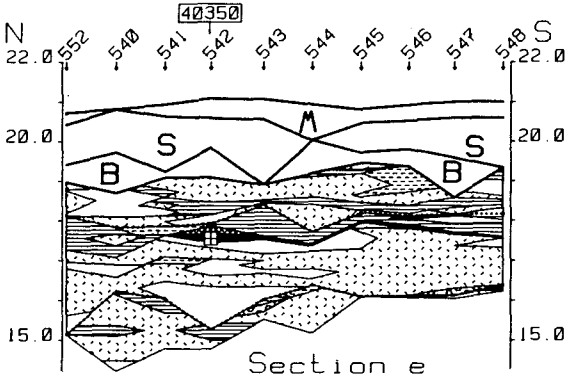

Section e

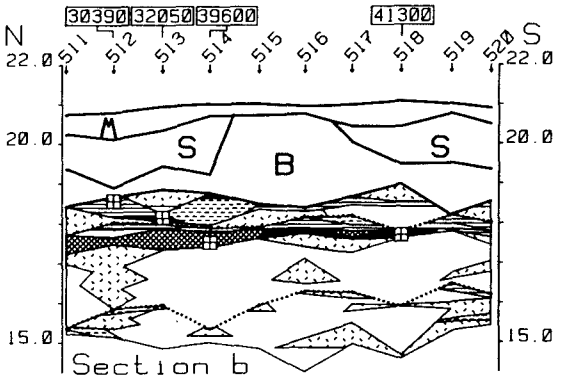

Section b

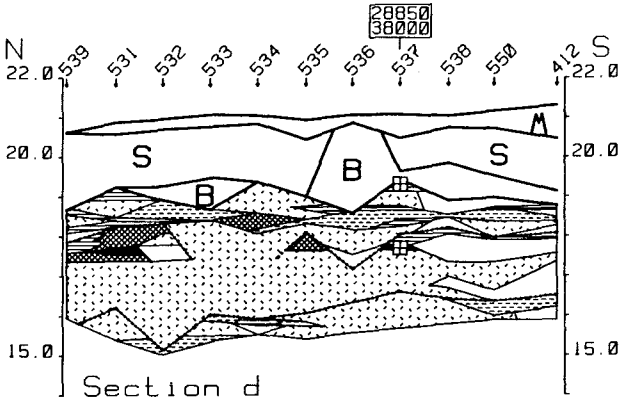

Section d

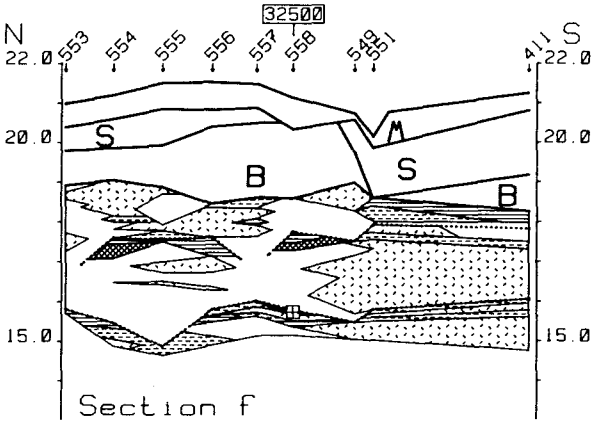

Section f

IV.4.1.2. Chronostratigraphy.

Two datings on peat which correlates with unit DT3, have been obtained from boring 24 in the Tilligte section (fig. IV.9) and boring 410 in the Laarhuis-Rammelbeek section (fig. IV.10, 11). These indicate ages of 36.53 and 37.5 ka for unit DT3, maximally 38.7 ka. Both datings are confirmed by an extract dating. Boring 24 is located only a few meters west of boring 500 of the detailed grid site, boring 410 is situated at the southern edge of the mapped area, and correlation of the dated peat layers with the base of DT3 is certain. The datings obtained in the sections of fig. IV.18 from the basal part of DT3 in this area are listed below in table IV.2. Several of these datings prove to be significantly older than the preceding two datings.

Boring	Dating	Laboratory nr: GrN-	Material
506	41100 ± 900	12181	gyttja
508	39300 ± 850	12182	gyttja
509	41500 ± 1400	12183	peat/gyttja
514	39600 ± 1100	12186	gyttja
518	41300 ± 1000	12187	peat
537	38000 ± 850	12189	peat
542	40350 ± 950	12190	peat

Table IV.2. Datings from unit DT3 in the Tilligte detailed grid area.

Nevertheless, lithostratigraphical correlation of DT3 with the 40-42 ka silt/peat complex in the Tilligte section (fig. IV.9) would lead to unlikely constructions. Also, the datings on DT4 (table IV.3) show that ages over 39 ka for unit DT3 might be too old, as this would yield an unlikely large hiatus of at least 7000 years between DT4 and DT3. Therefore, especially the ages over 40 ka in table IV.2 are erroneous. Also the datings themselves give some indications, as they vary markedly over short lateral distance. Secondly, the material of some samples (gyttja and peat gyttja intergrades) is suspect; unfortunately no other material was available for sampling. Also palaeobotanical evidence points to subaquatic environments (Ran, 1990). This type of sediment is well known for the risk of contamination by older carbon (par. IX.2). By contrast, the samples of boring 24 and 410 have been derived from relatively pure peat. The results show, that datings on gyttja may show ages which may be up to 3000 years too old.

Three datings have been derived from unit DT4 (table IV.3). Although these datings are not checked by extract datings, contamination by younger humic material is not very likely. In that case probably also the datings of DT3 would have been influenced. The datings are stratigraphically consistent, with

Figure IV.19 (next page). Synoptic fence diagram (E-W) of unit DT 2 and 3 in the detailed grid area south of Tilligte. Legend: see fig. IV.8. Boring 410 is part of the Laarhuis-Rammelbeek section (fig. IV.10).

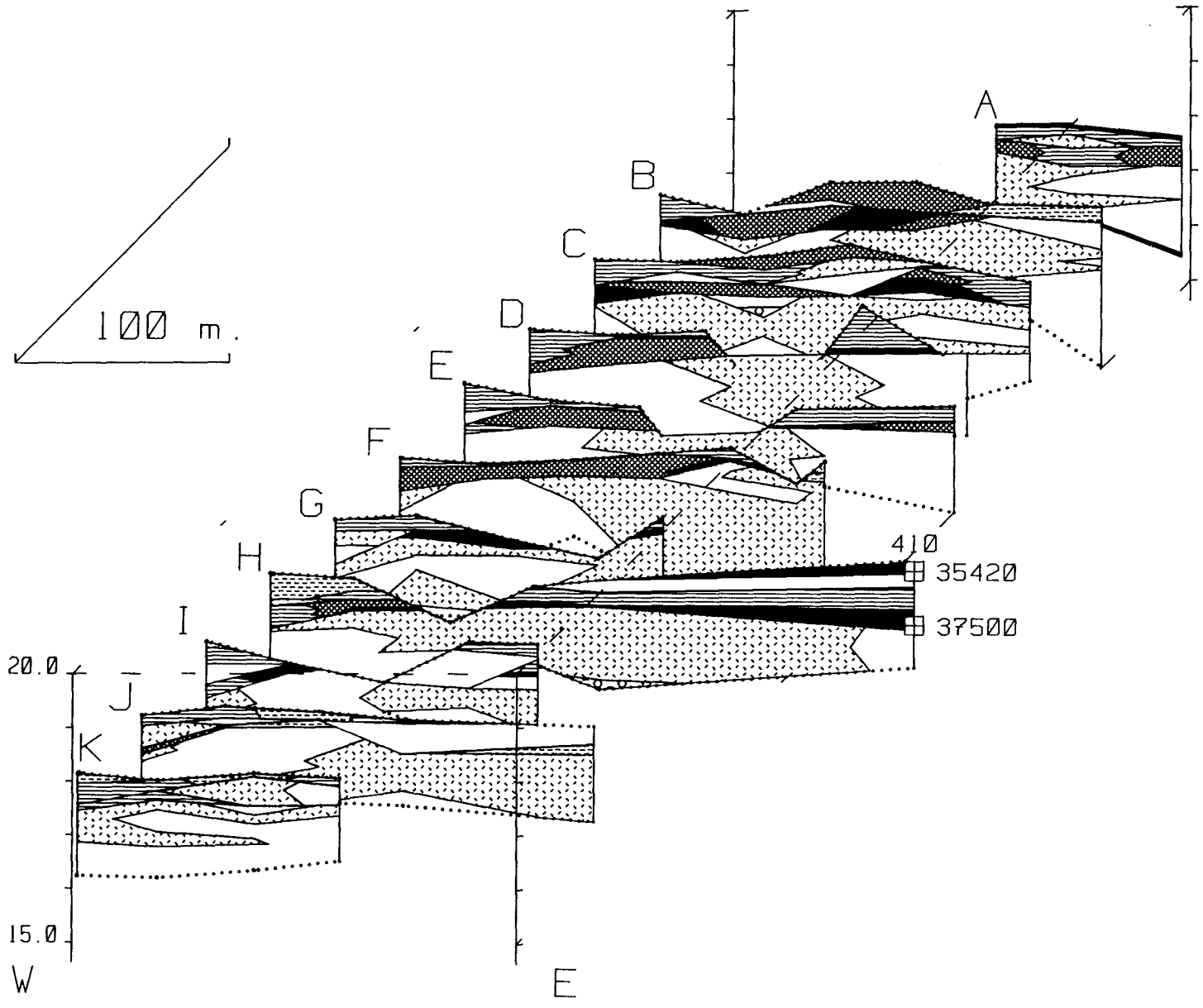
100 m.
A
B
C
D
E
F
G
H
I
J
K
410
35420
37500
20.0
15.0
W
E

Boring	Dating	Laboratory nr: GrN-	Material
512	30390 ± 370	12184	peaty silt
513	32050 ± 500	12185	peaty silt
537	28850 ± 470	12188	peaty silt

Table IV.3. Datings from unit DT4 in the Tilligte detailed grid area.

the youngest one occurring at the highest level. Especially the datings on boring 513 and 514 clearly demonstrate the existence of a hiatus between DT4 and DT3 of 4000 years.

An attempt has been made to date unit DT1. A peat sample from boring 558 yielded an age of 32.5 ka. This is clearly erroneous, an age over 40 ka should have been found. The cause might be contamination during sampling.

IV.4.2. Detailed boring programme north of Denekamp.

A stretch of the Lattrop-Denekamp section (C'C''), parallel to the former Dinkel Canal sections (Wijmstra and De Vin, 1971) has been studied with more detail, with a distance between the borings of at most 50 m. Two parallel sections (DD' and EE', fig. IV.20) also have been made which include hydraulic boring Dorpermeien (figs. III.3, IV.20).

The Asten Formation largely consists of an unusual thick clay unit with gyttja beds at the top. The Liendert Member of the Twente Formation again starts with a thick silt/clay unit, followed by sandy deposits with peaty intercalations. The Dinkel Member proves to consist of coarse sand and gravel with large peat and clay lumps. It becomes gradually finer towards the top. This is repeated at the base of the Tilligte beds, but the coarse sand levels are less massive than those of the Dinkel sand, and rapidly grade into finer sands. In the upper half of the Tilligte beds sediment with an extremely large amount of clay pebbles and a striking light grey colour is found.

These clay pebble beds are also found in most nearby borings and appear to represent the fill of a separate fluvial incision. In one boring (627 in section DD') the overlying clay contains humic matter which is dated at 28.6 ka. This dating provides the upper age boundary. In boring 644 clay pebble sediment overlies sediments dated between 42.2 and 35.5 ka. The latter dating might be too young, as indicated by its extract age. The datings suggest that incision and infilling have taken place between 35.5 (or possibly 42.2) ka and 28.6 ka. Most likely, this fluvial incision correlates with erosion level III.

The clay pebble beds prove to be restricted to the two southerly sections of this area. In the Lattrop - Denekamp section it has not been found. By its contrasting lithology the distribution of this sediment type easily can be traced in the sections. Its eastern and western boundaries prove to be very sharp, a complete return to the normal type of Tilligte beds sediment occurs within 25 m. The areal distribution indicates a predominantly WSW-ENE course of the river which caused the incision (fig. IV.21), at a right angle to the present drainage. With a more northerly course

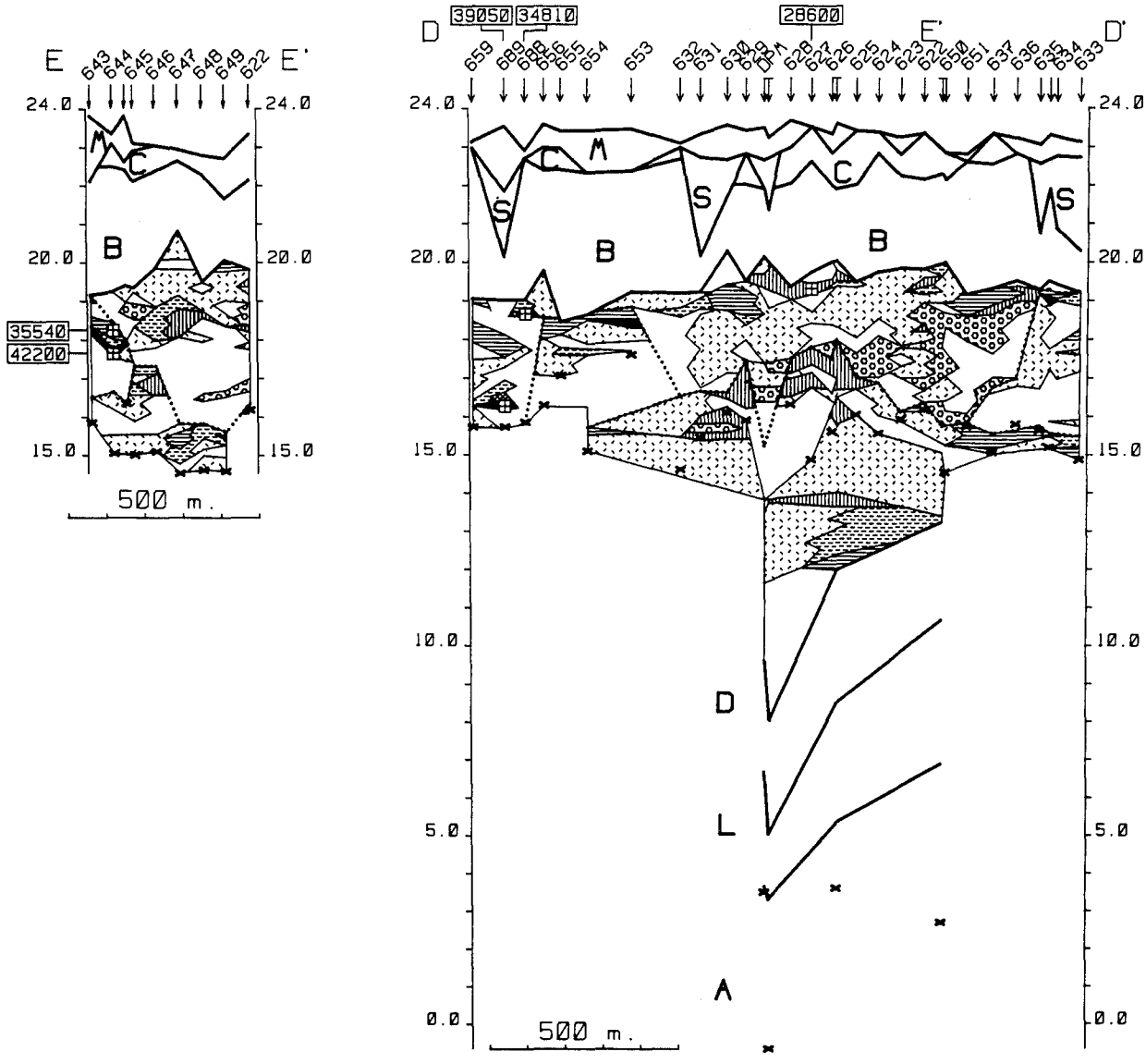

Figure IV.20. Detailed sections north of Denekamp. Location: see fig. IV.1 and IV.17. Legend: see fig. IV.8. DPM: boring Dorpermeien.

the clay pebble sediment should have been found also in the Lattrop- Denekamp section between boring 613 and 621. This agrees with the much more easterly course of the main drainage line of the valley during most of the Middle Pleniglacial, as derived from the distribution of the Puntbeek sands (par. IV.3.3, VIII.2.1). The fluvial incision associated with erosion level II in the middle part of the Lattrop-Denekamp section (par. IV.3.3) also shows approximately this direction.

Lithological evidence for erosion level II is present in the shape of silty sand with intraclasts between the two datings in boring 644. Furthermore, erosion level II and the associated fluvial incision fill (par. IV.3.3.2) have been found at the west side of section DD' (fig. IV.20). The datings of 36 and 39.6 ka in boring 688 and 689 also occur at an anomalous low position, and compare well with datings on the same depth levels in section C'C'' (fig. IV.13).

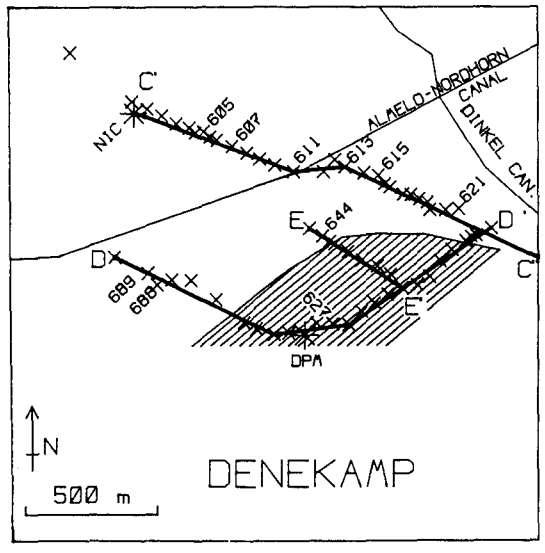

Figure IV.21. Distribution of clay-pebble beds (hatched area) within Tilligte beds NE of Denekamp. *: hydraulic core (DPM = Dorpermeien, NIC = Nicolaasstichting); X: boring. See also fig. IV.1 for location.

IV.5. Losser boring.

To obtain data from an area further upstream, a hydraulic boring (fig. III.3) has been made near the town of Losser (location: fig. IV.1). The substratum consists of sandy diamicton, interpreted as Drente Formation till. It is overlain by light-grey clayey sand, perforated by woody roots, which most probably correlates with the Asten Formation. The Liendert Member is represented by sand, with a silt bed at the top. Both units are thin, less than 1 m together. They are overlain by coarse sand with gravel, alternating with finer, silty sequences, the Puntbeek sands. At the top of this sequence, a thin peat bed is found which is dated at 42 ka. Apparently the boring occupies a transitional area between Puntbeek sands and Tilligte beds. The peat is overlain by Beverborg Member and Singraven Formation sediments.

The coarse development of the Middle Pleniglacial deposits is not unexpected in this upstream location. Still, some peat and silty sediments occur. This sequence represents the same coarse variety of the Mekkelhorst member as is found in the Beverborg section.

IV.6. Internal stratigraphy of the Middle Pleniglacial deposits in the Dinkel valley.

Although at first sight the Middle Pleniglacial sequence consists of a rather uniform alternation of sand and silt or peat beds, the borehole sections reveal clear facies differences and traceable erosion levels (fig. IV.22). The facies differences are related to spatial and temporal variations in the fluvial system and sediment sources, to be discussed in par. VIII.2.1. The most outstanding dissimilarity is the contrast between the Tilligte beds (sand/silt/peat beds) and the Puntbeek sands (only sand beds). From the Lattrop-Denekamp section and the Beverborg section it proves that both units are lateral equivalents. The

Puntbeek sands mainly represent deposits along the main drainage line of the valley and the basin.

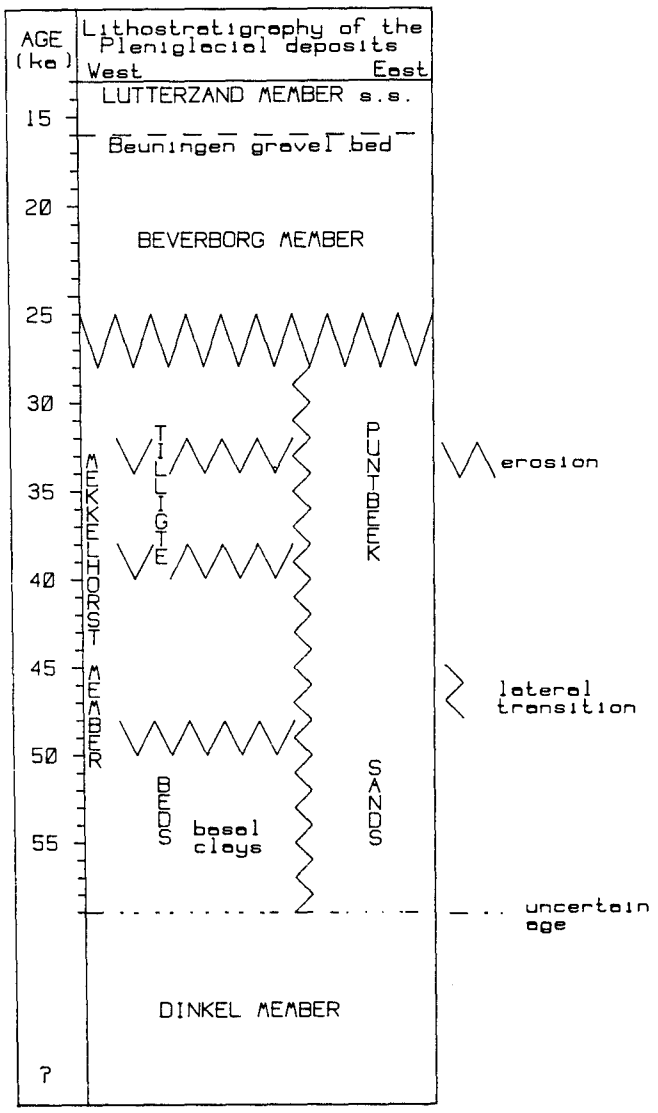

Figure IV.22. Schematic representation of the lithostratigraphy of the Pleniglacial deposits in the Dinkel valley.

Within the Tilligte beds several facies varieties can be discerned. In the basal clays the silt beds are generally thicker and contain more clay than in the remainder of the Tilligte beds. Also, the basal clays are always strongly calcareous, while in the overlying parts of the Tilligte beds lime may be absent. The age of the basal clays is older than 47 ka, but most radiocarbon datings characteristically show ages over 50 ka. A second facies of the Tilligte beds is the coarser sediment found in the Beverborg section and Losser area. Here, sands of the Tilligte beds are coarser than average and silt/peat beds are generally less frequent. A third facies is represented by the peat-rich sequences found in the western part of the Tilligte section.

Furthermore, three Middle Pleniglacial erosion levels can be discerned. These are associated either with channel deposits, or thinner erosion phenomena within overbank deposits. These levels can be traced in most of the sections by lithology and by ano-

malies in the radiocarbon chronology. Well defined overall differences in lithology are generally absent above and below the erosion levels. The erosion levels do not incorporate all erosion phenomena which may be found, and local erosional features are usually present between them.

The oldest erosion level (level I) is found at the top of the basal clays. Lithologically, it can be traced very well in most sections. In general it is rather flat and may be merely a facies change, but channel forms occur frequently. It is older than 47 ka, but most likely younger than 50 ka.

Level II is dated between 38 and 40 ka, and is the most well developed phenomenon. Channel deposits occur frequently, and in the centre of the basin a larger incision is found which itself has been filled with an alternation of silt/peat and sand beds. Erosion level II is found also in the Hengelo basin (par. VI.4).

Erosion level III is dated between 32 and 34 ka. Apart from possible deeper fluvial incision in the area north of Denekamp, erosion level III generally appears to be merely a hiatus indicated by the radiocarbon datings.

V. Petrographical analysis and sediment sources of the Late Pleistocene basin fill.

V.1. Mineralogical differentiation of the basin fill units.

The sands of the Twente Formation are considered to be derived mainly from the local substratum (Crommelin, 1964; Doppert et al., 1975). The mineralogy of the fluvial deposits reflects mixing of the substratum sediments, and mineralogical discrimination between different units within the Twente Formation therefore is likely to be difficult. Nonetheless, mineralogical variation within Weichselian valley fill sequences has been found (De Ploey, 1961; Vandenberghe & Krook, 1981, 1985; Haest, 1985; Lootens, 1987). These variations have been attributed to additions of allochthonous aeolian material, or different source areas within the fluvial sequence. Likewise mineralogical differences also may exist within the Late Pleistocene basin fill in the Dinkel valley. As these differences may be related to the sedimentary environment, a closer consideration is worthwhile.

Most exposures and some borings have been subjected to heavy mineral analysis. In most cases the 50-420 µm fraction has been used in the analysis. In some silt samples the 30-60 µm and 60-250 µm fractions have been counted separately. A number of 200 translucent grains in each sample has been identified. The following minerals or mineral groups have been distinguished:

- Garnet group;
- Epidote group (epidote, zoisite, clino-zoisite);
- Alterite and saussurite (translucent, grayish micro-crystalline aggregates, of which the original mineral components cannot be determined);
- Amphiboles (mostly green hornblendes, rarely brown hornblende);
- Augite and other pyroxenes, sphene; in the Netherlands tradionally grouped under the heading 'Volcanic minerals';
- Other stable minerals (zircon, rutile, anatase, brookite);
- Other unstable minerals (rare, less stable minerals: tremolite, glaucophane, apatite, detrital siderite, chloritoid);
- Staurolite;
- Topaz;
- Metamorphic minerals (kyanite, andalousite, sillimanite);
- Tourmaline group.

Erratic high percentages of siderite may sometimes occur which have been included in the group of rare unstable minerals. This siderite is not of authigenic origin but is reworked from older deposits. The grains are usually rounded and appear to have been subjected to both mechanical and chemical wear, as shown by scanning electron microscope study.

To highlight the differences within the heavy mineral diagrams and to assist zonation stratigraphically constrained cluster analysis has been applied. The analysis has been carried out with an adapted version of the CONISS cluster analysis program (Grimm, 1987). This program employs the method of incremental sum of squares (also known as Ward's method) which minimizes within-cluster sum of squares. As dissimilarity coefficient the chord distance has been used. In practice this involves a data transformation, by taking the square root of each entry of the data matrix, after which the squared Euclidian distance is computed. The effect is that for frequency data such as heavy mineral counts rare variables are up-weighted relative to abundant

variables (Grimm, 1987). The value of such a weighting has been suggested by a preliminary inspection of the heavy mineral diagrams.

Figs. V.2-4 display heavy mineral diagrams from borings, with zonation as derived from cluster analysis. In most cases a cut across the dendrogram at a dissimilarity level of 5 provides an acceptable number of zones. In boring Kamphuis the within-zone variation is somewhat larger, so a dissimilarity level of 6 has been used. The main zones in the borings are indicated by characters, further subdivisions by number suffixes (figs. V.2-4, table V.1).

Zone	Lithostratigraphical unit (see section III)	Boring				
		Losser	Kamphuis	28	Tilligte Vlierweg	Noord Deurn.
III	Lutterzand Member s.s. Beverborg Member	A	A_2, A_1	A	A1	absent
II	Mekkelhorst Member Dinkel Member	A	A_4, A_3	B_2, B_1	A_4 (top) A_3, A_2	A_2, A_1
I	Liendert Member (Twente Formation) Asten Formation	B	B	absent	A_4	B

Table V.1. Between-boring correlation of heavy mineral zones in the individual borings (figs. V.2-4) and correlation with the lithostratigraphy of the basin fill. Characters A and B represent main zones of each boring, number suffixes further subdivision.

Table V.1 shows the correlation between the heavy mineral zones of the individual zones, and correlation with the relevant lithostratigraphical units. Table V.2 and fig. V.5 display the mean composition for each zone and stratigraphical unit. In figs. V.2-4, the Asten Formation and the Liendert Member are separated at a generally high dissimilarity level from the younger units, and constitute mineral zone I. A clear decrease of the stable mineral group and tourmaline, combined with an increase of garnet, amphiboles, volcanic minerals and other unstable minerals occurs at the zone I-II transition (table V.2). The increase of the latter mineral group is due to the presence of detrital siderite. The transition from zone II-III coincides with the boundary between the Tilligte beds (Mekkelhorst Member) and the Beverborg Member. A sharp increase in garnet and a decrease in amphiboles occurs at that level (table V.2, fig. V.5). The mineralogical break between the Mekkelhorst Member and the Beverborg Member can be traced across the entire valley, also in locations where the Tilligte beds grade into the Puntbeek sands (fig. V.6).

In general, variability within zone II (Dinkel Member + Mekkelhorst Member) is high. Within several borings subzones of zone II are distinguished. In the Tilligte basin the Tilligte beds can be subdivided in a lower amphibole-rich part and an upper garnet-rich part (fig. V.3).

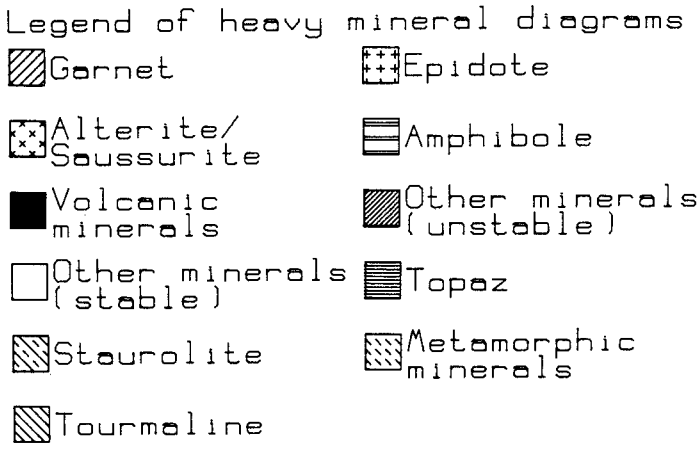

Figure V.1. Legend for the non-opaque heavy minerals in the diagrams of fig. V.2-10. High percentages of 'other minerals (unstable)' in the diagrams are mainly caused by presence of detrital siderite.

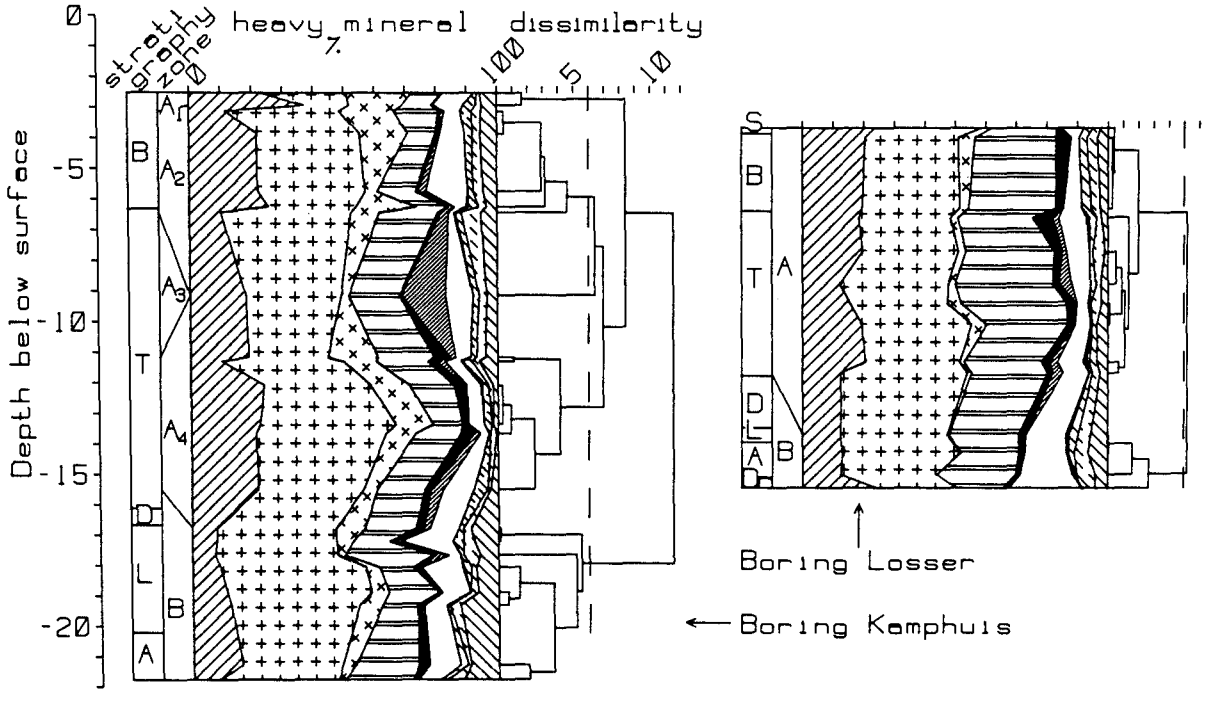

Figure V.2. Heavy mineral diagrams of boring Losser and Kamphuis, showing zonation with the help of stratigraphically constrained cluster analysis. The borings are located in the Dinkel valley upstream of Denekamp (fig. IV.1). Legend in fig. V.1.

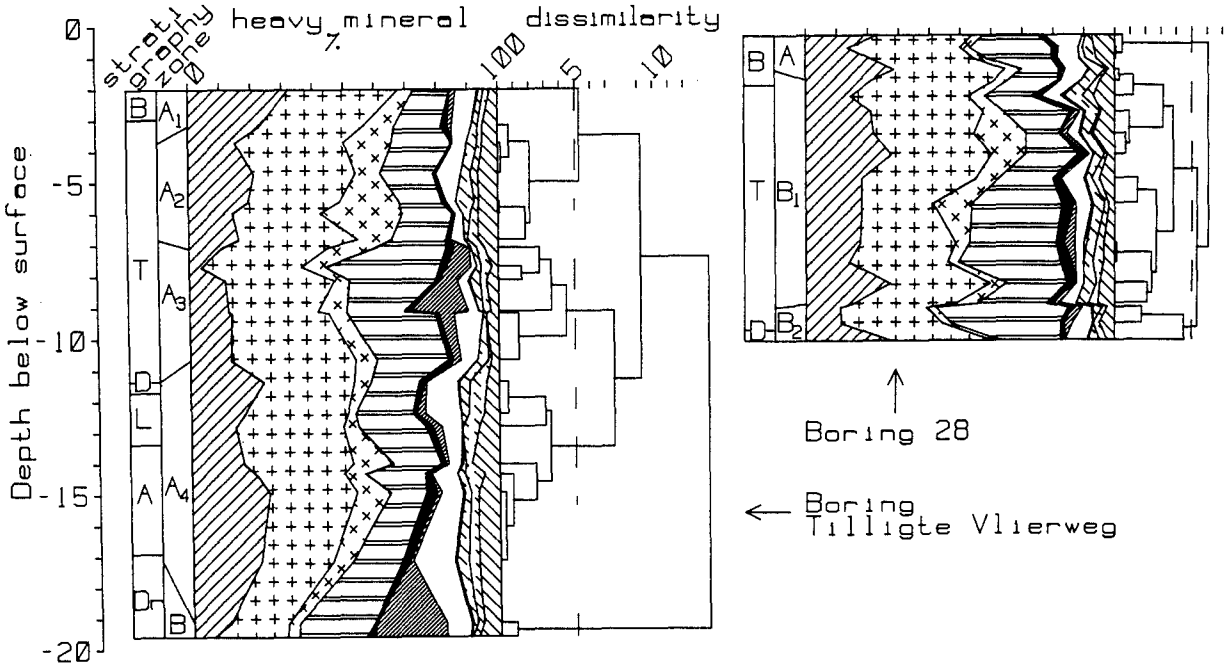

Figure V.3. Heavy mineral diagrams of boring Tilligte Vlierweg and 28, with zonation. The borings are located in the Tilligte section (fig. IV.1). Legend in fig. V.1.

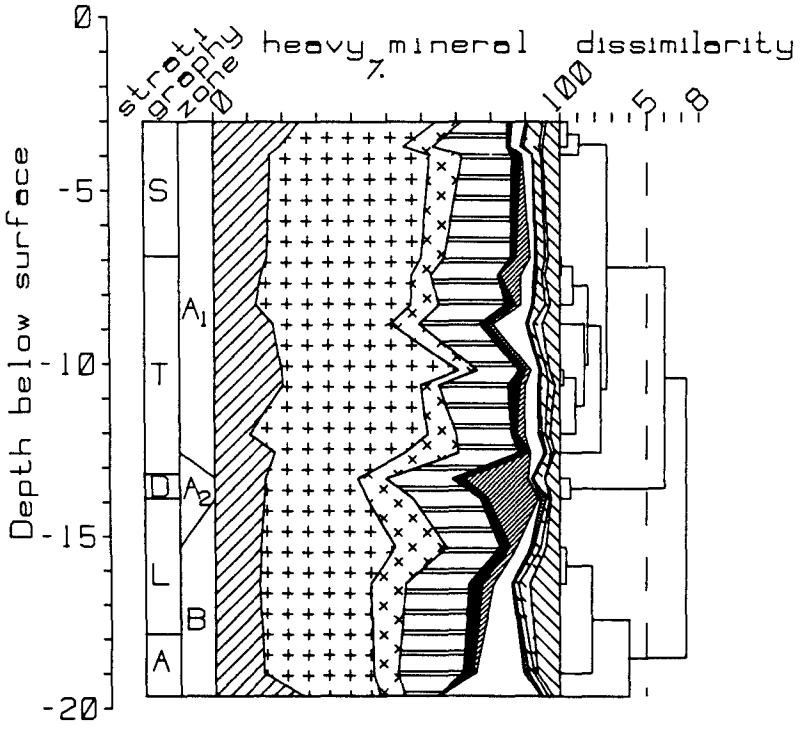

Figure V.4. Heavy mineral diagram of boring Noord Deurningen, showing zonation. The boring is located in the Lattrop-Denekamp section north of Denekamp (fig. IV.1). Legend in fig. V.1.

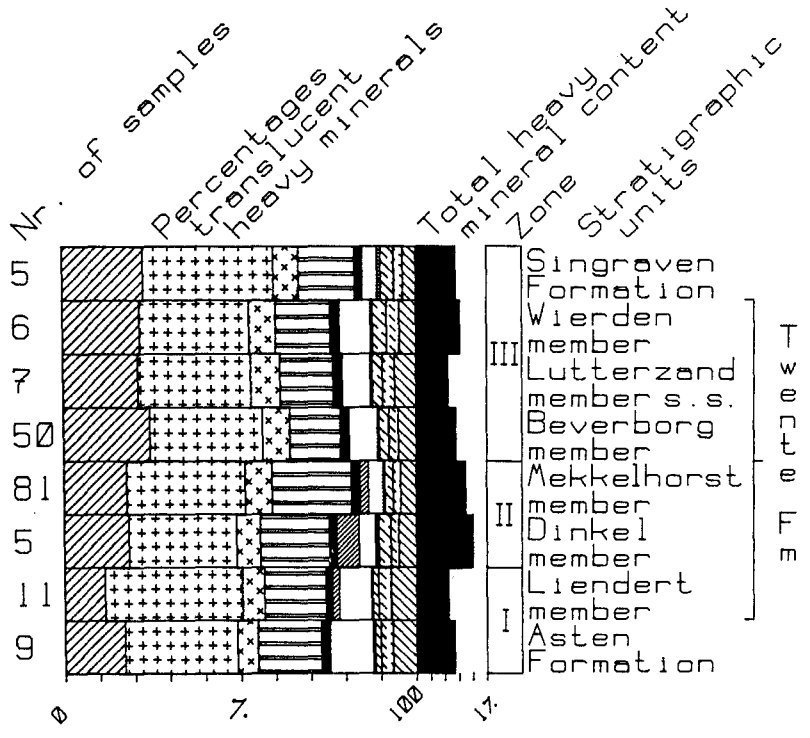

Figure V.5. Mean heavy mineral composition of the stratigraphical units in the Late Pleistocene basin fill, and correlation with the heavy mineral zones distinguished in the borings.

Mineral	Zone							
	I (n=20)		II (n=86)			III (n=63)		
	mean	std	mean	std	diff	mean	std	diff
Garnet	14.0	5.2	17.9	5.9	+	24.0	7.8	+
Amphiboles	17.8	5.1	22.5	7.6	+	14.6	5.8	-
Volcanic minerals	1.8	1.1	2.3	1.3		2.0	1.2	
Other minerals (stable)	10.6	6.0	4.3	2.6	-	8.1	3.8	+
Other minerals (unstable)	1.4	1.3	2.7	4.5		0.5	0.6	
Topaz + staurolite + metamorphic minerals	5.5	1.8	5.0	1.7		6.2	2.3	+
Tourmaline	7.0	2.5	4.4	2.3	-	5.1	2.0	
Total percentage heavy minerals (weight %)	0.5	0.7	0.7	0.8		0.6	0.8	

Table V.2. Average heavy mineral content of each mineral zone of the valley fill (std = standard deviation). Only the mineral percentages which clearly vary between the zones have been listed. The differences for the more abundant (>5%) minerals has been tested for significance with a t test (10 % two-sided significance level). +: significant positive difference with the underlying zone, -: significant negative difference. See also fig. V.5.

Figure V.6 (next page). Cross-valley correlation of heavy mineral diagrams in the Beverborg area (locations in fig. IV.1). Note that garnet-rich sediments occur mainly in the Beverborg, Lutterzand and Wierden Members.

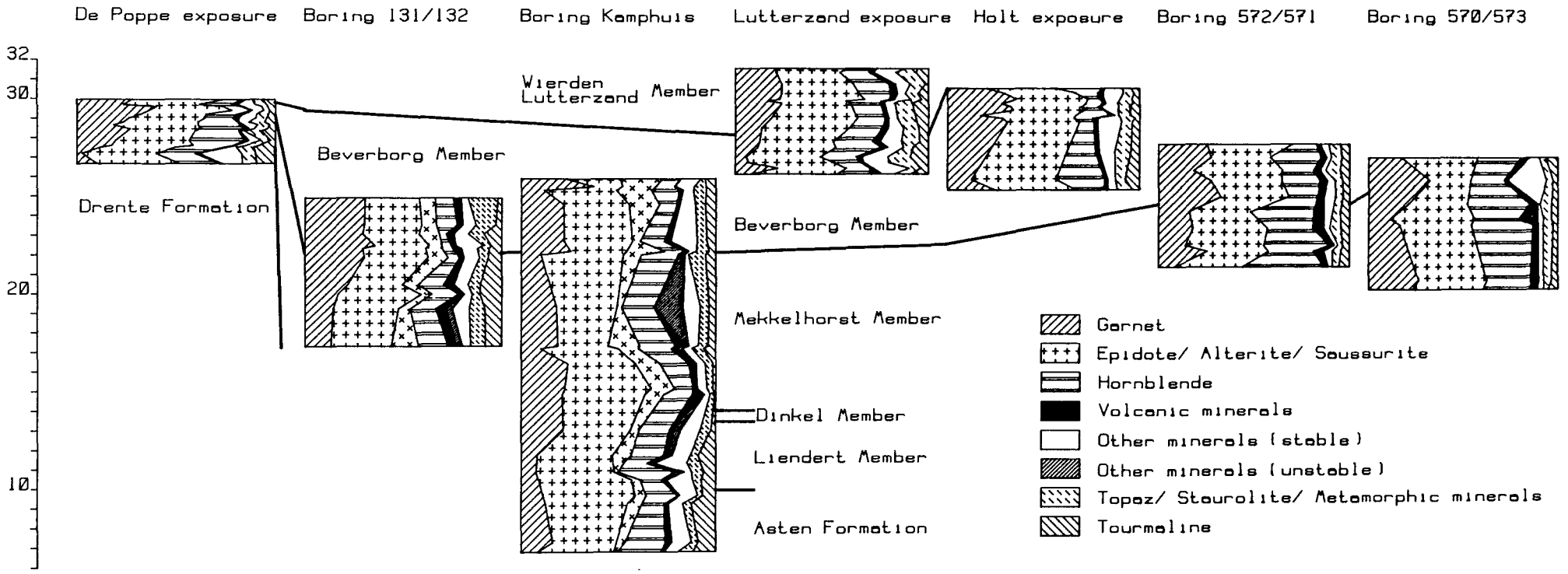
De Poppe exposure
Boring 131/132
Boring Komphuis
Lutterzand exposure
Holt exposure
Boring 572/571
Boring 570/573
32
30
20
10
Wierden Member
Lutterzand
Beverborg Member
Drente Formation
Beverborg Member
Mekkelhorst Member
Dinkel Member
Liendert Member
Asten Formation
Garnet
Epidote/ Alterite/ Saussurite
Hornblende
Volcanic minerals
Other minerals (stable)
Other minerals (unstable)
Topaz/ Staurolite/ Metamorphic minerals
Tourmaline

V.2. Sediment sources and processes influencing the basin fill mineralogy.

Theoretically the heavy mineral composition of the basin fill should be a mixture of the substratum heavy mineral assemblages, taking into account areal extent (fig. I.1) and total heavy mineral fraction of the substratum formations (fig. V.7).

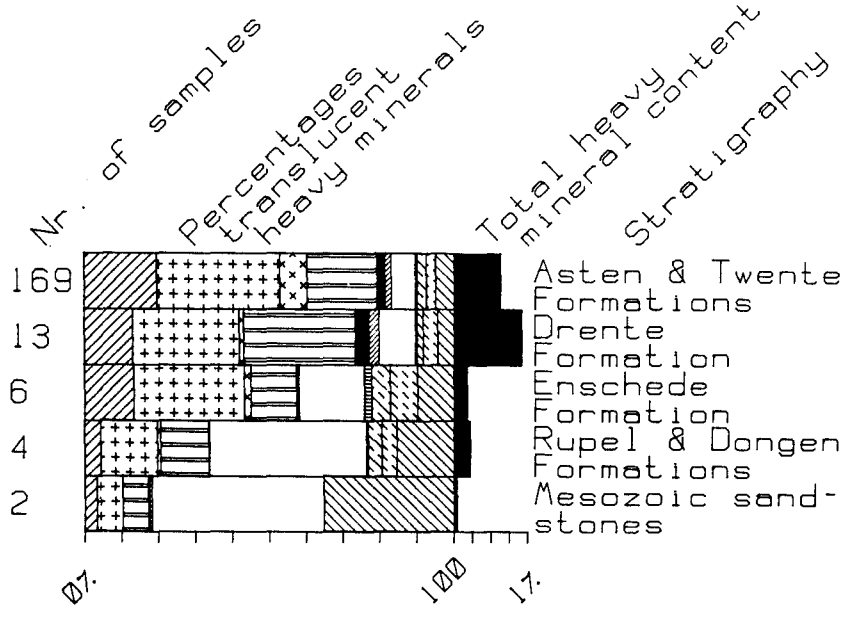

Figure V.7. Mean heavy mineral spectra from different basin substratum units (determined from samples collected by the author), compared with mean heavy mineral composition of the Late Pleistocene basin fill.

The Drente Formation is represented by till and - in the glacial basins - fluvioglacial sediments (par. I.2). At the edge of the basin thick till mantles occur (Van den Berg & Beets, 1987). Till beds occur in drainage divide positions on top of the Ootmarsum ice-pushed ridge (Van Huissteden, 1989), and suggest former presence of an extensive till cover. The heavy mineral association of the Drente Formation is the most unstable association in the drainage basin. Tills of the Twente region and its surroundings generally contain 25-40% epidote, 20-65 % amphibole, and 10-40% garnet (Rappol & Stoltenberg 1985, Rappol, 1987). This is confirmed by samples collected by the author (fig. V.7, table V.3). A special characteristic is the presence of a few percent of pyroxenes, minerals which are absent in the other substratum formations. Authigenic siderite is present locally. The Drente Formation also contains the highest weight percentage of heavy minerals. Lithology of several samples used for compilation of fig. V.7 and table V.3 indicates admixture of older material which may have led to an over-representation of stable minerals.

The Enschede Formation (coarse sands and gravel) occurs in elongated zones in the ice-pushed ridges (Van den Akker and Knibbe, 1963). The most important characteristics are the relatively high percentages of metamorphic minerals, staurolite, and presence of topaz (fig. V.7). Up to 20 % stable minerals may be found. Garnet percentages tend to vary strongly. Garnet-rich

variations of the formation may contain more than 30 % garnet (Doppert et al., 1975).

Sediments of Tertiary age dominate the ice-pushed ridges (Doppert et al., 1975). The Lower Tertiary formations (Dongen and Rupel Formations) consist of clays and glauconitic sands. These contain a stable heavy mineral association (fig. V.7). Upper Tertiary sediments with an unstable heavy mineral association (Breda Formation) are probably restricted to small areas in the northwestern part of the Ootmarsum ice-pushed ridge. The Lower Cretaceous sandstones in the German part of the drainage basin contain a stable association. Both the Tertiary and Cretaceous formations contain large amounts of opaque minerals, while their total heavy mineral content is very low.

Systematic stratigraphical variations on the average basin fill mineralogy, as determined by the substratum, may arise from:
(1) river capture;
(2) density or shape sorting of the minerals, related to sedimentation processes;
(3) selective erosion of substratum formations under varying climatic conditions;
(4) The amount and type of weathering of the substratum under different climatic conditions;
(5) Addition of allochthonous material from outside the drainage basin by aeolian transport.

Process 1 may have occurred in the upper course of the river (between Ahaus and Gronau, fig. I.1), but will not have involved a considerable substratum change. The other processes are environmentally sensitive. With respect to process 3 presence or absence of permafrost may be crucial. Very permeable formations which otherwise are less sensitive to erosion by overland flow, may become impermeable and erodible under permafrost conditions, as the numerous dry valleys on the sandy ice-pushed ridges in the Netherlands testify (e.g. Maarleveld, 1949). In the Dinkel drainage basin the Enschede Formation might have behaved this way.

As noted in other areas, process 5 could have been active during the Middle and Late Pleniglacial (Vandenberghe & Krook, 1981, 1985; Haest, 1985; Lootens, 1987). An allochthonous aeolian contribution must consist of a considerable amount of material with a deviating mineral composition, to exert a noticeable influence on the basin fill mineralogy. The source areas for this aeolian material may range from distant to regional (e.g. a neighbouring river basin). In the latter case, the mineralogy can be quite similar to that of the basin under consideration. The Upper Pleniglacial loesses and coversands are supposed to have originated partly from the North Sea basin (Mücher, 1986; Schwan, 1986). A possible source area in the North sea is characterized by the A and H mineral provinces (Edelman, 1933; Baak, 1936). The A province contains on average 31 % garnet, 27 % epidote, 24 % amphibole, and 13 % stable minerals + tourmaline; for the H province these values are respectively 30 %, 26 %, 14 %, 5 %. These values do not differ strongly from the valley fill in the Dinkel basin. The silt fraction of Tubantian loesses in the southern Netherlands and Belgium shows 5-9 % garnet, 45-49 % epidote, 23-29 % amphibole, 6-9 % stable minerals and 4-6 % tourmaline (Eden, 1980; Mücher, 1986). The silt fraction of 8 Upper Pleniglacial loess samples from the Belvédère site (Vandenberghe et al., 1985) show somewhat lower epidote and higher

stable minerals values (Krook, pers. comm., table V.6). It is likely that addition of allochthonous loessic material should be indicated by high epidote percentages in the silt fraction, as the substratum formations all contain much less epidote.

V.3. Interpretation of the mineralogical differences.

V.3.1. General evaluation.

Most of the basin fill sediment has been derived from the Drente Formation, as the mean heavy mineral composition of the Twente and Asten Formation closely resembles that of the Drente Formation (fig. V.5,7). Some deviations occur (table V.3). In all zones of the basin fill the amphibole percentages are significantly lower, while the amount of alterite is considerably higher in the basin fill. A considerable part of these alterites show gradations into green hornblende. The presence of these hornblende-alterites (Boenigk, 1983) suggests that part of the hornblende grains have been transformed into alterite by weathering processes. Also winnowing of the generally flattened, angular amphiboles could have played a role (Winkelmolen, 1969). The generally somewhat higher content of unstable minerals in the basin fill is difficult to explain. As noted above, the 13 till samples on which the mean heavy mineral content of the Drente Formation is based may not be entirely representative. Also aeolian material which is rich in unstable minerals has been added to the basin (see below).

Mineral	mean	standard deviation	differences Drente Formation - Basin fill mineral zones		
			I	II	III
Garnet	13.1	3.19	o	+	+
Epidote	28.6	5.32	+	+	+
Amphiboles	30.3	9.67	-	-	-
Other minerals (stable)	9.8	4.32	o	-	o
Topaz + staurolite + metamorphic minerals	4.4	2.88	o	o	o
Tourmaline	6.1	2.32	+	o	o

Table V.3. Comparison of heavy mineral percentages of the most abundant mineral groups in the Drente Formation and the basin fill zones. +: significant positive difference of basin fill with Drente Formation; -: significant negative difference; o: difference not significant (t-test with 10 % two-sided significance level). See also fig. V.5 and 7.

Combined grainsize and mineralogical analysis of a number of samples indicates to what extent mineralogical differences may be related to general grainsize differences of the units. Minerals with high densities occur mainly in smaller size classes because of hydraulic equivalence (e.g. Schuiling et al., 1985). The hydraulic equivalence effect should lead to a positive correlation of high density minerals with mean grainsize as expressed on

ø scale (finer sediment --> higher ø value). Only the stable minerals group and the topaz/staurolite/metamorphic group satisfy this relation however (table V.4). Garnets (density > 3.3 g/cm^3) correlate negatively with phi mean, while the relatively light tourmalines (< 3.3 g/cm^3) show a high positive correlation. This indicates that other processes occur besides the effects of sorting during transport. For tourmaline and garnet this is supposed to be the grainsize of the source material. As demonstrated by fig. V.7 part of the tourmalines may have been derived from the fine grained Tertiary formations. The garnets could originate partly from coarse, garnet-rich Enschede Formation sediments. Also epidote, with an intermediate density (ca. 3.3 g/cm^3), shows an unexpectedly high positive correlation with ø mean which may point to addition of fine-grained epidote-rich material.

garnet	epidote	amphibole	stable minerals	topaz, staurolite, metamorphic minerals	tourmaline
-0.14	0.57	-0.23	0.40	0.37	0.31

Table V.4. Correlation coefficients of mineral groups percentage with mean grain size (computed as phi mean) of 39 samples. Significant positive or negative correlations (|r|>0.32, 10 % two-sided significance level) are underlined. Note that higher phi mean indicates lower mean grainsize.

Mineral group	Correlation coefficients							
	Garnet	Epidote	Amphibole	Stable min.	Topaz Staur Metam	Tourmaline	Q/F ratio	Total %
Garnet	1.00							
Epidote	-0.72	1.00						
Amphibole	-0.55	0.21	1.00					
Stable minerals	-0.06	-0.06	-0.31	1.00				
Topaz, staurolite metamorphic min.	-0.27	-0.08	0.30	-0.12	1.00			
Tourmaline	-0.58	0.20	0.22	0.36	0.22	1.00		
Quartz/feldspar ratio	0.04	0.05	-0.39	0.21	-0.12	0.14	1.00	
Total heavy miner. content (weight %)	0.26	-0.09	0.14	-0.22	-0.33	-0.49	-0.57	1.00

Table V.5. Correlation matrix of mineralogical data from boring Kamphuis. Significant correlations (|r|>0.42, t test, 10 % two-sided significance level) have been underlined.

From the Kamphuis boring also the light mineral fraction has been investigated by Krook. These analyses have been summarized in a quartz/feldspar ratio. Combined with total heavy mineral percentage this provides an opportunity to validate the influence

of weathering and concentration processes on the heavy mineral percentage. The samples from boring Kamphuis (fig. V.8) have been subjected to a principal components analysis, of which the results are listed in table V.5 and fig. V.8,9.

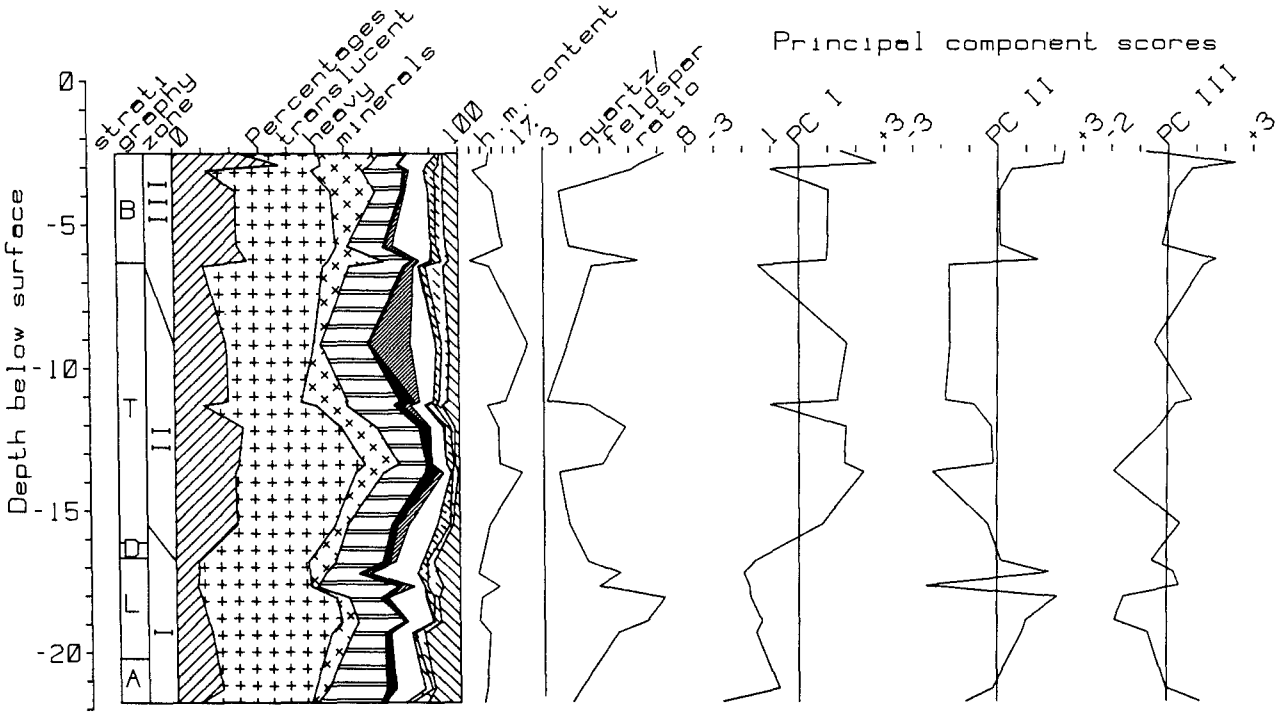

Figure V.8. Heavy mineral diagram of boring Kamphuis (see also fig. V.2). Separate curves indicate the total heavy mineral content (in weight %), quartz feldspar ratio in the fine fraction, and principal component scores. See table V.5 and fig. V.9 for results of principal component analysis.

The first principal component mainly represents the effect of density sorting. By this process lower density components of the sediment are removed by reworking, in favour of heavier components. Principal component loadings on garnet and total heavy mineral content are strongly positive, and strongly negative on the lightest minerals (fig. V.9). As shown by the principal component scores (fig. V.8), this process is active in zone II and III sediments (Pleniglacial). Density sorting can be expected to occur under conditions of frequent reworking of the sediment (Boenigk, 1983).

The second principal component shows high positive loadings on stable minerals and quartz/feldspar ratios, and negative on amphibole and total heavy mineral content (fig. V.9). This can be taken as an indication of the amount of weathering, or addition of sediment with a stable mineral association. Hornblende has been most susceptible to weathering. PC II scores are positive in zone I and III. Chemical weathering processes will be best expressed under conditions of relatively warm climatic conditions and slow substratum erosion.

The third principal component shows a high positive loading on topaz + staurolite + metamorphic minerals. As the amount of these minerals is highest in the Enschede Formation (fig. V.7), PC III most probably indicates addition of material from this formation.

A trend of gradual increase is visible in the PC III scores (fig. V.8). Addition of material from substratum formations, other than the Drente Formation, can be expected to increase in the course of time. The Drente Formation has formed a relatively thin cover on the older substratum, and is therefore a sediment source which will be depleted sooner or later, leaving the older substratum exposed to further erosion.

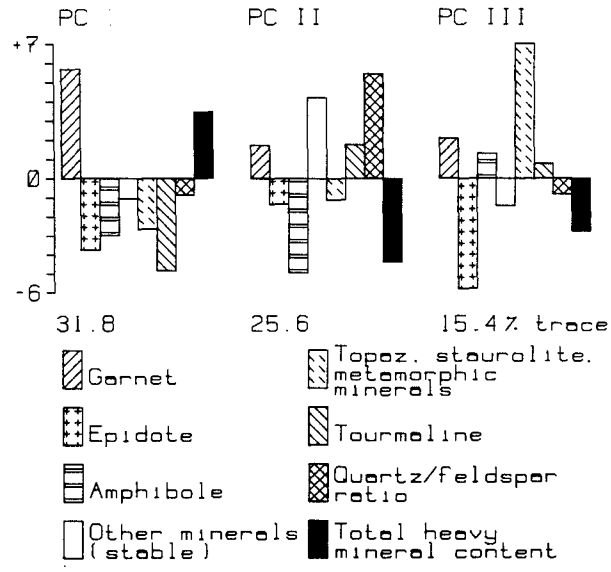

Figure V.9. Principal component loadings of mineralogical data from boring Kamphuis. The principal components have been calculated from percentages of garnet, epidote, amphibole, stable minerals, topaz + staurolite + metamorphic minerals, tourmaline, total heavy mineral content and quartz/feldspar ratio; '% trace' indicates the amount of variation in the data set accounted for by the principal components.

V.3.2. Processes related to specific zones.

Zone I. The heavy mineral composition of zone I of the basin fill deviates only slightly from that of the Drente Formation in fig. V.7. Compared with zone II, however, zone I shows a higher amount of stable minerals and tourmaline, and lower garnet and amphibole percentages. The principal component scores on PC II in boring Kamphuis are mainly positive. The sediment of zone I might have undergone more intense weathering than that of zone II. The high scores on PC II are most probably not caused by addition of stable substratum material, as abundant Drente Formation material should still have been available during deposition of zone I. Probably part of the sediment of zone I has been derived from weathered Eemian age soil profiles.

Zone II. The sediment in zone II of the basin fill (Dinkel Member, Mekkelhorst Member) shows the highest heavy mineral content and represents the most unstable material (fig. V.5). Especially the relatively high amphibole and pyroxene percentages indicate dominance of relatively unmodified Drente Formation material. Also the quartz/feldspar ratio is low (fig. V.8). The presence of erratic high amounts of detrital siderite is remarkable. The Drente Formation also will have been the source for the siderite grains (par. V.2). Siderite is extremely sensitive to weathering, especially under oxidizing conditions such as in

soils (Boenigk, 1983). Therefore the presence of detrital siderite is evidence of rapid erosion of the drainage basin substratum. Most siderite is found in the Dinkel Member and basal parts of the Mekkelhorst Member which have been deposited shortly after a period of fluvial downcutting. The development in the Hengelo basin is similar to that in the Dinkel basin. Also in the Hengelo A1 exposure (par. VI.2) unstable minerals percentages are very high, with high siderite percentages at the base of the sequence (fig. V.10).

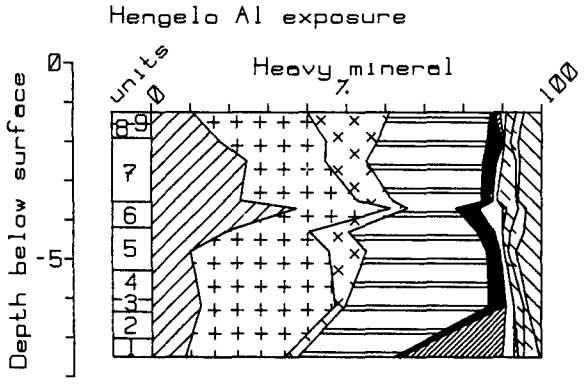

Figure V.10. Heavy mineral diagram of the Hengelo A1 exposure. Location in fig. IV.1, legend in fig. V.1.

As shown above, density sorting by frequent reworking of the sediment has been operative in zone II and III. Besides fluvial reworking, local aeolian reworking has been an important factor which is confirmed by presence of contemporaneous aeolian deposits and grain surface morphoscopy (par. VIII.3, VII.2).

Grainsize analysis of the silts of the Tilligte beds indicates the presence of a loessic component (par. VII.1.3.2.2). This should be confirmed by high epidote percentages in the silt fraction, relative to the substratum. Fractionated analysis of 10 silt samples shows that the silt fraction indeed contains considerably more epidote than any substratum formation. However, this is the case for the fine sand fraction as well (table V.6).

Source of samples	grain size ø	garnet	epidote	amphibole	stable minerals	topaz, staurolite metamorphic	tourmaline
Tilligte beds	4-5	12.7	35.9	30.8	11.1	3.9	2.4
Tilligte beds	2-4	14.0	37.1	34.6	3.3	3.6	2.9
Loess	4-5	6.6	39.9	25.1	15.6	1.4	6.6

Table V.6. Fractionated heavy mineral analysis of 10 Middle Pleniglacial floodplain silt samples, compared with analysis results from 8 typical loess samples from the Belvedere site (Krook, unpublished data). Grain size fractions: 32-63 µm (4-5 ø) and 63-250 µm (2-4 ø)

Grainsize distribution of tills in the Netherlands is characterized by a modal class of 2-3 ø/125-250 µm (Zandstra, 1983; Rappol & Stoltenberg, 1985). The fine sand fraction analyzed in the samples of table V.6 thus can be considered as representative

of tills also, and therefore should have shown similar epidote values as the till. As this is clearly not the case, part of the fine sand fraction is of allochthonous origin as well as the silt. Possibly the aeolian suspension material in this region did contain a larger fine sand fraction than typical loess, as the Dinkel basin has been situated closer to the source area of the loesses than the more southerly located typical loess regions (Mücher, 1986).

Besides the Drente Formation, also the Enschede Formation becomes increasingly important as sediment source during the Middle Pleniglacial. This is indicated by the PC III scores of boring Kamphuis, and raising metamorphic minerals and garnet percentages in the borings in the Tilligte basin (fig. V.3).

Zone III. At the transition from zone II to zone III amphibole and total heavy mineral content decrease; garnet, topaz + staurolite + metamorphic minerals and stable minerals increase. The latter again might point to more weathering of the sediment. However, the quartz/feldspar ratio in zone III of boring Kamphuis does not differ appreciably from that in zone II (fig. V.8). Instead an increased addition of stable substratum material could have caused the higher stable mineral percentages. Especially the increase in metamorphic minerals and topaz shows a further increase of the importance of the Enschede Formation as sediment source. As noted above, this may have been promoted by the establishment of a permafrost table in this very permeable substratum material.

An important feature of zone III is the strong increase of garnet. This is most conspicuous in the Beverborg Member. It is probably not a grainsize effect caused by the generally coarser texture of the Beverborg Member, as shown by the insignificant correlation between garnet and mean grainsize (table V.4). Density sorting has undoubtedly been a significant factor. Sedimentary structures of the Beverborg Member indicate besides fluvial sedimentation intense aeolian processes (Vandenberghe & Van Huissteden, 1988). The increase of garnet therefore may have been caused by augmented aeolian reworking of fluvial sediments.

Mineralogical evidence of allochthonous aeolian sand transport into the basin has not been found in the Dinkel valley sequence, although it should have occurred, especially during the Late Pleniglacial (e.g. Schwan, 1986). The aeolian Lutterzand Member s.s. has been found as infilling of upstream valley heads on the ice-pushed ridges (Van der Hammen, 1951; Van Huissteden, 1989) which points to intense aeolian sand transport across interfluvia. As suggested in par. V.2 allochthonous aeolian sand may have shown mineralogical similarity to the drainage basin substratum and the valley fill. In other regions with a different drainage basin substratum mineralogical evidence of aeolian sand transport across interfluvia has been found in sediments from Middle and Late Pleniglacial age (Vandenberghe & Krook, 1981, 1985; Haest, 1985; Lootens, 1987).

As a conclusion, four important processes appear to have caused the observed changes of the basin fill mineralogy:
- Weathering of the substratum during Eemian / Weichselian Early Glacial;
- Progressive erosion of the drainage basin substratum during the entire Weichselian;
- Fluvial and aeolian density sorting during the Pleniglacial;

- Addition of allochthonous aeolian material during the Middle Pleniglacial, as loessic suspension sediment.

V.4. Fine gravel petrography.

Local sediment sources are more strongly expressed in the gravel components than in the sand, and therefore provide an opportunity to evaluate the main sediment dispersal routes in the basin. The 3-5 mm fraction of a number of gravel samples from different units has been analyzed. The following components have been distinguished:
- Quartz;
- Crystalline components (quartz-feldspar fragments, feldspar, igneous or metamorphic aggregates, porphyry);
- Flint (grey and brown flint);
- Other components (different types of sedimentary rocks, quartzite).
Within the latter group, several typical elements have been distinguished separately: lydite and radiolarite, chalcedony, southern Mesozoic components. The latter have been derived from the drainage basin substratum upstream of the Nordhorn basin, and consist of claystone and shale fragments (e.g. 'Blatterschiefer'), white fine-grained sandstone (Bentheimer and Gildehauser sandstone), reddish sandstone (Buntsandstein type), soft white limestone and marl, and fossil fragments.

Besides the Mesozoic substratum, gravel sources for the basin sediment are the Drente Formation and the Enschede Formation. Both differ mainly in quartz and crystalline components. Pure glacigenic material from the Drente Formation (DG association, Zandstra, 1978) is characterized by high percentages (25-90 %) of crystalline components, low percentages (<16 %) of quartz and a variable amount of angular flint. By contrast, the Enschede Formation is rich in quartz (NN association, Zandstra 1978). Quartz percentages may exceed 75 %, together with additions of crystalline and other components, both in the order of 10 %. Flint is rare; typical is the presence of a few percentages of lydite and radiolarite (Maarleveld, 1956).

The gravel samples in the basin fill represent a mixture of the DG and NN associations (table V.7, fig. V.11). In the Beverborg area (Beverborg section, Lutterzand and De Poppe exposures, location in fig. IV.1) the difference between the Tilligte beds and Beverborg Member proves to be small. Only the flint percentage in the Beverborg Member is significantly higher.

Differences between the lithostratigraphical units are subordinate to regional differences. In the Beverborg area the Beverborg Member contains less quartz and more crystalline components than its equivalent in the Tilligte section. The difference is attributed to contrasting source areas. The Ootmarsum ice-pushed ridge from which the sediment in the Tilligte basin has been derived, consists for a larger part of quartz-rich Enschede Formation material than the Oldenzaal ice-pushed ridge.

Within the Tilligte beds also a significant difference in crystalline components is found between different areas. The Tilligte beds in the Lattrop-Denekamp area (Lattrop-Denekamp section and eastern part of Laarhuis-Rammelbeek section) contain less crystalline components than in the Beverborg area. This is also attributed to the dominance of sediment sources on the Ootmarsum ice-pushed ridge for the Lattrop-Denekamp area.

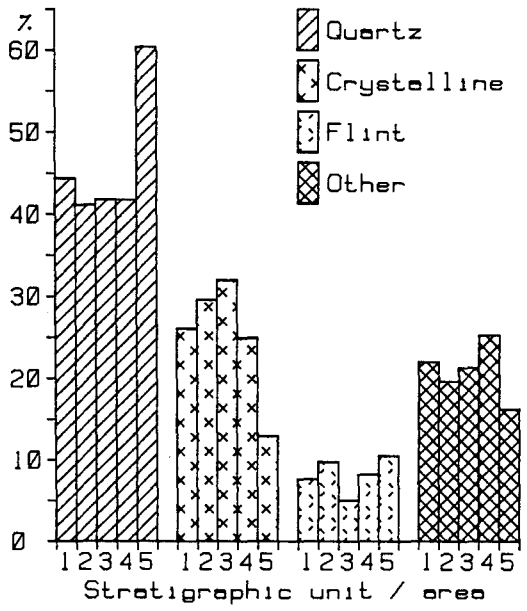

Figure V.11. Fine gravel petrology of different areas and units. Percentages indicate mean values. 1: All samples (50 samples); 2: Beverborg Member, Beverborg section (10 samples); 3: Tilligte beds, Beverborg section (11 samples); 4: Tilligte beds, Denekamp/ Lattrop area (15 samples); 5: Beverborg Member and Singraven Formation, Tilligte section (6 samples).

Component	Sample group					Differences		
	1	2	3	4	5	2-3	2-4	3-5
Quartz	44.4	41.1	41.8	60.4	41.7		-	
Crystalline	26.0	29.5	31.9	12.9	24.9		+	+
Flint	7.6	9.7	5.0	10.5	8.2	+		--
Other	22.0	19.6	21.3	16.2	25.3			

Table V.7. Mean fine gravel composition of basin fill units in different basin areas. 1: All samples (n = 50 samples); 2: Beverborg area, Beverborg Member (n = 10); 3: Beverborg area, Tilligte beds (n = 11); 4: Tilligte section, Beverborg Member (n = 6, partly Holocene reworked); 5: Lattrop-Denekamp area, Tilligte beds (n = 15). See also fig. V.11. +: significant positive difference, -: significant negative difference (t test, 10 % two-sided significance level).

In fig. V.12 the crystalline components percentage within the Tilligte beds is mapped. The highest values occur in the Beverborg area south of Denekamp. Lowest percentages occur northwest of Denekamp, intermediate percentages east of Denekamp. In that area mixing has taken place between sediment originating from the western Ootmarsum ice-pushed ridge and material from the southern Dinkel valley. It shows the presence of a general northeastward drainage of the Nordhorn basin during most of the Middle Pleniglacial which is confirmed by the borehole sections (par. IV.4.2, VIII.2.1).

Variations on this general pattern appear to have occurred however. In fig. V.13 the percentage of Mesozoic components in the Tilligte beds is mapped. With a few exceptions, most of the samples confirm the northeastern drainage in the Nordhorn basin, derived from the crystalline components. Low percentages of Mesozoic components occur northwest of Denekamp, high values south of Denekamp, intermediate values to the east. However, north of Denekamp three samples with an extremely high amount of Mesozoic material are found. These samples are all situated in channel deposits within the basal clays of the Tilligte beds. Apparently an important SSE-NNW drainage line existed during deposition of the basal clays. This has been a continuation of the drainage established during the Early Pleniglacial (fig. IV.7). The samples which indicate the more easterly drainage direction all postdate erosion level I. Apparently erosion level I is associated with a shift from dominantly SSE-NNW drainage towards SW-NE drainage in the Nordhorn basin.

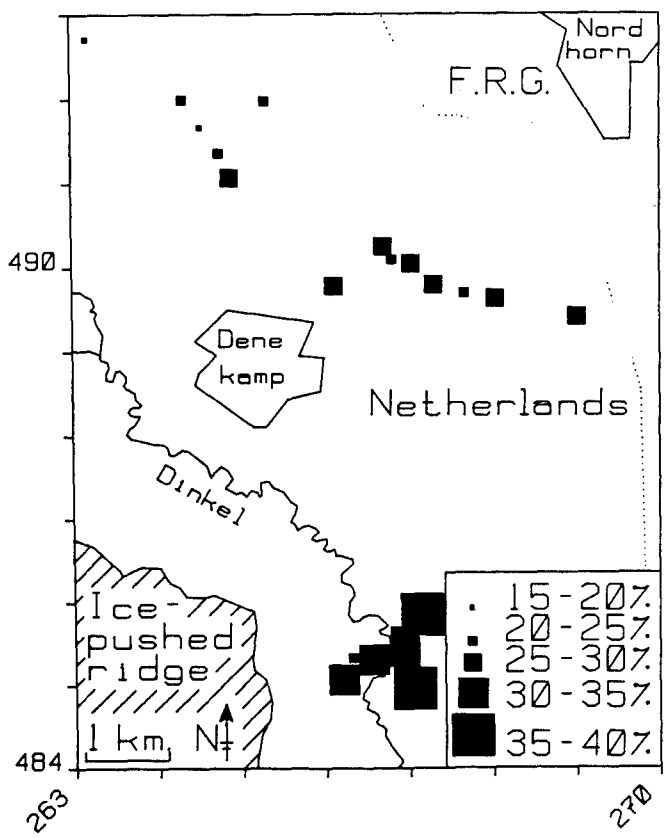

Figure V.12. Crystalline component percentages in the Mekkelhorst Member. The distribution shows influx of crystalline-poor material from the eastern part of the basin, mixing with crystalline-rich material from the south.

Figure V.13 (next page). Mesozoic components percentages in the Mekkelhorst Member. Main source of this material is the Dinkel valley. Extremely high values are associated with coarse channel deposits within the Lattrop beds, indicating a possible northwesterly course of the Dinkel at the start of the Middle Pleniglacial. Lower values occur in samples derived from younger levels.

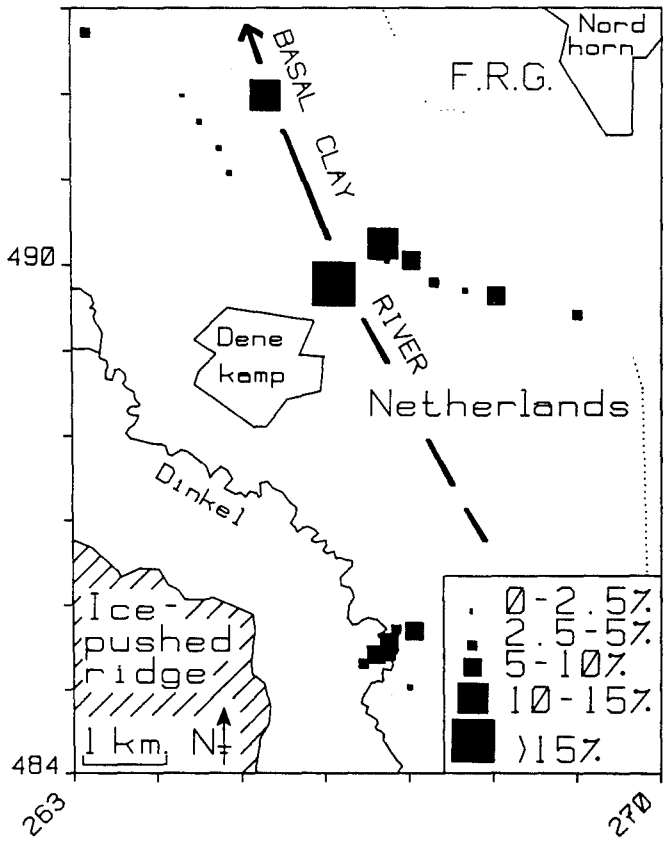
Nord horn
F.R.G.
BASAL CLAY
RIVER
Dene kamp
Netherlands
Dinkel
Ice-pushed ridge
1 km
N
0-2.5%
2.5-5%
5-10%
10-15%
>15%
490
484
263
270

VI. Stratigraphy and sedimentary environment in the Hengelo basin.

VI.1. Introduction.

Exposures reaching into the Middle Pleniglacial sediments are rare within the Dinkel basin. Therefore two exposures from the neighbouring Hengelo basin have been taken into consideration. The locations of the exposures have been indicated on fig. IV.1. The Twente Formation stratigraphy of the Hengelo basin (fig. VI.1) has been described extensively by Zagwijn (1974).

Because of the importance of sedimentary structure and periglacial phenomena descriptions in this section, a short discussion of the terminology with regard to this topic is useful. In the description of sedimentary structures the terminology of Reineck & Singh (1975) and Collinson & Thompson (1982) has been followed which is a slightly modified version of the terminology developed McKee & Weir (1953) and Campbell (1967). The legend for schematical representation of the sedimentary structures (fig. VI.2) has been derived partly from Selley (1970).

The terminology for the description of soil deformation structures of supposedly cryogenic nature follows that of Vandenberghe (1988). Six basic types of deformations are discerned using criteria as symmetry, amplitude, wavelength, and pattern of occurrence. Type 1 involutions are individual folds of small wavelength and amplitude. Type 2 involutions are regular, symmetrical and intensely convoluted forms with amplitudes above 0.6 m. Type 3 involutions are of the same nature, but of smaller dimensions. Type 4 consists of solitary forms (drops and diapirs) of different size. Type 5 deformations are upward directed structures in platy 'dikes', solitary or arranged in polygons. Type 6 represents irregular structures. In the exposures described below exclusively type 1, 2 and 3 occur. Other structures of cryogenic origin are frost cracks or fissures (Dylik & Maarleveld, 1967; Maarleveld, 1976). These are usually less than 10 cm wide. Ice wedge pseudomorphs or casts are larger fissure structures which show evidence of the erstwhile presence of ice which has been replaced by overlying or surrounding sediment upon thawing (Harry & Gozdzik, 1988). Characteristic evidence is the presence of slump structures, downturned laminae, and faulting in the adjacent sediments (Vandenberghe, 1983a,b).

VI.2. The Hengelo A1 exposure.

VI.2.1. Lithostratigraphy and sedimentary structures.

In 1986 a large exposure on the northeast side of the town of Hengelo has been made for highway construction works (location: fig. IV.1). This exposure has been nearly 300 m long and up to 8 m deep. It is situated in the Hengelo basin which presently belongs to the Regge drainage system. With exception of the uppermost units (11 and 12) the entire sequence in the exposure is of Middle Pleniglacial age (fig. VI.3). The sequence description starts at the base.

Unit 1: medium to coarse calcareous sand, finer towards the top. In the few locations where this unit has been exposed, it shows planar and scour-and-fill cross-bedding (photo VI.1). The foresets are overlain by cross-laminated sand with silty layers.

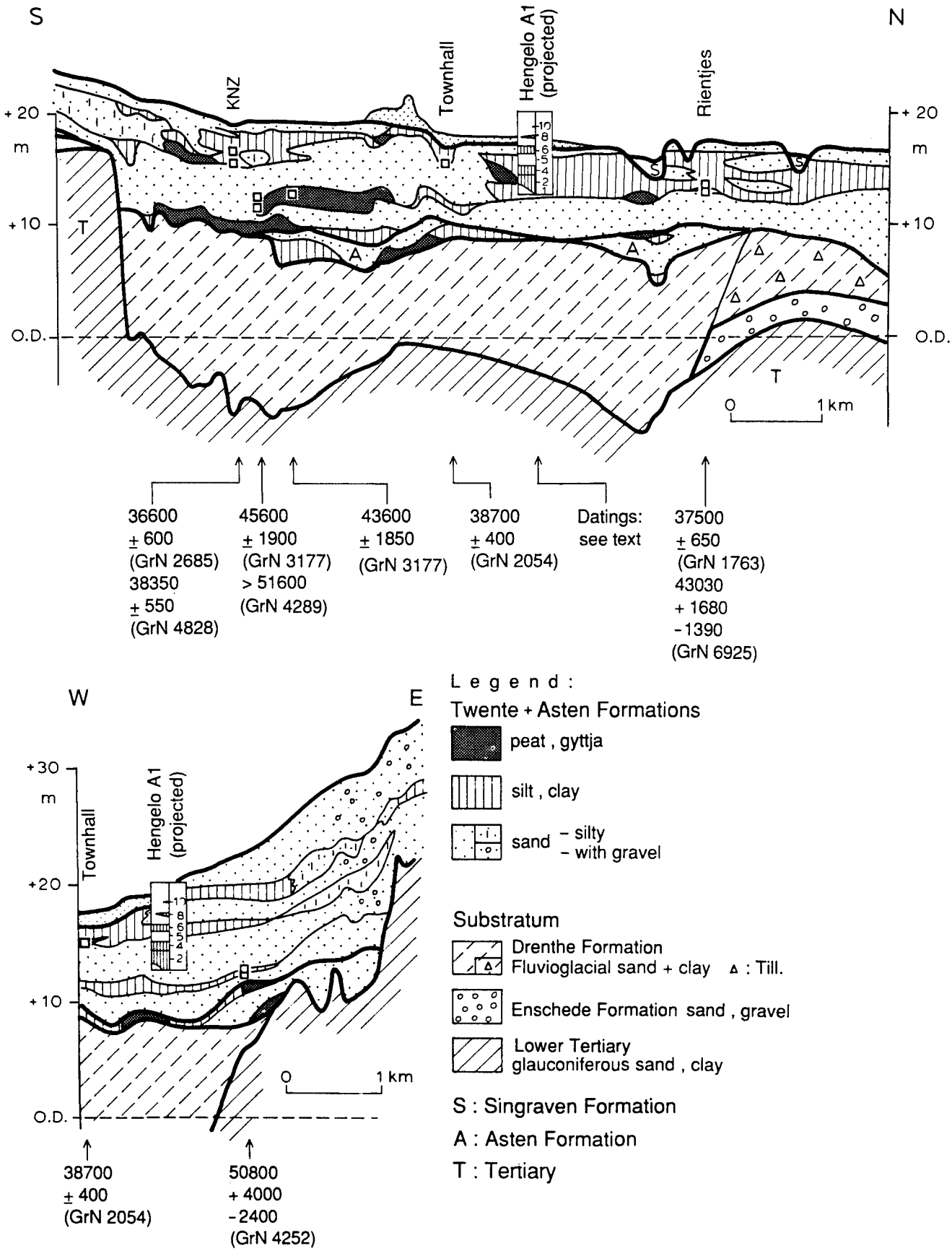

Figure VI.1. Sections through the Hengelo basin (simplified, after Zagwijn, 1974). The Hengelo A1 exposure is projected on both sections. Vertical scale in m relative to O.D.

LEGEND OF EXPOSURE SECTIONS

LACQUER PEELS

Column I: composition

Column II
Sedimentary structures and texture: grainsize indicated by width of column. or vertical line: sorting indicated by vertical line.

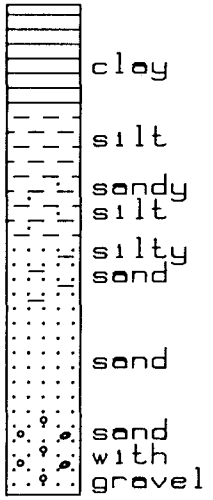

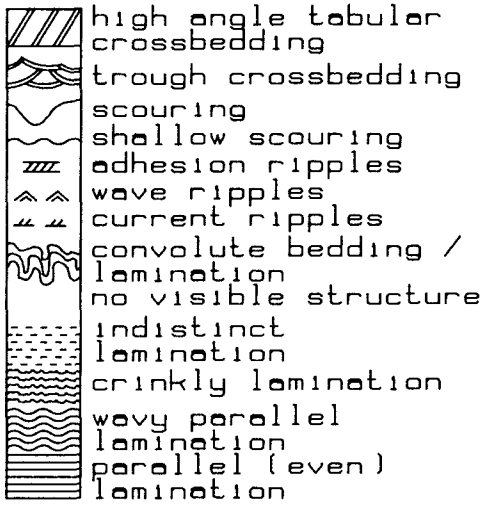

Thicker lines indicate prominent bedding planes

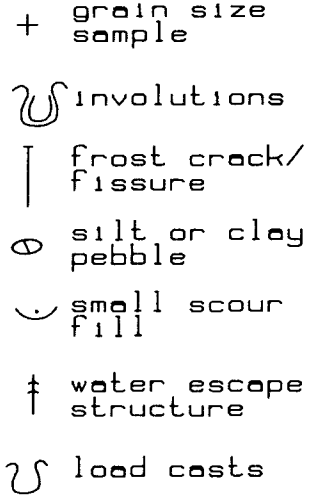

PIT FACE DRAWINGS

Figure VI.2 (previous page). Legend to sedimentary structure representations in lacquer peels and core logs, and legend of exposure drawings.

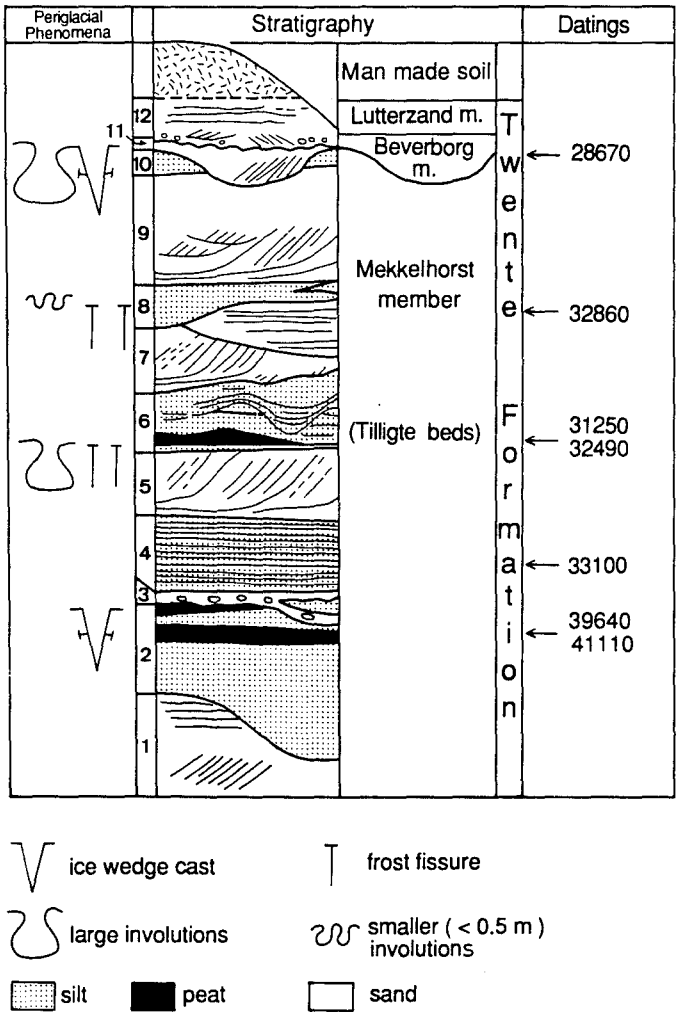

Figure VI.3. Stratigraphy of the Hengelo A1 exposure. See fig. IV.1 for location.

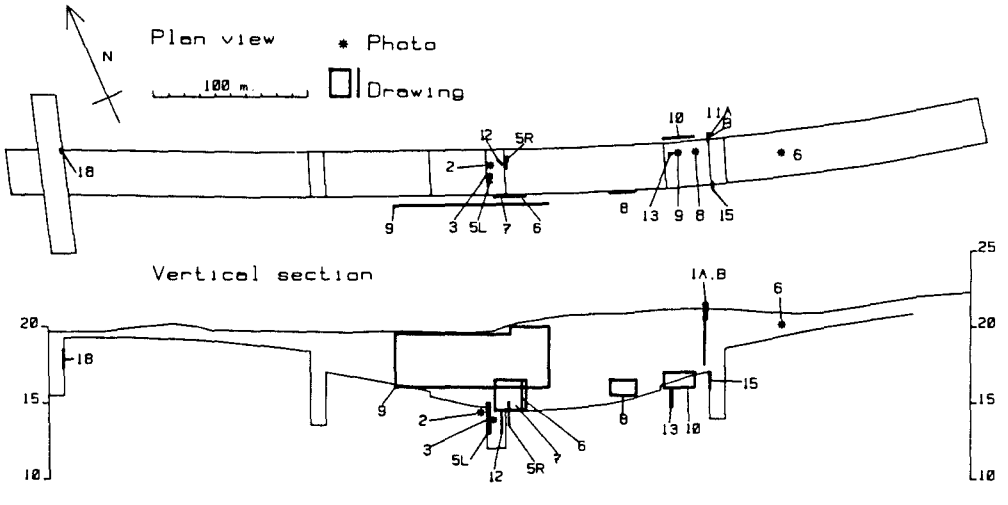

Figure VI.4. Overview of the Hengelo A1 exposure, with location of figures and photos. Vertical scale in m relative to Dutch ordnance datum.

The transition towards units 2 is locally sharp, but gradual in most places.

Unit 2: calcareous light grey silt with sand beds in the lower part of the unit. The thicker sand layers may contain some gravel (fig. VI.5). Also wave ripples have been found. The top of the unit consists of largely structureless silt. One or two peaty-humic layers are intercalated. Above this peat some lenses of whitish, extremely calcareous material occur. Detailed sedimentary structures in the top of unit 2 appear to have been obliterated after deposition. This homogenization may be of pedogenic or cryogenic origin. A conspicuous feature of unit 2 is the presence of well developed ice-wedge casts which penetrate unit 2 from above, forming a polygonal network with a polygon diameter of ca. 20 m (photo VI.2,3). Small gully fills overly the ice wedge casts (photo VI.4).

Unit 3: A 10 cm thick bed of coarse sand with some gravel and much angular lumps of peat and silt (fig. VI.5). Unit 3 truncates unit 2 and the ice wedge casts horizontally. The erosion surface extends itself over the gully fills above the ice wedge casts as a zone of coarser material.

Unit 4: dark grey, calcareous, sandy silt with undisturbed even parallel lamination. Darker laminae contain finely divided organic matter (fig. VI.5).

Unit 5: rather well sorted medium sand, cross-bedded with large foresets. The transition from unit 4 to 5 is gradual. Towards the top of unit 4 sandy layers increase in thickness and number. The top of unit 5 is strongly disturbed by type 3 involutions and frost fissures. The cross-bedding consists of a single layer with foresets, approximately 0.8 m. thick. The foresets resemble delta-foresets with well developed toesets attached at the base (fig. VI.6). Throughout the entire exposure the foresets are remarkably straight and the strike direction is very uniform (around N 315° E), varying within some 20° only. Rare local deviations are present, for example on the left side of figure VI.6. At distances varying between 2 and 6 m the foresets are covered by silt drapes. Along the toesets these silt drapes merge gradually with the horizontally bedded sand/silt transition between unit 4 and 5 (fig. VI.6,7). The silt drapes show small-scale slump structures and wave ripples. The topsets which belong to the delta-like foresets are obscured by the involutions at the top of unit 5. The transition of unit 5 to the silty clay at the base of unit 6 is usually sharp. Locally sand with a large amount of fine silt granules occurs at the top of unit 5.

Unit 6: Olive brown to dark grey, humic and peaty calcareous silt. The typical sequence within this unit consists of dark grey clay - peat - silt with peaty layers - laminated sandy silt with sand layers. The clay is usually strongly involuted with the sand of unit 5 underneath, the remainder of the unit is only slightly deformed. Clearly, the involutions postdate deposition of the basal clay bed of unit 6. Near the top a small channel with

Figure VI.5 (next page). Hengelo A1 exposure: Transition from unit 1 to unit 2 and erosion surface associated with unit 3, and top of an ice wedge cast (left). Larger numbers in drawing refer to units in fig. VI.3. See fig. VI.2 for legend, fig. VI.4 for location in the exposure, table VI.1 for information on the radiocarbon datings, table VII.1 for grainsize samples. Palaeobotanical results have been published by Ran et al. (1990).

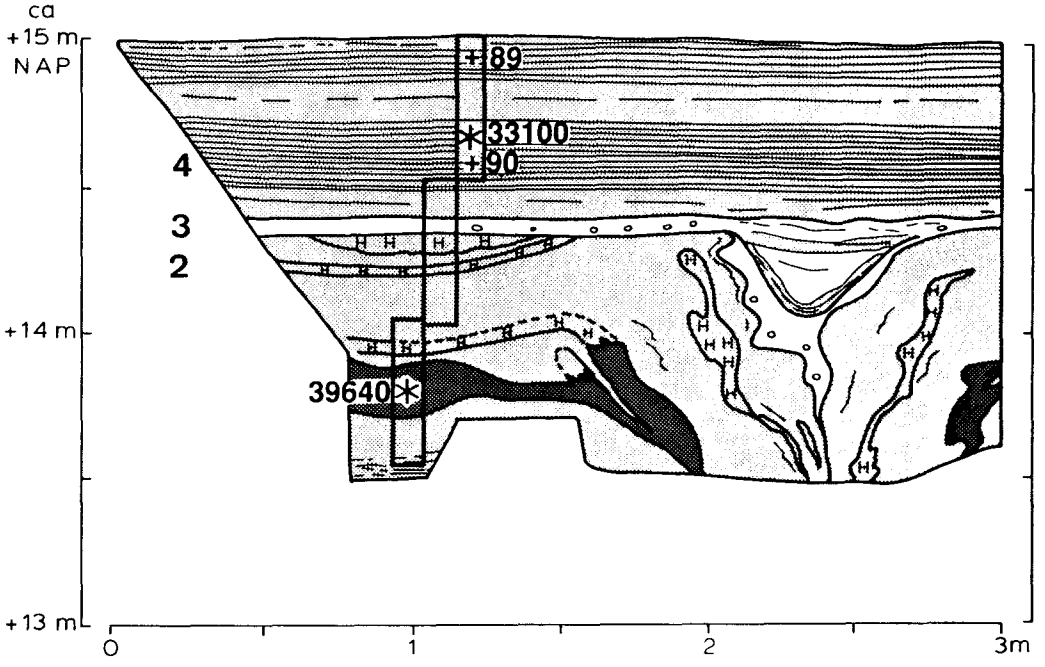
ca
+15 m
NAP
+89
33100
+90
4
3
2
+14 m
39640
+13 m
0
1
2
3m

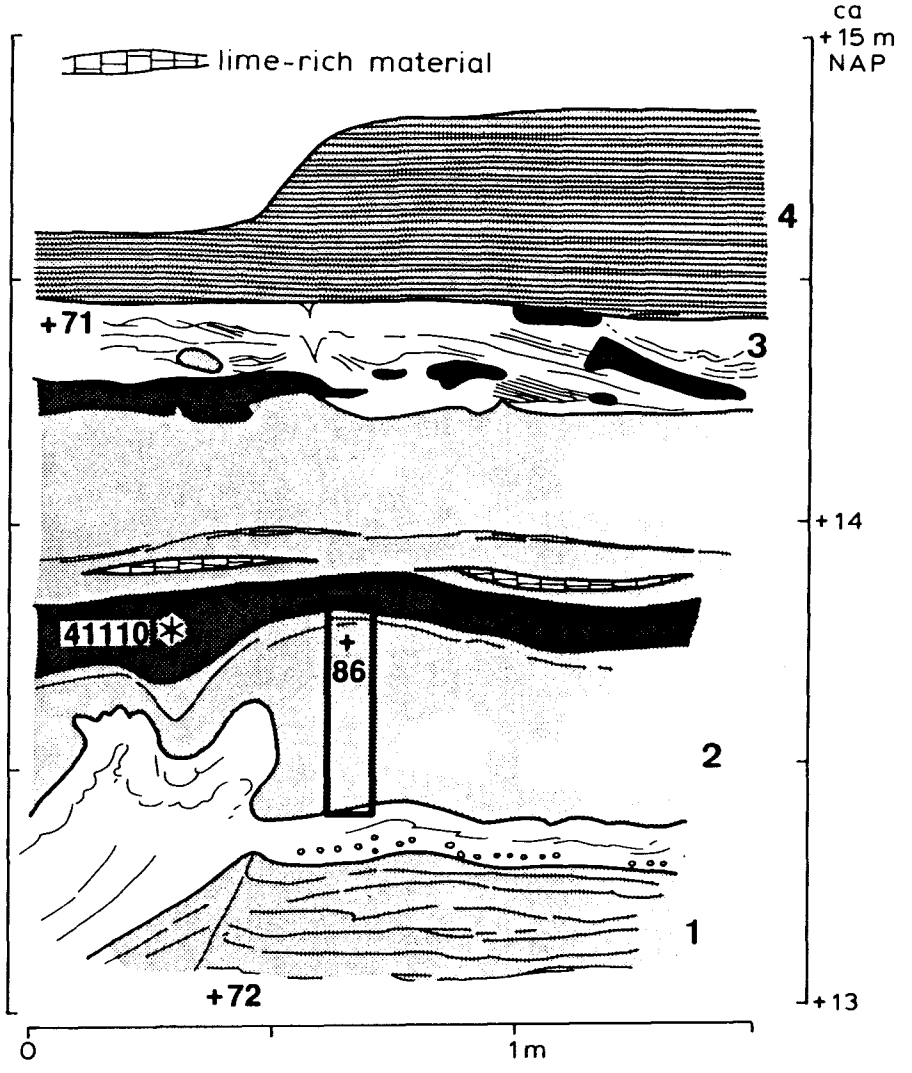
lime-rich material
ca
+15 m
NAP
4
+71
3
+14
41110
+
86
2
1
+72
+13
0
1m

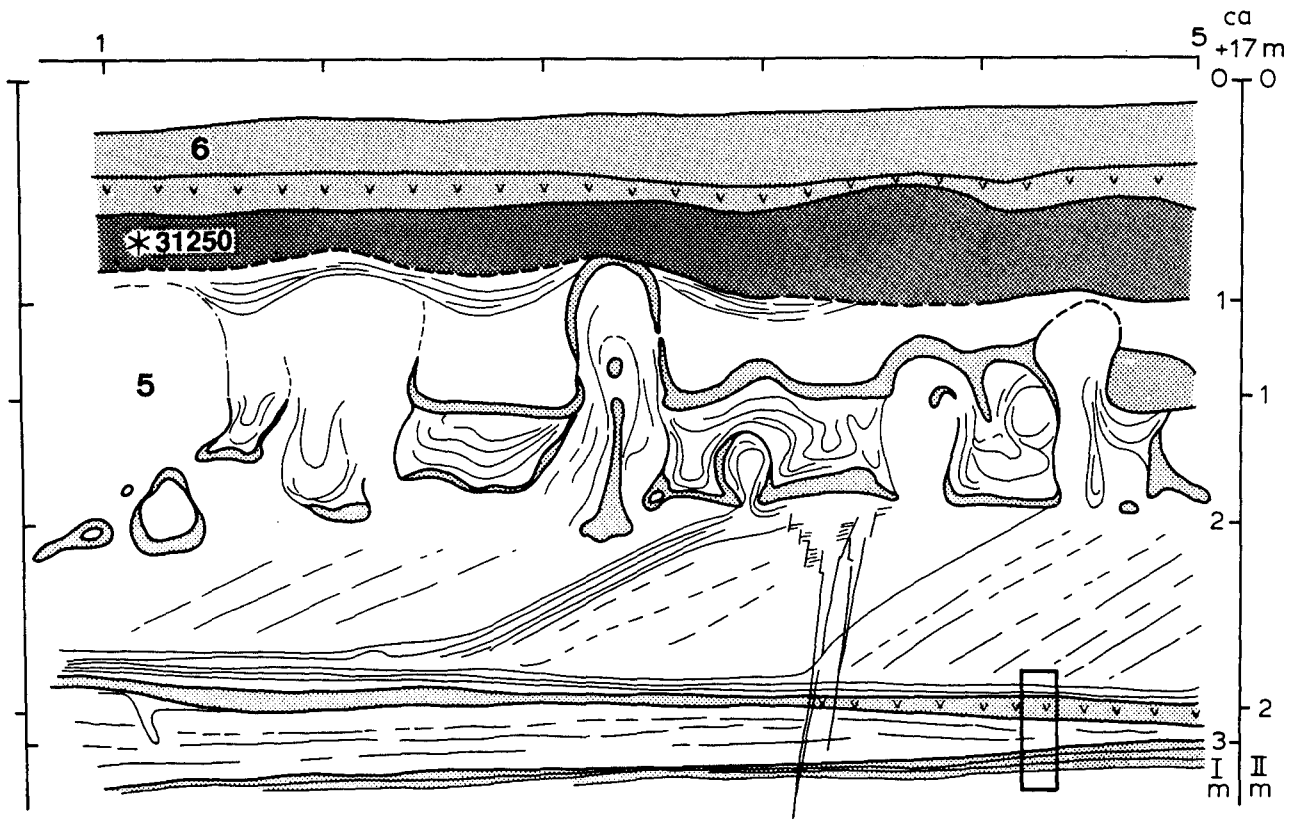

Figure VI.6. Hengelo A1 exposure: Sedimentary structures in unit 5. Numbers in the drawing refer to units in the fig. VI.3. See fig. VI.2 for legend, fig. VI.4 for location in the exposure, table VI.1 for information on the radiocarbon dating. Scale I: vertical scale along pit face; scale II: true vertical scale. Palaeobotanical results have been published by Ran et al. (1990).

associated levees has been found (fig. VI.8). The base of the channel has not been exposed. The channel fill mainly consists of parallel laminated sandy silt. It laterally changes into the top sediments of unit 6 which overlies the levees.

Unit 7: well sorted medium sand. The transition from unit 6 to 7 is gradual, but locally sharp. The sand is not calcareous. Like unit 5, unit 7 also consists of a single unit with large foresets of a delta-like appearance (fig. VI.9). The toesets merge with interlayered silt/sand at the top of unit 6. The only difference with unit 5 is the less prominent development of silt drapes on

Figure VI.7 (next page, top). Hengelo A1 exposure: Foresets with silt drapes in unit 5. Numbers in the drawing refer to units in the fig. VI.3. Lacquer peel: fig. VI.14. See fig. VI.2 for legend, fig. VI.4 for location in the exposure. Scale I: vertical scale along pit face; scale II: true vertical scale.

Figure VI.8 (next page, bottom). Hengelo A1 exposure: Channel with associated levees near the top of unit 6. The channel is overlain by lacustrine silt at the top of unit 6 and foresets of unit 7. Numbers in drawing refer to units in fig. VI.3. Oblique hatching: substratum of the channel. See fig. VI.2 for legend, fig. VI.4 for location in the exposure, table VI.1 for information on the radiocarbon dating, table VII.1 for grainsize samples. Scale I: vertical scale along pit face; scale II: true vertical scale.

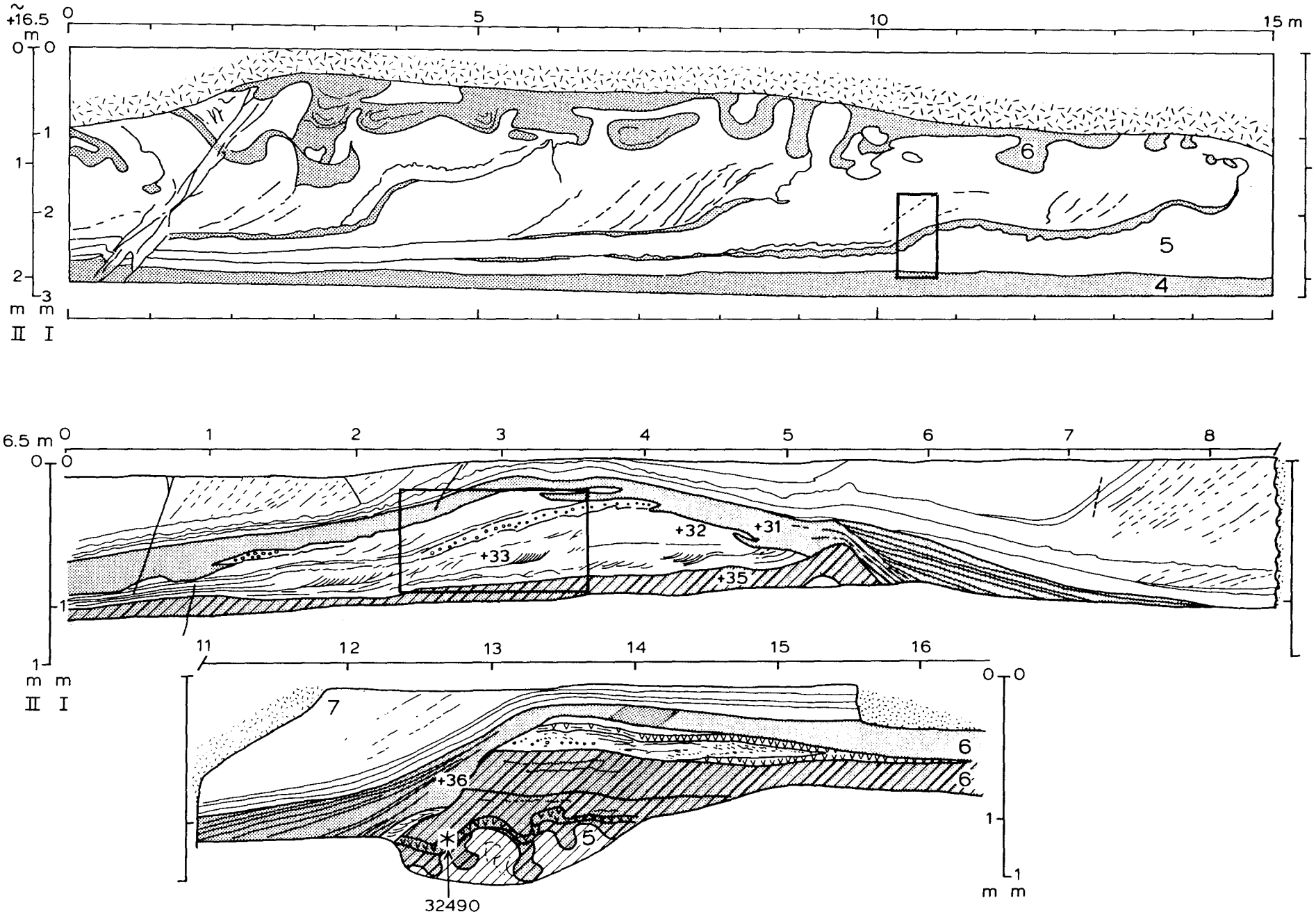
~
+16.5
m
0
5
10
15 m
0
1
2
3
m m
II I
6
5
4
16.5 m
0
1
2
3
4
5
6
7
8
+32
+31
+33
+35
11
12
13
14
15
16
7
6
6
+36
5
32490
1
m m

the foresets (fig. VI.9). The direction of the foresets also has been changed somewhat, as it varies around N 0° E (fig. VI.10). The top of unit 7 is disturbed by type 3 involutions also, but these involutions are generally smaller and more localized than those at the top of 5.

On the west side of the exposure the sedimentary structure of unit 7 changes into predominantly even, parallel bedding and lamination. The transition to unit 6 is erosive below this facies, with many scours (fig. VI.9). Bed tracing reveals that the parallel laminated facies partly overlies the foresetted facies, and grades into the topsets of the latter. The foresetted facies rapidly disappears between the horizontally laminated facies and the top of unit 6.

Unit 8: grey silty clay with many sand intercalations. Unit 8 is discontinuous, it wedges out between unit 7 and 9. The base of unit 8 is disturbed by type 3 involutions at many places. Locally, these also occur within unit 8 above sand intercalations (fig. VI.9). At the base a thin peat bed is found, consisting of mosses. Also wave ripples have been found (photo VI.5).

Unit 9: mainly well sorted, medium sand. The sedimentary structures in unit 9 are largely obliterated by both involution and soil formation. As far as could be observed, two types of lithofacies occur: delta-like foresets as described from unit 5 and 7 and coarse sand with some gravel showing sets of tabular cross-bedding (fig. VI.11). The latter facies is probably of local occurrence only.

Unit 10: humic and peaty sandy silt. This unit occurs as isolated 'balls' in the centre of intensely convoluted type 2 deformations (photo VI.6). These are the same deformations which are responsible for the disturbance of unit 9. Unit 10 is best preserved, where the overlying units 11 and 12 are well developed. The thickest occurrences are found in the easternmost part of the exposure. Insofar structures are preserved, these consist of thin parallel bedding and lamination caused by differences in sand and organic matter content.

Unit 11: coarse sand with some gravel. The unit is probably at most 0.75 m. thick, and cannot be traced with certainty throughout the whole exposure because of intense deformation and pedogenesis. Where unit 11 is well preserved (generally where unit 12 is thickest), its base proves to have taken part in the type 2 deformations which influenced unit 9 and 10. The deformation is less intense however. In these locations, unit 11 consists of shallow, wide channel fills. The top of unit 11 is marked by gravel strings and shallow scours (fig. VI.11). The unit is probably absent or very thin in most of the exposure.

Unit 12: fine to medium sand with even lamination. Unit 12 occurs only locally, underlying positive relief elements of the present-day surface.

Figure VI.9 (next page). Hengelo A1 exposure: General overview of unit 6-10 in the western part of the exposure. Numbers in drawing refer to units in fig. VI.3. Lacquer peels (from west to east): fig. VI.16, 17. See fig. VI.2 for legend, fig. VI.4 for location in the exposure, table VI.1 for information on the radiocarbon dating, table VII.1 for grainsize samples. Scale I: vertical scale along pit face; scale II: true vertical scale.

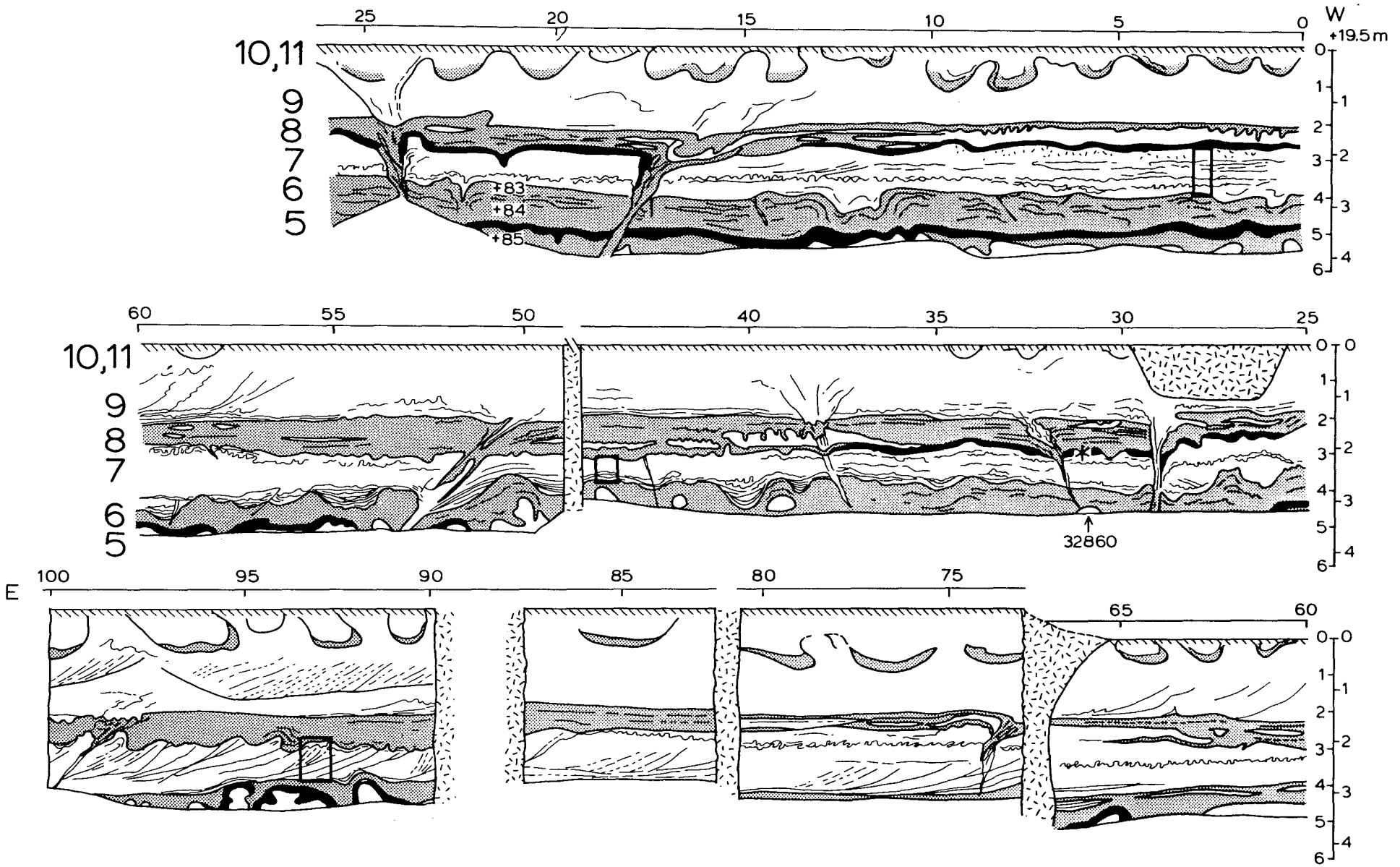
25
20
15
10
5
0
W
+19.5 m
10,11
9
8
7
6
5
+83
+84
+85
60
55
50
40
35
30
25
32860
100
95
90
85
80
75
65
60
E

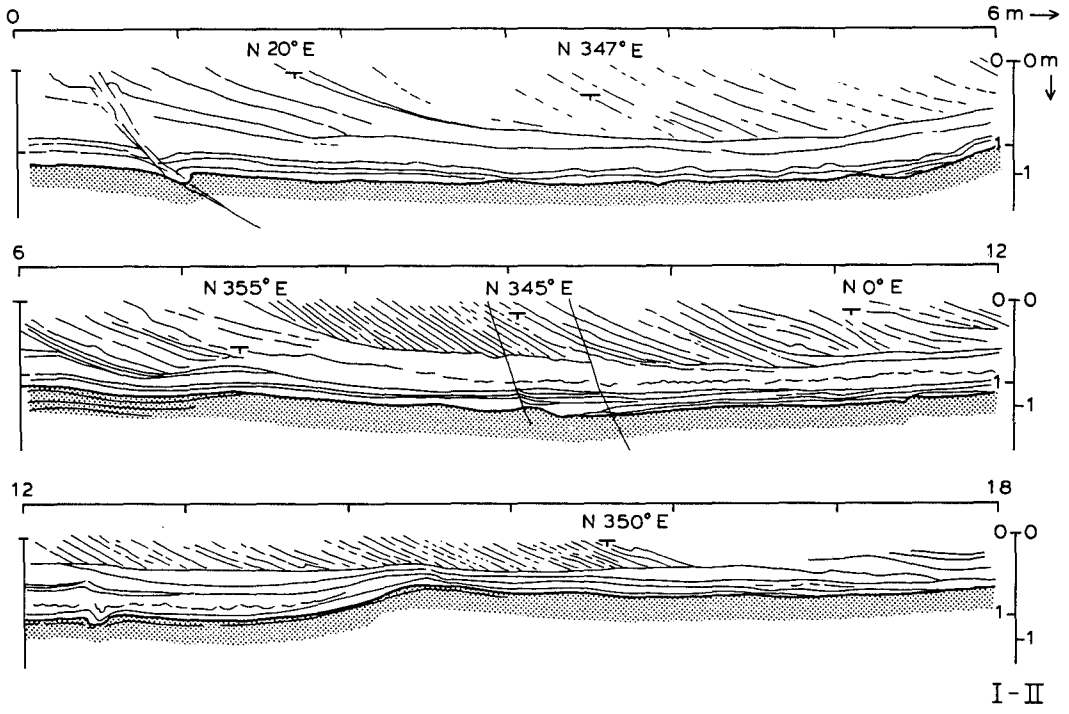

Figure VI.10. Hengelo A1 exposure: Foresets in unit 7, with strike directions. Numbers in drawing refer to units in fig. VI.3. See fig. VI.2 for legend, fig. VI.4 for location in the exposure. Scale I: vertical scale along pit face; scale II: true vertical scale.

VI.2.2. Chronostratigraphy.

Ice wedge casts from Early and Late Pleniglacial age are widely known in the Netherlands (Van der Hammen et al., 1967; Zagwijn & Paepe, 1968; Maarleveld, 1976; Vandenberghe, 1985). In this location however, the lowermost ice wedge cast level is of Middle Pleniglacial, rather than Early Pleniglacial age. This has been derived from the radiocarbon datings (table VI.1). The datings on the peat bed in unit 2 just below the first ice wedge cast level indicate an age between 39 and 42 ka. There are no reasons to doubt these results, since the extract and residue datings of the first sample closely overlap, and are reproduced by a second dating from the same peat bed.

Unit	Material	Residue dating	Extract dating	Laboratory nr.
2	peat	41110 ± 480	39200 +1800 -1500	GrN 13427/14221
2		39640 ± 370		GrN 14215
4	silt	33100 ± 600		GrN 15123
6	peat+silt	31250 ± 600		GrN 15124
6	peat	32490 ± 160	30040 ± 450	GrN 13426/15146
8	peat	32860 ± 270	27350 ± 210	GrN 13424/13425
10	silt	28670 ± 110	27780 ± 230	GrN 13428/13429

Table VI.1. Radiocarbon datings on the Hengelo A1 sequence.

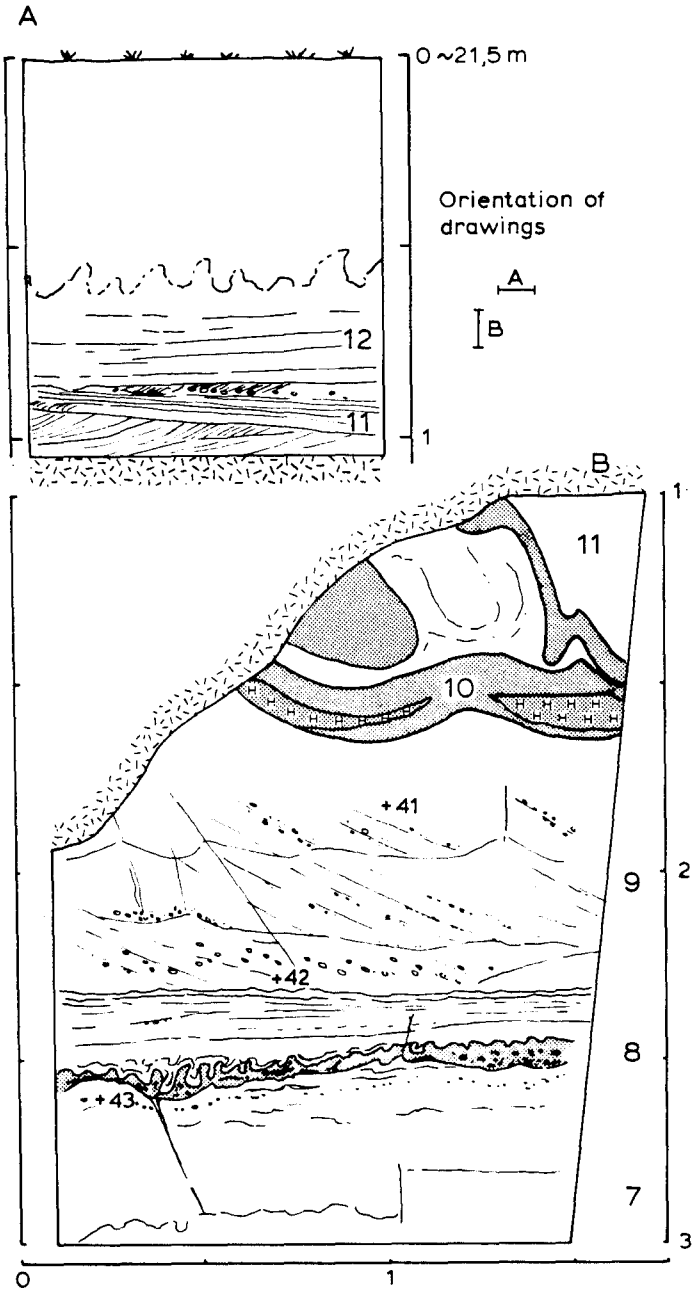

Figure VI.11. Hengelo A1 exposure: sedimentary structures associated with the pinching out of unit 8 on the eastern side of the exposure, and coarse crossbedded facies of unit 9. Numbers in drawing refer to units in fig. VI.3. See fig. VI.2 for legend, fig. VI.4 for location in the exposure, table VII.1 for grainsize samples.

Also lithostratigraphical correlation points to a Middle Pleniglacial age of unit 2. The top of the 'Lower Clay Member' (Zagwijn, 1974) which represents the oldest Middle Pleniglacial sediments in the Hengelo basin, is found at the same level, or deeper as unit 2 in this exposure (fig. VI.1). According to penetration cone soundings and borings made for geotechnical site investigations clay and peat occur slightly below the deepest level of the exposure (at ca. 10 m. + O.D.). These beds probably

correlate with a peat/clay bed in the sections of Zagwijn (1974) which has pollenanalytically been dated as Late Eemian (fig. VI.1). Furthermore, high lime content such as that of unit 2 is in the Dinkel basin more characteristic for Middle Pleniglacial silts than for Early Glacial fine grained deposits.

An upper age limit of the ice wedge casts is 33.1 ka as indicated by the dating on unit 4. However, the radiocarbon ages obtained from units 4-8 are most likely too young. Besides the significantly differing residue and extract ages in unit 6 and 8, the datings show stratigraphical reversal and yield an improbably high sedimentation rate for these units. By correlation with other sites described by Zagwijn (1974) the age range for the ice wedge cast formation can be further delimited. In the nearby Rientjes and KNZ exposures (Zagwijn, 1974) large type 2 involutions (indicating permafrost degradation) are overlain by an erosion level and lacustrine deposits which can be correlated with units 3 and 4 in the Hengelo A1 exposure. Datings from the Rientjes and KNZ exposures bracket the age of the type 2 involutions respectively between 43.03 - 37.5 ka, and 38.35 - 36.6 ka. Consequently, the ice wedge casts are not younger than 37.5 ka.

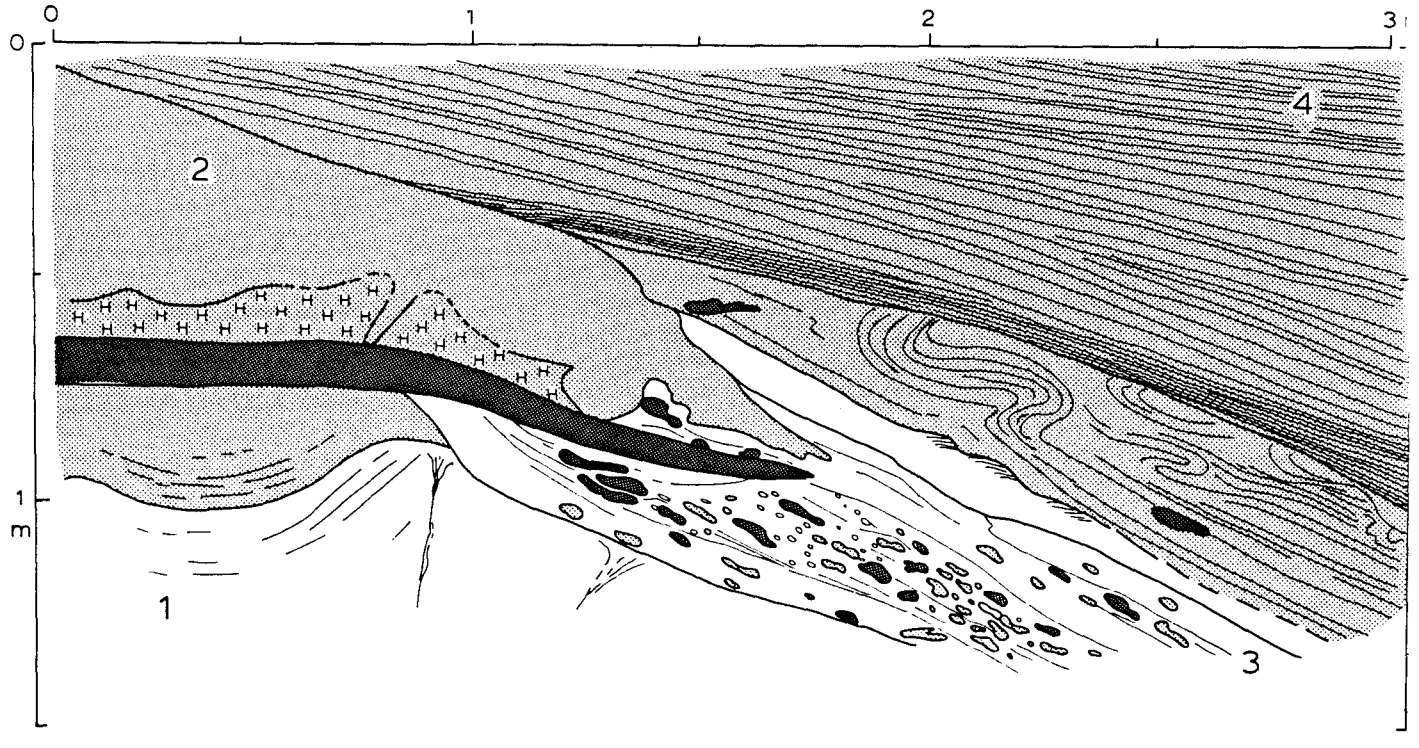

Figure VI.12 (next page). Hengelo A1 exposure: Bank and infilling of a channel, incised in unit 2. See fig. VI.2 for legend, fig. VI.4 for location in the exposure. Numbers in drawing refer to units in fig. VI.3.

Well documented reports on Middle Pleniglacial ice wedge casts in the Netherlands are scarce, and do not include sites where their age is delimited closely by radiocarbon datings above and below. A site near Breda (fissures structures overlain by gyttja, of which the base has been dated at 37000 ± 600, GrN 2515) has been reported by Van der Hammen et al. (1967); according to Zagwijn (pers. comm.) a Middle Pleniglacial age is likely. Photos show that these fissure structures (developed in fine, silty

sands) are rather narrow and appear to be forms which are possibly transitional between frost fissures and true ice wedge casts. Another site where ice wedge casts of Middle Pleniglacial age (> 35 ka) have been found is a large temporary exposure near Den Helder (NW Netherlands; De Mulder, undated; Ruegg, 1978). In more southerly located loess sequences, also occasional ice wedge casts dating from the Middle Pleniglacial occur, in the time range between 38.6 and 45.6 ka (Haesaerts, 1985). Other ice wedge cast levels of possible Middle Pleniglacial age have been reported by Kolstrup & Mejdahl (1986) from Denmark, dated at 39 ± 5 ka (Thermoluminescence dating). Although these datings allow wide age ranges for these fissures and ice wedge casts it is likely that their age is similar to that of the ice wedge casts in the Hengelo A1 exposure. Apparently, on favourable sites permafrost with active ice wedges did exist in a time range of approximately 37.5 to 42 ka.

The remainder of the sequence also is largely of Middle Pleniglacial age (table VI.1). Unit 1, which is genetically related to unit 2, is also assumed to be of Middle Pleniglacial age. The entire sequence from unit 1 up to unit 10 is correlated with the Mekkelhorst Member in the Dinkel valley. The erosion associated with unit 3 is of the same age as erosion level II in the Tilligte beds (par. IV.6).

The dating of unit 10 confirms that the overlying topmost ice wedge cast level dates from the Late Pleniglacial. Unit 12 represents the Lutterzand Member s.s. A peculiar feature of this exposure is the small thickness of the Beverborg Member (unit 11), as compared with the borehole sections in the Dinkel valley. Since at least the base of unit 11 has been cryoturbated with the underlying sediments, unit 11 may be considered as contemporaneous with, or older than the ice wedge casts or involutions. The top of unit 11 represents the Beuningen gravel bed. An association of this gravel bed with shallow scours is also known from the Lutterzand exposure (Wijmstra & Schreve-Brinkman, 1971). Consequently unit 11 also may be correlated with the Beuningen gravel bed alone. The near absence of sediments between the Middle Pleniglacial deposits and the Beuningen gravel bed also has been noted by Zagwijn (1974). The insignificant thickness of the Beverborg Member may be explained by local factors, such as remoteness from prominent sediment sources.

VI.2.3. Environmental interpretation of the periglacial phenomena.

VI.2.3.1. The Middle Pleniglacial ice wedge casts in unit 2.

According to Péwé (1966) mean annual air temperatures should be below -6° to -8° C for ice wedge formation. The lithology of unit 2 (clayey silt, peat) is extremely favourable material for ice wedge development (Romanovsky, 1976, 1985; Pissart, 1987). Romanovsky (1976, 1985) indicates mean annual ground temperatures lower than -2.5° C for fine grained sediments like those of unit 2. Conversion of soil temperatures to air temperatures is uncertain, but climatological data (Walther & Lieth, 1960) from the region which is indicated by Romanovsky (1985) as the area where ice wedges in silt and clay are found, indicate mean annual air temperatures below -4.5° C. Ice wedge development in sands requires lower mean annual ground temperatures, below -5.5° C

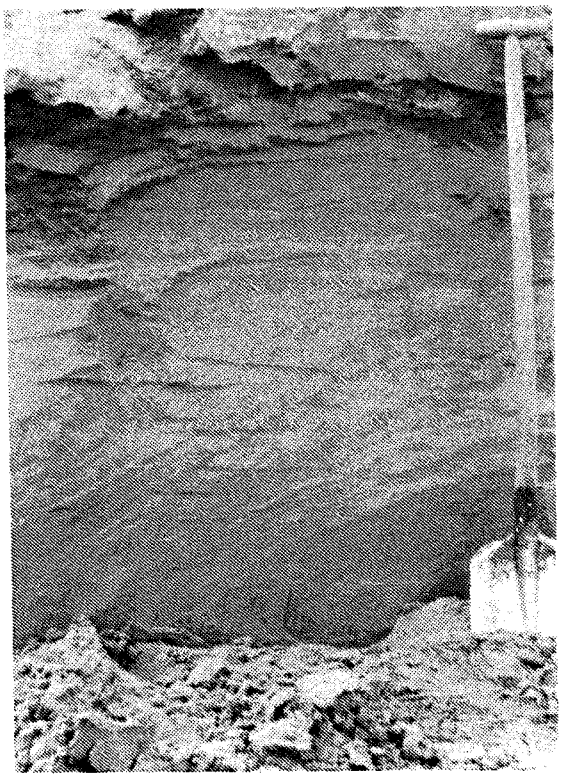

Photo VI.1 (top left). Hengelo A1 exposure: Crossbedding in unit 1. Location ca. 5 m east of fig. VI.12. Length shovel: 1 m.

Photo VI.2 (top right). Hengelo A1 exposure: Part of a polygonal network of ice wedge casts at the top of unit 2. See fig. VI.4 for location in the exposure. Shovel: 1 m.

Photo VI.3 (below). Hengelo A1 exposure: Ice wedge cast in the top of unit 2. See fig. VI.4 for location in the exposure. Shovel: 1 m.

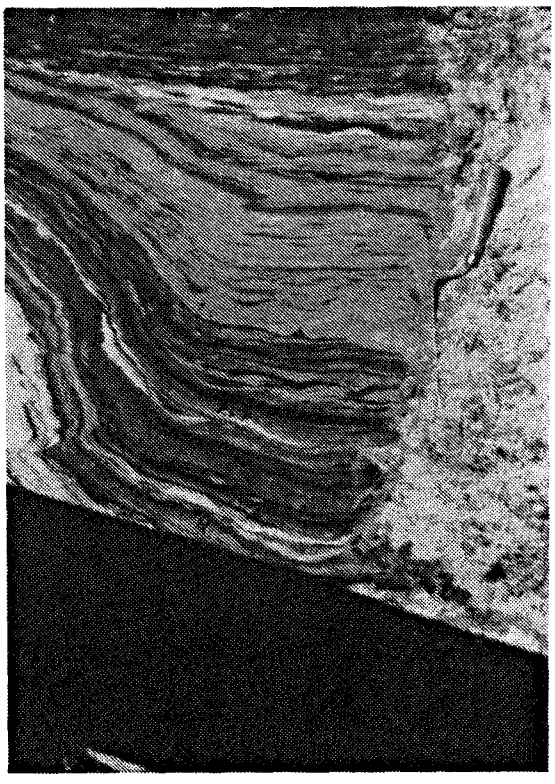

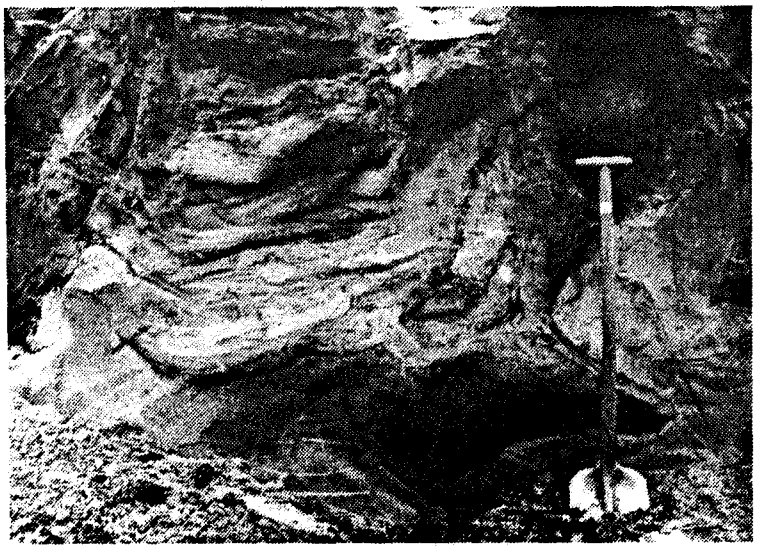

Photo VI.4 (top left). Hengelo A1 exposure: silty channel fill sediment above ice wedge cast in unit 2. Jointer: 17 cm.

Photo VI.5 (top right). Hengelo A1 exposure: Wave ripples in unit 8, horizontal section. Jointer: 17 cm.

Photo VI.6 (below). Hengelo A1 exposure: Very large involutions with remnants of unit 10 in the centre. The involutions are of Late Pleniglacial age. See fig. VI.4 for location in the exposure. Shovel: 1 m.

Photo VI.7 (top). Hengelo A1 exposure: Slump structure in evenly laminated silt in a channel infill, incised in unit 2. See also fig. VI.12. Jointer: 17 cm.

Photo VI.8 (right). Hengelo A1 exposure: Plan shape of involutions at the top of unit 5. See fig. VI.4 for location in the exposure. Shovel: 1 m.

Photo VI.9 (left). Hengelo A1 exposure: Plan shape of involutions at the top of unit 5. See fig. VI.4 for location in the exposure. Shovel: 1 m.

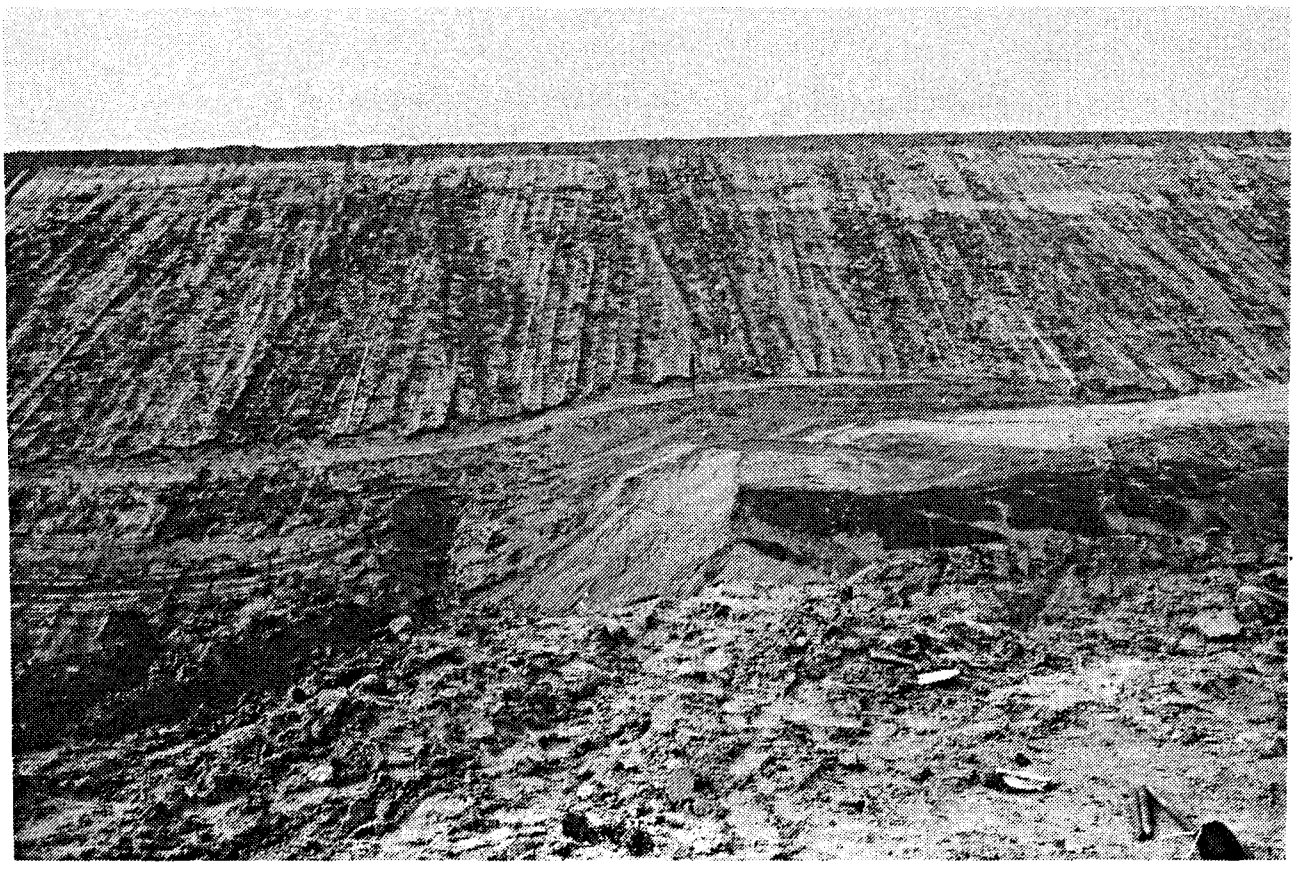

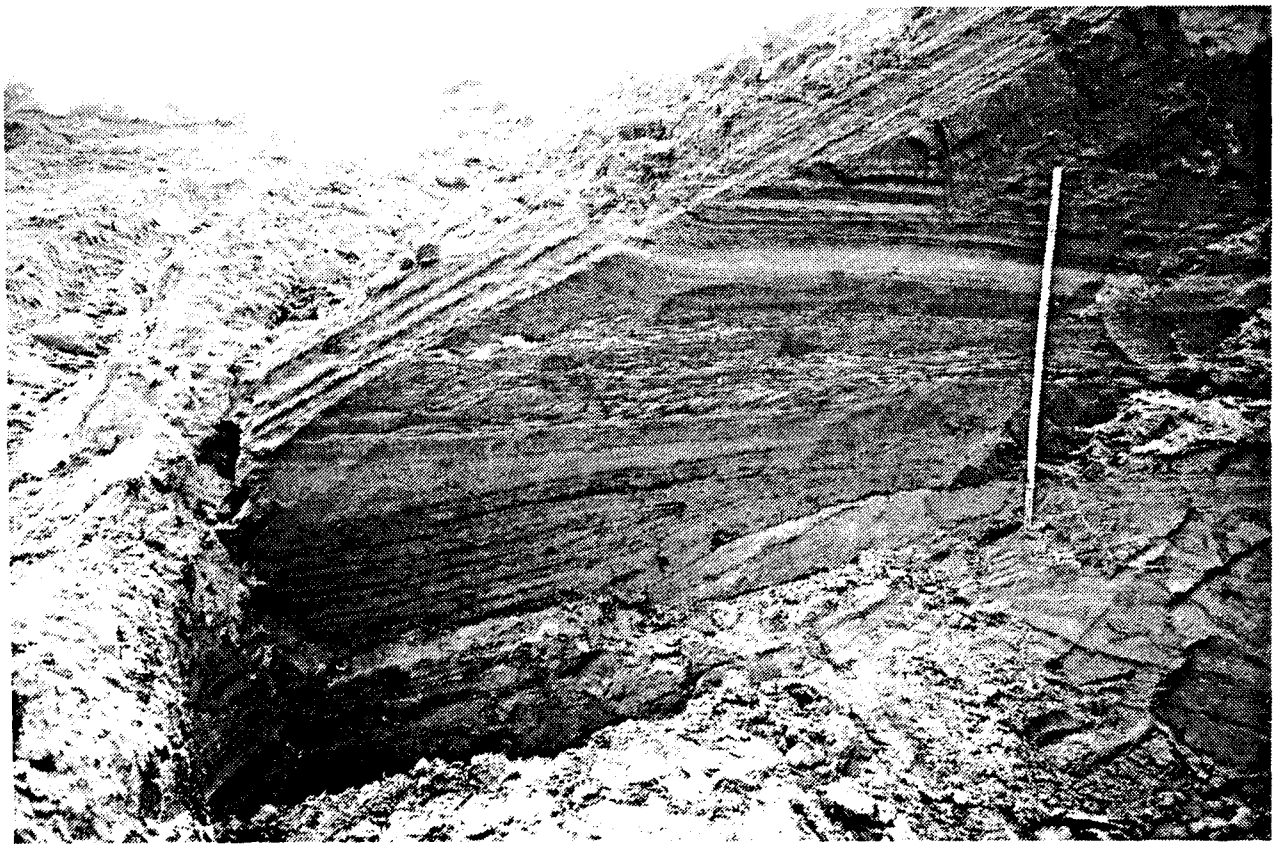

Photo VI.10 (above). Rientjes brickyard: Detail of units 1-4 at bank of southwestern channel. See also fig. VI.21.

Photo VI.11 (below). Rientjes brickyard: Detail of channel-fill cross bedding in unit 4. The sequence consists of channel-fill crossbedding, current ripple cross-lamination, followed by (wave?) ripple formsets at the base of unit 5. See also fig. VI.21. Scale bar 1.5 m.

(Romanovsky, 1976, 1985); mean annual air temperatures could be below -8° C in that case. The upper temperature limit of -6° of Péwé (1966) can be considered as a more conservative estimate (Washburn, 1979).

As shown in the previous paragraph, reports of ice wedge casts of similar age as to those of unit 2 in this exposure do not include well developed ice wedge casts in coarse sands. Most likely therefore, the mean annual air temperature has been well above the -6° to -8° C which is necessary for ice wedge development in sands. Further important prerequisites for ice wedge formation are mean minimum temperatures of the coldest month below -20°, sudden and strong temperature drops and a not too thick snow cover (Karte, 1979). Special local circumstances also might have applied, such as a surface which regularly has been blown free from snow.

Palaeobotanical analysis points to an aquatic environment for unit 2, changing towards a semi-terrestrial environment in the first peat bed at the top (Ran et al., 1990). The whitish calcareous lenses in the top of unit 2 probably point to soil calcification, indicating the presence of a summer evaporation surplus and a fairly dry climate (Tedrow, 1977). Evidently this peat marks the transition to a terrestrial environment which allowed the development of the ice wedge casts. The establishment of terrestrial conditions may have been stimulated by relatively dry climatic conditions.

Besides the ice wedge casts, only few cryogenic features occur within unit 1 and 2. At the transition of unit 1 and 2 a small frost fissure has been found. A diapir-like intrusion of unit 1 material into the silt of unit 2 in fig. VI.5 may have been caused by pile driving operations.

VI.2.3.2. Permafrost degradation and thaw lake formation.

The sequence of events associated with the ice wedge casts in unit 2 and the overlying units 3 and 4 indicates permafrost degradation accompanied by the formation of a thaw lake.

The secondary infilling of the casts has been derived largely from the host material. This material has filled the void left by the melting ice by slumping and flowing into it (photo VI.3). Additionally, coarse sand with some gravel is found in the centre of the fill. The casts are overlain by layered silty sand, deposited in small channels which apparently have been developed above the ice wedges. The silty sand shows an alternation of curved parallel lamination and current ripple cross-lamination (photo VI.4). The channels vary in size, photo VI.3 shows a larger one. Most of the silty channels fills has not been incorporated deeply in the fill of the cast.

The coarse sand in the centre of the ice wedge casts most likely represents material deposited during formation of the channels. As this material has been incorporated deeply within the wedge casts, the wedge ice still should have been present during formation of the channels. During the deposition of the silty sand in the channels, the wedge ice had not yet disappeared completely, since this sediment has been disturbed afterwards by faulting and minor slumping. Apparently the current velocity in the gullies has been reduced strongly during deposition of the silty material. The occurrence of parallel lamination even indicates deposition from suspension in stagnant water.

A larger channel (fig. VI.12) correlates with the gully fills above the ice wedge casts. Like in the smaller channels, the coarse material with intraclasts at the base of the channel changes upwards into finer sand with cross-lamination, followed by evenly laminated sandy silt, draped on the channel banks. This points to fully stagnant water in the channel, shortly after its incision. Convoluted lamination has been caused by slumping of the waterlogged silt down the erstwhile channel banks (photo VI.7).

The gully fills are overlain by a strictly horizontal erosion level, represented by unit 3. The strict horizontality of the erosion surface practically excludes fluvial erosion. The intraclasts in unit 3 probably have not been fluvially transported, as this would have led to a more rounded appearance, if they would have survived transport at all. It is assumed that the erosion surface of unit 3 represents an abrasion plane, caused by wave action along a lake shore. The transition to stagnant water sedimentation in the gullies below unit 3, and the lacustrine deposits which overly unit 3 further support this hypothesis. Wave action might have been a very effective erosion agent of (possibly still ice-rich) material of unit 2.

The erosion has been followed soon afterwards by deposition of evenly laminated sandy silt (unit 4). The fine mm-scale lamination in the silt has been well preserved. This silt represents lacustrine sediments, and may consist partly of reworked material from unit 2. The lake must have been sufficiently deep to prevent reworking of the bottom sediment by wave action or bioturbation. Only in the lowest parts of unit 4 wave ripples have been found.

The sequence of events can be summarized as follows: ice wedge growth - gully development and erosion along the ice wedge polygon trenches, accompanied by ice wedge degradation - rapid transition to stagnant water - cutting of an abrasion platform by wave action - lacustrine sedimentation. The sequence as a whole is taken as evidence for the development of a thaw lake, caused by subsidence after melting of excess ice in unit 1 and 2.

Necessary condition for the formation of thaw lakes is the presence of excess ice in the substratum. Especially unit 2 may have contained a large amount of excess ice. Black (1969a) cites ice contents between 75 and 91% for clayey silt and peat. The lower value already would produce a subsidence of roughly 0.8 m due to ice melting from unit 2 alone. Most of the literature concerning thaw lakes pertains to plan morphology of the lakes and associated processes (e.g. Black, 1969a). Caving in of the lake margins due to thawing and wave action is assumed to be the process by which the lakes are enlarged after their initial formation. Along the lake margins gully erosion takes place, following the trenches above ice wedges (Hopkins, 1949; French, 1976). According to Tedrow (1969) part of the material eroded from the lake banks by caving and wave action becomes suspended and is deposited again in other parts of the lake. Also deposition of clumps and slabs close to the banks takes place.

Hopkins & Kidd (1988) give a description of the actual sedimentary sequence resulting from thaw lake formation. This matches well with the sequence of unit 2-4. According to these authors a typical thaw lake sequence consists of: (1) a sandy, organic rich basal detrital unit between 0.1 and 1.0 m thick, and (2) an overlying unit of fine-grained, thin-bedded central basin deposits between one and ten m thick. The basal unit overlies ice

wedge pseudomorphs, contains peat lumps, and shows current cross-bedding. It is deposited near the actively enlarging lake margin and is as such a time-transgressive unit. In this case unit 3 represents the basal unit, and unit 4 the overlying basin deposits. The development of gullies in the ice wedge trenches matches well with the morphological descriptions cited above.

The initiation of permafrost degradation does not necessarily indicate warmer climatic conditions. Several non-climatic causes can be cited (Black, 1969a; Washburn, 1979; Burn & Smith, 1988). Possibly ground ice thaw has been initiated by a fluvial erosion phase, as might be derived from the gully development and channel incision preceding the thaw lake. On the other hand the erosion features may as well have been caused or at least enhanced by ground ice thaw. It is very difficult to separate the effects of climatic change from geomorphological processes in this case. Palaeobotanical data from unit 4 (Ran et al., 1990) suggest that the climate has been somewhat wetter, with more winter precipitation, than during formation of the ice wedges.

VI.2.3.3. Periglacial phenomena in the upper part of the sequence.

In the top of unit 5 frost fissures occur which may have had some infilling of ice, as can be seen from normal faults alongside the fissures (fig. VI.6). One of these structures approaches the width of an ice wedge cast (fig. VI.13), but it is a solitary feature. The structures do indicate, that the climate has been sufficiently cold for repeated frost crack development. According to Maarleveld (1976), seasonal frost cracks may form with mean annual temperatures up to 0°. Karte (1979) indicates mean temperatures below -1° for these features. A second requirement is

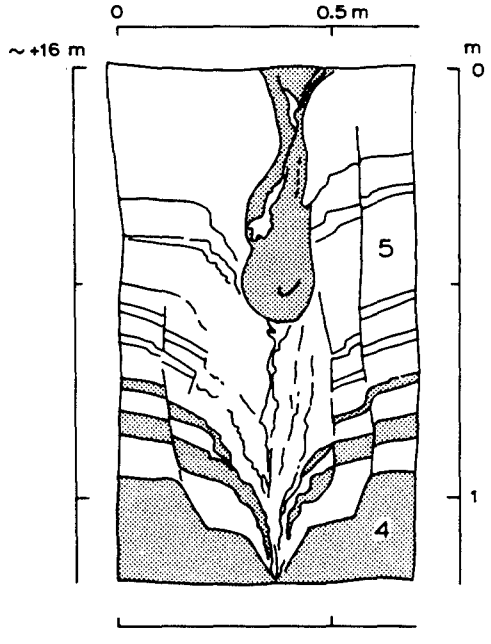

Figure VI.13. Hengelo A1 exposure: solitary fissure structure originating from the top of unit 5, showing evidence of a primary infilling with ice. See fig. VI.2 for legend, fig. VI.4 for location in the exposure. Numbers in drawing refer to units in fig. VI.3.

sudden temperature drops in the order of at least 10°, while presence of an insulating snow cover may impede cracking (Dylik & Maarleveld, 1967; Washburn, 1979). Temperatures might have been only slightly higher than those during the development of the ice wedge casts in unit 2.

The involutions at the top of unit 5 postdate both the fissure structures and the deposition of the basal clay bed of unit 6. They are of the 3a type (Vandenberghe, 1988). Their form suggests that the clay at the base of unit 6 has sunk down into the sand of unit 5, forming loadcast-like structures. This indicates that they have been developed from loadcasting of liquefacted material (e.g. Vandenberghe & Van den Broek, 1982; Vandenberghe, 1988), instead of differential heave during frost penetration in the soil (e.g. Van Vliet-Lanoë, 1985). The amplitudes are ca. 0.5 m, with a wavelength of approximately 0.8 m. The base is often flattened, and sometimes indications of two stages of formation can be found (fig. VI.6,7) which may result in a somewhat exaggerated size. Usually the basal clay of unit 6 has sunk downward into the sand. It has formed small necks which display in some places a polygonal network in plan (photo VI.8), while on other locations a pattern of single drops is more common (photo VI.9). The deformations do not necessary point to the presence of a permafrost table (Maarleveld, 1981), but may be formed also as a result of local, excessive water pressures during thaw in an environment of seasonally frozen ground (Vandenberghe, 1988). In this case the regular occurrence over a large area in the exposure may indicate the presence of a local permafrost table, although the climate evidently has been too warm for the development of ice wedge casts.

Apart from the basal layer, unit 6 is not strongly disturbed. Type 1 deformations (folds of small amplitude, Vandenberghe, 1988) occur frequently (fig. V.9). In this case the cryogenic origin is doubted, since also deformation by non-cryogenic loading may have occurred. Somewhat stronger deformation of possible cryogenic origin occurs below the horizontally bedded part of 7 which represents a subaerial environment (see below). Also frost fissures are very abundant in this part of unit 7, starting from different levels.

At the transition of unit 7 to 8 only locally type 3a involutions occur. These grade into smaller amplitude wave-like forms (fig. VI.9). Besides at the base of unit 8, the involutions also occur above thicker sand intercalations within unit 8. Usually they display a typical drop form. The process evidently has operated on a more local scale than the involution formation at the top of unit 5. There is no indication for the presence of a permafrost table.

The very large type 2a involutions (amplitude over 1 m, photo VI.6) in the centre of which unit 10 is found, occur at the same level as the top of the Late Pleniglacial ice wedge casts. They are likely to be associated with permafrost degradation (Vandenberghe & Van den Broek, 1982; Vandenberghe, 1983b, 1988).

Sedimentary structures of unit 6 and 8 indicate a - at least partly - lacustrine environment (see below). The question can be raised, if the formation of these lakes has been induced by ground ice melting also, analogous to the thaw lake deposits of unit 4. If this is true, a cycle of thaw lake formation - lake filling -ground ice formation - thaw lake formation could be responsible for the silt/sand alternation in this site. However,

there are important differences between the sequences of unit 2/3/4 and 5/6 or 7/8:
1. Especially in unit 7/8 there is no certain indication of the former presence of permafrost.
2. Both in sequence 5/6 and in sequence 7/8 involution formation took place after, and not before the first silt or clay deposition.
3. Features indicating the deepest lake phase in unit 6 - well laminated silts, see below - occur at a considerable time after the development of the involutions; consequently, there is no clear relation between both features.
4. The sequences 5/6 and 7/8 involve sand bodies, in which less excess ice could be formed than in the silt of unit 2.

A temperature limit for the type 3 involutions is difficult to give (Maarleveld, 1976; Washburn, 1979; Vandenberghe 1988). French (1986) suggests for similar cryoturbations that extremely warm and wet summers may have promoted formation.

Combination of the sedimentary environment of the deposits and the periglacial phenomena in the upper part of the sequence indicates, that cryogenic deformation starts as soon as a sedimentation surface becomes exposed to air. As such, climatic perturbations cannot be derived from it with sufficient certainty.

VI.2.4. Sedimentary environment of the Middle Pleniglacial deposits.

VI.2.4.1. Fine-grained floodbasin deposits.

The fine-grained units (2, 4, 6 and 8) have in common that shallow lacustrine conditions did occur during some stage of their deposition, as is indicated by the presence of wave ripples. The genesis of unit 4 as a thaw lake deposit already has been discussed in par. VI.2.3.2. The well preserved lamination in unit 4 points to absence of bioturbation, and therefore indicates a relatively deep and permanent lake. In the other fine-grained units layering is often only crudely developed. In unit 6 a crude centimeter-scale bedding is expressed by varying quantities of vegetal matter, caused by vegetation growing at the site. Involuted levels within unit 8 (fig. VI.9) indicate that this unit has been deposited in a very shallow pool, where frost could penetrate in the subsoil. The silts of unit 6 and 8 have been deposited at sites which may have been flooded for only part of the year.

The environmental sequences in unit 6 and 8 are very similar. At or near the base peat beds are found which indicate a semi-terrestrial environment. Also the clay at the base of unit 6 probably has not been deposited in permanently standing water, as this should have prohibited formation of involutions. Termination of peat deposition in both units indicates increased clastic deposition. At the top of these units evidence for a higher water level is found. At the top of unit 6 well preserved lamination occurs which by analogy with the laminated silt of unit 4 should indicate deeper water. Both units are overlain by foreseted sands which have been deposited in lakes of some depth (par. VI.2.4.2).

Especially on the western side of the exposure, unit 8 gradually disappears through an increase in thickness and number of

sand intercalations (fig. VI.9). The sand supply apparently came from the west. To the east, it changes into a humic/silty sand level accompanied by frost fissures (fig. VI.11), indicating subaerial exposure. The presence of layers with silt granules associated with unit 8 in fig. VI.11 is attributed to frequent shallow erosion by running water or waves.

The sequence in unit 2 differs markedly from unit 6 and 8, as it shows a transition from lacustrine to terrestrial environment. Indications of lacustrine conditions (wave ripples) or episodic running water (coarse sand beds) occur in the lower part. Unit 2 appears to consist partly of a fine-grained channel fill (par. VI.2.4.4) which might explain why the unit 2 sequence differs from the other silty sequences. Terrestrial conditions occur in the upper part of unit 2, shown by peat growth, soil formation, and ice wedge development. As grainsize analysis indicates, the top of unit 2 consists mainly of loessic material. The development of a terrestrial environment at the top may have been enhanced by frost heave during permafrost establishment, or the establishment of a drier climate.

VI.2.4.2. Crevasse splay and levee deposits.

The peculiar type of foresets in the sands of unit 5, 7 and 9 justify a closer discussion of their origin. The foresets are clearly of a different nature than the tabular cross-bedding produced by sand wave or bar propagation in a river channel environment, or foresets created by aeolian dune migration. The absence of basal erosion, the well defined toesets, the silt drapes and the uniform direction throughout the whole exposure indicate deposition in stagnant water, analogous to delta foresets. Presence of frost fissures and involutions at their top points to sub-aerial exposure.

However, if the sand was transported into the lake at the mouth of a channel, a roughly semi-circular arrangement of the foresets should have been found instead of the remarkable uniform direction. Obviously the foresets are not produced by a point source, but rather by a linear source. A probable linear source is a levee system along relatively straight stream channels. The 'delta' foresets then represent the distal facies of crevasse splays, terminating in a lake.

The topsets of this system are ill preserved, caused by cryoturbation at their surface. Generally the topsets appear to consist of parallel lamination, in which silt granules may be found. Most likely this lamination has been produced under upper flow regime conditions by shallow sheetflow over the crevasse splay surface. Rare high width/depth ratio scour-and-fill structures occur as part of the topsets. This agrees with observations on crevasse splays in present-day environments (Smith et al., 1989). On young stage crevasse splays sheetflow and high width/depth ratio channels occur. On further maturation this is gradually converted into channels with lower width/depth ratio. The crevasse splays at this site appear to be of a rather simple, 'immature' type.

The foresets are frequently steeper than the subaquatic angle of rest of sand, especially near the top. This type of oversteepening may be by caused shear forces exerted by the water current on partly liquefacted sand which is a phenomenon associated with rapid deposition (Collinson & Thompson, 1982).

Alternatively, oversteepening may be caused by post-sedimentary disturbance: cryoturbation, and post-depositional loading of the sand on underlying waterlogged lacustrine deposits.

Unit 7 has been the most widely exposed foresetted unit. The absence of thick silt drapes in unit 7 points to smaller time lags between the successive stages of foreset propagation than in unit 5. The foresetted part of unit 7 increases in thickness in an eastern direction which must be attributed to depth variations of the lake in which the crevasse splay has been deposited. Detailed analysis of the sedimentary structures of the parallel bedded part of unit 7 indicates frequent occurrence of upper flow regime running water, alternating with subaerial exposure (par. VI.2.4.3.2). The transition of unit 7 to 6 is erosional below this parallel bedding, as indicated by frequent scours at the top of unit 6 (fig. VI.9). This facies of unit 7 probably represents a proximal, subaerial part of a crevasse splay while the cross-bedded facies is the distal part. West of the section of fig. VI.9, coarse cross-bedded sands have been found which correlate with unit 7. Unit 6 is locally absent at this site, due to erosion. The source channel of the crevasse splay should have been situated at or close to this site.

Relatively straight river channels associated with crevasse splays terminating in shallow lakes, might be expected from the anastomosing river systems as described by Smith (1983) and Smith et al. (1989), or deltaic distributary and interdistributary bay systems (Axelsson, 1967; Dahlskog, 1966, Elliott, 1974). Two examples of levee/lake interaction involving thermokarst lakes (cf. unit 4/5) are described by Wallace (1948) and Walker (1978). Although descriptions of internal bedding and lamination types of crevasse splays terminating in lakes are lacking, crevasse splays of the type described here undoubtedly can occur in these situations.

VI.2.4.3. Structural details of the crevasse splays.

Lacquer peels from the crevasse-splay foresets in unit 5 and 7 reveal interesting details on processes which did occur during deposition of these units. In general structures point to very rapid deposition by water with a high sediment load and high flow velocities. Waterlogged conditions leading to liquefaction are common. During progradation of the foresets the water level may have risen appreciably in the lakes, and considerable bottom currents did occur in front of the foresets. Foreset progradation has been episodic. Most likely, each progradation phase represents a single river flood. Another general feature is the coarsening upward sequence produced by crevasse splay progradation. A coarsening upward sequence also has been found in present day crevasse splay deposits (Smith et al., 1989).

VI.2.4.3.1. Unit 5.

The lower part of the lacquer peel in fig. VI.14 shows a conspicuous coarsening upward sequence. The lowest beds (at A in fig. VI.14) are an alternation of thin parallel silt and sand beds which are slightly convoluted. The sand has been settled from suspension, and represents the toesets belonging to foresets at some distance (ca 10 m) from the peel location. Upwards the sand beds are becoming thicker and coarser, showing cross-lamina-

tion (B); silt beds disappear. Flow has been approximately in the same direction as the migration of the large foresets. This sequence is truncated by shallow scouring, followed by ripple foresets which are in turn overlain by a first set of large foresets (C). The ripple foresets are evidence of considerable bottom currents in front of the prograding delta-foresets.

The basal lamination of the foresets shows two modes of foreset propagation. Partly the lamination is produced by settling from suspension on both the slope and toesets, resulting in lamination which follows the underlying relief (D). This alternates with regular avalanching which produces foreset lamination abutting against the toesets at the base (E). Avalanching also produces small unconformities (F) on the foresets. The sedimentation occurred very rapid as the repeated oversteepening and suspension deposition on the foresets indicates.

The deposition of the first set of foresets terminates rather abruptly. At the base of the foresets coflow current ripples (G) have been formed. Near the transition between foresets and toesets these grade into backflow ripples (H). The last foresets in the backflow ripples have a finer texture due to a rapidly waning current. Thereafter the silt drape (I) has been settled from suspension. Some wave reworking also has occurred, as the clean sand lenses within the horizontal part of the silt drape suggest. The next phase of foreset propagation shows the same alternation of suspension and avalanche deposition as discussed above. In the basal part the lamination is strongly disturbed due to slumping on the inclined sedimentation surface (J). Also part of the topsets is visible. Although the lamination in this reach is disturbed by cryogenic processes, the structures are essentially plane bedding and faint parallel lamination (K) which point to upper flow regime conditions on the crevasse splay surface. The distortions marked L in fig. VI.14 are due to a frost fissures.

The most remarkable phenomenon is gradual rising of the nickpoint between topsets and foresets (arrow in fig. VI.14). This points to a rise in water level during sedimentation, either by increasing discharge over the topsets or a rising lake level. The last hypothesis is most likely, since increasing discharge also would lead to higher current velocities; a trend of accordingly coarser sediment is not visible. Fig. VI.7, which is a sketch of the neighbourhood of the peel, also shows evidence of fluctuating water level. The step-like appearance of the silt drapes is striking. Apparently the water level in the floodbasin rose strongly during flooding and varied considerably in the course of the year.

VI.2.4.3.2. Unit 7.

Fig. VI.15-18 show peels derived from unit 7 which document a transition from foresets deposited in deeper water in the eastern part of the exposure, towards subaerial crevasse/splay levee

Figure VI.14 (next page). Hengelo A1 exposure: Lacquer peel showing silt drape on crevasse splay foresets in unit 5. Characters refer to comment in text, numbers to grainsize samples in table VII.1. See fig. VI.2 for legend, fig. VI.7 and VI.4 for location in the exposure. Column I: composition/texture, II: grainsize, III: sorting (poor/medium/well).

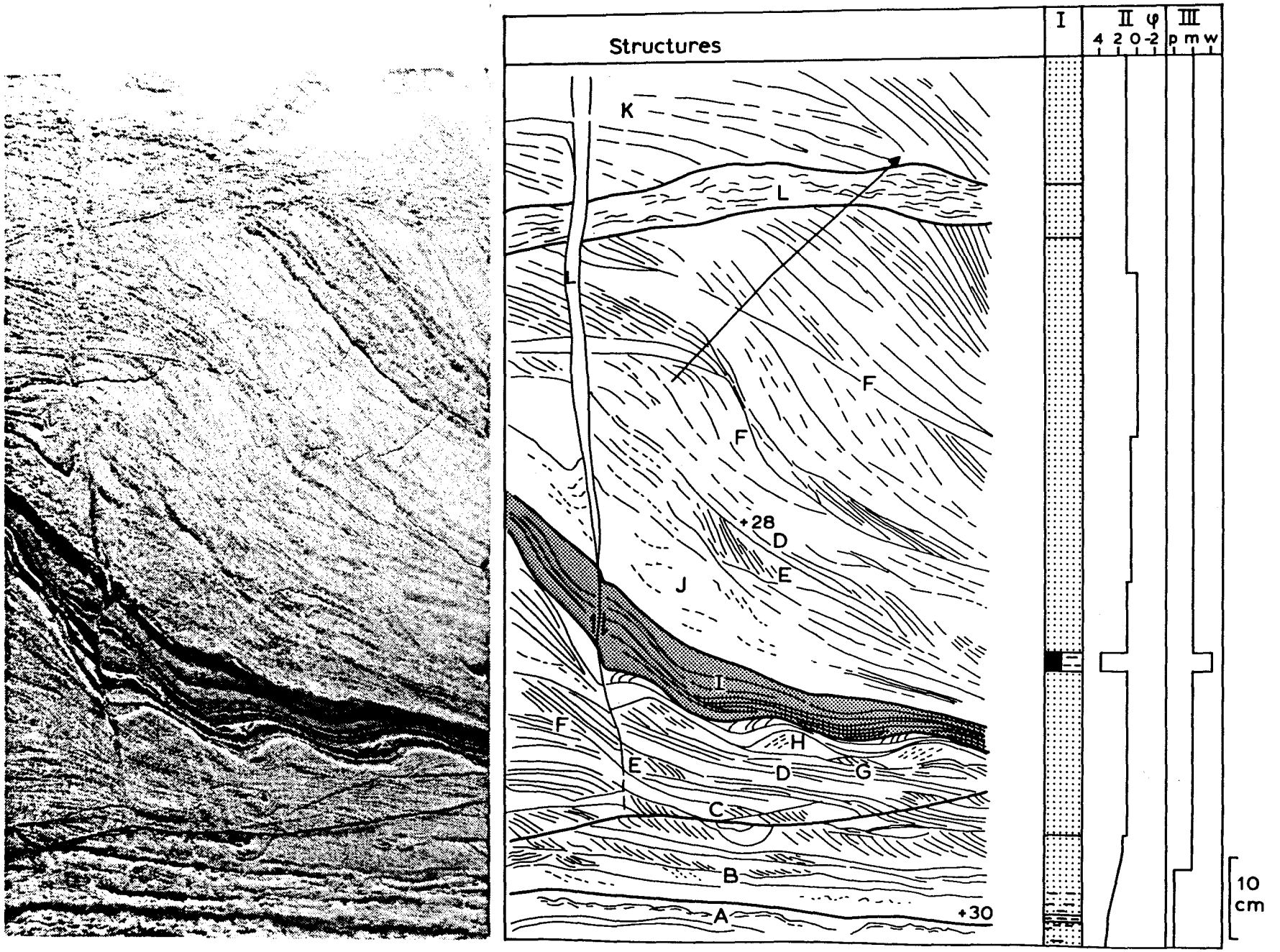
Structures
I
II φ
4 2 0 -2
III
p m w
K
L
L
F
F
+28
D
E
J
I
I
F
H
E
D
G
C
B
A
+30
10
cm

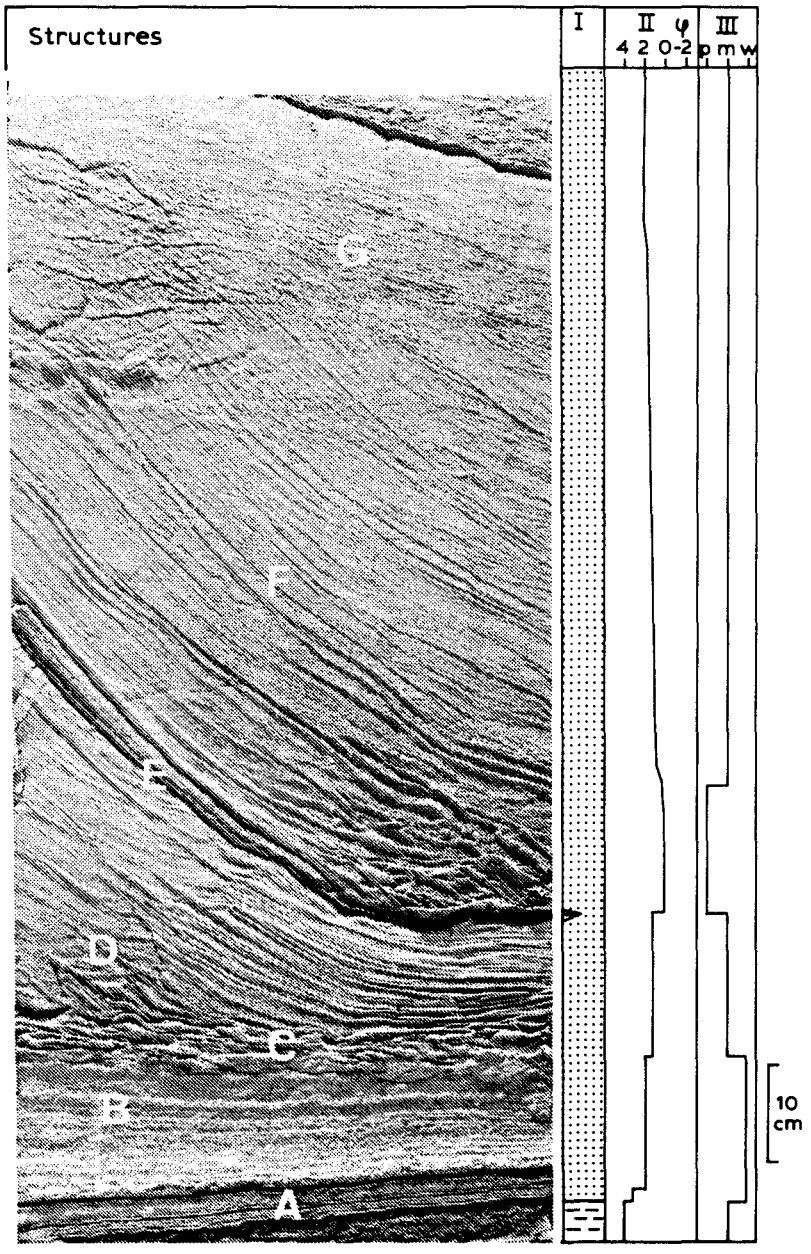

Figure VI.15. Hengelo A1 exposure: Lacquer peel from unit 7 showing crevasse splay foresets at eastern side of exposure. Characters refer to comment in text, numbers to grainsize samples in table VII.1. See fig. VI.2 for legend, fig. VI.4 for location in the exposure. Column I: composition, II: grainsize, III: sorting (poor/medium/well).

deposits and channel deposits on the western side of the exposure. Current velocities have been modest at the start of the crevasse splay progradation into the unit 7 lake, as bottom current phenomena are absent at the oldest, westernmost foresets. Later current velocities have been higher which may point to a gradual increase of discharge diverted by this crevasse splay into the floodbasin.

The lacquer peels of the foresets in unit 7 show the same pattern of development, as is shown by fig. VI.15. The basal deposits are evenly laminated toesets (at A in fig. VI.15). The

last thick bed (B) of these is clearly coarsening upwards. This is followed by cross-laminated sand (C), deposited under influence of bottom flow induced by the floodwater entering the lake. The first set of crevasse splay foresets shows well defined interfingering of avalanche material on the foreset slope with suspension sediments of the toesets (D). At E a thin silt drape separates two progradation phases. Deformation of the lamination by slumping can be seen at F. Towards the top the foreset direction changes (G).

The foresets in the second peel (fig. VI.16) are lower than those of the first site, indicating a lower water depth during formation than at the site of fig. VI.15. Bottom current indications are absent. The foresets are produced mainly by avalanching as they are abutting against the toesets (A in fig. VI.16). The lamination in the topsets is disturbed by liquefaction (B). Part of the lamination may have originally represented current or wave ripple lamination, drawn into chevron folds. The topmost sediment

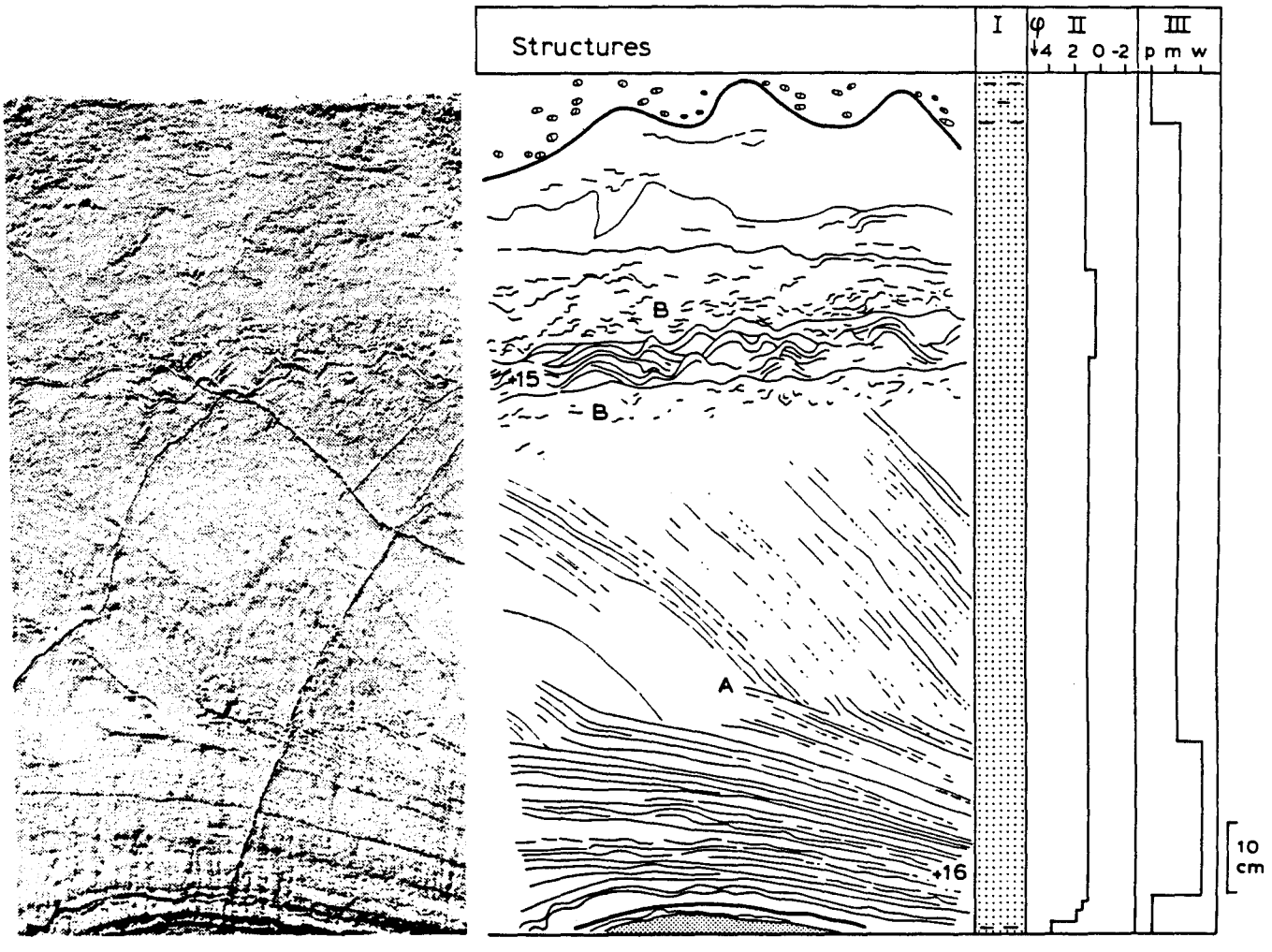

Figure VI.16. Hengelo A1 exposure: Lacquer peel from crevasse splay foresets in unit 7, west of fig. VI.15. Foreset height is considerably smaller than in the previous sites. Characters refer to comment in text, numbers to grainsize samples in table VII.1. See fig. VI.2 for legend, fig. VI.9 and VI.4 for location in the exposure. Column I: composition, II: grainsize, III: sorting (poor/medium/well).

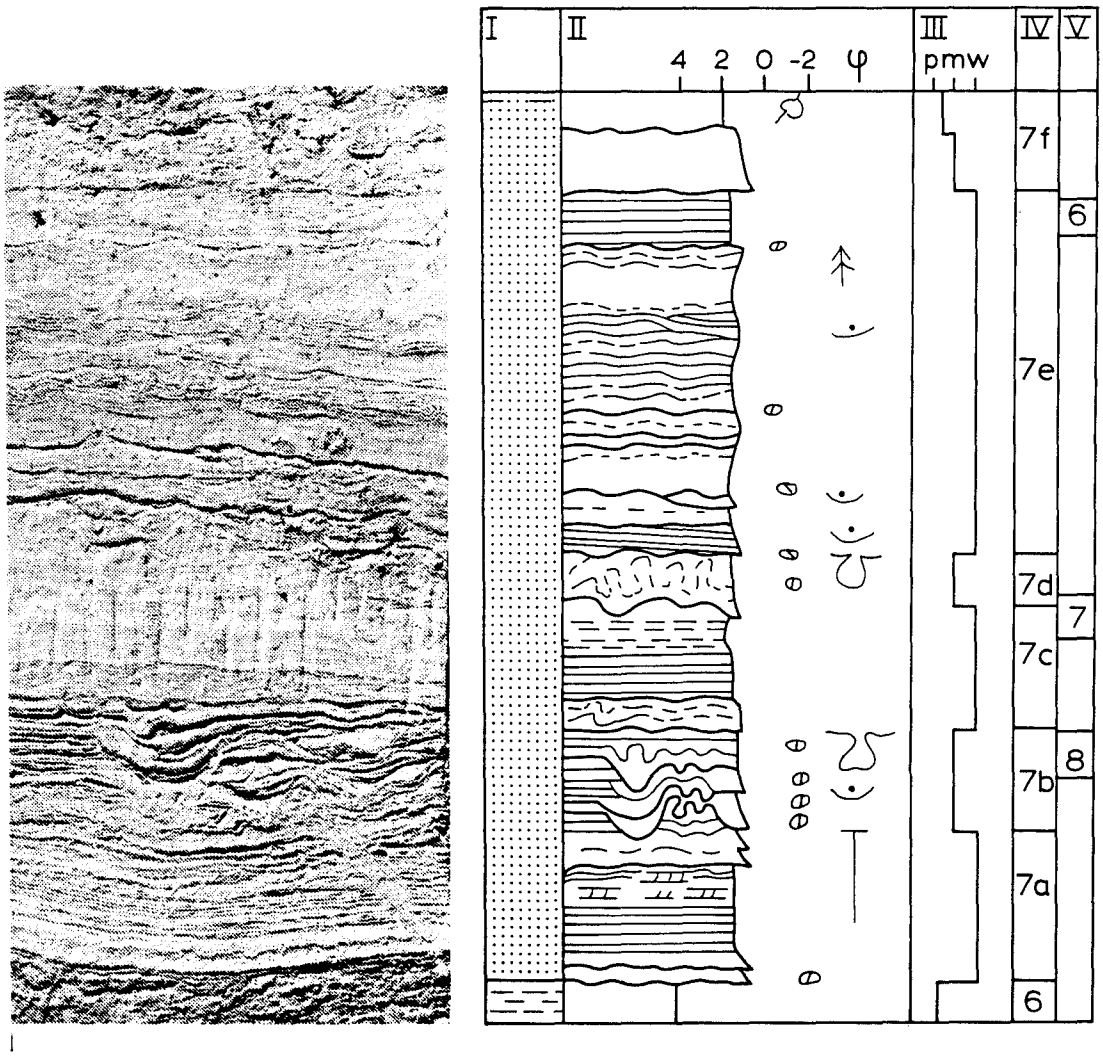

Figure VI.17. Hengelo A1 exposure: Lacquer peel of horizontally bedded facies of unit 7. See fig. VI.2 for legend, fig. VI.9 and VI.4 for location in the exposure. Column I: composition; II: structure and texture; III: sorting; VI: subunits (see text); V: grainsize sample numbers (table VII.1).

consists of a mixture of sand and silt granules. The low amplitude wave-like deformation of the lacustrine silt at the base of the peel is attributed to loading of the sand into waterlogged silt below. It is unlikely that this deformation has been caused by frost action, as the top of the silt should have been located below the water table.

Fig. VI.17 shows a lacquer peel from the parallel bedded part of unit 7. The material is well sorted, and is dominated by parallel bedding and lamination. The sand is much coarser than the average Twente Formation aeolian sand (par. VII.1.3.2.1; Schwan, 1988a). On closer inspection, many irregular erosional unconformities prove to be present. Most of these unconformities are lined with small silt granules. These features practically exclude aeolian deposition. Only in the top of subunit 7a (fig. VI.17, table VI.2) indications of aeolian sedimentation are found.

U-nit	Description	Interpretation
7f	Homogenized, graded beds with erosive base	Running water (scour and fill?).
7e	Even, parallel lamination; irregular unconformities lined with silt granules; low angle scours. Lamination is partly obliterated or shows undulating appearance through local upturning along vertical structureless zones (dewatering structures)	Upper flow regime plane bedding; disturbed by liquefaction. Rapid sedimentation.
7d	Strongly disturbed by convolution; original structure probably cf. 7b	As 7b
7c	As 7e	As 7e
7b	Contains silt granules; stacked small scours laterally grading into thin, even parallel bedding; synsedimentary convolution, loading	Deposition from suspension alternating with erosion.
7a	Thin, normally graded, even/wavy parallel lamination and bedding; beds have erosive base. Adhesion ripples and frost fissure at top.	Subaquatic deposition from suspension alternating with erosion; wet aeolian subaerial deposition.
6	Silt	Standing water.

Table VI.2. Description of sedimentary structures in lacquer peel of fig. VI.17.

The top of unit 6 has been truncated erosively. Just to the right of the lacquer peel a scour is present (fig. VI.9). Subunits 7a and b indicate frequent standing water after flooding, as erosional scouring alternates with suspension deposition. These subunits probably have been deposited contemporaneously with the first foresets that appear to the east of this site; the convoluted level of 7b appears to overly these foresets (fig. VI.9). Most of subunit 7c-f indicates shallow water depths and high flow velocities, resulting in upper flow regime plane bed sedimentation. This alternates with subaerial exposure, as is shown by frequent frost fissures throughout the sequence and aeolian reworking at the top of 7a. The frequent convolution, loading and liquefaction phenomena point to waterlogged conditions caused by rapid sedimentation. According to Reineck & Singh (1975) upper flow regime plane bed and convolution phenomena are of common occurrence in levees and crevasse splays. It is assumed, that this sediment represents a subaerial part of a crevasse splay or a levee, situated in a position more closely to the channel than the foresets in unit 7.

The lacquer peel of fig. VI.18 has been taken at the westernmost site where the sediments of unit 7 have been exposed. The basal subunit (7a) shows traces of scouring, current ripple

cross-lamination and parallel lamination at the top. The structures have been obliterated largely by liquefaction. Unit 7b displays scouring at the base, and contains a large lump of peaty silt, probably derived from unit 6. The original structure appears to have been trough cross-bedding at the base, at the upper part mainly current ripple lamination. After a second shallow scour it changes into predominantly parallel lamination with many silt intraclasts. This parallel lamination probably points to upper flow regime conditions. The overlying parallel bedded silt with type 3 involutions probably correlates with unit 8 elsewhere in the exposure. It indicates a rather sudden transition to mainly standing water deposition. The silt has been truncated by scouring, after which the cross-bedded sand of unit 9 has been deposited. Near the base the cross-bedding appears to be of the planar type, changing upwards into trough cross-bedding.

With exception of unit 8, all units point to high energy current flow. Subunit 7b further shows evidence of rapid sedimentation and decreasing water depth, after which current activity has stopped. Unit 9 shows renewed channel activity. The structures show that the site of this lacquer peel is situated at, or very close to the site of the channel from which the crevasse splay of unit 7 has been deposited. Unit 8 represents temporary inactivity of the channel. The reactivation shown by unit 9 is associated with the crevasse splay foresets of unit 9.

The relatively large distance between the proximal crevasse splay/levee facies and the channel is only apparent, as the exposure cuts the strike of this system at an angle of about 45°. The true distance between the channel deposits at the site of fig. VI.18 and the crevasse splay deposits of unit 7 in the main exposure is 200 m at most (fig. VI.4). Unit 7 is not exposed between the western tip of the main exposure and the site of fig. VI.18. Penetration cone soundings indicate that thicker channel deposits associated with unit 7 may be present in the unexposed part. If the parallel bedded facies of unit 7 indeed represents the levee of the system, it is only a low relief feature. This also explains why such a large amount of fairly coarse material could have been deposited at considerable distances from the channel. Neither do the channel deposits appear to represent a very well defined deep channel, although exposure is incomplete in this case. Most likely this channel itself is not a primary river channel, but represents the feeder channel of a crevasse splay system (fig. VI.19).

VI.2.4.4. Channels.

In three cases it is possible to make inferences with regard to channel morphology. These pertain to small channels which probably did play only a minor role in the floodplain drainage. Sedimentary structures indicate that the channels at the top of unit 2 and 6 may have been short-lived phenomena which have functioned in floodbasin drainage only.

The oldest indications for channel morphology originate from the unit 1/2 boundary. Locally this boundary is sharp and shows channel-like depressions. The base of unit 2 contains reworked vegetal detritus in these locations and is underlain by coarse sand with fine gravel. This suggests that part of unit 2 has been

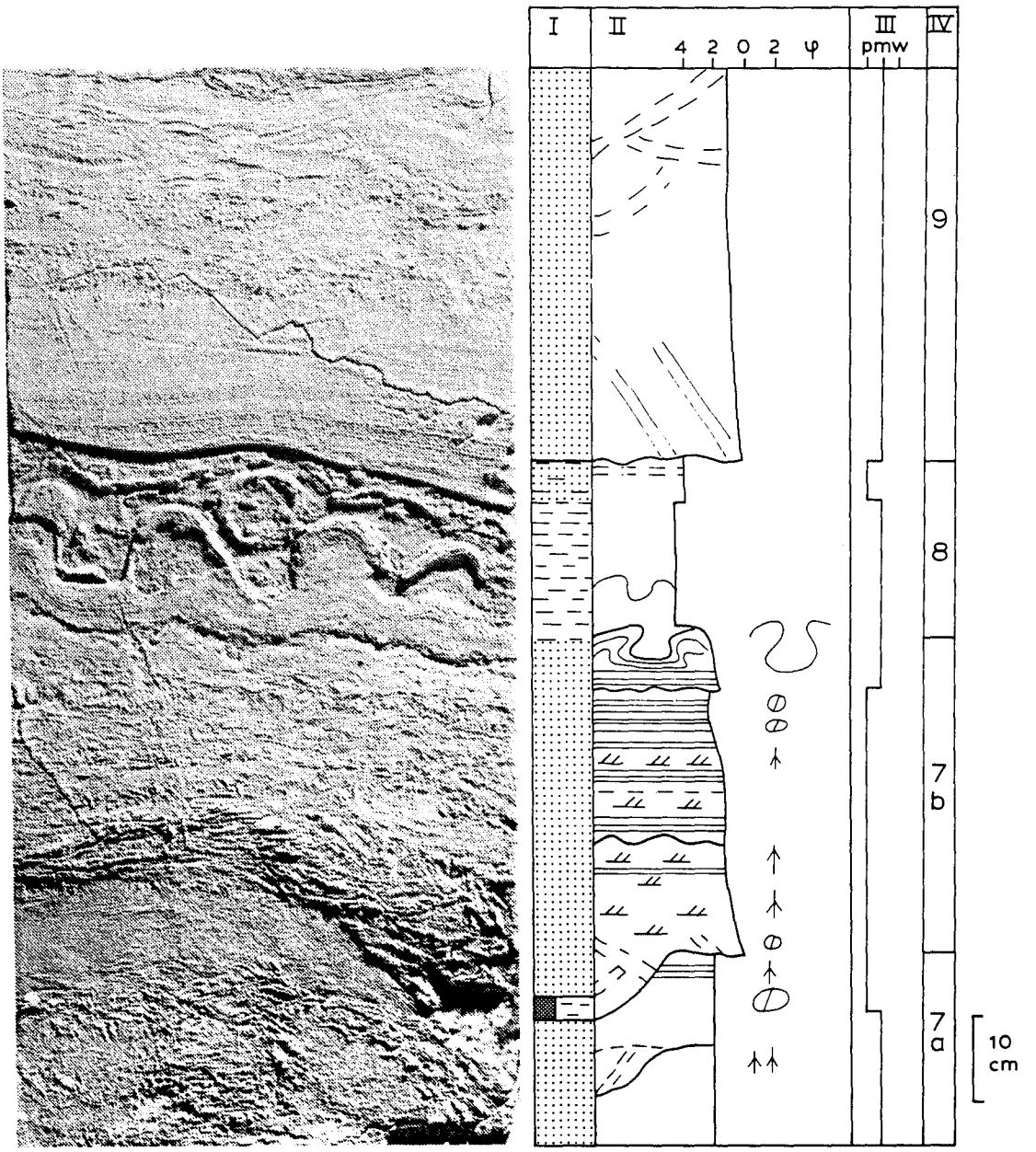

Figure VI.18. Hengelo A1 exposure: Lacquer peel of channel fill sediment in unit 7, extreme western part of exposure. See fig. VI.2 for legend, fig. VI.4 for location in the exposure. Column I: composition; II: structure and texture; III: sorting; VI: (sub)units (see text).

deposited as a fine-grained channel fill. This channel fill displays a low width/depth ratio, although its exact size could not be determined.

A second channel is found incised into unit 2; it is associated with the gullies found above the ice-wedge casts in unit 2 (fig. VI.12). The channel bank which could be observed is interesting because of clear bank undercutting phenomena. The coarse material with clay and peat lumps at the base of the channel partly underlies a protruding remnant of the silt and peat of unit 2. After deposition of the coarse material failure did occur in the silt/peat bank, by the development of a small crack. Again the size of the channel could not be determined,

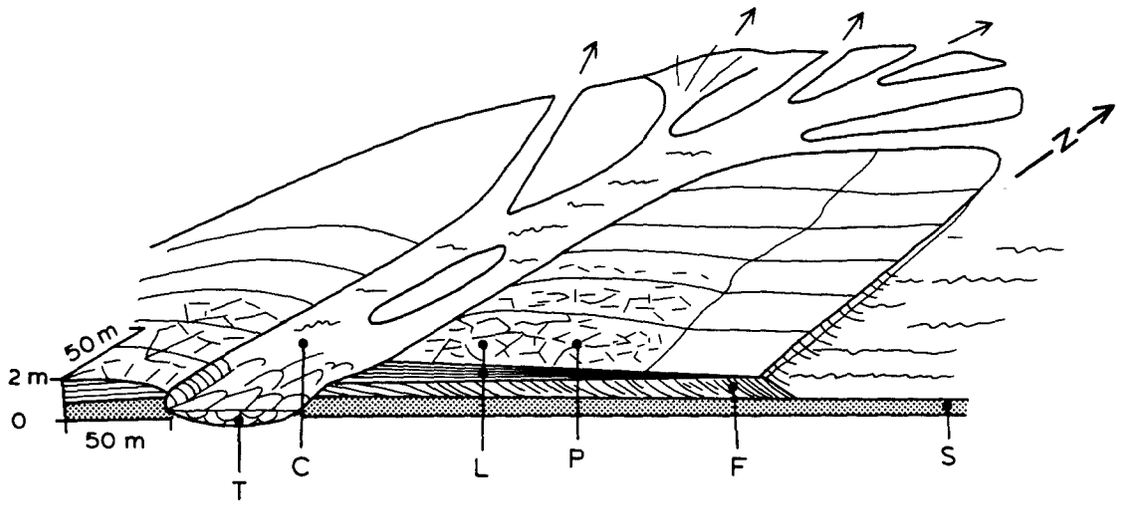

Figure VI.19. Possible configuration of the crevasse splay represented by unit 7 in the Hengelo A1 exposure. S: lacustrine silt; F: foresets created by crevasse splay progradation in lake; L: levee or proximal crevasse splay sediment with upper flow regime plane bedding; P: frost crack polygons; C: low width/depth ratio feeder channel of crevasse splay; T: trough cross-bedding in channel.

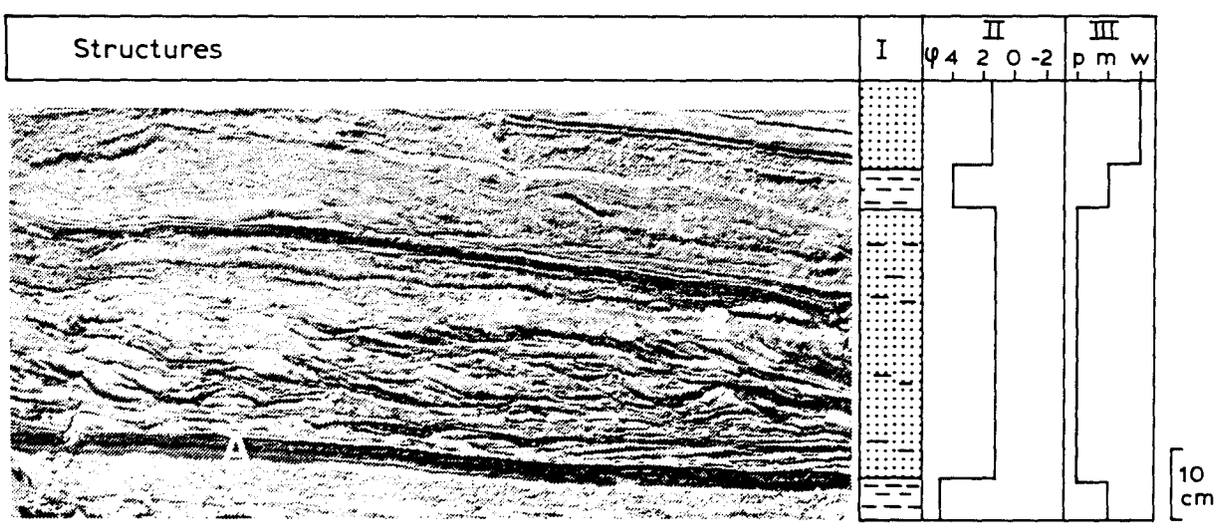

Figure VI.20. Hengelo A1 exposure: Lacquer peel showing internal structure of a small levee near a channel at the top of unit 6. Characters refer to comment in text. See fig. VI.2 for legend, fig. VI.8 and VI.4 for location in the exposure. Column I: composition/texture, II: grainsize, III: sorting (poor/medium/ well).

since only one bank has been exposed. The steep bank which is visible suggest a low width/depth ratio.

Near the top of unit 6 a small channel with associated levees has been found (fig. V.8). The width/depth ratio of this channel has been considerably smaller than 10.2. The laminae in the channel fill have been draped over the channel and levees, indicating settling from suspension after the channel has become inactive. The levees consist of medium to coarse cross-laminated sand with much reworked peat and small silt pebbles.

A lacquer peel from one of the levees gives an impression of the life cycle of this channel (fig. VI.20). The start of the channel erosion is marked by deposition of a layer of reworked peat and silt pebbles (A in fig. VI.20) at the base of subunit 6b (the levee). This is followed by the levee sediment: sand with silt granules and reworked peat. The dominant structure is current ripple cross-lamination, with the foresets directed away from the channel. At B a microdelta has formed, at C upper flow regime plane bedding. Sets are bounded by irregular layers of reworked peat, or erosional unconformities with silt clasts. The layers of reworked peat are best developed at some distance from the channel. If each set is taken as a separate flood deposit, the channel has been active during 10 - 12 floods at most. Subunit 6c represents lacustrine silt draped over the channel and levee. Unit 7 contains the toesets of crevasse splay deposits. The channel has become entirely inactive during deposition of the lacustrine silt. From its small size and short lifetime it appears that the channel represented only a temporary crevasse channel.

The absence of larger or more abundant channel structures in this large exposure is striking. Most of the exposed sediment is clearly fluvial material, but has been deposited in overbank environments. The large volume of relatively coarse sands in the overbank deposits suggests that the floodbasins play an important role in transporting the water and sediment volumes of major floods. This might have been caused blocking of channels by snow and ice in early spring (par. II.3.3).

VI.3. The Rientjes brickyard.

VI.3.1. Stratigraphy.

North of Hengelo Twente Formation clays have been dug for brick fabrication. A large exposure, the Rientjes brickyard, has been described by Zagwijn (1974). Further data have been collected in 1972 by the Rijks Museum voor Geologie en Mineralogie at Leiden, the Rijks Geologische Dienst and the Hugo de Vries Laboratorium of the University of Amsterdam. This resulted in an unpublished palaeobotanical report (Vermij & Heukeshoven, 1974). This report mainly deals with palynological data, but in addition provides good drawings and photos of the clay pit. Unfortunately this unique Twente Formation exposure cannot be studied any more. To complete the information on the Middle Pleniglacial palaeo-environment of the Hengelo basin data from this exposure have been included here. The lithology and sedimentary structures described below have been derived from the section drawings and photos by Vermij & Heukeshoven (1974). Mr. J. de Jong of the Rijks Geologische Dienst kindly provided additional information.

Unit 1 consists of sand, overlain by gyttja or peaty clay, ca. 0.25 m thick. At the base the gyttja is strongly involuted. The photos suggest that unit 1 has a rather firm consistence. A Mammuthus molar found in the exposure probably originates from this bed. A radiocarbon dating from unit 1 yields an age of 43030 +1680 -1390 y B.P. (GrN 6925). Unit 1 forms an erosion remnant at the base of the section, overlain by a horizontal

Figure VI.21 (next page). Rientjes brickyard: overview section. Location see fig. VI.1. Numbers refer to units in text.

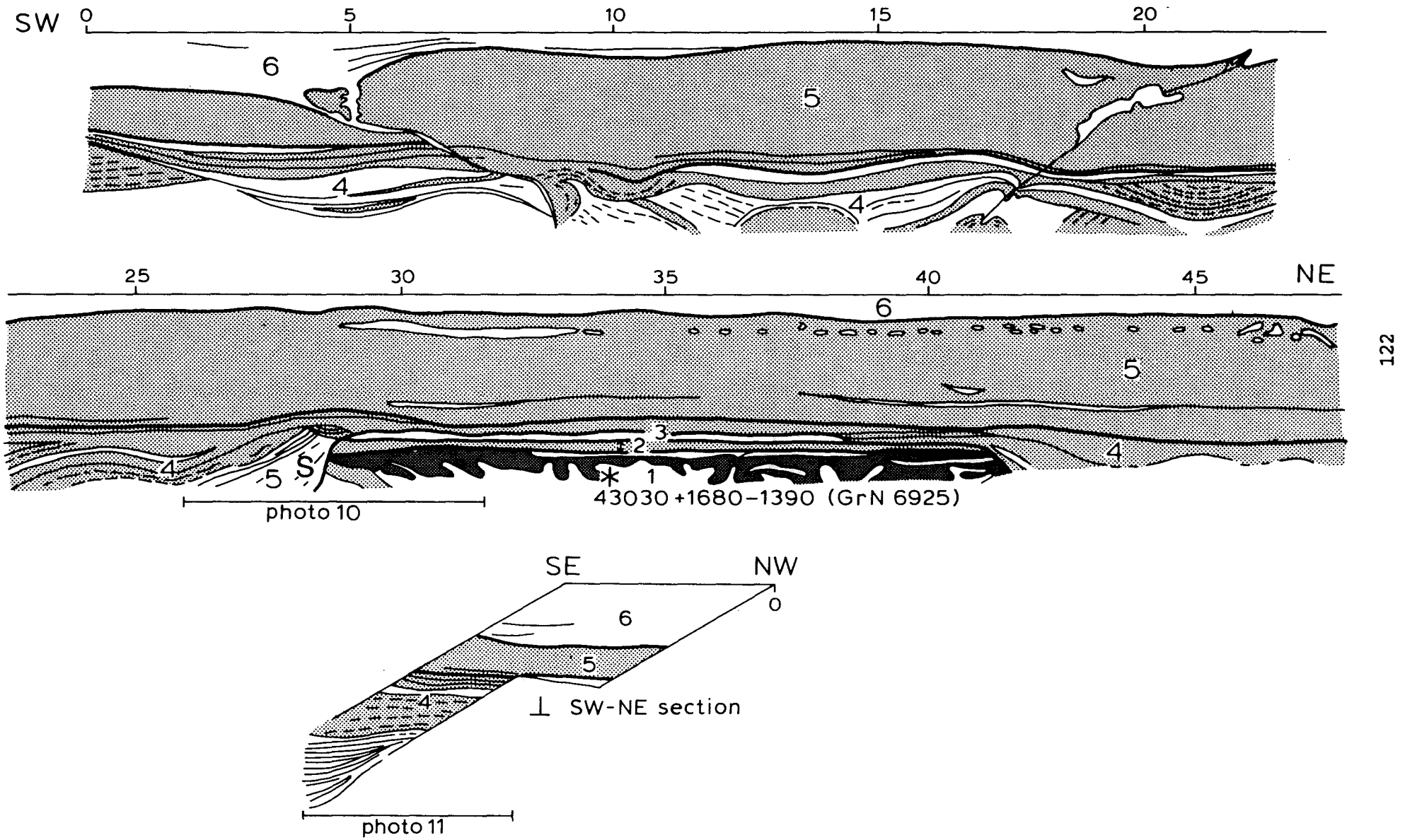
SW
0
5
10
15
20
6
5
4
4
25
30
35
40
45
NE
6
5
3
2
4
4
5
S
1
43030 +1680–1390 (GrN 6925)
photo 10
SE
NW
0
6
5
4
⊥ SW-NE section
photo 11

erosion surface and cut off on both sides by channel banks (unit 4).

Unit 2 is a layered clayey deposit with a sand bed at the base. It overlies the horizontal erosion surface above unit 1.

Unit 3 also is confined to the area where unit 1 occurs. It overlies unit 2 and consists a 0.25 m thick bed of sand with foresets.

Unit 4 replaces unit 1-3 on the southwest and northeast side of the section. The transition is erosive, with steep erosion planes cut into units 1 and 2. The unit consists of beds ranging from sand to silt with thin bands of organic debris. The structure is predominantly channel fill cross-bedding (cf. Reineck & Singh, 1975). Zagwijn (1974) also published a radiocarbon dating from the base of the exposure, with an age of 37500 +/- 650 y B.P. (GrN 1763). This dating has been obtained from silt rich in plant debris found within unit 4, near the base of the exposure (De Jong, pers. comm.).

Unit 5 is a clay unit which is up to 3 m thick locally. The transition between 4 and 5 is gradual, with a decreasing number of sandy intercalations. Also at the top of unit 5 sand lenses occur.

Unit 6 consists of sand. On the southwest side of the section the base of 6 shows a channel-like structure, cutting into unit 5. Several ice-wedge casts start from this unit; according to Vermij & Heukeshoven (1974) the top of the casts is situated at the base of unit 6. However, since unit 6 sediment also fills the wedges, these will be younger than most of unit 6.

By virtue of their lithology, units 1 through 5 correlate with the Tilligte beds. A lithostratigraphical correlation of the sequence of unit 1-2 with the sequence of unit 2-3-4 in the Hengelo A1 exposure is evident. The erosion level at the base of unit 2 is probably the same erosion level as is represented by unit 3 in the Hengelo A1 exposure. This is further confirmed by the radiocarbon ages of the underlying sediments in both exposures. Consequently units 4 and 5 in this exposure are of approximately the same age as units 5-10 in the Hengelo A1 exposure. The dating of 37.5 ka on unit 4 serves as an upper age limit for the erosion level.

Unit 6 correlates according to Vermij & Heukeshoven (1974) with the Older Coversand II (Van der Hammen, 1971). The possible presence of a fluvial channel structure at the base of unit 6, however, indicates that unit 6 also might contain the Beverborg Member.

VI.3.2. Sedimentary structures.

The fact that only photos and drawings from this exposure are available, hampers the description and interpretation to a certain extent. Estimates of the silt content and humic matter content have to be derived from grey-tones of the photographs, and the nature of bedding and lamination cannot be studied in detail. Still an interpretation can be given in rather general terms.

The sand and gyttja of unit 1 (fig. VI.21) are strongly disturbed by rather irregular type 2a involutions (photo VI.10). According to Vandenberghe (1988) type 2a involutions indicate permafrost conditions. The correlation with unit 2 in the Hengelo

A1 exposure, in which ice wedge casts have been developed, confirms the permafrost origin of the involutions.

Unit 1 is an erosion remnant of limited extent. The horizontal erosion surface above unit 1 is the oldest erosion feature. After the erosion the layered clay or silt of unit 2 has been deposited, indicating a lacustrine environment like that of unit 4 in the Hengelo A1 exposure. On the SW side a sandy lens is intercalated in this silt. The lacustrine silt is overlain by a sand layer with tabular cross-bedding (unit 3). It consist of two foresetted beds, apparently with silt drapes. The foresets are sigmoidal and resemble - with exception of their smaller size- the crevasse splay foresets in the Hengelo A1 exposure. After deposition of unit 3 the channel banks have been cut into the deposits of units 1-3. As the sandy deposits of unit 2 and 3 indicate, the channels already did exist at that time, and merely moved closer to the site.

The bank of the southwestern channel is covered by a large slump block which consists of the sandy non-cohesive material of unit 3 (S in fig. VI.21). The block must have slumped down the bank in frozen condition, as the original sedimentary structures, including a frost fissure have been preserved (photo VI.10; De Jong, pers. comm.). The actual channel bank is very steep, and apparently the cohesive material of unit 1 largely has been eroded away before the overlying sand unit toppled down. According to its length in the drawing, the block might have overhung the bank for at least 2 m. Possibly such a deep cavity is the result of thermo-erosional niche development.

Unit 4 represents a low current velocity channel fill deposit. Silty material with inclined bedding, overlying the slump block of unit 3, might represent a lateral accretion deposit. Towards the base unit 4 is somewhat coarser. The channel fill cross-bedding in unit 4 is directed approximately parallel to the pit face, as can be judged from the gentle bedding slopes. Locally current ripple lamination is visible (photo VI.11). The festoon-like cross-bedded units intersect each other repeatedly (fig. VI.21). Some of the fill units appear to consist mainly of layered silt. Towards the top of the channel fill parallel bedded silt dominates, and possibly also wave ripples occur (photo VI.11). This indicates a gradual transition to standing water. The channel fill of the northwestern channel largely consists of silt, apparently the channel fill cross-bedding is situated deeper. The channel evolution started with active erosion and lateral displacement which was followed by vertical accretion and low current velocities. Channel activity ceased gradually. Both channel sections observed in the pit face are most likely part of the same channel, oriented roughly parallel to the SE-NW directed pit face. Probably units 1-3 have been left over as an erosion remnant in a channel bend. Compared to the channels in the Hengelo A1 exposure, this channel has been a feature of considerable magnitude.

Unit 5 consists of lacustrine clay. In most of the exposure, it is two meters thick. It is mainly parallel bedded, with some thin sandy beds intercalated near the base. This lacustrine deposit, overlying both the channel of unit 4 and its banks, is a clear demonstration that the silting up of the channels coincided with a gradually rising water table at the site.

In summary, the sequence at the Rientjes brickyard represents a transition from a fluvial environment towards a purely lacus-

trine situation, after an initial erosion phase between ca. 43 and 37.5 ka. The erosion phase is accompanied by permafrost degradation phenomena, as is the case in the Hengelo A1 exposure. The apparently long-lasting lacustrine deposition (unit 5) without fluvial interference indicates impeded drainage of the basin.

VI.4. Middle Pleniglacial evolution of the Hengelo basin and correlation with the Dinkel valley sequence.

Within the Twente Formation, Zagwijn (1974) distinguishes two main clay/peat levels, the Lower and Upper Clay Member. Both units are of Middle Pleniglacial age. Unit 1 in the Rientjes brickyard and unit 2 in the Hengelo A1 exposure are correlated with the Lower Clay Member. The overlying silts and clays in both exposures correlate with the Upper Clay Member, dated by Zagwijn (1974) as younger than 39 ka. The fact that both units are separated by only a thin sand layer in these exposures, is not in contradiction with the sections published by Zagwijn (1974, fig. VI.1). Lithostratigraphical correlation of the Upper and Lower Clay Members with the Mekkelhorst Member in the Dinkel valley is obvious.

Information on the sedimentary environment of the Lower Clay Member is scanty, therefore it is not certain whether it differs markedly of that of the Upper Clay Member. The sections of Zagwijn (1974) point to more prominent peat deposition. Very thick clay deposits, like those of the Upper Clay Member, appear to be absent. In the Upper Clay Member sedimentation takes place in a fluvial environment with a pronounced lacustrine component in the floodbasins, locally grading into a fully lacustrine environment. This sedimentary environment indicates incomplete drainage of the basin.

The Rientjes and Hengelo A1 exposures show that after ca. 39 ka and before 37.5 ka permafrost degradation and the development of an erosion level occurred. A similar change is found in a third exposure described by Zagwijn (1974), the Hengelo KNZ pit. In this location cryoturbatic peat, dated at 38350 ±550 (GrN 4828) is overlain by undisturbed gyttja (dated 36600 ±600, GrN 2685). In all three exposures strongly cryogenic disturbed sediments are erosively truncated and overlain by lacustrine deposits.

The radiocarbon datings above show that the erosion level in these exposures is of the same age as the Middle Pleniglacial erosion level II in the Dinkel valley sequence. Erosion level I in the Dinkel valley appears to be lacking in the deep Hengelo A1 exposure; also the data of Zagwijn (1974) do not indicate its presence. The same holds for erosion level III between 33 and 35 ka.

Clearly, erosion level II is the most widely occurring phenomenon. This erosion level is associated with both permafrost degradation and fluvial incision. Fluvial incision is most prominent in the Dinkel basin. The sequence in the Hengelo A1 exposure suggests that fluvial erosion probably has preceded permafrost degradation.

VII. Sediment composition, grain size and grain surface texture analysis.

VII.1. Grain size, lime and organic matter content.

VII.1.1. Analysis methods.

To support the interpretation of the sedimentary environment, grainsize, organic matter and lime content have been determined from a number of sediment samples. Organic matter percentages have been estimated using the ignition loss method. Lime content of the samples has been determined by the Scheibler method.

All grainsize samples have been pretreated using concentrated H_2O_2 to remove organic matter, followed by boiling with 1 N HCl to remove lime. The fine fractions have been peptisized by boiling with 0.24 N $Na_2P_2O_7.10H_2O$ (Sodium Pyrophosphate) at a neutral pH. Silt and clay have been separated from the sand fraction using Atterberg cylinders. For size grades larger than 53 µm separation of grainsize fractions occurred by sieving, finer size fractions have been determined using the pipette method. All size fractions are given as weight percentage of the total sample without lime and organic matter. The samples for grain surface texture analysis have been derived from the 150-210 µm fraction of the grainsize samples.

VII.1.2. Lime content.

Lime is present in most Middle Pleniglacial sediments, especially those from deeper levels. Both sands and silts contain lime and show effervescence with HCl, but sands contain considerably less lime than silt. Silt-poor samples (less than 10% silt/clay) have on average only 2.1% lime, while those with higher silt/clay percentages contain on average 6.0% lime. In the latter group, lime contents up to 20% have been found. Sediments with high organic matter content are usually not calcareous. The correlation of organic matter with lime content is negative (correlation coefficient r=-0.3). This reflects syndepositional decalcification by humic acids of vegetation at the sedimentation surface. Near the top of the Mekkelhorst Member limeless sediments are abundant. Since an appreciable change in lithofacies does not occur, this carbonate decrease indicates either postdepositional decalcification or changes in the sediment sources. The environmental significance of lime content is ambiguous.

VII.1.3. Statistical evaluation of the grain size data.

VII.1.3.1. Evaluation methods.

Traditionally several methods have been used to derive conclusions about the depositional environment from grainsize data. Usually the data are summarized first, by graphical or computational derivation of a few parameters from the set of grain size classes. Often these parameters are based on an idealized statistical model of the grainsize distribution, or on depositional process models. Well known examples are the graphical moment measures of Folk and Ward (1957), the texture diagrams of Doeglas (1946), the CM patterns of Passega (1964), and statistical moment measures (e.g. Friedman, 1961). More recently, multivariate

statistical methods have been employed (Klovan, 1966; Davis, 1970; Allen et al., 1972; Chambers & Upchurch 1979; Brown, 1985).

The Twente Formation is shows large variations in depositional environment. Besides fluvial deposits, also aeolian or colluvial sediments may occur. Mixing and reworking of sediments from different environments and characteristics inherited from parent material further add to the complexity. As a consequence most grainsize histograms show complex, multi-modal distributions.

Distinction between complex grain size distributions cannot be made using parameters which summarize the grainsize distribution (e.g. moment measures) or use only a part of the distribution (e.g. percentile-based parameters). Multivariate statistical methods have the advantage that essentially the entire grainsize distribution can be taken into consideration. It allows distinction of the grainsize fractions which control the variation in the analysis results. This will assist an efficient grouping of the grainsize distributions into environmentally meaningful groups.

Samples from exposures and samples from boreholes with more fragmentary sedimentary structure information have been included in the analysis. By comparing both groups the environmental information from the first group can be extrapolated to the second group. The samples have been split into two large groups, one group of samples with more than 10% silt and clay (the silty group), and sands with a lower silt and clay percentage of which only the sieve fractions have been determined (the silt-poor group). With the silty group also the amount of organic matter has been taken into consideration. This has not been done with the silt-poor group, since organic matter content in practically all these samples proves to be negligible.

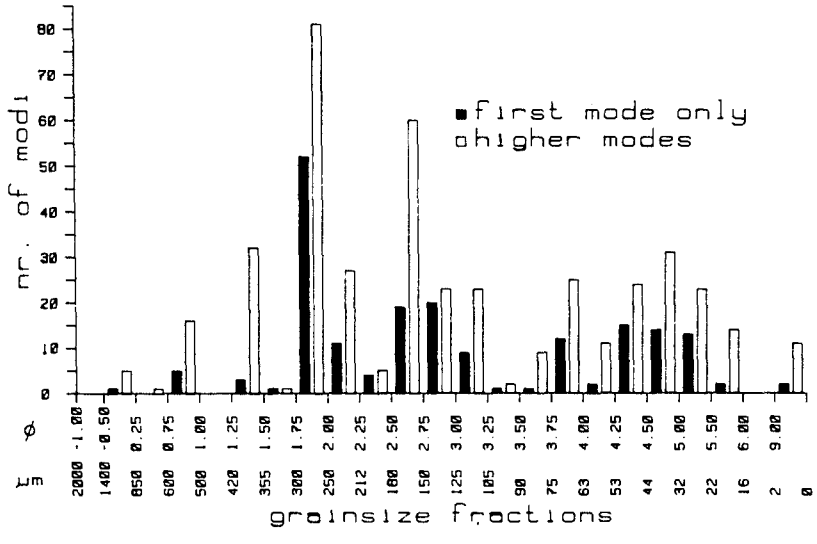

Figure VII.1. Frequency distribution of grainsize histogram modi. Modes are concentrated in the 250-300 µm, 105-180 µm and the silt fractions.

The fine division of the grainsize scale into 1/4 ø units poses problems when using multivariate statistics. The large number of grainsize fractions (24 fractions in the case of silty samples) leads to unduly large data matrices. Moreover, adjacent grainsize fractions are strongly correlated. If the weight percentage in one particular fraction is high, the adjacent

fractions are likely to show high values also. In this way a large amount of redundant information is introduced into the analysis beforehand. A method to overcome this problem is either lumping fractions together, or deleting fractions from the distribution. Deleting some fractions has the advantage of opening the data matrix. The bias introduced beforehand in this way is outweighed by the advantage of more effective and manageable analysis.

The grainsize distributions are composed of different subpopulations which can be related to distinct transport modes (Visher, 1969; Allen et al., 1972; Middleton, 1976; Sagoe & Visher, 1977; Bridge 1981). Modal fractions of the grainsize distribution contain the mean of the different subpopulations which make up the grainsize distribution (Clark, 1976). The modal fractions therefore should be highly sensitive to environmental variation. From a comparison of the modal size fractions of all samples it appears that modi tend to occur in a few fractions only. The most prominent of these is the 1.75 - 2.00 ø (250-300 µm) fraction (fig. VII.1). The fractions which are selected for further statistical analysis (fig. VII.2) are those fractions in which most modi tend to occur.

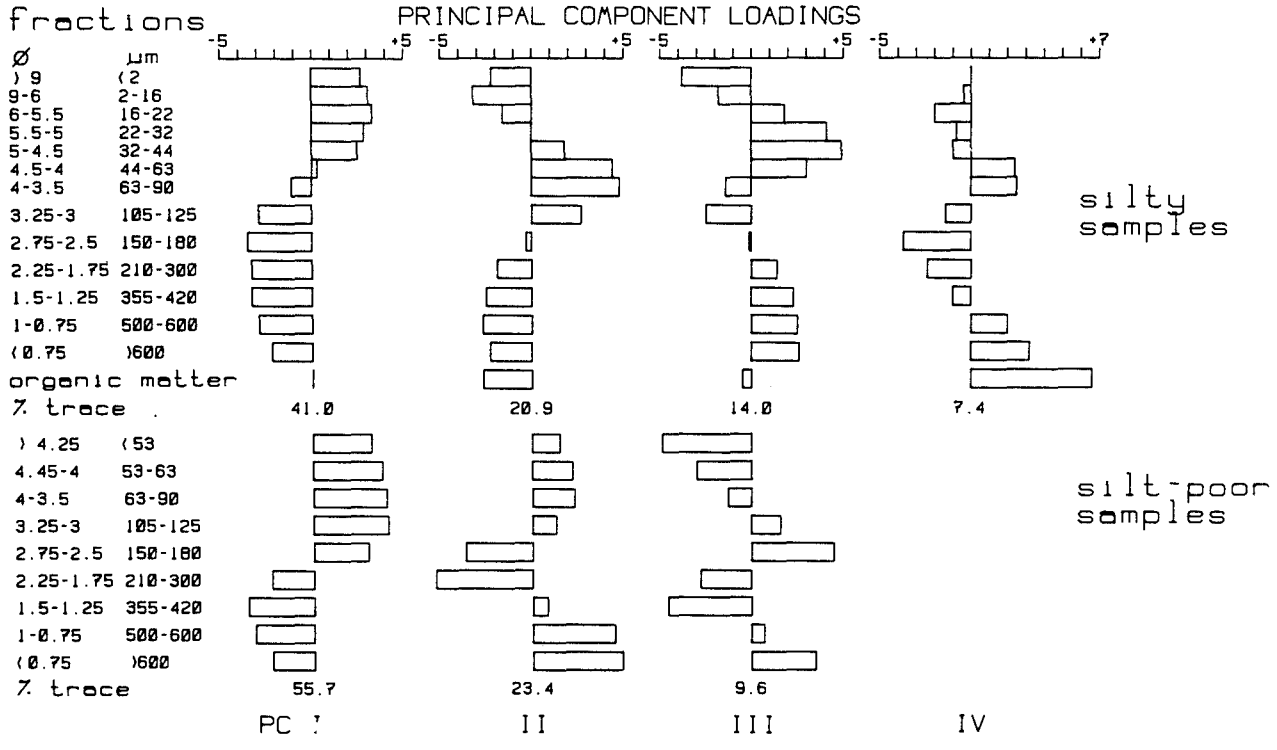

Figure VII.2. Principal component loadings of the grainsize fractions. Left side: fractions taken into consideration for the pricipal components analysis. Percent trace indicates the amount of variation in the data set accounted for by the principal components.

VII.1.3.2. Principal components analysis.

Principal components analysis is a simple multivariate technique which lends itself well to the analysis of the grainsize data set (see e.g. Davis, 1986). After selection of the suitable grainsize fractions the datamatrix has been standardized and a correlation matrix calculated. High correlations between neighbouring size

fractions still exist, but have been reduced to an acceptable minimum. The eigenvectors of the correlation matrix represent the principal components. Fig. VII.2 is a graphical representation of the loadings of each grainsize fraction on the most important principal components. The principal component scores of the samples have been employed to discriminate groups or clusters within the data set (fig. VII.3, 4, 5).

To facilitate interpretation of the principal components, also samples from characteristic sedimentary environments in other Twente Formation stratigraphical units have been treated with the same principal component transformation. Firstly, since aeolian contributions to the sedimentary environment are of interest, loess samples from the Belvedere site (Vandenberghe et al., 1985) and aeolian coversand from the Lage Egge and Nordlohne sites close to the Dinkel valley (Schwan, 1986, 1987) have been used. Secondly, information on the sedimentary structures from the borehole and exposure descriptions is included (table VII.1). Thirdly, log-probability plots of the cumulative grainsize distribution curves facilitate an interpretation of the relation of subpopulations to sedimentation processes (Visher, 1969; Allen et al., 1972).

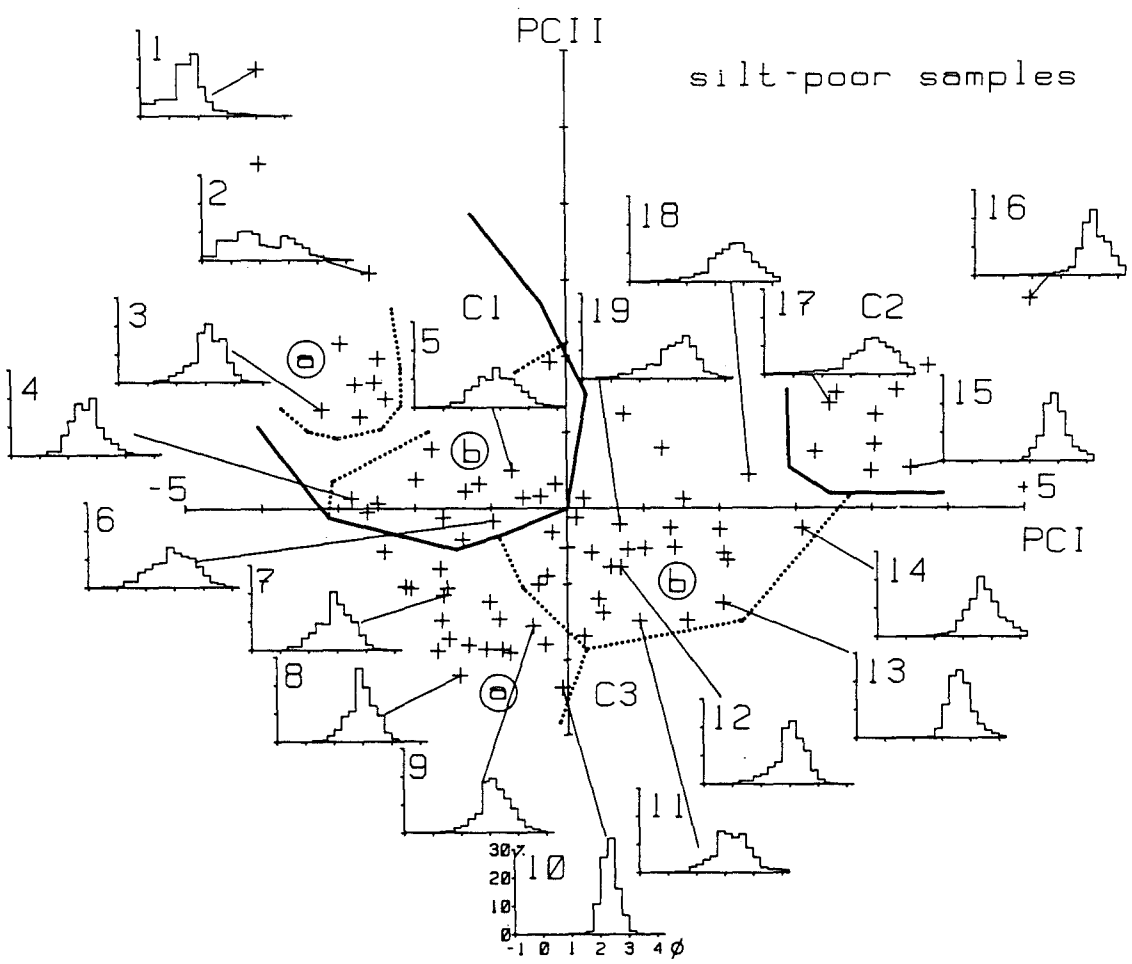

Figure VII.3. Scatter plot of principal component scores of the silt-poor samples, with classification of the samples in three main groups. Histograms show representative grainsize distributions; sample names and location in Appendix 2.

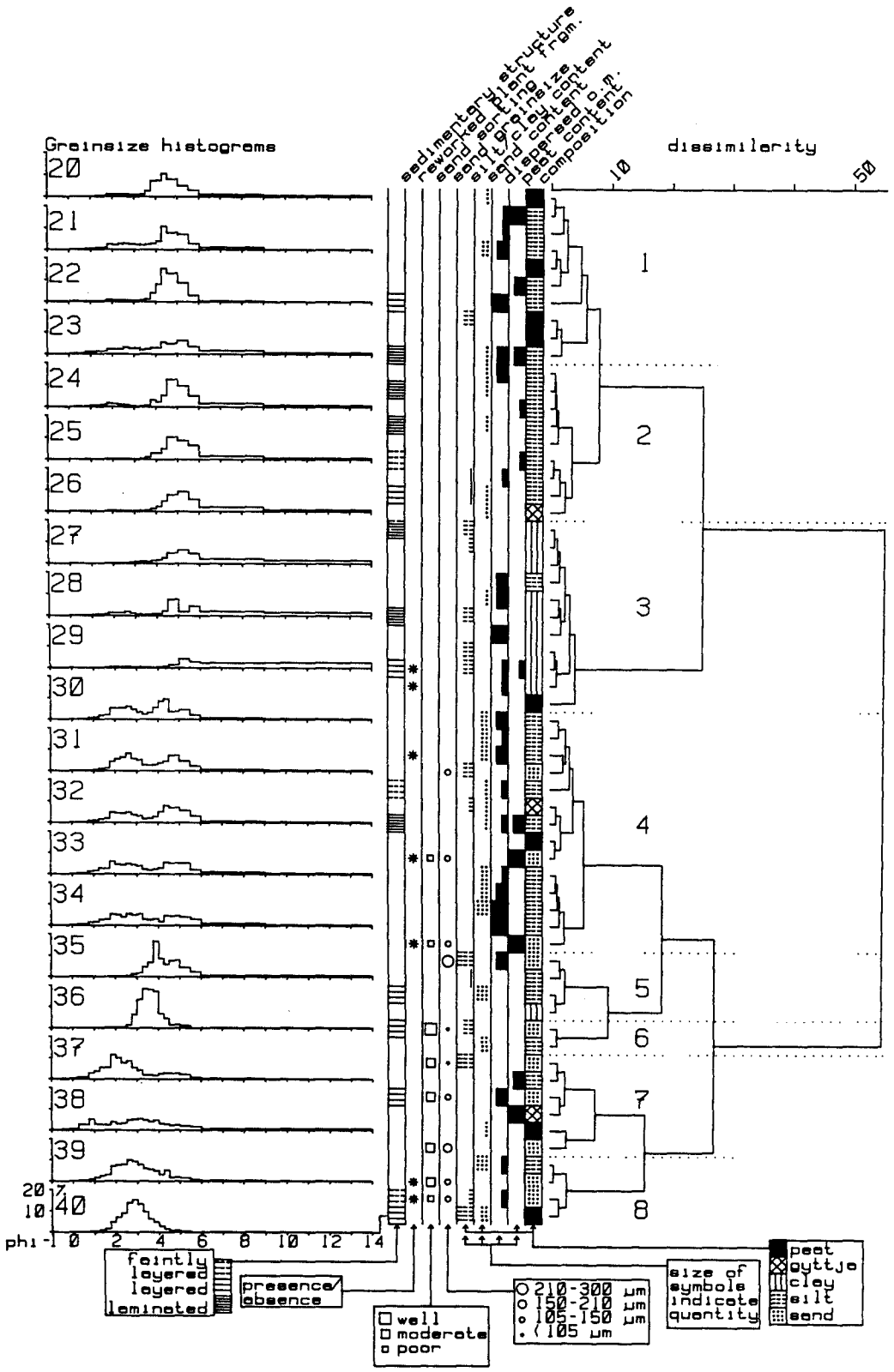

Figure VII.4. Cluster analysis on principal component scores of silty grainsize samples. Left: representative grainsize frequency distributions (sample names and locations in Appendix 2). Middle: field description sedimentary properties of the samples. Right: tree diagram.

For the silt-poor sample group the first two principal components explain nearly 80 % of the variation. Addition of the finest fractions and organic matter content introduces additio-

nal variation. With the silty samples, an acceptable level is reached with the fourth principal component. The first principal component of both groups of samples exhibit the same pattern of loadings (fig. VII.2). High positive loadings occur on the coarse fractions, and negative loadings on the finer fractions. Clearly the proportion of the coarse and fine fractions is the most important variable in the whole data-set; fine grained samples score high on the first principal component. Comparing with moment measures, this corresponds to the mean of the grainsize distribution. This is not an unexpected result. Also in other studies the proportion of fine and coarse fractions has emerged as the most important parameter, as it is related to the energy levels of the depositional environment (Davis, 1986).

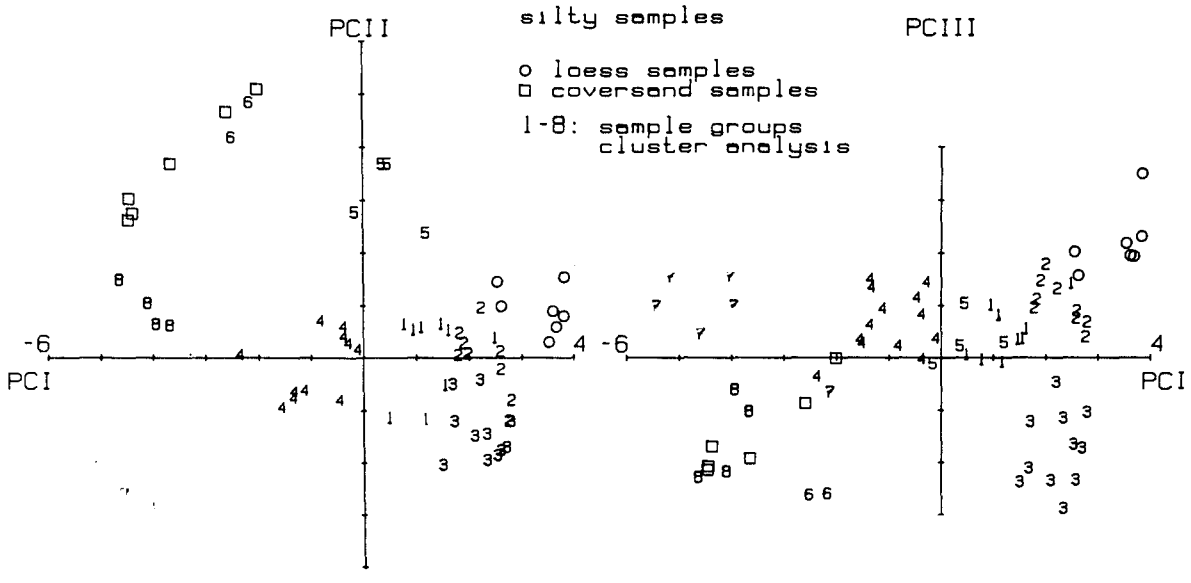

Figure VII.5. Scatter plots of principal component scores of the silty samples, combined with samples from aeolian deposits of other Twente Formation units (Lutterzand Member s.s., loesses; see text for origin of these samples).

VII.1.3.2.1. The silt-poor samples.

The second principal component (PC II) in the silt-poor sample group explains 23.4 % of the total variance. The two coarsest size fractions show a high positive loading, while the 150-180 µm and 210-300 µm fractions show a strongly negative loading. The cumulative curves (fig. VII.6) indicate that the latter fractions are carried in intermittent suspension (Middleton, 1976; Eschner & Kircher, 1984), or represent the 'saltation population' distinguished by Visher (1969). The coarser fractions represent the sediment carried along the bed by a variety of processes, such as sliding, rolling, and saltation (Middleton, 1976), or may be interpreted as lag sediment. Therefore the second principal component is interpreted as an indication of the presence of either coarse bedload sediment, or erosional processes leading to lag deposit development. Fluvial channel deposits are expected to show generally positive scores on PC II.

The scatter plot of the principal component scores of the samples on PC I and PC II (fig. VII.3) reveals clear groupings of the samples. As is shown by sedimentary structure information of

several samples, the C1 and C3 groups consist predominantly of fluvial sediments. The separation between these groups is rather gradual. The C2 group stands out well as a separate group on the scatter plot, and represents sediments with a possible aeolian component.

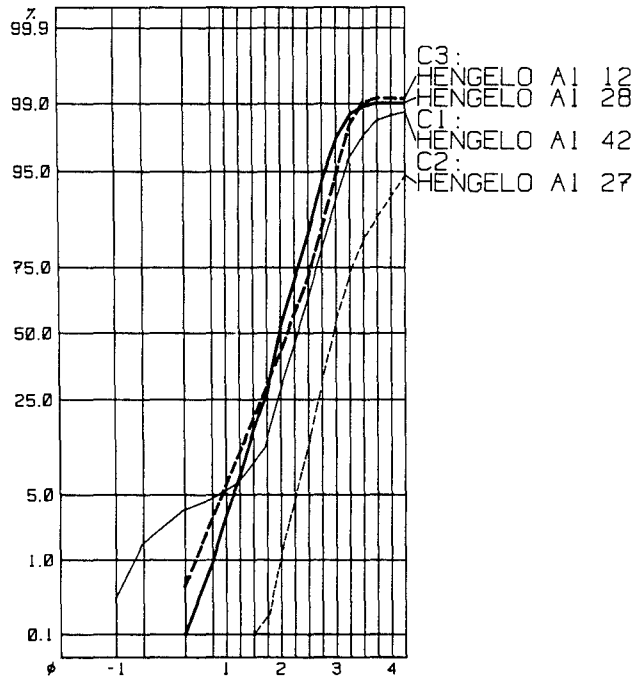

Figure VII.6. Representative cumulative curves of the silt-poor sample group. C1, C2, C3: grainsize distribution type distinguished in fig. VII.3.

Group C1, with negative scores (<-1) on PC I and positive or slightly negative scores on PC II, represents samples of a fluvial channel origin. All samples have coarse subpopulations which dominate in the extreme outliers of this group. Two subgroups can be discerned (C1a and C1b, fig. VII.3). C1b contains samples with a conspicuous amount of sediment in the 125-250 µm range. One of the samples with the highest positive scores on PC II originates from very coarse gravelly sand with peat clasts and clay pebbles. The presence of gravel or intraclasts has been noted frequently in the field descriptions of these samples (fig. VII.7). Hence, the interpretation of this group as being fluvial channel deposits is justified, and is consistent with the interpretation of the principal components given above. In the Hengelo A1 exposure, some coarser crevasse splay topset and foreset samples are found in group C1 which reflects the presence of a certain amount of coarse material transported by rolling and sliding (table VII.1).

Group C2 consists of fine sands. As such, these are characterized by positive scores on PC I (>3). Also on PC II these samples have positive values, because PC II gives a slightly positive weight to the fine fractions besides the coarsest fractions. The field descriptions often note a layered structure. The rightmost outlier of this group originates from Middle Pleniglacial fluvio-aeolian deposits in a small exposure in the Dinkel valley (De Poppe exposure, par. VIII.3.1). When the principal component scores of the 'coversand' samples from the

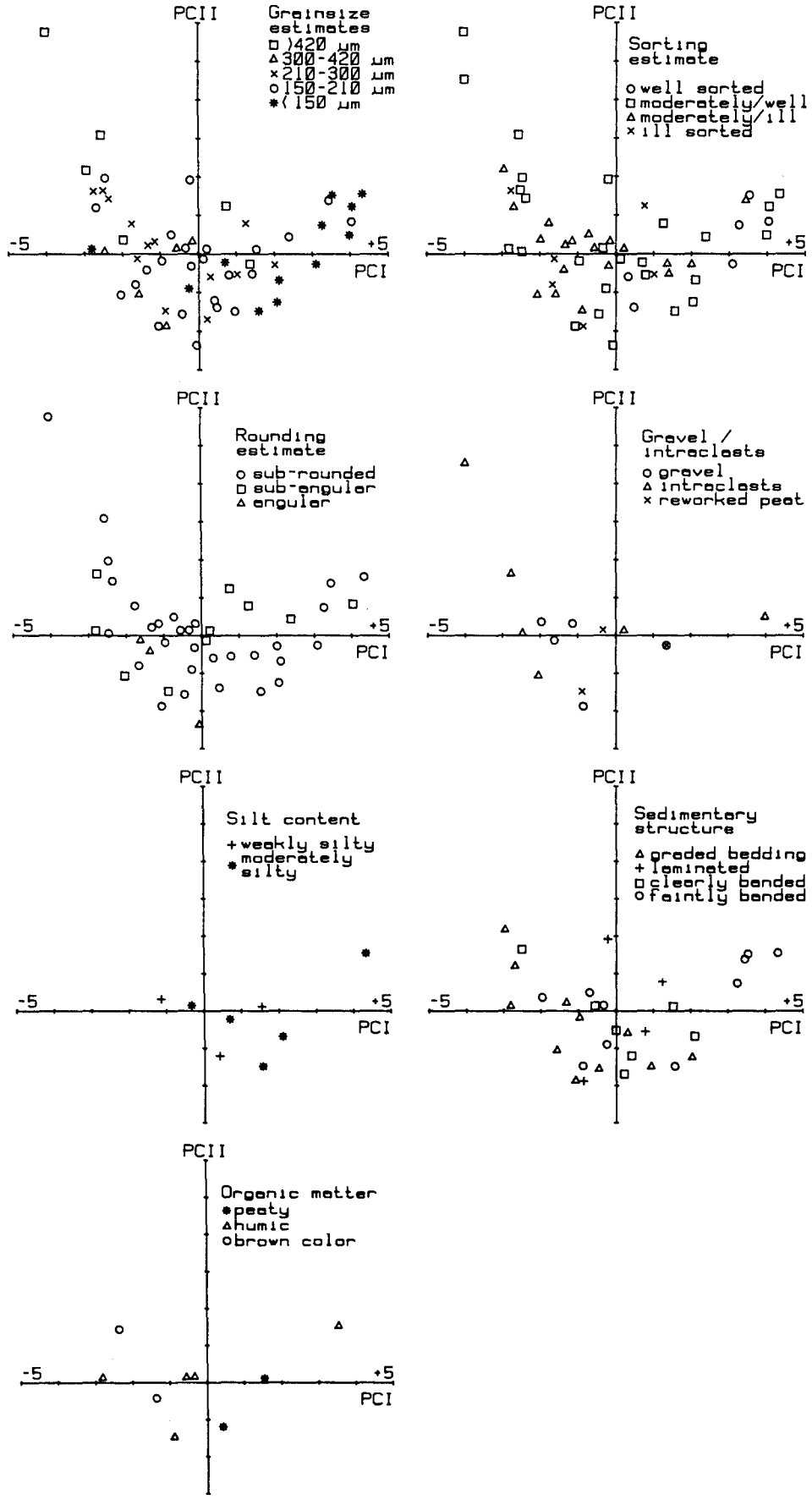

Figure VII.7. Relation between field description of the silt-poor samples and their location on principal component scatter plots.

Lage Egge and Nordlohne sites (Schwan, 1986, 1987) are calculated, most of these samples also prove to plot within this group (fig. VII.8). This applies especially those sands which are of the horizontal alternating bedding type frequently found in the Lutterzand Member s.s (Schwan, 1986). Hence, the grain size distribution strongly resembles that of coversands. Sands of the aeolian alternating bedding type may incorporate aeolian suspension material which constitutes the finest fractions of these samples (Schwan, 1988a).

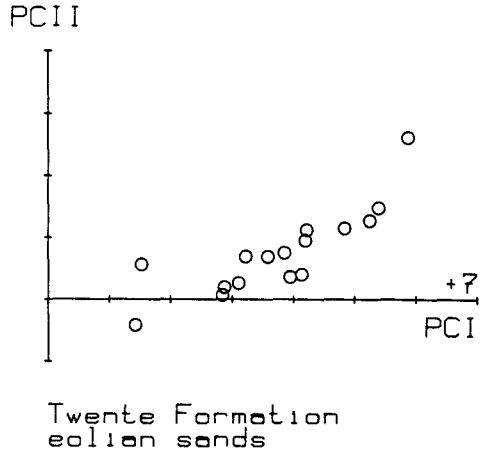

Figure VII.8. Principal component scatter plot of aeolian sands from other Twente formation units (Lutterzand Member s.s., Wierden Member; see text for origin of these samples).

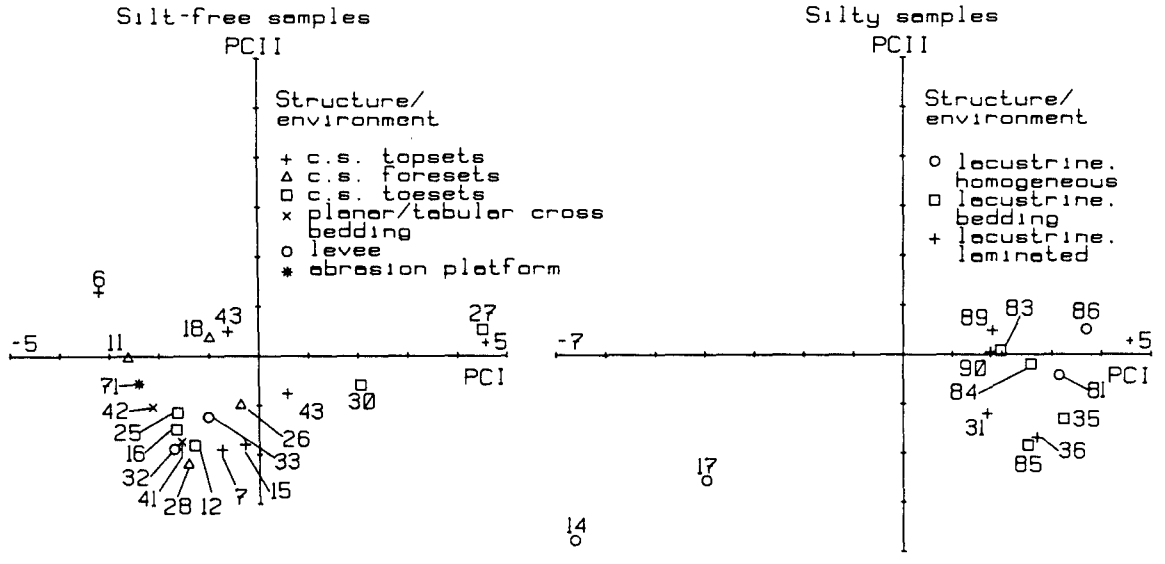

Figure VII.9. PC I-II scatter plot of samples from Hengelo A1 exposure, with indication of sedimentary environment. Numbers correspond to sample numbers in the figs. VI.8-24.

However, in several of the group C2 samples sedimentary structures contradict an aeolian origin: current ripple cross-lamination, presence of intraclasts (fig. VII.7). One sample originates from the toesets of the crevasse splays in the Hengelo A1 site (table VII.1). In general most C2 samples are less well

sorted than the typical coversands (Schwan, 1988a). Hence most of the samples in this group represent low-energy fluvial environments. The probable cause of the resemblance to aeolian sands of these fluvial deposits is reworking of aeolian deposits.

The third and largest group (C3) has negative or slightly positive scores on PC II and intermediate values on PC I. The usually negative scores on PC II indicate that the graded suspension load dominates these samples. These samples originate from environments where scouring and lag deposit formation is minimal, and intermittent suspension transport dominates over bedload traction. Subgroup C3a (strongest negative scores on PC II, negative on PC I) contains samples with a peak in the 250-300 µm range. Subgroup C3b (negative on PC II, positive on PC I) generally contains finer sediments, dominated by subpopulations in the 125-250 µm range.

Group C3 represents samples from overbank environments, and possibly lower energy channel environments. Sands which are transported from channels into overbank environments can be expected to contain largely (intermittent) suspension fractions, while sedimentation in general will be rapid, without scouring. The crevasse splay deposits from the Hengelo A1 site (par. VI.2) largely belong to subgroup C3a (table VII.1, fig. VII.9). Other cross-bedded sediments also plot in this group. Subgroup C3a therefore represents environments in closest proximity of the channels. In subgroup C3b probably more distal overbank sediments occur, sediments with an aeolian component might be included. Some samples from the Nordlohne site, especially those belonging to the coarser aeolian facies (Schwan, 1987) plot in this subgroup (fig. VII.8).

VII.1.3.2.2. The silty samples.

In general the grainsize distributions of the silts is more intricate than those of the sands. Most distributions are markedly bi- or multimodal (fig. VII.4). Cumulative log-probability plots (fig. VII.10) show various breaks in the slope of the curves. At least five subpopulations appear to occur. Some curves in fig. VII.10 show pronounced steps, indicating intermixing of sediments deposited at quite different energy levels. This points to alternation between different depositional mechanisms (e.g. current flow versus standing water).

In most samples the size fraction smaller than ca. 16 µm is present in only low amounts, and the coarsest silt fractions (32-63 µm) dominate completely. Both fractions belong to the wash load which consists of sediment produced by slopewash in the drainage basin (Richards, 1982). It is not very likely that one particular group of size fractions is over-represented in the highly variable drainage basin substratum, causing dominance of a particular grainsize fraction in the valley fill sediment. Also the tills of the Drente Formation do not show exceptionally high silt percentages (Zandstra, 1983). The coarser silt fractions may be preferentially deposited as the finest material will be carried longer in suspension (Walling & Moorehead, 1987). However, this does not explain the conspicuously high values of the coarsest silt fraction in all silt and clay beds, compared with the very low values of the finer silt fractions (2-16 µm, fig. VII.1 and 4). Even the most clay-rich sediments still have a first mode in the coarse silt fractions. Therefore the 32-63 µm

fractions should represent some specific sediment source, independent from the drainage basin substratum and depositional selection processes. It most probably represents addition of loess which mainly consists of material in this grainsize range (literature review by Mücher, 1986). Also in present-day wetlands in Alaska significant inputs of aeolian silt occur (Ford & Bedford, 1987). The remaining fractions in the sand range roughly correspond to the subpopulations in the silt-poor samples. A break between graded suspension bedload and rolling transport at 1.75 ø (300 µm) is not clearly present in the more fine-grained samples.

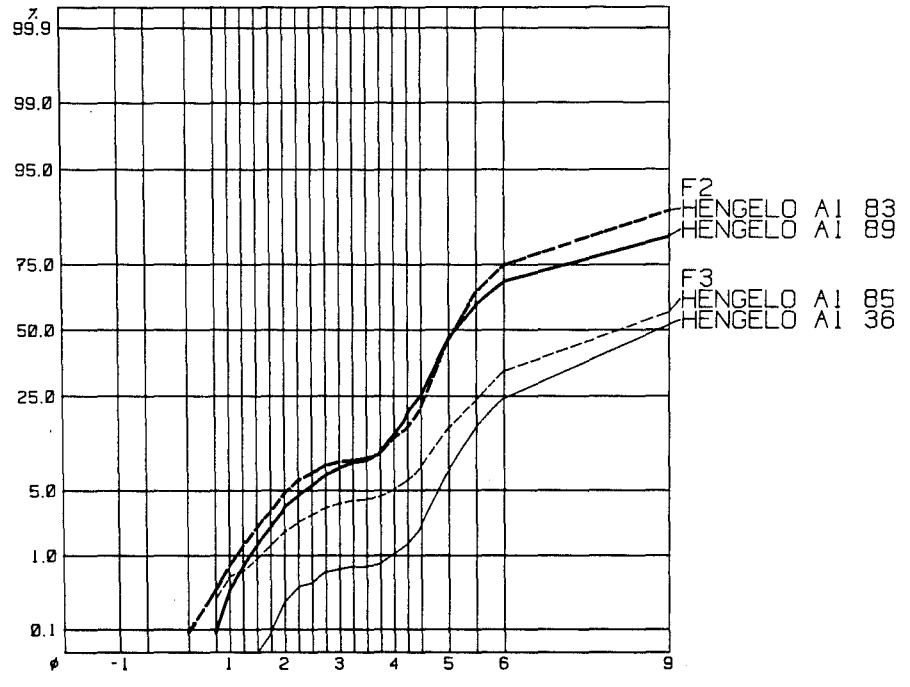

Figure VII.10. Representative cumulative curves of the silty sample group. F2, F3: grainsize distribution types (fig. VII.4).

As mentioned above PC I is an indication of the general coarseness of the sediment. PC II emphasizes the coarse silt and fine sand fractions. The finest fractions and the coarser sand fractions receive negative loadings. This principal component is responsible for 21 % of the variation in the data set. The finest sand and coarsest silt fractions represent a coarse fluvial wash load fraction. The clay fraction, however, has a negative loading. PC II therefore might separate purely lacustrine environments where also the finest material settles out, from temporary flooded environments where the finest sediment is carried away during flood recession. A negative loading on PC II indicates prolonged standing water. Alternating bedding coversands and loesses also show positive scores on PC II (fig. VII.5). Therefore positive scores on PC II also might express the addition of a (reworked) aeolian suspension component.

PC III explains 14 % of the variance. The coarsest fractions show positive loadings, together with a strongly positive loading on coarse silt fractions and a negative loading on the clay fraction. PC III apparently expresses regular occurrence of current flow carrying a certain amount of coarse bedload.

PC IV accounts for only 7 % of the variation. Nevertheless it is still worth considering, since the organic matter content receives the highest loading in this principal component. Clearly, there is no strong relation to organic matter content and the type of clastic sediment which is deposited. This also has been observed in a modern subarctic fluvial/deltaic environment. Dahlskog (1966) shows that in a Northern Scandinavian river delta vegetation rather reacts on sedimentation conditions instead of influencing them. The clastic sedimentation appears to determine organic matter content. If large amounts of clastic sediment are deposited in a relatively short time on a certain site, the organic matter content of the sediment will be low, in spite of the presence of vegetation on the site. Sedimentation rate data from the palaeobotanical analysis confirm this (Ran, 1990). In the correlation matrix organic matter content only shows positive correlations with the finest silt fraction and the coarsest sand fraction. This agrees with the two possible sources of the organic matter in the sediment: growth in situ on quiet sites of the alluvial plain, and fluvially transported organic debris.

As scores on at least the three first principal components have to be incorporated, a classification of the silty samples is more difficult to establish. Therefore cluster analysis has been applied to assist in developing a partitioning of the data set, using the first four principal component scores of the samples. The clustering algorithm used is known as Ward's method which constructs groups by minimizing the within-group sum of squares (Ward, 1963; Mather, 1976). This method yields several groups in the data set (fig. VII.4). The first three groups (F1, F2, F3) lie closely together on the scatter plot of the PC I and II principal component scores. These groups all have positive scores on PC I, and positive or negative on PC II and III.

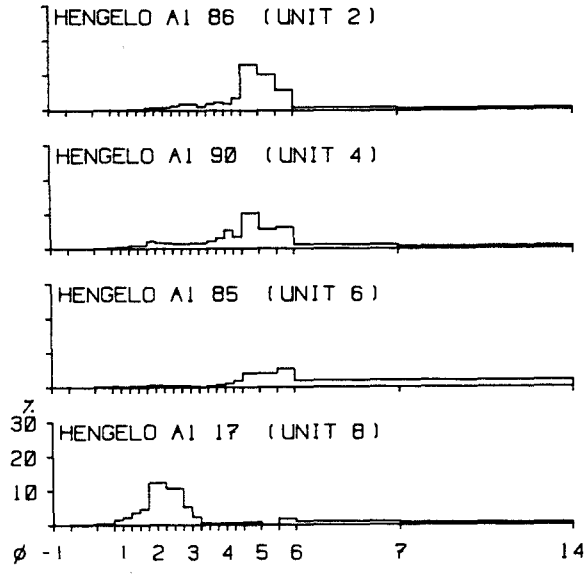

Figure VII.11. Grain size histograms of different types of silt beds from the Hengelo A1 exposure. Unit numbers refer to lithostratigraphical units in section VI. Unit 2: homogeneous silt; unit 4: laminated sandy silt; unit 6: layered clayey silt; unit 8: layered clayey sand/silt.

Sample number	Sedimentary structure	Unit	Environmental interpretation	Sample location fig.	Class
H 6	parallel lamination	7	crev. splay topset	VI.17	C1a
H 11	foreset cross-bedding	7	crev. splay foreset	VI.15	C1b
H 18	foreset cross-bedding	7	crev. splay foresets		C1b
H 43	sand wit silt pebbles	7/8	crev. splay topsets	VI.11	C1b
H 27	parallel lamination	7	crev. splay toesets		C2
DP VI.5	parallel bedding/lamin.	3	aeolian sand		C2
H 32	cross-lamination	6	small levee	VI.8	C3a
H 33	cross-lamination	6	small levee	VI.8	C3a
H 15	cryoturbated	7	crev. splay topsets	VI.16	C3a
H 16	parallel lamination	7	crev. splay toesets	VI.16	C3a
H 12	parallel lamination	7	crev. splay toesets	VI.15	C3a
H 25	parallel lamination	7	crev. splay toesets		C3a
H 28	foreset cross-bedding	5	crev. splay foresets	VI.14	C3a
H 41	planar-tabular cross-bedd	9	channel bedform	VI.11	C3a
H 42	planar-tabular cross-bedd	9	channel bedform	VI.11	C3a
H 71	cross-lamin./intraclasts	3	abrasion platform	VI.5	C3a
H 26	foreset cross-bedding	7	crev. splay foresets		C3b
H 30	parallel bedding	5	crev. splay toesets	VI.14	C3b
H 7	parallel lamination	7	crev. splay topsets	VI.17	C3b
H 86	homogeneous	2	floodplain	VI.5	F2
H 89	parallel lamination	4	thaw lake	VI.5	F2
H 90	parallel lamination	4	thaw lake	VI.5	F2
H 35	parallel bedding	6	shallow lacustrine	VI.8	F2
H 81	involuted/homogenized	6	shallow lacustrine	VI.6	F2
H 83	parallel bedding	6	shallow lacustrine	VI.9	F2
H 84	parallel bedding	6	shallow lacustrine	VI.9	F2
H 31	parallel lamination	6	shallow lacustrine	VI.8	F3
H 36	parallel lamination	6	fine gr. channel fill	VI.8	F3
H 85	parallel bedding	6	shallow lacustrine	VI.9	F3
H 14	involuted/homogenized	8	shallow lacustrine	VI.16	F7
H 17	involuted/cross-lamin.	8	shallow lacustrine		F7

Table VII.1. Grainsize samples from exposures (H = Hengelo A1, DP = De Poppe, par. VIII.3.1), with classification in sample groups as developed above. crev.splay = crevasse splay.

Both F1 and F2 grainsize distributions are dominated completely by the coarse silt fraction (fig. VII.4) and therefore may contain a loessic component. This is illustrated by the topmost F2-type grainsize distribution in fig. VII.11 (top of unit 2 in the Hengelo A1 exposure, par. VI.2.1) which has a grainsize distribution strongly resembling that of genuine loess. The main differences between F1 and F2 are the organic matter content, sedimentary structures and a somewhat higher fine sand content in F1. Group F1 contains peat and humic or peaty silt, and most samples have a modus in the 4-4.25 ø (63-53 µm) fraction. The occurrence of peat within F1 suggests mainly (semi-)terrestrial environments. The somewhat higher fine sand content relative to fine silt is not in contradiction with this origin. During

flooding, these somewhat higher floodplain sites will experience slightly higher current velocities on average. Another sand source in these environments may be aeolian sand.

F2 samples have lower organic matter content, and therefore the sedimentation rate probably has been higher. Also the fine silt content is somewhat higher. Samples in F2 may be partly of lacustrine origin (e.g. samples from the finely laminated thaw lake deposits in the Hengelo A1 exposure belong to this group; fig. VII.11, table IV.1). In general, samples from F2 tend to display lamination and bedding more often than those of group F1. Samples with a less well developed lamination probably represent shallower lacustrine or mainly terrestrial environments (par. VI.2.4.1).

Group F3 contains sediments with a large amount of clay. Organic matter content varies strongly. The high amount of clay in these samples suggests a distal backswamp or lacustrine origin, with less fluvial influence and less silt influx than F2. The low scores on PC III show a relatively low amount of the coarse silt fractions. It appears that within the Dinkel basin group F3 sediments most frequently occur in the basal clays of the Tilligte beds. In the Hengelo A1 exposure this type of sediment is of common occurrence in the younger Middle Pleniglacial unit 6 (table VII.1, fig. VII.11).

Groups F4 to F8 represent more sandy sediments. Group F4 contains strongly bimodal sediments with modes in the silt and sand fractions; the silt mode dominates. The organic matter content is generally high; also peat and gyttja samples occur within this group. This group represents the same type of overbank environments as groups F1 and F2, but with a more important influx of coarse material, and consequently a position closer to river channels.

Group F5 and F6 each contain only a few samples. F5 consists of bimodal sand/silt mixtures, F6 represents rather well- sorted fine sands. Typical coversand samples from the Lutterzand Member s.s. plot in approximately the same range as in group F6. Organic matter is generally absent. Therefore F5 and F6 can be considered as a somewhat siltier equivalent of group C2 discussed above, with a similar aeolian component.

Groups F7 and F8 represent sands with variable organic matter content, some samples have been classified as peat or gyttja. F7 contains ill-sorted samples in which the sand fraction dominates, up to the coarsest fractions. The presence of the coarsest fractions point to overbank environments in the vicinity of fluvial channels. The fine fraction may have been derived from reworked silt pellets, from an alternation of sand deposition by running water and deposition from suspension, or wave reworking in silty floodbasin environments. The latter process is illustrated by a sample from unit 8 in the Hengelo A1 exposure, a shallow lacustrine deposit with sandy intercalations and wave ripples (fig. VII.11, table VII.1). Group F8 is related to F7, but contains better sorted, silt-poor samples. Apart from the somewhat higher silt content (just over 10 %), these resemble samples from group C3b. A similar origin is assumed.

VII.2. Grain surface morphoscopy using the scanning electron microscope (S.E.M.).

VII.2.1. Introduction.

As physical and chemical processes during transport and sedimentation may leave their imprint on sand grain surfaces, a study of surface features may yield information on these processes (e.g. Krinsley & Donahue, 1968; Margolis & Krinsley, 1971; Krinsley & Doornkamp, 1973; Smart & Tovey, 1981; Culver et al., 1983). Limitations of the method are caused by the fact that many surface features may have been produced in more than one environment (Brown, 1973; Manker & Ponder, 1978). Furthermore inheritance of features from previous erosion/deposition cycles plays a role (Margolis & Krinsley, 1973; Elzenga et al., 1987), as does the variance in the analysis results caused by observer bias (Culver et al., 1983). These limitations can be overcome by considering combinations of surface features, counted from a statistically representative number of quartz grains (Margolis & Krinsley, 1973; Culver et al., 1983). Several types of grain surface features can be produced experimentally (e.g. Kuenen, 1960; Margolis & Krinsley, 1971; Nieter & Krinsley, 1976; Lindé & Mycielska-Dowgiałło, 1980). Literature on grain surface features of sand from periglacial environments shows that also in this case meaningful conclusions about sedimentary environment can be derived from quartz grain surface features (Krinsley & Cavallero, 1970; Vincent, 1976; Korotaj & Mycielska-Dowgiałło, 1982; Kowalkowski & Mycielska-Dowgiałło, 1983; Kowalkowski & Brogowski, 1983; Elzenga et al., 1987).

Within the Twente Formation discrimination between aeolian and fluvial sedimentation is of both palaeo-climatic and stratigraphical significance. Wijmstra et al. (1971) have applied a crude form of morphoscopic analysis to the Twente Formation sequence of the Mekkelhorst boring in the study area, by determining the percentages of dull and translucent sand grains. This showed stratigraphically consistent differences within the Twente Formation. Elzenga et al. (1987) have shown that differences in quartz grain surface features within Twente Formation sediments are related to both depositional environment and geographical location. In the Twente region grain surface features of chemical origin prove to be more abundant than in the southern Netherlands which is attributed to parent material differences.

In this study grain surface morphoscopy has been used to support conclusions about aeolian or fluvial origin derived from grainsize analysis. The quartz grains may have inherited features from different processes during their transport history. Experimental data indicate, however, that aeolian abrasion occurs relatively rapid compared to abrasion in aqueous environments (Kuenen, 1960; Lindé & Mycielska-Dowgiałło, 1980). Frequent occurrence of aeolian reworking therefore should be readily detectable by an increase in grain surface features attributed to aeolian abrasion.

VII.2.2. Analysis method and feature description.

Analysis has been restricted to samples of which also grainsize information is available. Besides samples from the Tilligte beds

and Puntbeek sands, also a sample from the Dinkel Member and one from the Liendert Member have been included (table VII.2).

From each sample 30 grains in the size range of 150-210 µm, retained from the size analysis, have been picked at random. The number of 30 grains has been suggested by Culver et al., 1983. Elzenga et al. (1987) present a description of 29 types of surface features which have been found on Twente Formation quartz grains. The same list of surface features has been used in this study (table VII.3). For each sample, the S.E.M. study resulted in a tally matrix with the number of grains on which a specific surface feature has been observed.

Sample name	Nr	Sample location (section or exposure)	Age estimate chronology or chronostratigraphy
Scholtenhave 367-370	1	Laarhuis-Rammelbeek	36-40 ka
Scholtenhave 401-404	2	Laarhuis-Rammelbeek	36-40 ka
Scholtenhave 827-829	3	Laarhuis-Rammelbeek	47-51 ka
Scholtenhave 987-989	4	Laarhuis-Rammelbeek	47-51 ka
N. Deurn. 1240-1244	5	Laarhuis-Rammelbeek	>50 ka
N. Deurn. 1085-1089	6	Laarhuis-Rammelbeek	>47 ka
571/605-611	7	Gildehaus	<39 ka
572/449-455	8	Gildehaus	<39 ka
Venweg 1312	9	Laarhuis-Rammelbeek	Early Pleniglacial
Dorpermeien 472	10	Denekamp sections	<36 ka
Hengelo A1 26	11	Hengelo A1	<39 ka
Hengelo A1 30	12	Hengelo A1	<39 ka
Hengelo A1 6	13	Hengelo A1	<39 ka
Hengelo A1 7	14	Hengelo A1	<39 ka
Venweg 753	15	Laarhuis-Rammelbeek	40-47 ka
Venweg 1007	16	Laarhuis-Rammelbeek	47-50 ka
Scholtenhave 1284-1287	17	Laarhuis-Rammelbeek	Early glacial

Table VII.2. Sample numbers and origin. Name or first number refers to boring, other numbers in boring samples denote depth below surface in centimeters. See figures of section VI for location of exposure samples.

Because of the high frequency of features of apparent chemical origin some detail has been added in table IV.3. Frequently, irregular scaling of a secondary silica layer has been observed on the grains. If this occurred over large areas it has been classified as chemical disintegration. Often this surface scaling (photo VII.1) resembles cryothermal scaling described by Kowalkowski & Brogowski (1983) and Kowalkowski & Mycielska-Dowgiallo (1983), thus this feature might be attributed to cryogenic weathering as well.

Minor amendments have been made to two of the surface characteristics in table IV.3. Conchoidal fractures have been split in two size groups, fracture planes having either a larger or smaller diameter than 15 µm. Conchoidal fractures of either size occur on virtually all grains, but during analysis it was noted that only the smaller conchoidal fractures occurred as fresh features on strongly abraded or chemically modified grains. The smaller fractures therefore could be of different origin than the larger fractures. Especially abundant large conchoidal fractures

Name of surface feature	Generally supposed formative mechanism and/or environmental significance
Roundness	degree of abrasion
High microrelief	degree of grain surface modification since removal from parent rock
Conchoidal fractures	breakage by high energy grain-to-grain collision, glacial environment, freshly mechanically weathered rock
Semi-parallel steps	associated with conchoidal fractures, shear stress
Arc-shaped steps	associated with conchoidal fractures
Semi-parallel lines	movement of sharp objects along grain
Straight scratches	grain-to-grain collision
Curved scratches	grain-to-grain collision
Mechanical V-shaped pits	impact features, relatively high energy environment
Scratches with satellite V's	idem
Imbricated breakage blocks	glacial environment
Disc-shaped concavities	associated with conchoidal breakage patterns, aeolian environment
Meandering ridges	caused by intersection of conchoidal breakage patterns, aeolian environment
Upturned plates	crystallographically oriented plates, produced by mechanical wear
Graded arcs	percussion fractures, aeolian environment
Chattermarks	grains skipping along one another
Flat cleavage planes	cleavage, especially smaller grains, inherited from parent rock or in glacial and subaquatic environment
Fresh cleavage planes	associated with conchoidal fractures
Irregular small fractures	high energy impact features
Precipitation of silica as upturned plates	crystallographically oriented precipitation
Oriented etch V's	crystallographically oriented etching
Irregular precipitation/ solution surface	solution/precipitation
Silica plastering	diagenesis, glacial environment
Chemical disintegration	chemically aggressive environment
Solution pits	chemical solution
Surface scaling	chemical or cryogenic abrasion
Smooth precipitation surface	rapid precipitation of silica
Arc/ circle/ polygonal cracks	associated with chemical precipitation surface, probably caused by shrinkage
Quartz crystal growth	quiet, slow precipitation of silica
Orange-peel texture	upturned plates smoothed by precipitation/solution, aeolian environment
Adhering particles	glacial and aeolian environment

Table VII.3. Grain surface features distinguished on Twente Formation quartz grains, adapted from Krinsley & Doornkamp (1973), Higgs (1979), and Elzenga et al., 1987. Underlined features have been used in the statistical analysis.

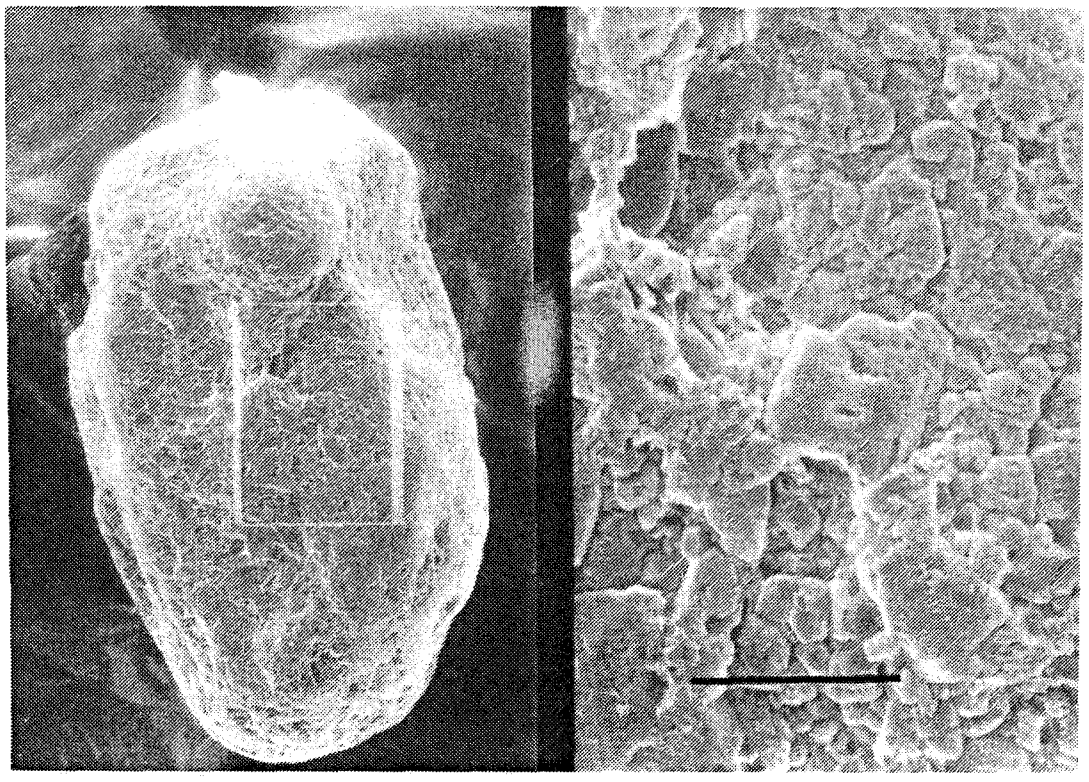

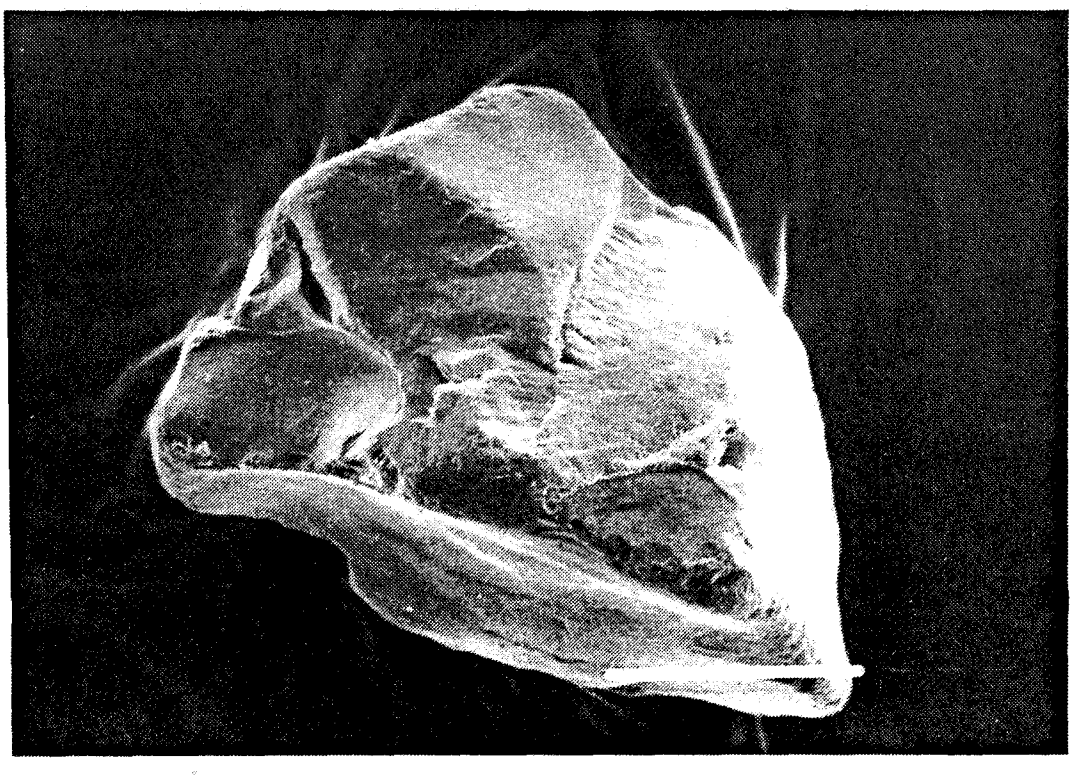

Photo VII.1 (top). Irregular surface scaling of presumed chemical or cryogenic origin. Sample 16, table VII.2; magnification right side 200 x, left side 1000 x; scale bar right side 100 µm, left side 20 µm.

Photo VII.2 (below). Typical angular grain with large conchoidal fractures and only minor abrasion of the edges. Sample 13, table VII.2; magnification 250 x, scale bar 100 µm.

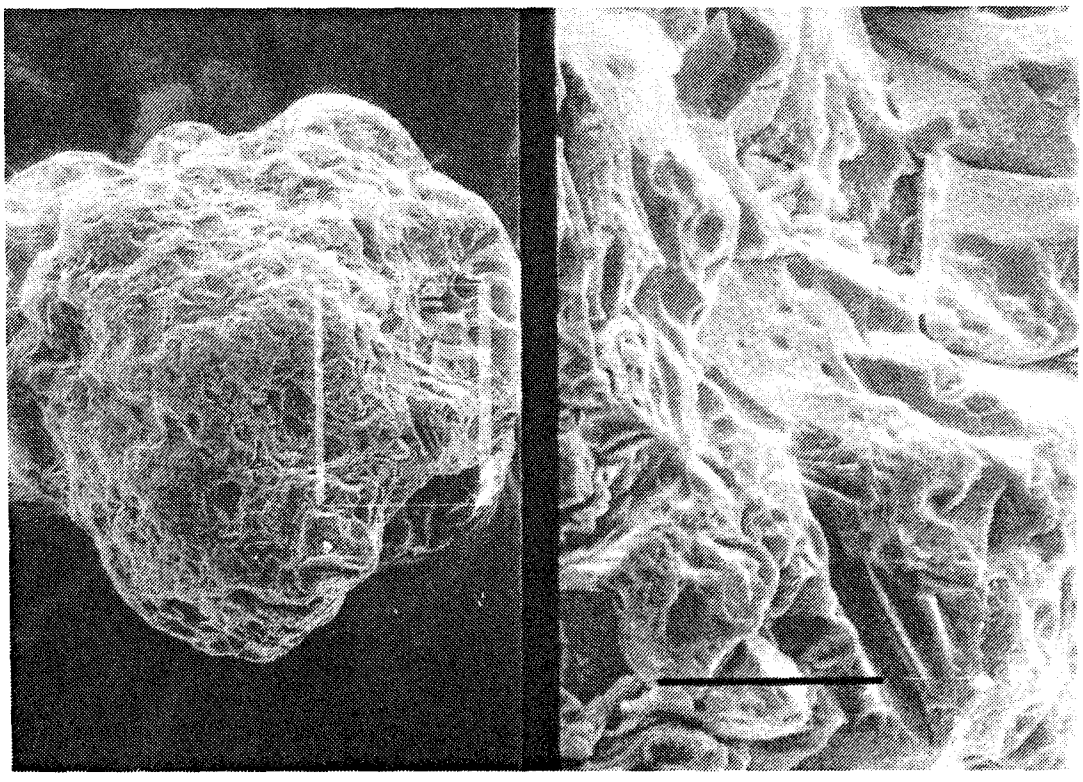

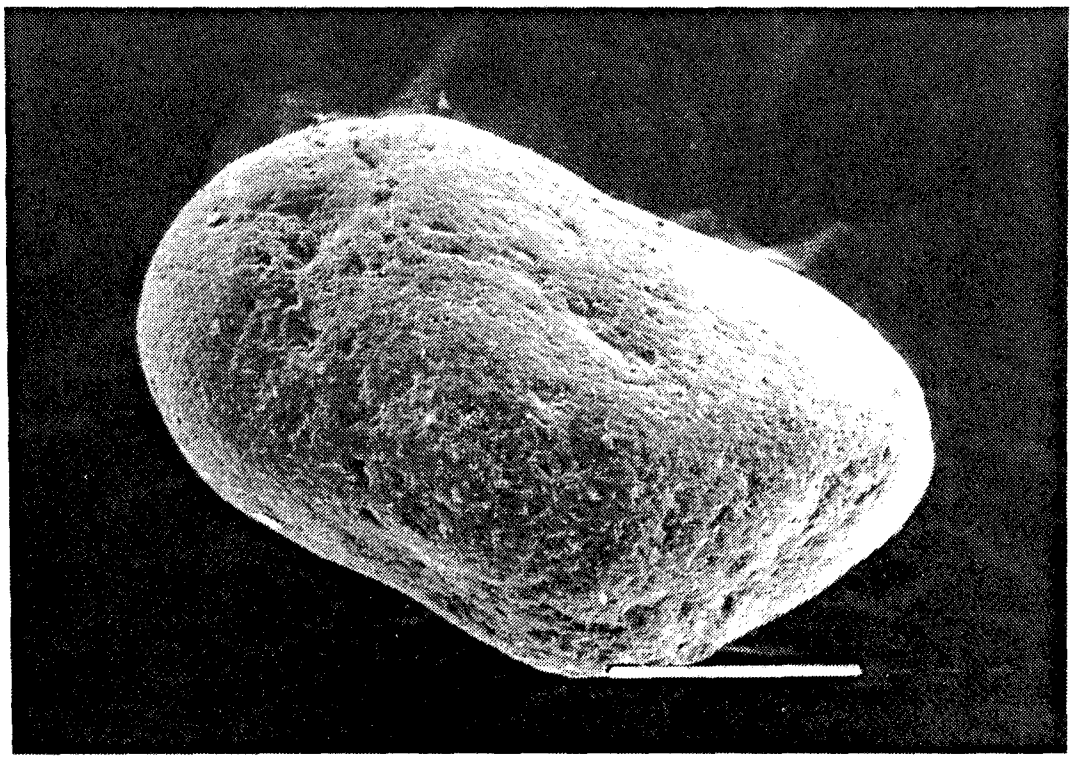

Photo VII.3 (top). Irregular grain with strongly modified surface features, both by mechanical and chemical wear. Features caused by chemical wear are irregular solution pits and scaled surface, mechanical wear is shown by small conchoidal fractures. Right side: detail of intersecting small conchoidal fractures which may have been caused by hydro-cryothermal splitting. Sample 16, table VI.2; magnification left side 215 x, scale bar 100 µm; magnification right side 1075 x, scale bar 20 µm.

Photo VII.4 (below). Well rounded grain, covered largely with orange peel texture and upturned plates. On the upper and lower side of the grain disc-shaped concavities are visible. Sample 15, table VII.2; magnification 250 x, scale bar 100 µm.

may be diagnostic for glacial grinding (Krinsley & Doornkamp, 1973; Nieter & Krinsley, 1976). The smaller conchoidal fractures are interpreted as impact features. If the fractures are grouped together and form a highly irregular surface, another possible origin is hydrocryothermal chipping (Kowalkowski & Brogowski, 1983; photo VII.3). For the orange-peel structure an areal coverage percentage has been estimated, distinguishing grains with this feature on only minor parts of the grain from grains dominated by this feature.

All samples show mixtures of grains of quite different aspect. 'End members' of the grain types are respectively:
- Angular grains dominated by large conchoidal fractures and fresh cleavage planes, showing only minor impact abrasion or chemical alteration (photo VII.2).
- Highly irregular, subangular grains, strongly chemically altered, with abundant features produced by both solution and precipitation of silica (photo VII.3);
- Rounded and strongly abraded grains, dominated by upturned plates or orange-peel texture (photo VII.4).

The first group of grains is assumed to represent relatively 'fresh' grains derived from glacial deposits. The second group of grains may have been derived from Tertiary deposits which show abundant evidence of chemical alteration (Mak et al., 1989). As most of the Middle Pleniglacial material appears to have been derived from the Drente Formation (par. V.3.1), it appears likely that also chemical features may be produced within the Middle Pleniglacial depositional environment. The third type of grains has undergone considerable transformation during transport which is not necessary only the latest (Middle Pleniglacial) transportation phase. In the Drente and Enschede Formation sands, also grains have been found which display these surface features (Mak et al., 1989).

VII.2.3. Statistical evaluation.

Seventeen samples, both from the Hengelo basin and Dinkel valley, have been analyzed. For statistical evaluation a non-parametric approach is most suitable, as the data matrix is derived from tallies. As suggested by Elzenga et al. (1987), the data matrix has been reduced by discarding all features which are either rare or abundant in all samples (< 20% or >80% of all grains). The features which have been used in subsequent analysis are underlined in table VII.3.

To investigate the differences between the samples a similarity matrix has been calculated, using Gower's similarity coefficient. A value of 0 indicates complete dissimilarity, 1 indicates complete similarity (Davis, 1986). Differences between the samples are minor; similarities range between 0.43 and 0.85. First it has been attempted to reduce the number of variables in the data set by principal coordinates analysis, by extracting the eigenvalues and eigenvectors of the similarity matrix (Davis, 1986). Unfortunately, it proves that the principal coordinates do not optimize the data set sufficiently. The first two coordinates account for only 30% of the variation in the data set; a level over 80% is reached only with the ninth principal coordinate. These results are undoubtedly due to the small differences between the samples, caused by their similar stratigraphical and

geographical origin. Within the data set of Elzenga et al. (1987) for instance the variation in those aspects is larger.

However, the similarity matrix lends itself well to application of cluster analysis, to detect groupings in the sample set. A furthest neighbour algorithm has been used. Although the similarities between the resulting clusters are high, the samples can be subdivided in two main groups. This subdivision proves to be associated with significant differences for several of the surface features. (fig. VII.12, table VII.4). Based on fig. VII.12, further subgroups can be differentiated within the main groups, each containing a few strongly similar samples.

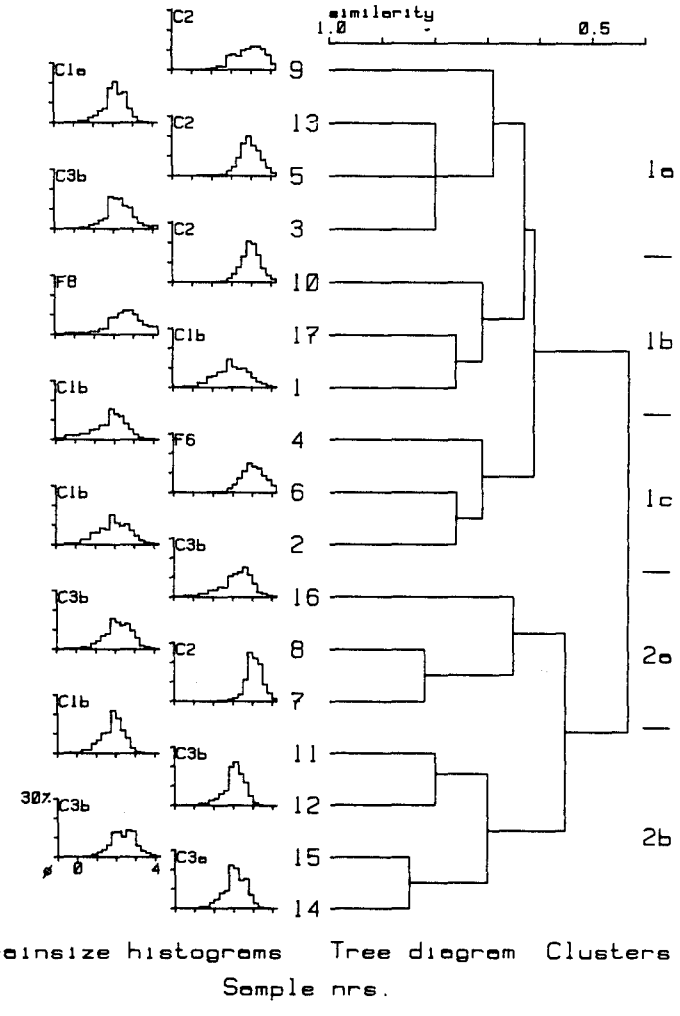

Figure VII.12. Cluster analysis on grain surface morphoscopy samples. Left: grain size histograms with histogram type classification (fig. VI.3,4); middle: tree diagram, constructed with furthest neighbour algorithm (similarity measure is Gowers' similarity coefficient); right: classification. Sample numbers refer to table VII.2.

Significance of the differences between the main groups has been tested using the Mann-Whitney T-test (Davis, 1986), with a two-sided 10% significance level. The differences are genetically meaningful. Group 2 has consistently better rounded grains, more chemical solution and precipitation features, and more features

which are commonly ascribed to aeolian processes, such as orange peel texture, meandering ridges, and disc-shaped concavities (table VII.4). Group 1, on the contrary, has more features which are associated with mechanical wear and glacial grinding, such as features which occur on large conchoidal fractures, cleavage planes and mechanically formed upturned plates. The group 1 samples have undergone less chemical modification and aeolian wear which tends to obscure these features. These samples probably consist for a larger part of material which has been derived freshly from the substratum. Notwithstanding the differences, both groups show abundant features related to transport in general (scratches, mechanical V-shaped pits).

The differences between the subgroups appear to be less genetically consistent. Subgroup 1a has somewhat more aeolian features than 1b and 1c, while subgroup 1b contains slightly more features which point to glacial source material (large conchoidal fractures, cleavage planes). Subgroup 2b might have undergone somewhat stronger chemical precipitation than 2a.

Grain surface feature	mean of sample group		Difference between main groups (mean 2 - mean 1)	Difference between subgroup means and main group mean				
				group 1			group 2	
	1	2	-5 0 +5	a	b	c	a	b
Roundness	16	23		+	-		-	+
High microrelief	12	10						
Conchoidal fractures	19	16						
Semiparallel steps	14	8						
Arc-shaped steps	7	4						
Straight scratches	17	18						
Curved scratches	8	7						
Mech. V-shaped pits	27	29						
Scratches with V's	4	2						
Disc-shaped concavities	14	19		+	-	+	+	·
Meandering ridges	7	15		+	-			
Upturned plates	18	12		-	+		+	·
Flat cleavage planes	5	1			+			
Irr. precip/sol. surface	17	20						
Silica plastering	3	3						
Precip. upturned plates	7	10						
Chemical disintegration	5	2						
Solution pits	5	4						
Smooth precip. surface	1	5						
Arc/circle/polygonal cr.	18	20					-	+
Orange-peel texture	17	24		+	-		-	+
Adhering particles	19	23					-	

Table VII.4. Differences in surface textures between sample groups established with cluster analysis. Only results of features with statistically significant differences have been listed. +: positive difference >2; -: negative difference >2

VII.2.4. Comparison of grain surface morphoscopy with grainsize, sedimentary structure, and stratigraphical position.

Grain size analysis results and sedimentary structures of the samples generally confirm the grain surface morphoscopy classification. With one exception all samples in group 2 have C2 or C3b -type grainsize distributions and therefore most likely represent overbank environments (fig. VII.12). This agrees with the abundance of chemical and aeolian features, since chemical alteration and aeolian reworking should be most prominent in these environments. By contrast, group 1 with its more unmodified grains contains relatively more C1-type grainsize distributions, representing fluvial channel deposits. A clear difference with regard to aeolian reworking between both groups is not apparent. Both group 1 and 2 contain samples with a C2-type grainsize distribution which indicates presence of (reworked) aeolian material. Sedimentary structure information of most of these samples contradict a purely aeolian origin. A classification in group 2 does not indicate a purely aeolian origin, despite the higher number of aeolian features on the grains of group 2. Rather it points to a relatively long stay in overbank environments in general, resulting in a higher chance of both chemical alteration and wind transport.

Evaluation of the stratigraphical position of the samples shows, that the oldest samples occur in group 1 (table VII.2, fig. IV.12). The samples from the Dinkel and Liendert Member are found in this group, as well as several samples with ages over 47 ka. In group 2 predominantly samples younger than 47 ka are found. Apparently the supply of freshly eroded substratum material decreased during the Middle Pleniglacial, leading to a relative increase of sediment which has undergone one or more floodplain reworking cycles. This is confirmed by the gradual decrease in sedimentation rate in the basin during the Middle Pleniglacial (par. IX.3).

The results of the morphoscopical analyses with the help of the S.E.M. confirm the morphoscopical analyses of Wijmstra et al. (1971) on the Mekkelhorst boring. These show an increase of grains with a dull surface texture after the Early Glacial. As shown by the S.E.M. analyses, the dull surface texture may have been caused by both aeolian wear and chemical processes.

As a conclusion, the grain surface textures themselves do not provide an exclusive indication of depositional environment. Differences between the samples are small. Clear indications for changes in intensity of aeolian processes are absent. Most of the aeolian deposits have been fluvially reworked. Nevertheless, the surface texture analysis provides additional information on the role of chemical alteration of sand grains in the depositional environment. Aeolian reworking and chemical modification appear to act together as common processes in alluvial overbank environments throughout the Middle Pleniglacial.

VII.2.5. Comparison with grain surface texture results from other units of the Twente Formation.

Only two samples from older units have been analyzed (par. VII.2.2). Elzenga et al. (1987) have analyzed samples from the Upper Pleniglacial and Late Glacial deposits (Beverborg, Lutterzand and Wierden Member) in the Dinkel valley and nearby loca-

tions. Only 2 of these 13 samples originate from distinctly fluvial deposits. This provides a possibility for comparison, although observer bias has to be accounted for. Furthermore, the counting method has been different for some properties. In the study of Elzenga et al. (1987) no estimates of aerial surface occupation of phenomena has been made, and conchoidal fractures of different size have not been distinguished.

Grain surface feature	Mean		Difference between mean 1 and 2 (only if difference is significant) -15 10 5 0 5 10 15 20+
	1	2	
Roundness	19	19	
High microrelief	15	11	
Conchoidal fractures	7	27	
Semiparallel steps	2	11	
Arc-shaped steps	3	6	
Imbricated breakage bl.	4	1	
Straight scratches	23	17	
Curved scratches	18	7	
Mech. V-shaped pits	30	28	
Scratches with V's	15	3	
Disc-shaped concavities	24	16	
Meandering ridges	11	11	
Upturned plates	28	16	
Graded arcs	3	1	
Flat cleavage planes	1	3	
Fresh cleavage planes	2	0	
Irregular small cracks	1	1	
Oriented etch V's	6	1	
Irr. precip/sol. surface	29	18	
Silica plastering	3	3	
Precip. upturned plates	14	8	
Chemical disintegration	5	3	
Solution pits	13	5	
Arc/circle/polygonal cr.	19	19	
Orange-peel texture	27	26	
Adhering particles	26	21	

Table VII.5. Comparison between grain surface texture counts in this study and Elzenga et al. (1987). Mean 1: mean of all relevant samples of Elzenga et al. (1987); Mean 2: mean of samples in this study.

Table VII.5 lists the differences between the samples used in this study and those of Elzenga et al. (1987). Some differences undoubtedly are due to observer bias. For example in this study most cleavage planes have been classified as 'flat cleavage planes' in stead of 'fresh cleavage planes'. The significance of the differences has been tested in the same way as the cluster analysis grouping in table VII.4. It proves that features produced by mechanical wear and chemical action are more abundant in the samples of Elzenga et al. (1987) which confirms the previously noted trend of increase through time of these features. Conchoidal fractures and related features occur more frequently in the samples used in this study. This is probably

largely due to a decrease in the amount of grains with large conchoidal fractures, freshly derived from glacial deposits. There is no obvious difference in typical aeolian features, for instance 'orange peel texture' and 'meandering ridges' did not show significant differences.

In the younger units of the Twente Formation, sedimentary structures pointing to aeolian sedimentation are abundant (Schwan, 1988a,b; Vandenberghe & Van Huissteden, 1988). Nevertheless, the typical 'aeolian' grain surface features do not show a concomitant increase. A conclusion of palaeo-hydrological significance may be drawn from this contradiction. Probably aeolian reworking has been of general occurrence throughout the Pleniglacial, and its intensity during the Middle Pleniglacial might not have differed much from that during the Late Pleniglacial. Only the intensity of fluvial reworking has decreased during the Upper Pleniglacial, resulting in a relative increase of deposits with aeolian sedimentary structures after the Middle Pleniglacial.

VIII. Sedimentary environment in the Dinkel basin and morphological model of the Middle Pleniglacial river plains in Twente.

VIII.1. Lithofacies classification of the Middle Pleniglacial sediments in the borehole sections.

Environmental interpretation of the large amount of borehole information in the Dinkel valley is simplified by classification of the layers in the core descriptions into genetically meaningful lithofacies classes. Several lithofacies classifications of fluvial sediments are known (e.g. Allen, 1970; Cant & Walker, 1976; Miall, 1973, 1977, 1978b). Miall (1977, 1978b) has developed a classification of lithofacies types for braided river deposits which has proved to be useful in many studies, also those pertaining to non-braided rivers. Based on this classification the approach of characterizing fluvial deposits by 'architectural elements' has been developed (Miall, 1985). For description of the borehole sections in this study, Miall's classification has two drawbacks, however. First, it heavily depends on sedimentary structures. In the core descriptions this information is of a fragmentary nature. Second, Miall pays comparatively little attention to the wide variety of overbank deposits which prove to be of special importance in this case. Therefore, a different classification has been developed here, adapted to the type of information which can be extracted from the borehole descriptions.

Besides the incomplete information on sedimentary structures, this poses problems with respect to data quality. All sediment properties in the borehole descriptions are estimates, expressed on nominal and ordinal measurement scales, with varying reliability. As a method to assess the quality and environmental significance of these estimates, the borehole descriptions have been compared with the grain size analysis results. Core description elements which almost uniquely occur in one or a few of the grainsize sample groups (fig. VII.4,7), will contain the most useful information on the sedimentary environment and can be used in the classification.

Table VIII.1 lists for each group of grain size samples, to what extent field description properties are related to a group of grainsize samples. Based on these data, the following field description elements have been selected for classification:

- Material
- Sand grain size
- Gravel content
- Presence of intraclasts
- Sedimentary structure
- Silt/clay content
- Sorting
- Organic matter content

Table VIII.1 (next page). Distribution of core description properties over grainsize sample classes. / : not noted; * : rare property; +++ property restricted to one sample group; ++ : property restricted to a few groups; + : generally occurring property, but most abundant in this group; o : generally occurring property, but rare in this group; − : generally occurring property; blank: absent.

Property	Sample group										
	C1	C2	C3	F1	F2	F3	F4	F5	F6	F7	F8
Sorting (sands)											
ill	++		++	/	/	/					
ill/moderate	-	-	-	/	/	/	++				++
moderate/good	-	-	-	/	/	/				+++	
good		++	++	/	/	/			*		
Rounding/angularity (sands)											
angular	*		*	/	/	/	/	/	/	/	/
sub-angular	-	-	-	/	/	/	/	/	/	/	/
sub-rounded	-	-	-	/	/	/	/	/	/	/	/
Grain size (sands)											
<150µm	o	+	+	/	/	/	-	-	-	-	-
150-210µm	-	-	-	/	/	/				*	
210-300µm	++		++	/	/	/		*			
300-420µm	++		++	/	/	/					
>420µm	++		++	/	/	/					
Silt content (sands)											
absent	-	-	-	/	/	/	++		++	++	++
low	++		++	/	/	/					*
moderate	o	+	o	/	/	/	*		*		
high				/	/	/		++		++	++
Gravel content											
absent	-	-	-	/	/	/	/	/	/	/	/
present	++		++	/	/	/	/	/	/	/	/
Intraclasts, reworked peat											
absent	-	-	-	/	/	/	/	/	/	/	/
present	+	+	o	/	/	/	/	/	/	/	/
Sand content (silty samples)											
absent	/	/	/	+	+	+	o	o	o	o	o
low	/	/	/	++	++	++				++	
medium	/	/	/	++			++		++		++
high	/	/	/				++	++			++
Peat content (clastic sed.)											
absent	-	-	-	o	+	+	+	+	+	o	+
low/medium		*		++	++	++	++			++	
high/mostly peat				++		++	++			++	++
Humic matter											
absent	-	-	-	o	+	o	o	o		+	o
low/medium	+	+	o	+	o	+	+	o		o	+
high				++		++	++				
Sedimentary structure											
not identified	-	-	-	o	+	+	o	+	+	+	+
laminated	++		++		++	++	++				
banded	o	+	+	-	-	-	-	-	-	-	-
graded bedding	++	++									
Composition											
peat				++		++	++			++	++
gyttja					*		*			*	
clay						++		++			
silt				o	+	o	+	+	+	o	o
sand	-	-	-				++	++	++	++	++

Categories of layers can be described by sets of query rules using the properties above, and the layer classification is carried out with the help of the query option of the core description database (par. IV.1). Experiments with different sets of query rules have been checked against field experience, exposure descriptions and the lacquer peels of the hydraulically cored borings (fig. VIII.1,2).

The classification of the sands can be based on grainsize, sorting, silt or gravel content, and sedimentary structure. However, the differentiation in lithological attributes of sands is poor, also of sands with distinctly different grainsize distributions. Sands with a C2 and C3 type grainsize distribution tend to show much overlap in lithological characteristics, but sands with a C1 type distribution show a more distinct set of attributes. Therefore, the sands have been split in only two relatively broad lithofacies groups: a group which contains rather coarse grained (C1 type) sands deposited mainly in channels, and overbank deposits which may include reworked aeolian material with a C2-type distribution. A third coarse-grained lithofacies, the intraclast beds, has been based on field experience.

The fine-grained deposits show a wider range of grainsize distributions which have been classified into a larger number of distribution types. Besides grainsize, organic matter content plays an important role as it depends on local clastic sedimentation rate (par. VII.1.3.2.2). Peats or gyttjas therefore form separate lithofacies classes. With respect to grainsize estimates (sand or silt content, table VIII.1), the fine-grained sediments can be split into two large groups: sandy material (F4-F8 type distributions) and silt or clay of which sand content has been estimated as low or absent (F1-F3 type distribution). Within the sandy group lithological attributes do not allow further distinction. A sand/silt intergrade lithofacies class is based on these mixed grainsize distributions. In the silt/clay group material with an F3-type distribution most often has been described as clay, and constitutes a separate lithofacies. Sedimentary structure is not a very reliable criterion for further classification within the fine-grained beds. As suggested by table VIII.1, it might be possible to distinguish a group of strongly laminated fine-grained sediments, but in the core descriptions such sediment proves to occur only rarely.

The final classification has been summarized in table VIII.2 which also shows the relation to the classification of the grain size samples and the possible correlation with the lithofacies types of Miall (1978b). The association of the borehole lithofacies classes with sedimentary structures has been derived from the exposure data and the lacquer peels from the hydraulic cores (fig. VIII.1,2). Table VIII.3 shows a count of sedimentary structures associated with the lithofacies classes in the cores. It reveals clear differences in sedimentary structure between the lithofacies classes and confirms their relevance for distinction of sedimentary environments. A further description of the lithofacies classes follows below.

Class A, Coarse channel sands. Sand, grainsize > 210 μm. Not silty, clayey or humic. Clay or silt layers are absent. These sands may contain gravel, intraclasts, or reworked peat, and may show graded bedding or faint lamination/banding. Finer sands (grainsize >150 μm) have been included if they show a moderate

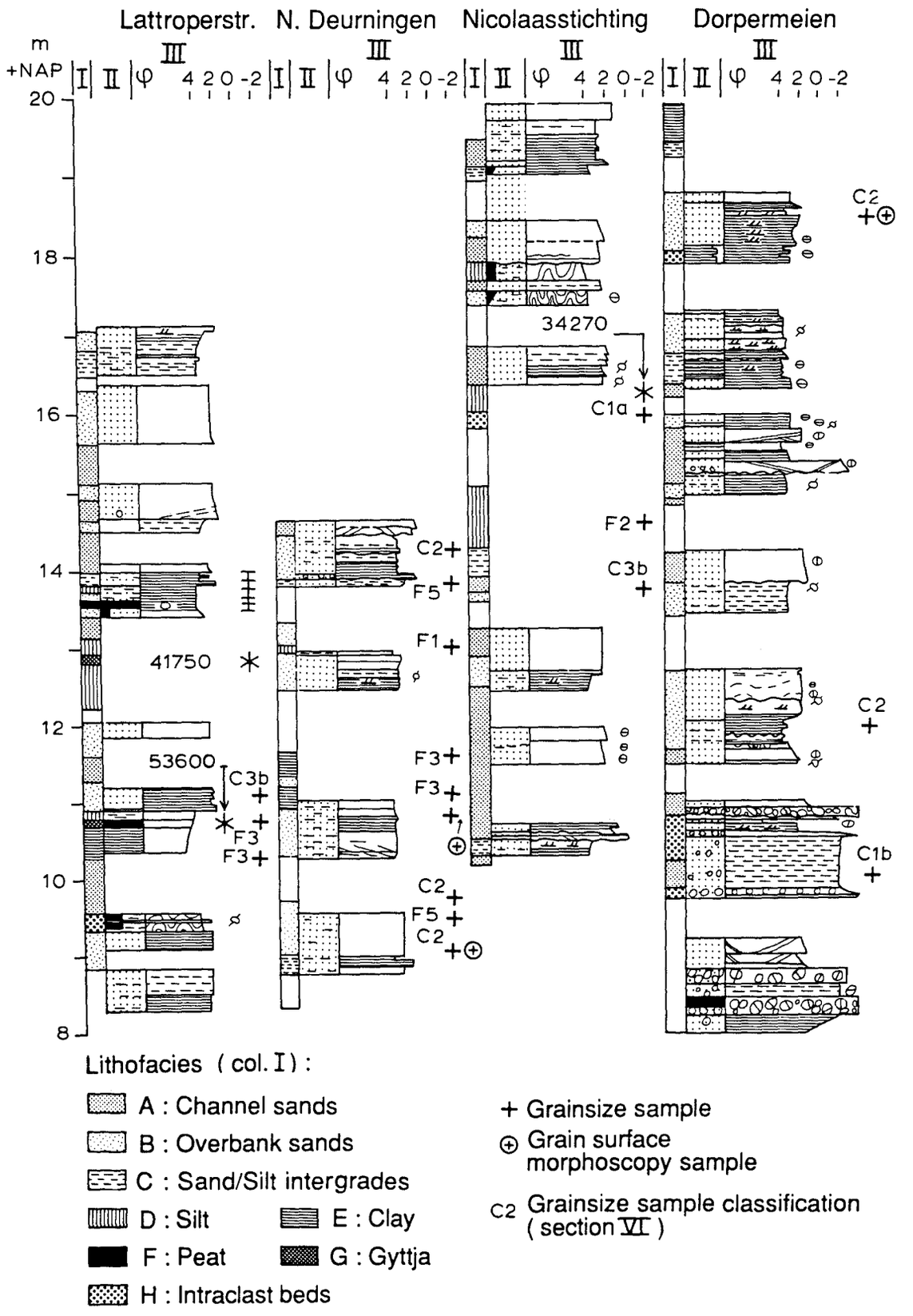

Figure VIII.1. Lacquer peel logs of hydraulic cores from the Tilligte beds. Legend for representation of sedimentary structures in fig. VI.2. Character codes near grainsize sample locations refer to grainsize sample classes in section VII.

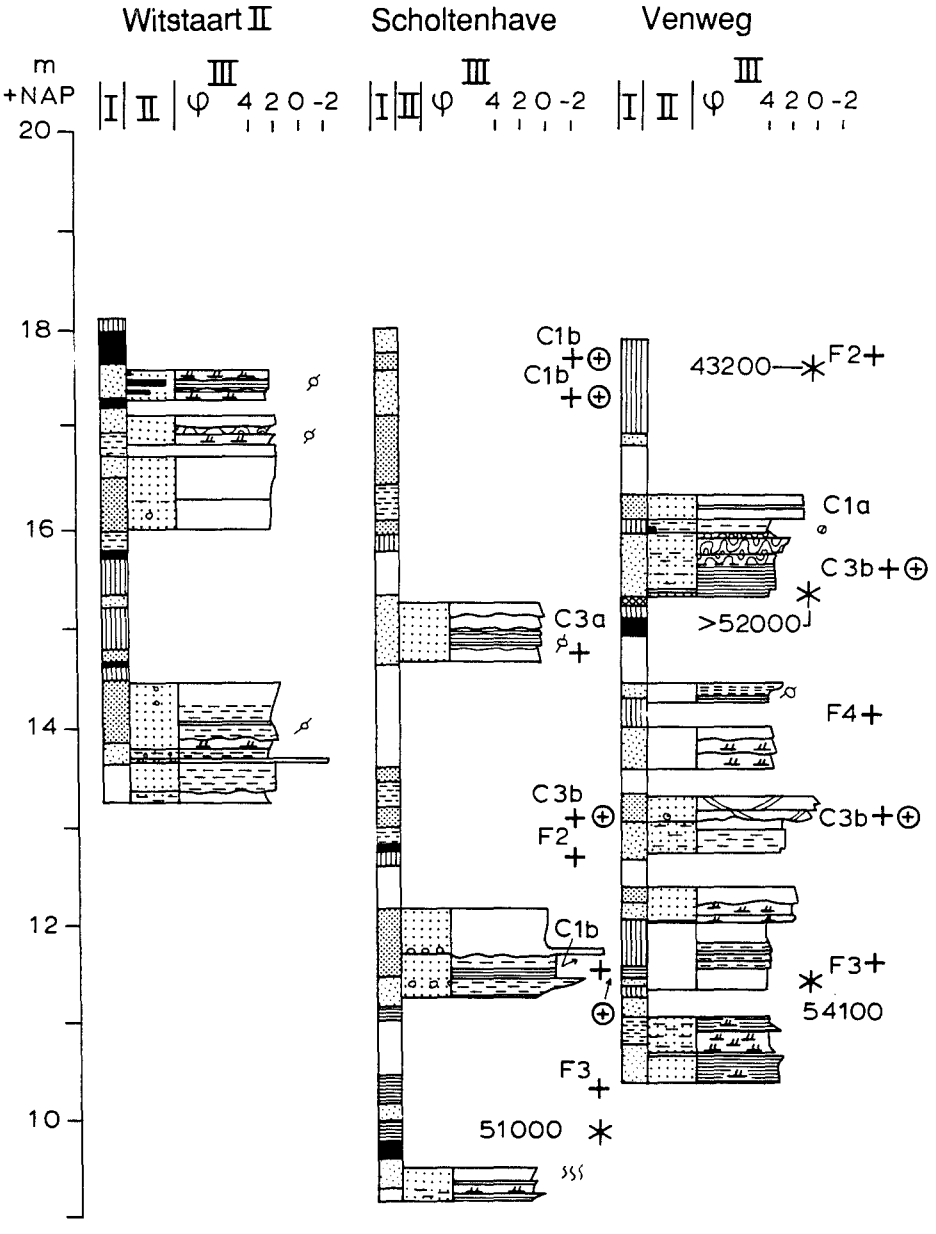

Figure VIII.2. Lacquer peel logs of hydraulic cores from the Tilligte beds. Legend see figs. VIII.1 and VI.2.

Lithofacies (based on core descriptions)	Grain size sample groups	Lithofacies Miall (1978b)
A Coarse channel sands	mainly C1, some C3	Se, Ss, St, Sp, (Sr)
B Overbank sands	C3, C2	Sr, Sh, Sl, (St, Sp)
C Sand/ silt intergrades	F4, F5, F6	Fl, Fsc, (Sr, Sl)
D Floodbasin silt	F1, F2, some F3	Fl, Fsc, Fcf
E Floodbasin clay	F3	Fl, Fsc, Fcf
F Peat	F groups, mainly F1	C
G Gyttja	F groups	C, Fcf?
H Intraclast layers	possibly F8	Se

Table VIII.2. Relation between lithofacies types in the boreholes, grain size sample groups and the lithofacies classification of Miall (1978b).

Lithofacies class	A	B	C	D	H	
parallel lamination	30	47	60	50	0	%
parallel bedding	35	16	0	50	75	%
cross-lamination	0	33	40	0	0	%
cross-bedding	35	4	0	0	25	%
Total	100	100	100	100	100	%

Table VIII.3. Sedimentary structures associated with lithofacies classes in the hydraulic cores.

or lower sorting estimate, and the absence of clear lamination or bedding except graded bedding. These sediments correspond to probably cross-bedded or cross-laminated fluvial sands, largely deposited in channels. Also some crevasse splay sands of the type which is found in the Hengelo exposure might be included, since these also consist largely of clean, rather coarse sands. Especially the top of crevasse splays is likely to contain sands with similar characteristics as channel deposits (Smith et al., 1989). The cored borings usually show high-angle crossbedding in this type of sediment. It is probably mainly composed of lithofacies types Se, Ss, St and Sp, and some Sr (scour fills, trough and tabular crossbedding, ripple cross-lamination; Miall, 1978b).

Class B. Overbank sands. This group contains finer sand and silty or humic sand. The cored boring lacquer peels often show ripple cross-lamination, well-developed horizontal lamination or thin bedding, although also some high-angle crossbedding has been found. These are mainly overbank deposits, such as crevasse splay sands or (fluvially reworked) aeolian sands. The predominance of ripple cross-lamination confirms a largely waterlaid origin. Also low energy in-channel deposits could be included; in fact, the transition between A and B type sands is likely to be gradational. Lithofacies Sr, Sh, Sl (cross-, horizontal lamination, low angle crossbedding; Miall, 1978b) dominate, with minor amounts of St and Sp.

Class C. Sand/ silt or clay intergrades. Sandy clay, moderately and strongly sandy silt, and strongly silty or clayey sand. Also strongly humic or peaty sand has been included. Sedimentary structures are mainly parallel lamination, thin bedding or - more rarely - ripple cross-lamination. This class mainly represents transitions from crevasse splay to floodbasin deposits. It may be comparable to lithofacies types Fl and Fsc (even or cross-laminated or massive silt and mud; Miall, 1978b) with minor amounts of Sr and Sl.

Class D. Floodbasin silt. Silt, only slightly sandy. Most silts display thin bedding and have been deposited in shallow lacustrine or frequently flooded floodbasin environments. Lithofacies types Fl, Fsc and Fcf (laminated or massive silts; Miall, 1978b) compare with this sediment type. The Hengelo A1 exposure indicates, that finely laminated silts may have been deposited in somewhat deeper water than the massive or crudely bedded silts. The common presence of a fine sand subpopulation in the grainsize samples of the silts points to deposition in floodbasins in the vicinity of channels, and presence of some current flow (par. VII.1.3.2.2).

Class E. Floodbasin clay. Only clay without sand is included. The same environment as that of the silt applies, the difference in clay content has been caused by lower current velocities during flooding. Probably the clays have been deposited in more distal environments than the silts, or in more outspoken lacustrine environments. The same lithofacies types (Miall, 1978b) apply as with class D.

Class F. Peat. All peats are sedge peat or moss (Amblystegiaceae) peat (Ran, 1990). Amblystegiaceae peat may grow in standing water of some depth (Ran, 1990). In the field usually no discrimination has been made between the peat types. Both represent floodbasin environments which have been cut off from clastic sediment sources. It is equivalent to lithofacies type C (Miall, 1978b).

Class G. Gyttja. Besides the much finer divided plant remains, gyttja displays a lighter brownish colour than peat. Many gyttjas are strongly calcareous, in contrast to peat which never contains lime. The gyttjas are lake deposits without strong fluvial influx, although most gyttjas still contain considerable amounts of mineral matter. It corresponds either to lithofacies type Fcf or C (Miall, 1978b).

Class H. Intraclasts layers. Peat, gyttja, clay or silt, where lithologic description codes indicate that these layers consist of reworked material. Also strongly sandy peat is included. These are residual deposits, remaining after erosion of finer sediments. In case of significant thickness of layers of this type, this sediment may be the equivalent of lithofacies type Se (Miall, 1978b).

VIII.2. Large scale facies pattern and sediment body geometry in the Middle Pleniglacial Dinkel basin.

VIII.2.1. Spatial distribution of the lithofacies types in the Middle Pleniglacial sediments.

Fig. VIII.3 shows the distribution of the lithofacies classes within the Mekkelhorst Member in different regions of the Dinkel valley (fig. IV.1). These regions are:

1. Tilligte area (Tilligte section, detailed mapping area, western part of Laarhuis-Rammelbeek section);
2. Denekamp-West (eastern part of Laarhuis-Rammelbeek and Lattrop sections, Denekamp detailed sections);
3. Denekamp-East, along the Dutch-German border east of Denekamp (easternmost borings of the Lattrop-Denekamp section);
4. Beverborg and Losser area, which is the main valley south of Denekamp (Beverborg section, Losser boring),
5. Gildehaus section.

In the three basin regions (Tilligte, Denekamp-W and Denekamp-E) a gradual transition from west to east is apparent. This is most clearly expressed by the amount of peat beds which decreases in eastern direction. By contrast, the amount of coarse sand increases in this direction. The number of peat beds is highest in the Tilligte basin, close to the present drainage divide between the Hengelo basin and the Dinkel valley system. This is considered as an extremely peaty variant of the Tilligte beds, deposited at a marshy drainage divide position (Tilligte section, fig. IV.9).

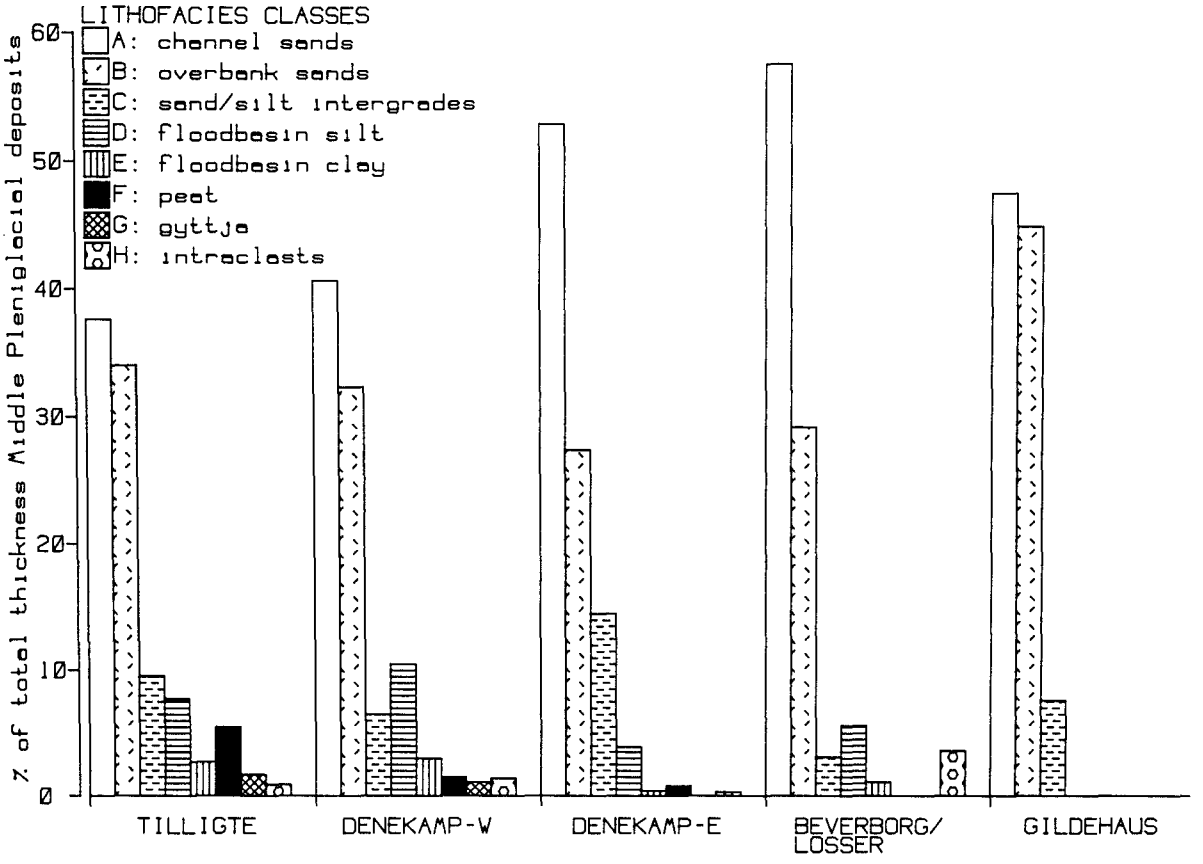

Figure VIII.3. Distribution of lithofacies types within the Middle Pleniglacial deposits in different regions of the Dinkel valley. Bars represent (total thickness lithofacies) / (total core length Middle Pleniglacial deposits) X 100 %.

The Denekamp-E region and the Gildehaus section show a very low amount of peat and silt beds, while sands dominate. Especially in the Denekamp-E region these are lithofacies A sands. This part of the basin did contain the major drainage line of the basin throughout most of the Pleniglacial. As shown in par. IV.4 and V.4, the trunk river followed a much more easterly course than at present. In the Gildehaus section lithofacies B sands are more important; these may comprise a considerable aeolian component in this section (par. VIII.3.2). The eastern parts of the Lattrop-Denekamp section and the Gildehaus section represent the sand facies of the Middle Pleniglacial deposits, the Puntbeek sands.

The Middle Pleniglacial deposits in the Beverborg section and Losser boring contain more coarse sands than the other areas which corroborates with the upstream position. The silt and clay beds are still present, however, therefore these deposits are considered as a coarser variant of the Tilligte beds. A relatively large number of intraclast beds occurs. It indicates that silt deposition in floodbasin has been a regular feature of the alluvial plain, but many silt beds have been eroded after deposition, indicating more active lateral channel shifting.

A vertical variation in the amount of certain lithofacies types can be observed especially in the Denekamp-W area, by the presence of the basal clays of the Tilligte beds (par. IV.6). The basal clays, the peat-rich deposits in the Tilligte basin, and the coarse deposits in the Beverborg section can be con-

sidered as 'end members' of the facies variation within the Tilligte beds.

VIII.2.2. Sedimentary structures and sediment body geometry of the Tilligte beds in the Dinkel valley.

VIII.2.2.1. Fine-grained deposits.

Like the fine-grained beds in the Hengelo A1 exposure (par. VI.2.4.1), the silt, peat and gyttja beds in the Dinkel valley are floodbasin deposits. An illustrative example is the complex of silt and gyttja beds in the Tilligte detailed grid area (unit DT3, fig. IV.18, 19). It appears to be a large sheet-like body of wider extent than the studied area; therefore, formation in a abandoned river channel is to be excluded. Locally it has been removed by erosion through vertical incision of a small channel. The horizontal lithofacies pattern of unit DT3 shows variations of clastic input. A gradual transition from gyttja and peat in the north to silt in the southern part of the area is visible. In the southeastern part the silt gradually grades into sand by an increasing number of sand beds.

The vertical development displays the characteristic pattern of rising local water level and increasing clastic deposition, also found in the Hengelo A1 exposure (par. VI.2.4.1). Vegetation grades from semi-terrestrial at the base to open water near the top, as is indicated by palaeobotanical analysis (Ran, 1990). A break in the development of DT3 is represented by a sand split which is found in many borings. This probably correlates with indications of stronger fluvial influx found in palaeobotanical analysis (Ran, 1990). Above the sand split the area with peat/ gyttja sedimentation is strongly reduced in favour of (sandy) silt deposition.

The other silty units (DT1, DT4; fig. IV.18) in the Tilligte detailed grid area show strong lateral variation and many discontinuities which can be attributed to cryoturbation. DT1 mainly consists of interfingering silt and sand beds; a single silt bed rarely can be traced over more than two borings. Unit DT4 shows similar characteristics; its internal stratigraphy may be characterized as chaotic on the level of detail provided by the boring grid. Near-vertical lithological boundaries are sometimes found in the cores from unit DT4. Especially the latter feature suggests that involutions are responsible for the disturbed appearance of this unit. A similar phenomenon has been found in the Lattrop-Denekamp section (par. IV.3.3, fig. IV.15). This short-distance lateral discontinuity appears to be a common feature of Middle Pleniglacial silt beds.

In the Lattrop-Denekamp section (fig. IV.12, 13, 14) more stratigraphical detail is available on the basal clays of the Tilligte beds. These do not consist of uniform contiguous clay beds. Sandy intercalations and lateral lithofacies transitions prove to be common within the basal clays. This shows the essential fluvial nature of the basal clays, although by analogy of similar deposits in the Hengelo basin the lacustrine component in floodbasins has been important (par. VI.4).

Fine-grained fills of abandoned channels also occur within the Tilligte beds, although these appear to be rare. An example is a 2.80 m thick uninterrupted silt sequence in boring 673 (fig. IV.11). It is an isolated occurrence which may represent a clay

plug in an abandoned channel. This is confirmed by the presence of coarse channel deposits underneath.

VIII.2.2.2. Sand bodies.

Within the sand units of the borehole sections lithofacies A and B sands interfinger with each other in a complex way. Most sand bodies tend to display a sheet-like geometry like the fine-grained deposits. Considerable thickness variations occur locally. In general the thickest parts of the sand units are composed of lithofacies A sands and represent channel deposits. The thinner, more sheet-like parts, largely consist of lithofacies B sands, and represent crevasse splay and levee deposits. Also in these cases intercalations of lithofacies A are common, and may represent crevasse splay topset or crevasse channel deposits, by analogy with the crevasse splays in the Hengelo A1 exposure (par. VI.2.4.2).

An example of channel deposits with associated sandy overbank deposits is unit DT2 in the Tilligte detailed grid area (fig. IV.18, 19). Its base (erosion level II) appears to dip downward both on the western and northeastern side of the area, where also lithofacies A sands are concentrated. This marks the presence of channel deposits, although a distinct channel shape cannot be distinguished. Where the base of DT2 is situated higher in the section mostly lithofacies B sands occur, indicating overbank rather than channel deposition. Lithological differentiation within unit DT2 is poor, the transition between channel and overbank deposits appears to be gradual. At the top of DT2 smaller channel fills have been found which mark the final activity of the system. These fills consist of coarse sand with reworked peat and are up to 0.6 m thick.

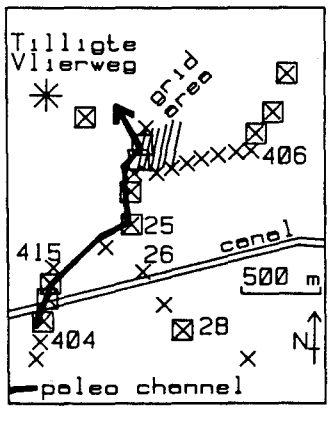

Figure VIII.4. Possible course of channel system associated with erosion level II in the vicinity of the Tilligte detailed grid area. *: hydraulic core; X: boring; squares indicate borings where thick lithofacies A sequences occur above erosion level II.

By combination of data from the detailed grid area, the Tilligte section and Laarhuis-Rammelbeek section, a palaeo-channel system has been reconstructed, associated with unit DT2 (fig. VIII.4). As inferred from its direction, this channel system should have belonged to the main drainage lines of the Tilligte basin. The channel deposits of unit DT2 are associated with erosion level II.

VIII.2.2.3. Erosion levels.

The erosion levels within the Tilligte beds are in most cases represented by simple subhorizontal hiatuses in overbank environments, or single channel incision/fill sequences. An illustration is a contour map of erosion level III in the Tilligte detailed grid area (fig. VIII.5). The elongated depression in the centre of the area represents an approximately south-north running small channel which cut through the underlying deposits of unit DT3 in most west-east sections (fig. IV.19).

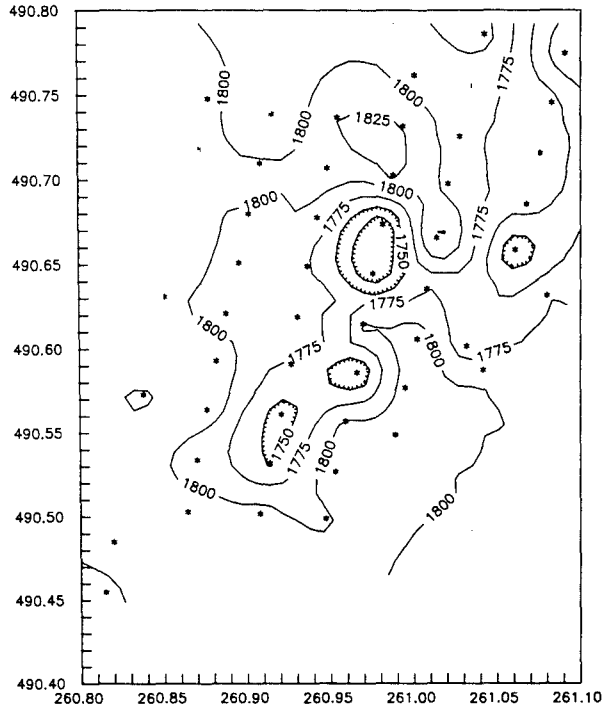

Figure VIII.5. Contour lines of erosion level III in the Tilligte detailed grid area. *: boring locations. Location see fig. VI.1.

Channel erosion appears to be most common in association with erosion level II (e.g. Tilligte section, fig. IV.9). The central part of the Lattrop-Denekamp section (fig. IV.13) shows a deeper fluvial incision associated with erosion level II. In this location two stacked sequences of lithofacies A/B sands, alternating with fine grained lithofacies types occur in the incision fill. In this downstream location the fluvial incisions associated with level II apparently have been sufficiently wide and deep for floodplain formation within the incisions.

VIII.2.2.4. Floodplain slope.

The main drainage line of the Nordhorn basin has been located farther to the east than at present, and has been directed towards the centre of the glacial basin (par. VIII.2.1). Consequently, drainage lines east of this area should have been directed towards the east or northeast which is confirmed by the clay-pebble channel in the detailed section area north of Denekamp (par. IV.4.2) and fine gravel petrography (par. V.4). However, a floodplain slope in this direction cannot be derived from the fine-grained beds and erosion levels in the sections,

e.g. the Laarhuis-Rammelbeek section. Instead, most silt/peat beds show an approximately horizontal attitude in the Laarhuis-Rammelbeek section.

An explanation for this lack of gradient may be tilting of the basin in a western direction. Possible tilting is indicated by a map of vertical movements with reference to Dutch ordnance datum, derived from precise levelling (Murre, 1985; cited by Steur et al., 1987). The Twente area rises rather strongly relative to Dutch ordnance datum. The amount of this rise is lower in the western part of Twente than in the east, resulting in tilting. Under the assumption of constant movement rates, a tilt of the studied basin reach in the order of a few meters could be possible (for sediments at the base of the Tilligte beds). This tilt is also reflected in sedimentation rate (par. IX.3) and in the present floodplain morphology. All rivers in the Nordhorn basin and Hengelo basin are deflected to the west. In the Nordhorn basin this deflection may have been established during the Late Pleniglacial, as the present river courses mainly follow the lower terrace associated with the top of the Beverborg Member.

VIII.3. Middle Pleniglacial aeolian sands in the Dinkel valley.

VIII.3.1. De Poppe exposure.

In 1983 a small road construction exposure in the Dinkel valley near De Lutte could be studied (fig. VIII.6). It is situated on the margin of the present Dinkel floodplain and shows a compressed but fairly complete Pleniglacial stratigraphy. The exposure has been described also by Van Huissteden et al. (1986a). Stratigraphy and sedimentary environments are summarized as follows.

Unit 1: Drente Formation; till. Green-grey sandy clay with scattered gravel and stones.

Unit 2: Twente Formation; residual slope deposit. Bluegreen, sandy diamicton. This unit is heavily cryoturbated, and contains pockets and small fissures filled with coarse sand. The overlying gravel string correlates with Steinsohle I (Zagwijn & Paepe, 1968).

Unit 3: Mekkelhorst Member, fluvio-aeolian sediment. Greenish grey silty sand with some coarse intercalations. Dominant sedimentary structures are thin parallel bedding and lamination. Locally small frost fissures occur. The unit has been erosively truncated by unit 4.

Unit 4: Beverborg Member; fluvial channel deposits. Cross-bedded light grey to yellowish coarse sand with gravel. Gradual transition towards unit 5.

Unit 5: Beverborg Member; fluvio-aeolian sediment. Medium to fine sands with indistinct wavy parallel bedding. Towards the top of unit 5 an increasing amount of gravel strings occurs. A large ice-wedge cast starts from this level. The topmost gravel bed is the Beuningen gravel bed.

Unit 6: Lutterzand Member s.s., aeolian sand. Fine to medium, evenly laminated sand.

The characteristic peat and silt beds of the Mekkelhorst Member (Tilligte beds) are lacking in this exposure. Unit 3 is correlated with the Mekkelhorst Member because of further lithological analogies (high silt content, similar mineralogy and

colour), and similar stratigraphical position. Unit 3 is considered to be a representative of the Puntbeek sands which occur in this location in a fluvio-aeolian facies. This is illustrated by fig. VIII.7 which represents a lacquer peel taken at the top of unit 3 (table VIII.4).

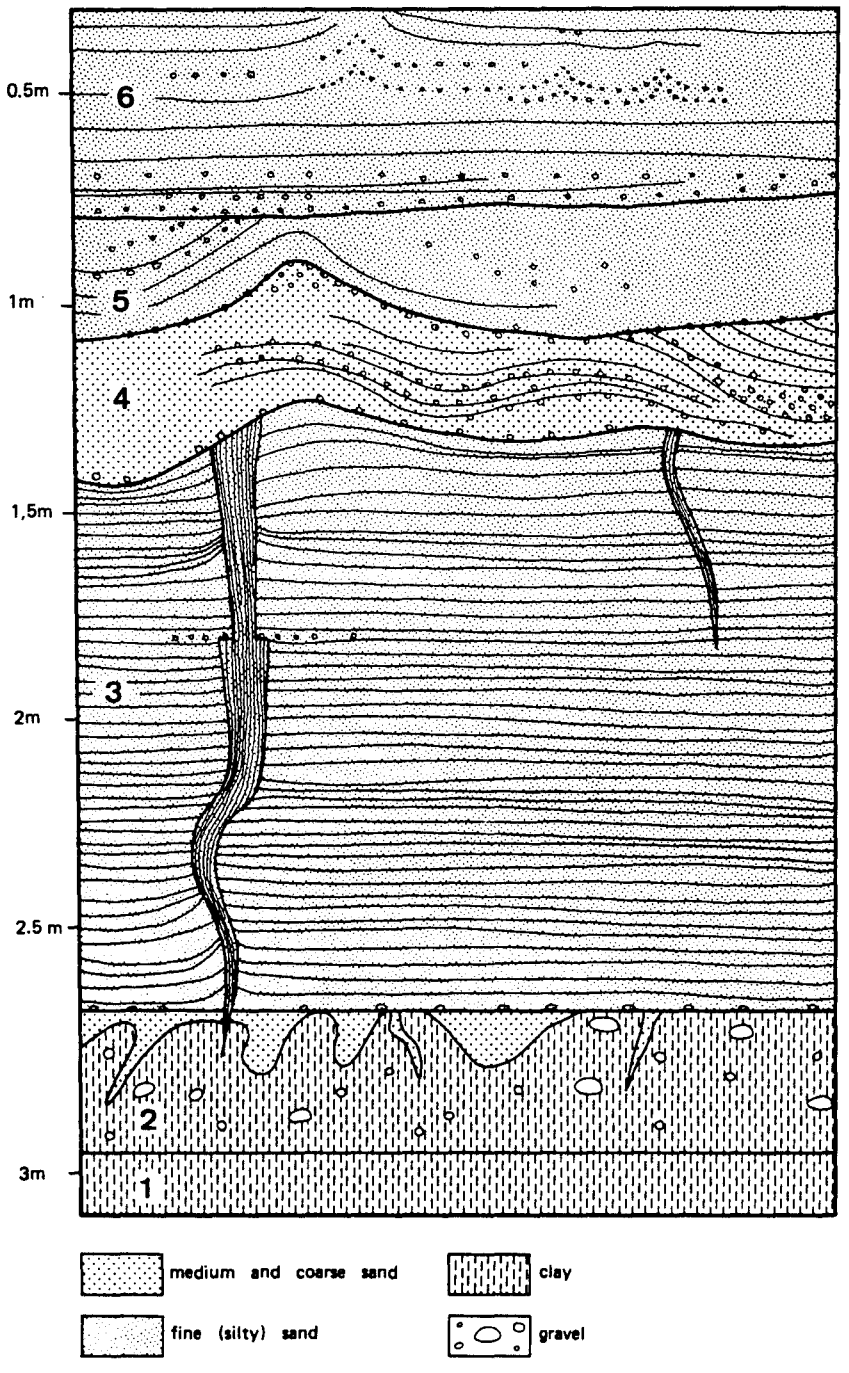

Figure VIII.6. De Poppe exposure: compound vertical section with lithological subdivision, sedimentary and periglacial structures. Depth in meters with respect to local ground level. Location: See fig. IV.1. After Van Huissteden et al. (1986a).

Subunit 3a represents a gradual transition from wet to dry aeolian deposition as is found frequently in this type of parallel bedded aeolian deposits (Ruegg, 1975). By comparison with

Twente Formation aeolian sands described by Schwan (1986), the coarser beds represent aeolian accretion under drier conditions, and the silty beds indicate settling from suspension on wet surfaces. Subunit 3b marks reworking of the aeolian material by superficial flooding.

Subunit 3c shows a return to aeolian deposition, with dry aeolian deposition at the base and wetter conditions at the top. The subhorizontal laminae at the base dip very slightly to the north. By virtue of the low angle of dip, and faint inverse grading in thicker laminae, it resembles the subcritically climbing translatent stratification, caused by wind ripple climbing (Hunter, 1977). The structures in subunit 3d point to running water reworking with frequent scouring. The sequence is truncated by unit 4 (Beverborg Member).

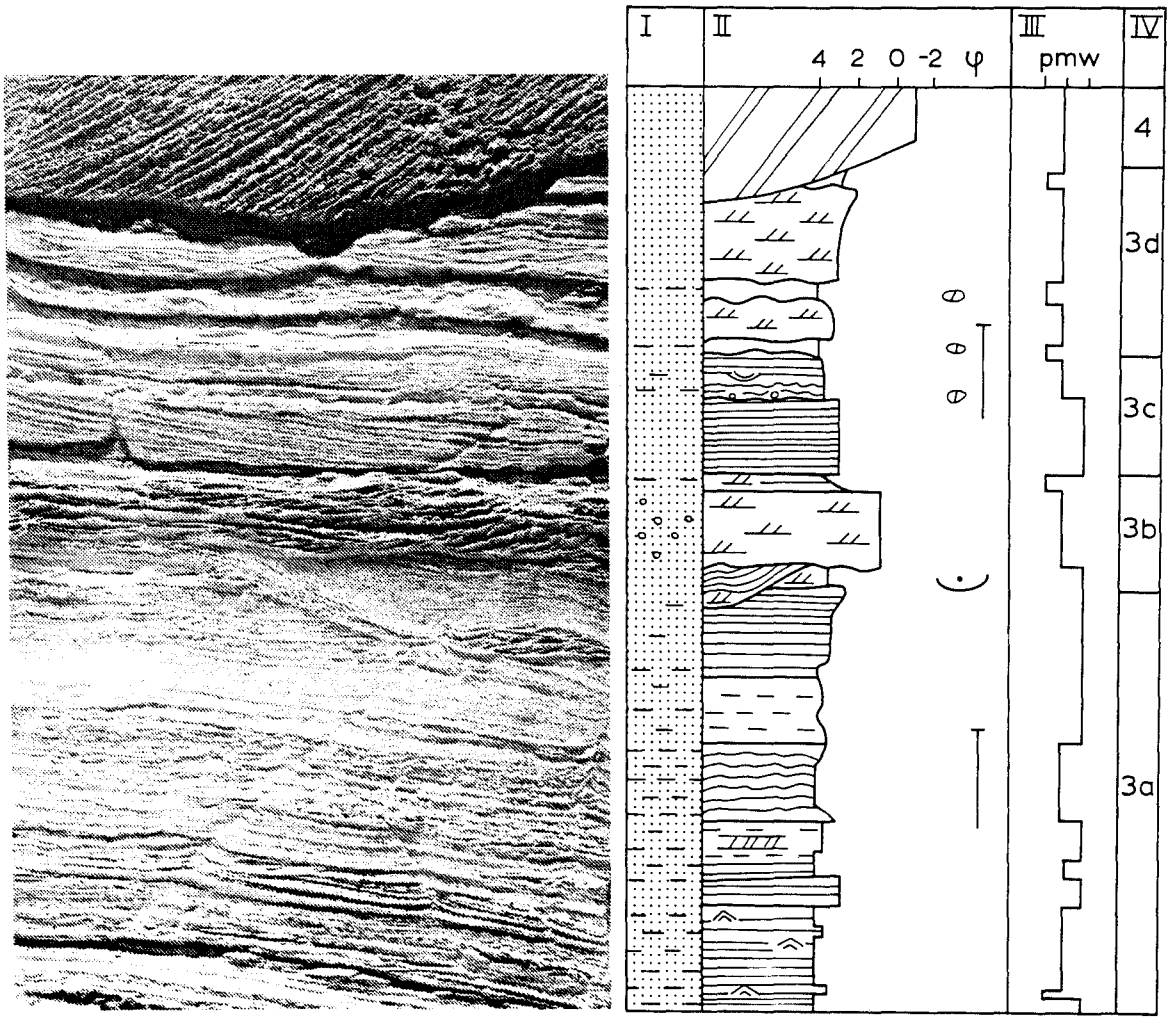

Figure VIII.7. Lacquer peel of the top of unit P3 in the De Poppe exposure. Column I: composition; II: structure and texture; III: sorting; VI: units in text. See fig. VI.2 for legend.

The structures in unit 3 show alternation of aeolian deposition and surficial running water, probably high stage river flooding. The aeolian sediments themselves contain a fairly large quantity of silt, pointing to aeolian suspension deposition. The nature of this sediment bears similarity to the fluvio-aeolian

deposits described by Vandenberghe & Van Huissteden (1988) from the Upper Pleniglacial deposits in the nearby Holt exposure. A difference is the better preservation of the lamination. Also the small-scale subvertical jointing, a characteristic element in the Upper Pleniglacial sands with similar facies, is absent. This might indicate less intense frost action. Evidence of frost action is present only in the shape of frost cracks (fig VIII.6).

U-nit	Description	Interpretation
4	Very coarse, gravelly sand with tabular cross-bedding	bar on river channel bed
3d	Coset of cross-laminated fine sand, alternating with thin, structureless ill-sorted silty sand beds. The ill-sorted beds mark irregular unconformities and contain silt granules.	deposition/ scouring by shallow running water
3c	Medium-fine sand with subhorizontal, even parallel lamination, truncated by an unconformity lined with silt granules; top: silty sand with wavy parallel lamination and a small scour fill	dry to wet aeolian deposition, erosion by running water
3b	fine-coarse sand with cross-lamination; at the base scour fills with lamination parallel to the scoured surface, at top current ripple cross-lamination in coarse sand overlain by silt drape	reworking by running water, at the top standing water
3a	silty sand with even parallel lamination; unconformities lined with silt granules; climbing adsion ripples; locally (wave ?) ripple formsets	wet to dry aeolian transition; surficial scouring and standing water

Table VIII.4. Description of lacquer peel in fig. VIII.7.

VIII.3.2. Aeolian sands in the borehole sections.

An attempt has been made to discriminate aeolian sands in the borehole descriptions. Based on the grain size analysis results of par. VII.1.3 and exposure observations several possible sets of criteria may be used. Most of the aeolian material will be included in lithofacies class B, or eventually C. Grain size distribution criteria alone are not sufficient; beds with a grain size distribution similar to that of coversand frequently show current ripple cross-lamination.

The search criteria with which the core description database has been consulted reflect characteristics of Twente Formation aeolian deposits observed in exposures (Holt, Lutterzand and De Poppe exposure) and descriptions from literature (Ruegg, 1975; Schwan, 1988a,b). The sands of aeolian origin are fine, well sorted, somewhat silty sands which exhibit well developed even lamination and bedding. These sedimentary structures should be observable in the small diameter cores also. The search has been

carried out using four slightly different sets of criteria which have in common the following basic features:
- fine to medium sand;
- absence of peat, other organic matter, clay, gravel or intraclasts;
- absence of graded bedding structures;
- moderate to well sorting.

The first category (1) of aeolian sands is determined by these basic conditions alone. For the second category (2), an additional constraint is put on sedimentary structure; lamination or thin bedding should be present. The third category (3) is restricted to fine sands, without restriction on structure. The fourth category (4) combines the restrictions of category 2 and 3 (well sorted fine sands only, with bedding or lamination). Fig. VIII.8 shows the percentage of Middle Pleniglacial sand beds which conform to one of these categories, for different valley regions (regions as in par. VIII.2.1).

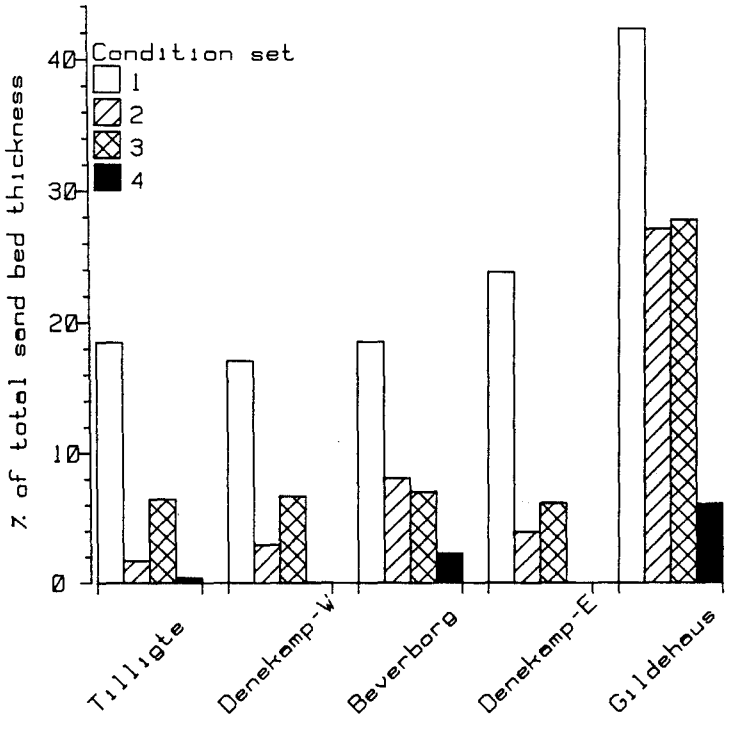

Figure VIII.8. Distribution of aeolian sands within the Middle Pleniglacial deposits in the Dinkel valley. Bars represent % possible aeolian sands of total thickness of Middle Pleniglacial sand beds. Condition set refers to different sets of database search criteria, see text for further description. Condition set 1 presents the most lenient, set 4 the most strict description of possible aeolian sands.

Not surprising, the most lenient definition of the aeolian sands (1) yields the largest percentage, while the most strict definition (4) yields the lowest percentage. Definition 1 will include a large amount of waterlaid sands from which the sedimentary structures have not been preserved in the cores, and is not very useful therefore. The constraints in the other definitions also do not exclude a waterlaid origin; current ripple cross-lamination, for instance, also may show up as undifferentiated

lamination in small diameter cores. Although it possibly may exclude some coarser aeolian sands, definition 4 is considered here as the closest possible description of aeolian sand in terms of the core descriptions, because of its agreement with exposed aeolian sands (De Poppe exposure, par. VIII.3.1; Schwan, 1988a,b).

All sets of definitions yield approximately equal percentages in all valley areas, except the Gildehaus area which shows distinctly higher percentages originating from the Puntbeek sands. Coarser fluvial sands appear to interfinger with finer aeolian sands in this area. Sedimentary structures in the finer sands most likely resemble those of unit 3 in the De Poppe exposure on the western margin of the Dinkel valley. Also the westernmost borings of the Beverborg section (fig. IV.16) indicate the presence of similar sediments. Apparently, a fluvio-aeolian facies exists within the Puntbeek sands besides the coarser fluvial facies of this unit in the Denekamp-E area. This facies is an analogue of the fluvio-aeolian deposits of the Upper Pleniglacial Beverborg Member, described by Vandenberghe & Van Huissteden (1988). However, the aeolian deposits of the Puntbeek sands are generally somewhat finer and siltier, which may point to an important loess component in the aeolian deposits. The fluvio-aeolian facies appears to occupy a marginal position in the Dinkel valley.

Mineralogy of the Puntbeek sands in the Gildehaus section does not differ significantly from the Tilligte beds (fig. V.6), and therefore channel bars on the alluvial plain represented by the Tilligte beds are the most likely source of the aeolian material. The fluvio-aeolian facies is absent in situations where larger areas of exposed channel sediments probably have been lacking, for instance in the Tilligte basin. Only in the presence of sufficiently large sandy bar surfaces a fluvio-aeolian valley margin apparently could develop, as probably has been the case in the Dinkel valley south of Denekamp. It might have occupied a somewhat higher floodplain level, as for instance the valley margin terraces with aeolian sedimentation described by Bryant (1983) and Good & Bryant (1985).

In the Dinkel valley the fluvio-aeolian facies appears to be more widespread on the eastern valley margin than on the western valley margin. On the western margin it occupies only a narrow strip as is indicated by the Beverborg section. This implies Middle Pleniglacial wind directions with an important westerly component. This confirms the hypothetical northwestern wind directions derived from grain surface morphoscopy data by Elzenga et al. (1987).

VIII.4. Markov chain analysis applied to lithofacies sequences.

VIII.4.1. Analysis procedure.

Investigation of vertical sequences in the Middle Pleniglacial sediments should provide more information on the type of changes which occur in the fluvial system. A well established technique is Markov chain analysis (e.g. Schwarzacher, 1975; Davis, 1986). Markov chain analysis is based on the transition frequency matrix which shows the number of upward transitions from one lithofacies to another in a vertical section. The transition frequency matrix (TFM) is converted into a transition probability matrix (TPM) by

dividing the entries of each row by the corresponding row total. The basic hypothesis to be tested is whether the lithofacies transitions follow a non-random pattern, or are generated by an independent random process. A non-random pattern in this case means that the occurrence of a certain lithofacies depends on the type of bed underlying it, instead of being determined by its relative abundance in the total sequence only.

The sequence which is used in the analysis should be homogeneous, that is, different parts of the sequence should provide the same TPM. Equality of the matrices can be tested using a Chi-square test (Schwarzacher, 1975). In this case it is difficult to apply such tests, as the partial TFM's will tend to have a too low number of counts for reliable use of the Chi-square test. However, the extent of vertical and lateral inhomogeneity is well known from the sections. The TPM is determined from borings in the Tilligte beds only, borings which include well developed portions of the basal clays have been discarded.

The facies transitions can be counted in various ways, by counting facies transitions at observed bedding planes, by counting at fixed intervals, or by counting at transitions to another facies only (Schwarzacher, 1975). Bedding planes can be difficult to determine with certainty in boreholes, especially in sand sequences obtained from the hand coring equipment. Fixed interval counting provokes the question which interval length should be chosen. Especially in this case it appears that one interval for all lithofacies types tends to over-emphasize the transitions between sands. The palaeobotanical data show that sands have been deposited much faster than fine-grained sediments (Ran, 1990), and it would therefore be justified to use larger intervals for counting the sand parts of the sequences than for the fine-grained parts. However, the choice of an interval length always will be arbitrary. Therefore transition counting which includes only transitions between different lithofacies types is applied here.

TPM's which include only transitions to different lithofacies types show zero values on the matrix diagonal ('structural zero's'). This is a non-random element which is introduced beforehand by the counting method, and therefore the usual procedure for testing the validness of an independent random sequence does not apply (Schwarzacher, 1975). Recently a method has been developed which overcomes the presence of structural zero's (Carr, 1982; Powers & Easterling, 1982). This test includes an iterative procedure to construct a matrix of expected transition probabilities, containing the transition probabilities generated by a quasi-independent sequence with the same percentage of lithologies (quasi-independence: independence, exclusive of the diagonal transition probabilities). The test is implemented in a computer program published by Wells (1989).

Another problem is to obtain a sufficient number of transition counts. The solution is either lumping of the more rare lithofacies classes, or lumping of a number of borehole sequences. The first procedure is not desirable, since objective selection criteria are lacking. The second procedure also must be applied with care. Lithofacies types deposited at the same time at closely spaced boring locations may be equal or laterally dependent (Schwarzacher, pers. comm., 1986). This may lead to over-representation of transitions. From the detailed borehole sections it proves that lateral facies changes generally occur

at very short distances, in the order of tens of metres. Possible lateral dependence can be avoided by selecting borings at a sufficient distance (order of kilometres) of each other. The elevation differences in the time lines, caused by the presence of fluvial incisions, provides a further chance to select a large number of transitions from different chronologic levels. The final selection of borings, based on distance, representativity for the Tilligte beds, and quality of the core description, is listed in table VIII.5. The analysis results are valid only for the Tilligte beds as found in the Tilligte and Nordhorn basins (par. VIII.2.1).

Boring	Section	Figure
Lattroperstraat	Lattrop-Denekamp	IV.12
Nicolaasstichting	Lattrop-Denekamp	IV.12,13
Dorpermeien	Detailed sections Denekamp	IV.20
Venweg	Laarhuis-Rammelbeek	IV.11
Tilligte Vlierweg	Tilligte	IV.9
Scholtenhave	Laarhuis-Rammelbeek	IV.10,11
Noord-Deurningen	Laarhuis-Rammelbeek	IV.11,12
Witstaartweg II	Tilligte	IV.9
663	Lattrop-Denekamp	IV.13
621	Lattrop-Denekamp	IV.13
607	Lattrop-Denekamp	IV.13
681	Lattrop-Denekamp	IV.12
632	Detailed sections Denekamp	IV.20
670	Laarhuis-Rammelbeek	IV.11
403	Laarhuis-Rammelbeek	IV.10
414	Laarhuis-Rammelbeek	IV.10
407	Laarhuis-Rammelbeek	IV.10
434	Laarhuis-Rammelbeek	IV.11
427	Laarhuis-Rammelbeek	IV.11

Table VIII.5. Borings used for Markov chain analysis.

VIII.4.2. Non-randomness of lithofacies transitions within the Tilligte beds.

Table VIII.6A shows the transition frequency matrix derived from the borings in table VIII.5, and table VIII.6B-H shows the results of subsequent analysis performed with the help of the computer program of Wells (1989). The transition probability matrix (TPM) indicates which transitions take place preferentially. In the TPM (table VIII.6B) the highest transition probabilities have been underlined. The matrix of semi-independent expected transition frequencies (table VIII.6C) is calculated from the row totals, using the iterative procedure proposed by Powers & Easterling (1982). Whether this matrix differs significantly from the observed TFM is determined with the help of a Chi-square test (table VIII.6D,E). The difference matrix (table VIII.6D) is obtained by subtracting the expected values (table VIII.6C) from the observed values (table VIII.6A). Table VIII.6E shows the individual Chi-square components and their summation. The observed frequencies differ significantly (level of signifi-

Table VIII.6. Analysis of a transition frequency matrix derived from the Tilligte beds (with the help of computer program by Wells, 1989). A: Transition frequency matrix; B: Transition probability matrix (highest values in each row are underlined); C: Expected transition frequencies (in case of semi-independent transitions); D: Difference matrix (observed - expected transitions); E: Sequence chi-square matrix, (significantly high values have been underlined); F. Binomial probabilities (probability < 10% have been underlined); G. Significantly favoured & disfavoured transitions (binomial probability < 0.1; extremely low probabilities, < 0.01 have been underlined); H: Asymmetry chi-square matrix.

A. TRANSITION FREQUENCY MATRIX.

Lithofacies		A	B	C	D	E	F	G	H	row totals
A	Channel sands	0	51	11	8	6	14	3	4	97
B	Overbank sands	57	0	25	16	14	14	2	4	132
C	Sand/silt intergrades	12	32	0	6	5	3	1	3	62
D	Floodbasin silt	19	20	6	0	0	4	6	2	57
E	Floodbasin clay	6	13	5	2	0	1	2	3	32
F	Peat	4	9	8	13	0	0	2	0	36
G	Gyttja	1	1	1	7	3	3	0	1	17
H	Intraclast beds	3	6	4	4	0	0	0	0	17
column totals		102	132	60	56	28	39	16	17	450

B. TRANSITION PROBABILITY MATRIX

Lithofacies	A	B	C	D	E	F	G	H
A	0.00	<u>0.53</u>	0.11	0.08	0.06	0.14	0.03	0.04
B	<u>0.43</u>	0.00	0.19	0.12	0.11	0.11	0.02	0.03
C	0.19	<u>0.52</u>	0.00	0.10	0.08	0.05	0.02	0.05
D	0.33	<u>0.35</u>	0.11	0.00	0.00	0.07	0.11	0.04
E	0.13	0.28	0.25	<u>0.40</u>	0.00	0.00	0.06	0.09
F	0.11	0.25	0.22	<u>0.36</u>	0.00	0.00	0.06	0.00
G	0.06	0.06	0.06	<u>0.41</u>	0.18	0.18	0.00	0.06
H	0.18	<u>0.35</u>	0.24	0.24	0.00	0.00	0.00	0.00

Table VIII.6 (continued)

C. EXPECTED TRANSITION FREQUENCIES

Lithofacies

	A	B	C	D	E	F	G	H
A	-	45.09	14.98	13.80	6.51	9.16	3.61	3.84
B	46.89	-	24.56	22.63	10.68	15.02	5.93	6.30
C	16.03	25.27	-	7.74	3.65	5.13	2.03	2.15
D	14.58	22.99	7.64	-	3.32	4.67	1.84	1.96
E	7.68	12.12	4.02	3.71	-	2.46	0.97	1.03
F	8.84	13.94	4.63	4.27	2.01	-	1.12	1.19
G	3.99	6.28	2.09	1.92	0.91	1.28	-	0.54
H	3.99	6.30	2.09	1.93	0.91	1.28	0.50	-

D. DIFFERENCE MATRIX

lithofacies

	A	B	C	D	E	F	G	H
A	-	5.91	-3.98	-5.80	-0.51	4.84	-0.61	0.16
B	10.11	-	0.44	-6.63	3.32	-1.02	-3.93	-2.30
C	-4.03	6.73	-	-1.74	1.35	-2.13	-1.03	0.85
D	4.42	-2.99	-1.64	-	-3.32	-0.67	4.16	0.04
E	-1.68	0.88	0.98	-1.71	-	-1.46	1.03	1.97
F	-4.84	-4.94	3.37	8.73	-2.01	-	0.88	-1.19
G	-2.99	-5.28	-1.09	5.08	2.09	1.72	-	0.46
H	-0.99	-0.30	1.91	2.07	-0.91	-1.28	-0.50	-

E. SEQUENCE CHI-SQUARE MATRIX

lithofacies

	A	B	C	D	E	F	G	H
A	-	0.77	1.06	2.44	0.04	2.56	0.10	0.01
B	2.18	-	0.01	1.94	1.03	0.07	2.60	0.84
C	1.01	1.79	-	0.39	0.50	0.89	0.52	0.33
D	1.34	0.39	0.35	-	3.32	0.10	9.38	0.00
E	0.37	0.06	0.24	0.79	-	0.87	1.09	3.75
F	2.65	1.75	2.45	17.87	2.01	-	0.70	1.19
G	2.24	4.44	0.57	13.40	4.82	2.33	-	0.40
H	0.25	0.01	1.74	2.23	0.91	1.28	0.50	-

Sequence chi-square sum: 106.866 | Degrees of freedom: 41

Table VIII.6 (continued)

F. BINOMIAL PROBABILITIES

lithofacies

	A	B	C	D	E	F	G	H
A	-	0.135	0.164	0.055	0.521	0.072	0.510	0.538
B	0.042	-	0.495	0.074	0.181	0.457	0.061	0.241
C	0.153	0.055	-	0.330	0.301	0.235	0.395	0.365
D	0.119	0.252	0.344	-	0.033	0.495	0.010	0.587
E	0.322	0.439	0.376	0.266	-	0.283	0.253	0.083
F	0.039	0.061	0.083	0.000	0.126	-	0.308	0.299
G	0.066	0.004	0.365	0.002	0.059	0.131	-	0.419
H	0.409	0.549	0.148	0.118	0.393	0.265	0.599	-

G. SIGNIFICANTLY FAVOURED & DISFAVOURED TRANSITIONS

Favoured transitions	Disfavoured transitions
Channel sands ↑ Peat	Channel sands ↑ Silt
Overbank sands ↑ Channel sands	Overbank sands ↑ Silt
	Overbank sands ↑ Gyttja
Sand/silt intergrades ↑ Overbank sands	
Silt ↑ Gyttja	Silt ↑ Clay
Clay ↑ Intraclast beds	
Peat ↑ Silt	Peat ↑ Channel sands
Peat ↑ Sand/silt intergrades	Peat ↑ Overbank sands
Gyttja ↑ Silt	Gyttja ↑ Channel sands
Gyttja ↑ Clay	Gyttja ↑ Overbank sands

H. ASYMMETRY CHI-SQUARE MATRIX

Lithofacies

	A	B	C	D	E	F	G
A	-	-	-	-	-	-	-
B	0.33	-					
C	0.04	0.86	-				
D	4.48	0.44	0.00	-			
E	0.00	0.04	0.00	2.00	-		
F	5.56	1.09	2.27	4.76	1.00	-	-
G	1.00	0.33	0.00	0.08	0.20	0.20	-
H	0.14	0.40	0.14	0.67	3.00	0.00	1.00

Asymmetry chi-square sum:	30.042
degrees of freedom:	27

cance 1%) from the expected values. Hence, the observed sequences are not the result of a semi-independent random process.

Sections generated by independent random processes are likely to be very rare (Schwarzacher, 1975). Rejection of the assumption of quasi-independence is genetically not very relevant. Also the significance of individual transitions should be taken into account. This is indicated by the difference matrix (table VIII.6D), the sequence chi-square matrix (table VIII.6E) and the calculated binomial probabilities (table VIII.6F) for the transitions.

In the difference matrix positive values indicate favoured transitions, and negative values indicate disfavoured transitions. The latter are not less important than the favored ones. The computer program of Wells (1989) provides two methods to determine whether a particular facies transition occurs significantly more or less than could be expected from the independent random model. First, the individual Chi-square scores can be used. According to Türk (1979), the residuals (the square root of the individual Chi-square components) are approximately normally distributed. Thus significance levels can be set for the individual Chi-square scores in table VIII.6E. Significant values (significance level 0.1) have been underlined in table VIII.6E. The second method is calculating the binomial probability of a given entry in the TFM (Harper, 1984). For favoured transitions the probability of obtaining at least the observed number of transitions applies, for disfavoured transitions the probability of at most the observed number. If the binomial probability is lower than the selected significance level (0.1), the transition is significantly favoured or disfavoured (underlined in table VIII.6F). It proves that the chi-square values yield more significant transitions than the binomial probabilities, especially from the rare lithofacies classes (peat, gyttja and intraclast beds). In the binomial probability calculation, the relative occurrences of the lithofacies classes apparently is weighted more accurately.

Combination of table VIII.6D, E, and F yields a list of transitions which deviate from expected values for an independent random succession (table VIII.6G). As can be seen from table VIII.6B these are not necessarily the most common transitions indicated by the TPM. In the latter the probabilities are also determined by the abundance of lithofacies classes.

Further analysis recommended by Powers & Easterling (1982) includes a test for asymmetry of the sequence which is also incorporated in the program of Wells (1989). The purpose is to test whether the sequence X to Y occurs as frequently as the sequence Y to X. The result is displayed in table VIII.6H. A high chi-square score in this case means that many non-reversible, unidirectional transitions occur. It proves that most transitions are reversible.

VIII.4.3. Entropy analysis of the transition probability matrix.

As shown above, a model of independent random lithofacies transitions does not hold for the Tilligte beds. This does not yet imply a sedimentological meaningful explanation of the observed dependent transitions. Another model, taking into account the possible sedimentary processes responsible for the dependencies, has to be developed.

Usually, it is assumed that the observed sequence consists of the sum of signal and random noise (Powers & Easterling, 1982). The 'signal' is considered to be the expression of an 'ideal' or fully developed cycle of events in the sedimentary environment. In general, two types of sequence may be present, symmetrical (e.g. X to Y to Z to Y to X) and asymmetrical (e.g. X to Y to Z to X to Y to Z).

Hattori (1976) provides a method to depict which type of sequences may be represented in the TPM, by calculation of entropy values. Entropy for row i in the n x n transition probability matrix is defined as

$$E_i^{post} = -\sum_{j=1}^{n} p_{ij} . {}^2\log p_{ij} \qquad (1)$$

in which p_{ij} denotes the transition probability from lithofacies number i to number j; the superscript 'post' denotes, that the entropy value pertains to the upward transition probabilities. Also the E^{pre} values for downward transitions can be calculated. E_i equals to zero when all p_{ij}'s in row i, except one, are equal to zero, maximum E_i occurs when all p_{ij}'s in row i (except p_{ii}) are equal to each other.

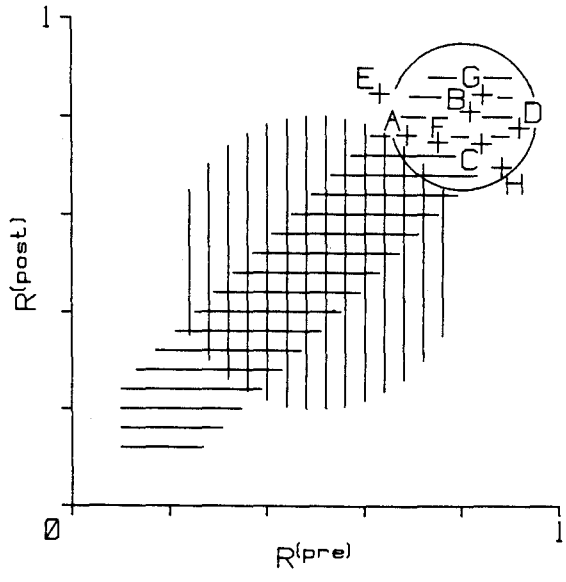

Figure VIII.9. Entropy set scatter plot (cf. Hattori, 1976) for the facies transitions in the Tilligte beds. R values are normalized entropy values for upward (post) and downward (pre) transitions. Hatched and encircled areas indicate theoretical entropy set distribution of different types of cyclic deposits cf. Hattori (1976). Vertical hatch: A4 type (truncated asymmetrical cycles); most fluvial deposits prove to show this type of entropy set distribution (Hattori, 1976). Horizontal hatch: B type (truncated symmetrical cycles). Circle: C type (Strongly disorganized succession). The Tilligte beds succession belongs to the C type.

For the purpose of comparison E_i is normalized by division with E_{max} which is the maximum possible entropy for each litho-

facies and depends on the total number of lithofacies only (E_{max} = 2.81 in this case). Normalization yields the value $R = E_i/E_{max}$.

The entropy set, a scatter plot of R^{post} versus R^{pre}, is used by Hattori (1976) to compare the observed TPM to TPM's of different theoretical cyclic successions. Every type of succession displays a typical pattern of points on the entropy set scatter plot. Fig. VIII.9 depicts the entropy set from the Tilligte beds. It is compared with the general point scatter pattern of two theoretical entropy sets conceived by Hattori (1976). These are: the A4-type entropy set which is generated by truncated asymmetric cycles, the B-type set, generated by truncated symmetric cycles. Especially the A4 type dominates in fluvial successions. However, all R values from the Tilligte beds prove to lie close to the maximum R values. The entropy set from the Tilligte beds therefore resembles Hattori's C-type sequence 'strongly disorganized cyclic succession'. In this type of sequence, none of the theoretical cycle models can be recognized.

Although Hattori (1976) denotes this type of sequence as 'essentially a random lithological series', it will be clear from the previous analysis, that randomness in the sense of a (quasi) independent random sequence does not hold for the Tilligte beds. The only justified conclusion is that a model assuming the presence of one or a few simple symmetrical or asymmetrical cycles does not hold for the Tilligte beds. The sequence may be a more intricate combination of different types of cycles, possibly combined with random perturbations. It is more complex than common fluvial sequences listed by Hattori (1976) which are usually of the asymmetric, truncated type.

VIII.4.4. Interpretation of the transition probabilities based on the preferred lithofacies transitions.

The Middle Pleniglacial floodplain is a complex system, in which sediment distribution and storage may be accommodated by several processes. Each of these processes may have generated one or more typical successions of its own. In addition random events such as extreme floods may have occurred. By consideration of the separate nonrandom facies transitions listed in table VIII.6G at least some of these processes are revealed.

Most transitions of organic into fine-grained clastic sedimentation are favoured: peat to silt, gyttja to silt, gyttja to clay and peat to sand/silt intergrades. The reverse transitions from fine grained clastic to organic sedimentation are less conspicuously favoured. As indicated by palaeobotanical data, the organic to clastic sedimentation transitions coincide with a change to wetter conditions (often open water) and an increased clastic sedimentation rate (Ran, 1990).

Direct transitions of peat or gyttja to sands are disfavoured. It appears that transition pathways from floodbasin sedimentation to channel sands tend to be gradual: favoured transitions are sand/silt intergrades to overbank sands and overbank sands to channel sands. This points to the presence of a gradual coarsening upward transition, in contrast to the generally assumed fining upward sequence model which is often found in literature on fluvial deposits (e.g. Allen, 1970; Miall, 1980; Reineck & Singh, 1975).

A process by which a similar coarsening upward sequence is created, is crevasse splay progradation (Elliott, 1974; Bridge,

1984; Smith et al., 1989). Also in this case the observed coarsening upward sequences represent crevasse splay sedimentation in floodbasin environments. An excellent example is the sequence in the Hengelo A1 exposure, where transitions from silt to crevasse splay sands also display a coarsening upward sequence (par. VI.2.4.2). In these cases, the sand/silt intergrades represent the toesets of prograding crevasse splay foresets. The coarsening upward sequences tend to repeat in vertical sections. The sedimentary process itself can be the cause of this cyclic behavior, by the following process.

Peat or gyttja sedimentation takes place in areas cut off from clastic influx. Since organic sedimentation rate is lower than clastic sedimentation rate, sedimentation in the area lags behind, in comparison with active sedimentation areas such as channel belts. This effect is especially likely to occur in cold climates with low organic matter production. If not already present, standing water bodies develop (section X). The resulting floodplain relief ultimately becomes unstable. Clastic influx will be restored by breaching of nearby levees or avulsion (formation of a new channel belt in a floodbasin). Restoration of the clastic sedimentation in a floodbasin after avulsion occurs by formation of crevasse splays which prograde into the basin and evolve gradually into a new channel system (Smith et al., 1989).

Levee breaching is assumed to have occurred as soon as organic sedimentation is replaced by clastic deposition. If a floodbasin is filled in by prograding crevasse splays, silt deposition will occur first in distal locations, later to be taken over by sand deposition of the actual crevasse splays (Smith et al., 1989). The process leads to the intercalation of a silt layer between organic sediments and crevasse splay sands; direct (erosional) transitions from peat to sand will be relatively rare, as is confirmed by the transition counts. Coarsest channel material will be found at the top of the crevasse splays (low width/depth ratio feeder channels), or intercalated within the crevasse splay sands (Smith et al., 1989).

The favoured transition from coarse sands to peat indicates that the termination of clastic sedimentation before peat growth starts, may be abrupt. Some transitions involving continued clastic deposition after sand sedimentation are even disfavoured (channel sands or overbank sands to silt). One obvious explanation for this transition is peat formation in abandoned channels. However, such situations are expected to be of limited areal extent, and therefore cannot be the sole explanation for the abundance of this transition. Also in the Hengelo A1 exposure the coarse top of crevasse splays is often covered immediately by peat. Therefore the frequent transition from coarse clastic sedimentation towards peat growth marks sudden termination of crevasse splay sedimentation. Also in present-day environments complete abandonment of crevasse splays in any stage of their development occurs, to be followed by vegetation growth (Smith et al., 1989). Since the splay surface is higher than the adjacent floodbasins, a continuation of sedimentation in a (semi-)terrestrial environment is most likely. This explains the preference for peat growth, while for instance lacustrine gyttja deposition immediately on overbank sand is disfavoured.

It appears that the common cycle of the Tilligte beds is generated by repeated crevasse splay progradation and avulsion in

floodbasin environments, as described by Smith et al. (1989). This common cycle is a coarsening upward cycle and consists of transitions from peat to floodbasin silt to overbank sands to channel sands, after which a return to peat deposition takes place.

However, the entropy analysis in the previous paragraph shows, that simple sequences are not readily to be found in the TPM. Considerable modifications may occur which consist of:
(1) truncation by erosion,
(2) incomplete development of a full cycle,
(3) combination with cycles generated by other processes,
(4) possible alternative transition pathways branching from the 'ideal' cycle or
(5) fully independent random events.

Type 1 complications will be related to channel erosion. A full cycle (2) may fail to develop as a consequence of high avulsion activity. In a periglacial environment, several processes may promote avulsion frequency (par. II.3). Type (3) modification is shown by silt/gyttja alternations. Besides gyttja to silt transitions, also silt to gyttja transition are favoured. This alternation is ascribed to shifting pathways of clastic influx within floodbasin lakes.

Clay beds also represent a distinct lithofacies which behaves in some respects differently from similar material like silt. Silt to clay transitions are significantly disfavoured. Other clay transitions are similar to those of silt, for instance the favoured gyttja to clay transition, indicating increasing clastic influx in a lacustrine environment. The clay beds probably represent a different type of floodbasin, more isolated from active river channels and with a more permanent lacustrine character. As such, the clays may be an example of type 4 modification.

A lithology which appears to behave independently is represented by the intraclast beds. The significantly favoured transition of clay to intraclasts may be spurious, as both clay and intraclast beds are relatively rare. Intraclast beds occur practically above any lithology, preferably those which will provide intraclasts upon erosion. Transition from intraclasts to sands are relatively rare, while those to silty material are common. Therefore the intraclast beds are not restricted to channel environments. Many intraclast beds are to be interpreted as erosion phenomena in floodbasin environments which may be caused by random events (type 5 modification). Examples may be extreme floods, or possibly thaw lake development, analogous to the intraclasts in the thaw lake sequence of the Hengelo A1 exposure (par. VI.2.3.2).

It is likely that the preference for coarsening upward sequences points to relatively little lateral channel migration. Typical erosional base/ fining upward sequence elements, caused by this process, are disfavoured. Vertical accretion in floodbasin areas dominates in the Tilligte beds over lateral accretion by migrating channels. The Middle Pleniglacial deposits in their most typical facies largely consist of overbank sediments, in which true channel deposits play a minor role. Fig. VIII.10 represents a scheme of the preferred transition pathways, based on the discussion above.

From a sedimentological viewpoint the above-mentioned process of sedimentation lag/crevasse splay formation suffices well as an

explanation for the observed repetitions of sand and peat/silt beds in the Middle Pleniglacial deposits. The alternation of sand and fine-grained deposits is not necessarily induced by climatic change, although it always remains possible that individual cycles are activated by climate-related increased flooding frequencies or increased sediment load.

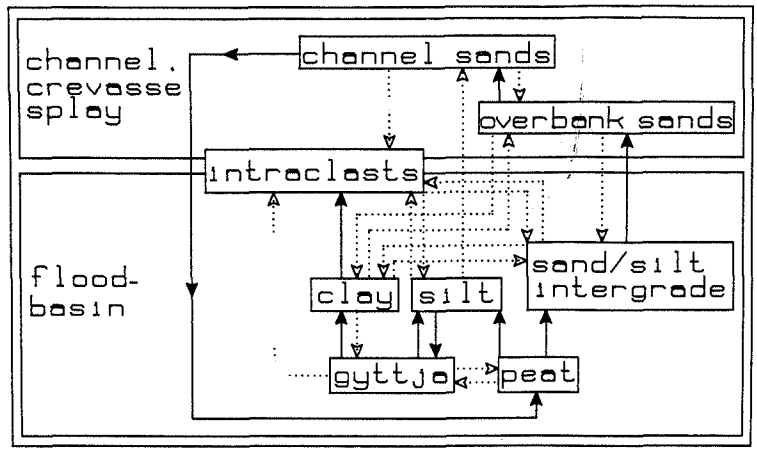

Figure VIII.10. Preferred lithofacies transition pathways in the Tilligte beds. Dotted lines : preferred transitions as indicated by positive values in the chi-square difference matrix (table VIII.6D). Solid lines: significantly favoured transitions as indicated by low binomial probabilities (< 0.1) of the transitions (table VII.6F,G).

VIII.5. Morphological characteristics of the Middle Pleniglacial fluvial environment in the Twente region.

A useful approach in description and classification of river deposits is the "architectural elements" analysis proposed by Miall (1985). In this method, emphasis is laid on description of the deposits in terms of a number of larger scale structures, rather than equating the deposits with the limited amount of data on present-day rivers. Although this method cannot be applied rigorously in this case (par. VIII.1), it is a useful guideline for the discussion below.

Channel deposits are not of wide extent throughout the Tilligte beds (par. VIII.2.2.2). Fining upward deposits with coarse channel lag deposits at the base do not stand out as a particularly frequent sequence in the Markov chain analysis (par. VIII.4.4). In the sections, the larger channel-like phenomena are associated with the erosion levels. The channels observed in the Hengelo basin exposures show steep, partly undercut banks due to their cohesive bank material (par. VI.2.4.4). Width/depth ratios could not be determined, but are not high. The mode of infilling is mainly vertical accretion, only the large channel in the Rientjes exposure shows evidence of some lateral migration (par. VI.3.2). In the Beverborg section, coarse sands are more common. The presence of fragmented, reworked silt or peat intraclast levels overlain by coarse sand point to more frequent reworking by lateral channel migration.

In the borehole sections most sandy deposits of the Tilligte beds consist generally of lithofacies B sands, with intercala-

tions of lithofacies A and C (par. VIII.2.2.2). These sands display different types of cross-bedding and horizontal lamination or bedding. The B- and C- type sands tend to grade into the fine-grained deposits, rather than overly these erosively. As the Markov chain analysis shows, a coarsening upward sequence dominates. Therefore most of these sands can be interpreted as crevasse splay deposits, with sedimentary structures similar to those observed in the Hengelo A1 exposure (par. VI.2.4.2,3). The crevasse splay sand bodies may contain smaller (crevasse) channels and levee deposits, or grade into channel deposits (par. VIII.2.2.2).

Levee deposits have not been identified in the borehole sections due to lack of sedimentary structure information, but they do occur in the Hengelo A1 exposure. These display upper flow regime horizontal lamination with scouring phenomena in larger systems, or smaller scale cross-lamination in small levees. Like the crevasse splay deposits, the levee deposits may appear in the borehole sections as lithofacies B sands interfingering with lithofacies A.

The overbank fines are sheet-like features as well. The silts have been deposited in typical floodbasin environments with shallow lacustrine or semi-terrestrial conditions, as is shown by the presence of wave ripples, and results from palaeobotanical analysis (Ran, 1990). Lithological variation within the overbank fines is generated by differences in clastic influx as discussed above. Peat and gyttja deposits originate in environments with strongly reduced clastic sedimentation. The basal clays in the Nordhorn basin and the thick clay deposits in the Hengelo basin point to more outspoken lacustrine conditions on the river floodplains. Fine-grained channel fills deposited in cut-off channel sections appear to be scarce. Examples are thick clay beds in boring 673 of fig. IV.11 (par. VIII.2.2.1) and part of unit 2 in the Hengelo A1 exposure (par. VI.2.4.1). Thaw lake deposits as observed in the Hengelo A1 exposure (par. VI.2.3.2) are rare as well (see below).

The scarcity of lateral accretion deposits, dominance of crevasse splay sand sheets and abundance of marshy to lacustrine deposits in the Tilligte beds point to similarities with the anastomosed rivers described by e.g. Smith & Smith (1980), Smith (1983, 1986), Smith et al. (1989), or model 8 of Miall (1985). These systems contain multiple, anabranching channels of low to high sinuosity, embedded in lacustrine and wetland environments. Within a single channel belt lateral accretion by meandering may occur, but the dominant mode of channel displacement is avulsion. Channel deposits tend to consist of ribbon-like sand bodies rather than extensive sheets. In general anastomosed river systems are rapidly aggrading, and peat growth may be prominent.

Nonetheless, the Middle Pleniglacial river plains in the Twente region show in several aspects some important deviations from this general description. The Tilligte beds tend to show a much smaller proportion of silt, clay, and peat, relative to sands. Three factors have influenced this difference. In the first place, it is partly an apparent difference, as compaction has reduced the thickness of the Middle Pleniglacial overbank fines to a greater extent than in comparable recent deposits. The two other factors are related to the periglacial environment of the rivers. The rate of organic matter production, and consequently also peat growth, will have been low in the cold Middle

Pleniglacial climate (Lieth, 1975; Zoltai & Pollet, 1983). Slower peat growth will decrease floodbasin sedimentation rate, leading to greater difference between channel belt and floodbasin sedimentation rates than would have occurred under warmer climatic conditions. Consequently, crevasse splay development and avulsion occurs more frequently. Next, a nival hydrologic regime, and blockage of smaller channels by snow or ice in early spring might have diverted a comparatively larger part of flood flows out of the channels, promoting extensive overbank deposition of coarser sediment (par. II.3).

A further cold-climate aspect of the anastomosed river deposits in this study is the possibility of ground ice formation in the overbank fines. If ground ice thaw is initiated, it may lead to thaw lake development and floodplain erosion. The thaw-lake sequence found in the Hengelo A1 exposure is a very specific sequence: a thin (<15 cm) layer with intraclasts, resting on floodplain silt or peat, and overlain by laminated silt. Nevertheless, only one occurrence of such a sequence has been found in the core descriptions. Possibly the rather frequent occurrence of intraclast to (sandy) silt transitions found by Markov chain analysis (par. VIII.4.4) also represent thaw lake sequences. The number of these transitions (8) is still low, however, and alternative explanations (extreme floods in floodbasin environments) may hold. Most lacustrine environments in the Middle Pleniglacial deposits have been ordinary floodplain lakes, and thaw lakes have been relatively rare.

A striking characteristic is the small-scale lateral variation within the deposits. Firstly, a scale factor must be taken into account. Especially in the Tilligte basin the 'rivers' will have been rather small streams originating from the surrounding ice pushed ridges. Another source of short distance variation may have been the tendency for high avulsion frequency, noted above. This should lead to higher channel deposit density (par. II.3). A very important source of apparently haphazard short distance lateral thickness variations of beds is the presence of cryoturbatic phenomena, as demonstrated by the intensely deformed silt beds in the Hengelo A1 exposure (par. VI.2.3.3). In borehole sections such cryoturbatic phenomena are hardly detectable and may pose serious problems in stratigraphical correlation (par. VIII.2.2.1).

Another peculiarity is the general occurrence of aeolian processes on the alluvial plains, as the lateral transition towards a fluvio-aeolian facies in the Puntbeek sands, and the grain surface morphoscopy data suggest (par. VII.2.4, VIII.3). It even may have occurred on crevasse splay or levee surfaces enclosed by lakes, for which evidence is found in the Hengelo A1 exposure. Aeolian reworking of levee sediments also has been reported from deltaic distributaries in subarctic and arctic areas (Dahlskog, 1966; McCloy, 1970). Most aeolian deposits probably occurred on channel bar, levee or crevasse splay surfaces, with a high chance of being reworked during flooding. Preserved aeolian sand deposits of some extent appear to be associated only with the larger channel belts, as found in the main valley of the Dinkel system south of Denekamp (fluvio-aeolian facies of the Puntbeek sands). Also the loessic material which has been deposited in the basin has been fluvially reworked, and finally re-deposited in the floodbasins. Fluvial

activity has been sufficiently high to prevent preservation of significant amounts of purely aeolian deposits.

Possible channel geometry in the Puntbeek sands ranges between an active, laterally migrating single channel river, to braided channels with low width-depth ratio. Most of the Puntbeek sands appear to have been deposited along the main drainage line of the valley, as these consist mainly of coarser sands. The fluvio-aeolian facies of the Puntbeek sands along the valley margins south of Denekamp (par. VIII.3.2) shows similarities with the Upper Pleniglacial fluvio-aeolian deposits (Van Huissteden & Vandenberghe, 1988).

On a large scale the geographical variation in sedimentary environment is more striking than the vertical variation along the time axis. This geographical variation is due to the position with respect to the major drainage lines, and basin/valley topography (par VIII.2.1). Vertical variation in the deposits is found in the shape of the erosion levels discussed in par. IV.6. The erosion levels are to be taken as intervals where erosion appears to be more common. Distinct downcutting associated with these levels is rare, it is mainly associated with level II. In many locations merely a hiatus is found. Level II is the most well developed erosion level which has been identified in the Hengelo basin as well as the Dinkel valley. It is accompanied by ground ice thaw features in the Hengelo basin. The thawing of ground ice probably has enhanced these erosion features in the Dinkel valley also.

IX. Radiometric datings and their implications for sedimentation rate and environmental changes.

IX.1. General chronology of the Late Pleistocene sequence in the Dinkel valley.

Pollenanalytical and radiometric dating provide a chronological framework for the stratigraphy of the Late Pleistocene basin fill as discussed in section III. Eemian age organic sediments have been dated in two borings. Peat beds in boring Kamphuis (2030-2110 cm below surface) and in boring Noord Deurningen (1786-1878 cm) are of Late Eemian age, as shown by pollen analysis (fig. IV.5, 6; Van Geel et al., 1986; Van Geel, pers. comm.). As is demonstrated by the latter boring, sedimentation continued throughout Eemian and Early Weichselian apparently without major erosional breaks.

In addition to palynological dating Uranium-Thorium datings have been carried out on Eemian and Weichselian age peats (Van der Wijk, 1987). Unfortunately samples from the Dinkel basin show extremely low U concentrations which leads to datings with large uncertainties and considerable deviations from expected ages (table IX.1). Especially Middle Pleniglacial sediments have been affected by this problem. The ages have been corrected for possible thorium exchange between mineral and organic matter of the sample. This correction depends on assumptions with regard to the exchange mechanism which are as yet not fully understood. According to Van der Wijk (1987) uncorrected ages often tend to agree better with expected ages. Indeed, the uncorrected ages from some of the Early Glacial/Eemian samples appear to yield realistic ages, although the standard deviations are still large. The ages of 100 +15 -13 ka for the Eemian peat in boring Kamphuis and 89 ±8 ka for an Early Glacial peat between 1322-1337 cm in boring Scholtenhave are not unlikely.

The remainder of the Weichselian sequence falls within the time range for application of radiocarbon dating. The Lower Pleniglacial Dinkel Member does not contain datable organic matter. Practically all datings from the Tilligte beds show finite ages between 27.5 and 55 ka (appendix II). Considering the large standard deviations of the oldest datings and their sensitivity to contamination, the base of the Mekkelhorst Member may be older than 55 ka. A limiting age is the 89 ±8 ka U-Th dating from the Liendert Member in boring Scholtenhave. As shown by the sedimentation rate estimated for the basin (par. IX.3), ages up to 60 ka for the oldest levels of the Mekkelhorst Member could be possible.

The Beverborg Member and the Lutterzand Member s.s. also show a deficiency of datable material. The youngest underlying datings range between 27.5 and 28.7 ka (Beverborg section, Hengelo A1 exposure; figs. IV.16, VI.3). The oldest overlying dated material yields an age of 13.31 ka (Boring Lattroperstraat, Lattrop-Denekamp section, fig. IV.12). This confirms the correlation of Beverborg Member with the Weichselian cold maximum. Apparently environmental conditions excluded organic matter deposition at that time.

Late Glacial datings have been obtained from the Laarhuis-Rammelbeek section, the Lattrop-Denekamp section (figs. IV.11,12) and a small exposure in the vicinity of boring Lattroperstraat (De Braak, appendix I, fig. IV.1). The youngest ages (<11.4 ka)

have been obtained from gully fills, while older datings (>12.3 ka) occur in relatively high positions beside these gully fills (e.g. De Braak, boring Lattroperstraat; fig. IV.12). This suggests an age of the deepest point of the Late Glacial fluvial incision between 11.4 and 12.3 ka at these locations.

Boring + depth (cm)	U-Th age (ka) with standard deviation		Expected age (ka)	^{14}C age	Lab. Nr. (GrN)
	Uncorrected	Corrected			
Witstaart I					
300-310	93 +8 -7	55 +8 -7	42		
310-316	169 +23 -18	136 +32 -18	42-45		
552-560	223 +93 -48	160 +89 -39	46-48	40.4	12198
670-673	130 +24 -19	ca. 21	48-55		
Witstaart II					
235-241	144 +19 -15	78 +13 -11	<42		
Scholtenhave					
1145-1152	122 +10 -9	44 +12 -10	ca. 51	51.0	11544
1322-1337	89 +8 -8	14 +15 -13	>55		
1451-1458	infinite	ca. 75	>70		
Kamphuis					
2060-2067	100 +15 -13	87 +62 -34	>100		

Table IX.1 U-Th datings from the Dinkel valley (after Van der Wijk, 1987). Borehole logs in fig. III.3.

IX.2. Error sources in the radiocarbon datings.

IX.2.1. Evaluation criteria.

In the evaluation of radiocarbon dating results the possibility of dating errors should be carefully considered. This justifies a discussion of the assumptions by which the datings have been evaluated. Appendix I shows a list of the radiocarbon datings performed on behalf of this study by the Groningen Isotope Physics Laboratory. For each dating possible errors have been listed, based on the stratigraphical evaluation in par. IV.3-5.

Radiocarbon samples in the age range considered here are especially sensitive to contamination by younger carbon (type A,B,C in table IX.2; Geyh, 1971; Mook & Van de Plassche, 1986). Contamination by younger humic acids can be detected by separately dating the alkali extractable organic fraction of the sample, and the residue after alkali extraction. If younger humic acids are present in the sample, these should be concentrated in the alkali extract (Mook & Streurman, 1983). If both dated fractions of the sample do not yield significantly different ages, type C contamination most likely is absent. Also type D error (table IX.2) might produce an extract age which is younger than the residue age (e.g. the middle dating of boring Venweg, par. IV.3.2.2). In that case the residue contains the reworked ma-

terial and may be erroneous, while the extract age may be correct (Schoute et al., 1981,1983).

Type	Process	After formation of sample	During formation of sample
A	Contamination during sample handling	*	
B	Contamination by root penetration	*	
C	Contamination by younger humic acids	*	
D	Contamination by reworked older carbon		*
E	Hard water error		*
F	Reservoir effects		*

Table IX.2. Processes which may lead to deviation of radiocarbon age from true age of the dated sediments.

It is difficult to attach a significance level to the difference of the extract and residue datings. In case of contamination by younger humic acids, a considerable difference between extract and residue age does not necessary indicate an erroneous residue age, as alkali extraction is assumed to remove most of the contamination. A large difference between the two ages indicates that the residue age may be suspect, but this should still be checked against other stratigraphical evidence.

With exception of a few very small samples all samples have undergone alkali extraction, although the amount of extracted material may have been insufficient for dating. Datings on samples which received only acid treatment can be considered as minimum ages only. In the absence of a check by extract dating possible contamination is evaluated by correlation with the nearest (preferably overlying) stratigraphical level with both extract and residue datings. Another indication of possible contamination is significant chronological reversal of samples in a vertical sequence, or otherwise unacceptable stratigraphical relations.

Especially fluvial environments are sensitive to type D contamination (table IX.2). Besides larger organic particles, river and sea water also contain very finely divided or colloidal organic matter which may be incorporated in overbank sediments (Schoute et al., 1981; Mook & Van de Plassche, 1986). In general, the influence of this contamination depends on the carbon content of the sample. The risk of this type of contamination is highest in clay or silt samples with low organic matter content.

Often lake water shows a lower $^{14}C/^{12}C$ ratio than air which is known as the reservoir effect (Olsson, 1986). Plants which assimilate under water consequently will show a too high age. The apparent age of lake water CO_2 may have been derived from dissolution of older carbonate rocks in the surrounding ("hard water error"). In this case dates may be in error as much as 3000 to 4000 years (Donner et al., 1971). Another source of old carbon may be ground water seepage into the lake (Olsson, 1986). Specifically in thaw lakes melting permafrost ice may contribute old carbon (De Gans, 1981). Reservoir effect is counteracted by exchange of CO_2 with the atmosphere at the lake surface. This

exchange will be most efficient in large and shallow lakes (Zagwijn, 1983; Mook & Van de Plassche, 1986). Most lakes on the Middle Pleniglacial floodplain will have been shallow at least, although their extent may have been restricted. Type D, E and F errors are difficult to detect. On the other hand, these are also more interesting from a palaeo-environmental point of view, if positively identified.

IX.2.2. Possible hard water effect in the Middle Pleniglacial sediments.

The Middle Pleniglacial sediments are usually rich in lime, and also palaeobotanical data point to lime-rich environments (Brinkkemper et al., 1987). This pertains not only to lake deposits; also peat deposits could have been influenced (Shotton, 1972). *Drepanoclades* and *Scorpidium* mosses which are the most important peat formers of the Tilligte beds, also can assimilate under water. It is important, therefore, to assess the risk of this type of error. As noted in par. IV.4.1.2 several datings from unit DT3 in the Tilligte detailed grid area appear to be too old. Part of this unit consists of lime gyttja. It is not impossible therefore that deviating ages are the result of hard water error.

Possible carbonate sources are Cretaceous carbonate-rich marine sediments in the upstream area of the river, lime-rich glacial sediments of the Drente Formation, or loess (Van Huissteden et al., 1986a). In the latter cases the carbonate should have been derived also from older marine carbonate rocks in the source areas of these sediments.

Carbon-containing materials of various sources can be characterized by their ratio between the stable carbon isotopes ^{13}C and ^{12}C (Burleigh et al., 1984). Normally, this ratio serves to correct ^{14}C datings for isotope fractionation during formation of the material (Olsson & Osadebe, 1974). It is expressed as $\delta^{13}C$, given by

$$\delta^{13}C = \left[\frac{(^{13}C/^{12}C)_{sample}}{(^{13}C/^{12}C)_{PDB\ standard}} - 1 \right] \times 10^3\ {}^{o}/_{oo}$$

(e.g. Mook & Van de Plassche, 1986). The standard which is referred to in this formula is a belemnite of Cretaceous age. Marine carbonates have $\delta^{13}C$ values around $0^{o}/_{oo}$, while atmospheric CO_2, most land plants, wood, peat and humus have lower values (generally $< -20^{o}/_{oo}$).

source of material	nr. of samples	mean	minimum	maximum	range	standard deviation
peat	29	-28.09	-28.90	-26.86	2.04	0.51
unit DT3	7	-27.69	-28.43	-26.82	1.61	0.58

Table IX.3. $\delta^{13}C$ values from peat samples from the entire Dinkel valley compared with gyttja/peat samples from unit DT3 in the Tilligte detailed grid area (par. IV.4.1).

If during deposition of unit DT3 the vegetation assimilated CO_2 derived from older lime-rich material, the samples should show relatively high $\delta^{13}C$ values. However, table IX.3 shows that there is no significant difference between the gyttja/peat samples of unit DT3 and other peat samples in the Dinkel valley. Neither do the values deviate from those of peat samples, published by Olsson (1986). Higher $\delta^{13}C$ values, as occur in many gyttja samples in that publication, are not found in unit DT3, or in any other of the Dinkel valley samples. It is unlikely, therefore, that assimilation of old carbon derived from lime has influenced the dating results, in spite of the generally lime-rich nature of the sediment. CO_2 exchange between lakewater and atmosphere apparently occurred rapidly, to counteract any hard water effects which otherwise should have occurred in this lime-rich environment. The exchange of lakewater CO_2 with the atmosphere is promoted by the shallow depth of the lakes, and exposure to wind as shown by the frequently found wave ripples in the sediment (par. VI.2.4.1).

Nevertheless, several samples have been found which appear to be too old (par. IV.3-5, appendix 2). As dissolved older CO_2 has not been the cause of the deviating ages, there should have been other sources of older carbon in the lake represented by unit DT3 in the Tilligte detailed grid area. The alternative source is reworked older organic matter, transported into the lake by floodwater. For unit DT3, river flooding is confirmed by the palaeobotanical and sedimentological data (Ran, 1990; par. VIII.2.2.1). As unit DT3 is situated closely above erosion level II, it is not unlikely that a large amount of organic material has been derived from older deposits.

IX.3. Sedimentation rate during the Middle Pleniglacial.

Linear regression of the height above O.D. on the mean age of the samples provides an estimate of the sedimentation rate (table IX.4). Fig. IX.1 shows time-depth diagrams, constructed from the datings in appendix 1. Datings which are considered as unreliable, and datings of which the elevation might have been influenced by differential compaction at the basin edges have been excluded. The diagrams have been constructed for two separate areas, the Tilligte area (Tilligte section, SW part of the Laarhuis-Rammelbeek section) and the Denekamp area (southern parts of the Lattrop-Denekamp section, eastern part of Laarhuis-Rammelbeek section).

In the Denekamp-Lattrop area the scatter of the datings around the regression line is much larger than in the Tilligte area. This is caused by the presence of more pronounced fluvial incisions and the larger size of the area. For the Tilligte area the first order regression results in a slope coefficient of the regression line of -0.35, or a mean sedimentation rate of 0.35 mm/y. The sedimentation rate in the Denekamp-Lattrop area is lower: 0.16 mm/y. Also, sedimentation appears to have started at a somewhat higher level in this area. This difference between the two areas confirms the hypothesis of a gradual tilting of the basin in a western direction (par. VIII.2.2.4). This tilt has favoured a higher sedimentation rate in the more westerly locations, such as the Tilligte area. It also may have caused the more pronounced development of fluvial incisions associated with erosion level II in the more easterly Denekamp-Lattrop area.

In the Tilligte area a second degree regression fits significantly better. The resulting regression line shows a tendency of a decreasing sedimentation rate in the course of time, although the regression line itself may over-emphasize this effect, as it is checked by only a few datings in the upper and lower time ranges.

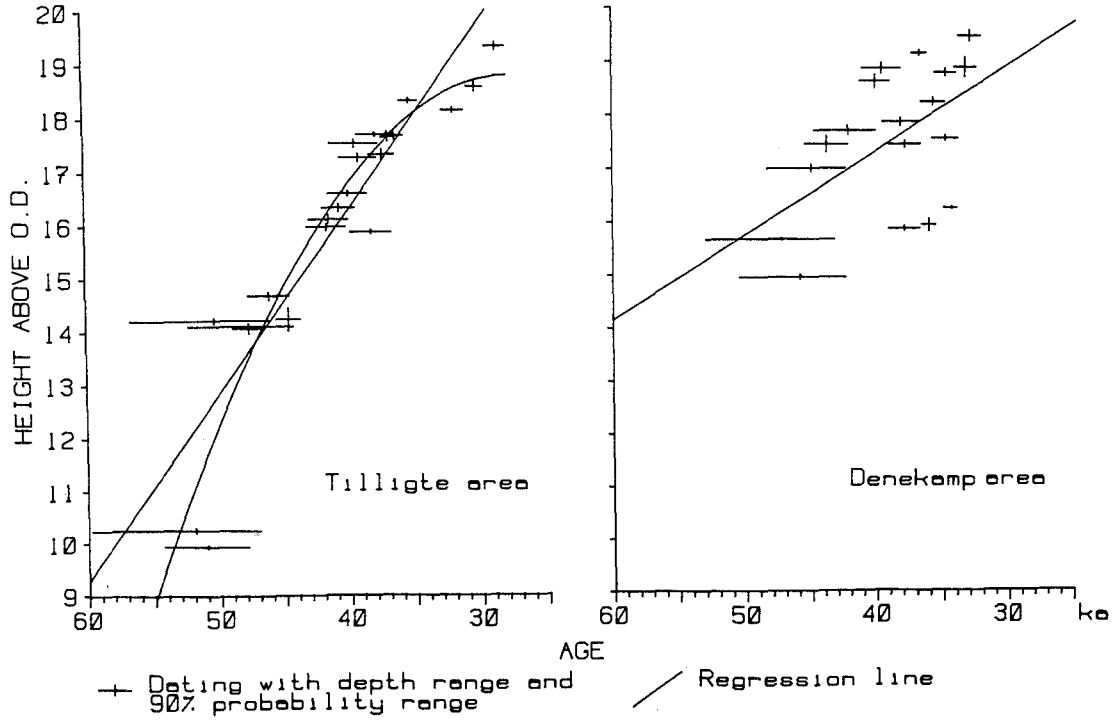

Figure IX.1. Time-depth diagrams derived from the radiocarbon datings in the borehole sections. Each dating is represented by a horizontal line, indicating the 90 % probability interval based on its standard deviation, and a vertical line representing the depth interval. Parameters from regression lines are listed in table IX.4.

parameters	Tilligte area (24 datings)	Denekamp/Lattrop area (20 datings)
1st degree regr.	D= 30.39 -0.35A	D= 23.63 -0.16A
2nd degree regr.	D= 8.29 +0.75A- 0.01A^2	D= 18.92-0.09A-0.003A^2
goodness of fit (1st)	0.83	0.32
goodness of fit (2nd)	0.90	0.33
F (regression)	103.90 (significant)	8.14 (significant)
F (quadratic addition)	12.23 (significant)	0.09

Table IX.4. Linear regression results of elevation above O.D. on the mean age of the samples. F test with 5% significance level. D = height above O.D. (m); A = mean age (ka).

IX.4. Distribution of datable material in time.

IX.4.1. Background and problems of radiocarbon dating distributions.

Van der Hammen et al. (1967) used the clustering of radiocarbon datings in certain time intervals to support the chronostratigraphical subdivision of the Middle Pleniglacial into three interstadials (Denekamp, Hengelo, Moershoofd Interstadials). It is assumed that climatic amelioration has been the cause of an increased deposition of datable organic material. Unfortunately only a small number of Middle Pleniglacial radiocarbon dates was available at that time, which precluded statistical analysis. At present the number of datings has considerably increased, and it is worthwhile to subject this dating population to further analysis.

The formation of many datable materials is determined by very specific edaphic conditions which are sensitive to environmental change. Such environmental changes may operate on a local scale only, for example avulsions on a river floodplain affecting a single floodbasin locality. Taken over a large area (comprising several river basins) the formation of datable material then will be randomly distributed in time. Alternatively, the formation of datable material may be affected by environmental processes operating in larger areas, for example climatic changes or tectonic movements. In that case the distribution of datable material in time is not random, and may show distinct peaks or gaps. A well known example is the effect of Holocene marine transgressions on peat formation in coastal sedimentation areas (e.g. Roeleveld, 1974; Geyh, 1980, Berendsen, 1984). Of more specific significance in this study is the dating of fluvial activity phases (Knox, 1975) and the dating of the Middle Pleniglacial interstadials (Van der Hammen et al., 1967; Geyh & Rohde, 1972).

Usually a histogram is compiled which shows the distribution of datings in an array of time intervals. Peaks or gaps in this histogram may indicate environmental change. Furthermore, peaks and gaps are introduced by fluctuations in atmospheric ^{14}C activity (Geyh, 1980). Sampling strategy is very important. Often more than one sample from the same layer in an exposure or borehole has been dated which will produce erratic peaks. Older, less well exposed stratigraphical levels may be under-sampled. Dating errors will tend to obscure any environmentally significant peaks or gaps. A population of samples which represent quite different sedimentary environments can have the same effect, since these environments may react in contrasting ways on climatic events.

The statistical significance of peaks and gaps in the histogram is a second problem. Peaks and gaps may be present also in a randomly distributed dating population, especially when only few datings are available (Shennan, 1979). The probability distribution of the number of randomly generated instantaneous events occurring within a certain time interval follows the Poisson distribution (Schwarzacher, 1975; Davis, 1986). Geological examples of instantaneous events are earthquakes or volcanic eruptions. If in those cases significant deviations from the Poisson distribution are found this can be taken as evidence for a non-random process.

Unfortunately radiocarbon datings cannot be considered as instantaneous events. A radiocarbon dating is represented by a normal probability distribution, with a not negligible standard deviation. When a distribution histogram of the datings is compiled this standard deviation should be accounted for. Considering older Middle Pleniglacial datings, the 90% confidence interval of the datings is of the same order of magnitude as the phenomena searched for (interstadials with a duration of a few thousand years). In this case the Poisson distribution (which is a discrete distribution) does not apply, although the resulting continuous distribution should have similar shape properties as the Poisson distribution.

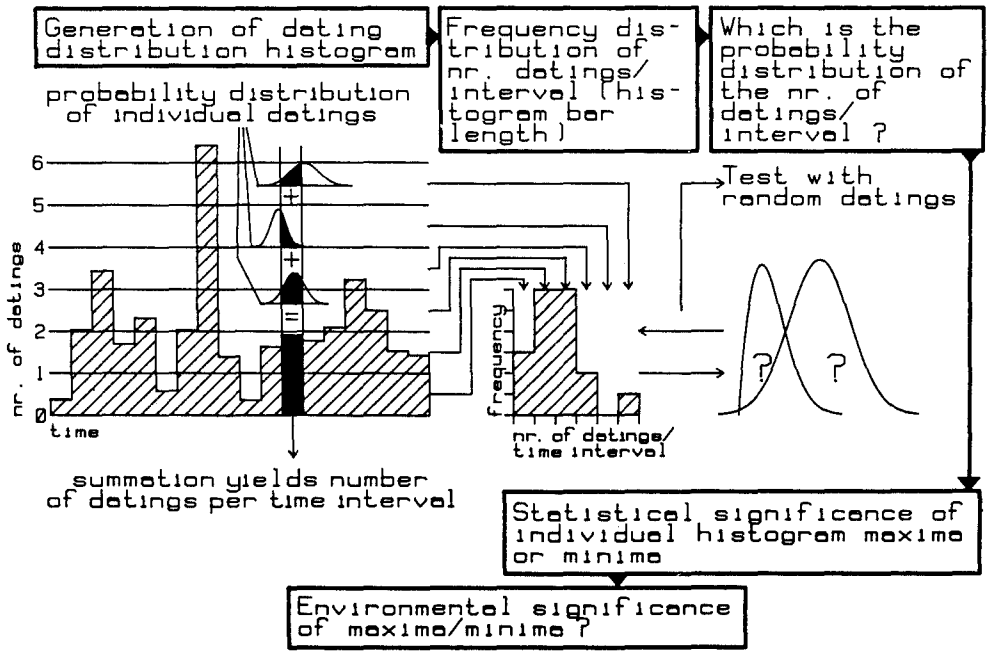

Figure IX.2. Outline of the statistical analysis of the radiocarbon dating distribution. The first step is compilation of the distribution histogram, by summing the contribution of each dating to each interval. This has been executed first with randomly generated datings. Next the frequency distribution of the histogram bar lengths has been determined. A comparison of this frequency distribution with gamma, Weibull, and normal probability distribution fits best to this frequency distribution. The probability distribution of the bar lengths in this histogram indicates the chance of occurrence of the extreme values in dating distribution histograms derived from real populations.

Much attention has been paid to the number of datings which is necessary to construct a dating distribution histogram (Shennan, 1979; Geyh, 1980). The latter author considered histograms with less than 4 datings per class interval as unreliable, as real gaps in the histogram cannot be distinguished from statistically generated gaps. In principle, however, even with a low density of datings it should be possible to evaluate at least the significance of the peaks in the histogram, if their probability distribution is known. Below a few probability distributions have been tested for their validity with the help of Monte Carlo simulations of dating populations. Next a radiocarbon dating

population from Northwest Germany, the Netherlands, and Belgium has been analyzed with the help of a suitable probability distribution. Fig. IX.2 shows schematically the steps taken in the ensuing statistical analysis.

IX.4.2. Quantitative analysis of the distribution of datable material throughout the Middle Pleniglacial.

IX.4.2.1. The probability distribution of the number of datings per time interval in a dating distribution histogram.

The probability that a dating occurs within a certain time interval is computed by integration of the associated normal (Gaussian) probability density function with mean μ (mean age of the sample), and σ (standard deviation), over the time interval under consideration. Let h_i be the sum of all datings occurring in the i-th interval of a dating distribution histogram. The lower and upper boundaries of the time interval i are respectively t_{i-1} and t_i. Then h_i can be computed by

$$h_i = \sum_{j=1}^{N} \int_{t_{i-1}}^{t_i} f(u,\sigma_j,\mu_j)\,du \qquad (1)$$

where N is the total number of datings taken into consideration, and f(u) is the normal probability density function of dating number j with parameters σ_j and μ_j. The integral is calculated using an iterative algorithm (e.g. Press et al., 1986). In practice it is not necessary to integrate all N datings over all intervals, since the contribution of a dating to h_i with a mean age far outside a interval is negligible. The quantity h_i/N is the chance of finding datable material in the interval.

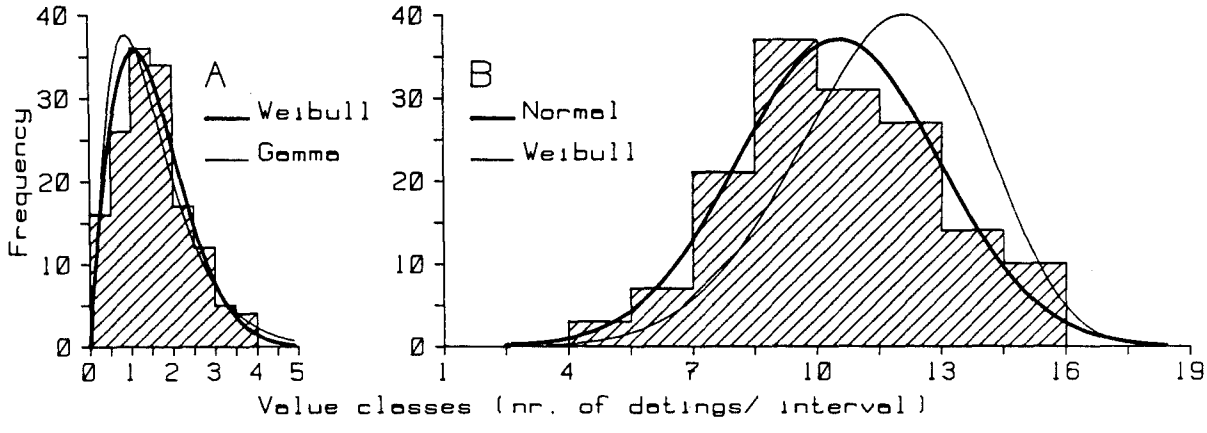

Figure IX.3. Frequency and probability distributions of the histogram bar length (number of datings / time interval, h_i) in dating distribution histograms. A: Gamma and Weibull distributions, fitted to results of 15 simulation runs of 30 random datings (time range 30 - 45 ka, interval width 1 ka). B: results of the same experiment as A, now with 200 datings in each simulation run. Normal and Weibull distributions are fitted. See table IX.5 for distribution parameters.

The probability distribution of all h_i's in the histogram should be known to evaluate whether a peak or gap in the histogram is significant or not. Following Shennan (1979), simulation experiments with randomly generated datings have been carried out (fig. IX.2,3). To approach a realistic dating population also the standard deviation of each dating has been generated at random, taking into account the tendency of standard deviations to become larger with higher age. A linear relation has been assumed between the mean age and standard deviation, with parameters determined by a linear regression of standard deviation on mean age of a set of real datings. At ages over 40 ka the standard deviation increases more rapidly with age than at lower ages, as is usual with real datings.

From the randomly generated datings distribution histograms have been compiled, and used to test which probability distributions best describe the variation of h_i. Fig. IX.3 shows the results for two different simulation experiments. A set of 15 simulations with a low number of datings (30) and a high number (200) has been run. The simulated datings have ages between 28 and 47 ka, distribution histograms have been computed for a range of 30 to 45 ka, with an interval width of 1 ka. Because of the large standard deviation at higher ages, the peaks and gaps in the distribution histograms tend to be much less pronounced then at low ages. Therefore, in a first approach only the range between 30 and 40 ka has been used for testing probability distributions.

Testing the fit of a certain probability distribution to the observed data is achieved by determining the frequency distribution of the observed h_i values, and comparing these with the expected frequencies computed from the theoretical probability distribution. A chi-square test can be used to determine whether the two deviate significantly (Davis, 1986).

Simulation experiment	Distribution	Distribution parameters		Chi-square value (5 degrees of freedom)
		μ b	σ (normal) c (Weibull, gamma)	
200 datings	Normal	10.506	2.421	2.896
	Weibull	11.485	5.458	14.229
30 datings	Weibull	1.696	1.817	2.761
	Gamma	0.674	2.378	8.099

Table IX.5. Results of probability distribution fitting to the numbers of datings per histogram interval, arising from random dating generation experiments. b and c are scale and shape parameters of the Weibull and gamma distributions, analogous to μ (mean) and σ (standard deviation) of the normal distribution.

As noted in the previous paragraph randomly generated instantaneous events lead to a Poisson distribution, and the distribution which is generated by real radiocarbon datings should have similar properties. If the expected number of events per interval is high, the normal distribution is a good approach of the Poisson distribution. Indeed, in the case of 200 randomly genera-

ted datings, the h_i's prove to follow a normal distribution fairly closely (fig. IX.3B, table IX.5). The chi-square value in table IX.5 is well below the 10% rejection level.

The choice of a probability distribution for cases with a low number of datings per time interval is more critical. A Poisson probability density function is a strongly skewed or continuously decreasing function for a low number of datings per interval. Continuous probability density functions with the same shape properties are those of the gamma and Weibull distributions. The gamma distribution has been applied in several geological and geographical problems, mainly in cases where distances between successive points are involved (e.g. bed thickness distributions: Schwarzacher, 1975; distance between boundaries on soil maps: Burgess & Webster, 1984). The Weibull distribution is often applied as a failure rate distribution in industrial quality control (Johnson & Kotz, 1970). Bridge & Leeder (1979) have applied it as a distribution of avulsion rate in a computer simulation of fluvial deposition. Both the gamma and Weibull probability density functions are characterized by a scale parameter (b) and a shape parameter (c). The range of both probability density functions is $0 \leq x \leq +\infty$, and the density functions are given by:

Gamma:
$$f(x) = \frac{(x/b)^{c-1}\,[\exp(-x/b)]}{b\Gamma(c)} \qquad (2)$$

where $\Gamma(c)$ is the gamma function with parameter c:

$$\Gamma(c) = \int_0^{\infty} \exp(-u)\,u^{c-1}\,du \qquad (3)$$

Weibull:
$$f(x) = (cx^{c-1}/b^c)\exp[-(x/b)^c] \qquad (4)$$

The parameters b and c from (2) and (3) can be estimated with the help of mean and variance of the observed h_i values. In practice these are less accurate estimators, since the distributions are strongly skewed. Maximum likelihood estimation performs better; procedures are described by Johnson & Kotz (1970) and Burgess & Webster (1984).

In the case of 30 randomly generated datings the distribution of h_i indeed proves to be skewed (fig. IX.3A). Both the gamma and Weibull distributions fit adequately, none yielding significantly high chi-square values (table IX.5). The Weibull distribution appears to approach more accurately the distribution of h_i than the gamma distribution, as shown by the considerably lower chi-square value in table IX.5. The fit appears to be especially better with respect to the mode and right hand tail of the distribution. The difference between gamma and Weibull is even more conspicuous if the age range of the dating distribution histograms is extended towards higher ages, where the effect of higher standard deviations reduces the variation of the h_i's. In that case the gamma distribution has to be rejected while the chi-square value of the Weibull distribution still remains below the 10% significance level. In case of a high number of datings

per interval the normal distribution in turn fits better than the Weibull distribution (table IX.5).

Consequently, the probability distribution of the number of datings/interval (h_i) of the dating distribution histograms can be approximated by a normal distribution if the mean number of datings per interval is sufficiently high (the mean of h_i should be higher than 3 x its standard deviation). If the expected number of datings per interval is considerably lower, the Weibull distribution is a good approximation.

IX.4.2.2. Analysis of Middle Pleniglacial datings from the Netherlands, Belgium and Northwest Germany.

As will be shown below, fluctuations in the formation of peat have occurred during the Middle Pleniglacial. However, these fluctuations do not coincide with the classical Middle Pleniglacial interstadials (Denekamp, Hengelo and Moershoofd Interstadials).

To obtain a well documented population of Middle Pleniglacial radiocarbon datings, the radiocarbon dating database of the Groningen University Isotope Physics Laboratory has been consulted. A number of 246 datings on Middle Pleniglacial sediments has been selected. Further selection could be carried out with respect to dated material, laboratory treatment, sample location, and presence/absence of an extract dating. Dating distribution histograms have been calculated for a time range of 25 to 55 ka, subdivided into 30 intervals with a width of 1 ka.

A first test includes all datings which have received an alkali-acid-alkali treatment. This excludes the datings which may have the strongest contamination errors. The resulting histogram is displayed in fig. IX.4A. Most datings concentrate between 27 and 45 ka, and further discrimination between periods of increased and reduced peat growth is poor.

Statistical evaluation of the histograms has been restricted to the interval where most datings occur (27-45 ka). The distribution of the number of datings in each interval (h_i) does not deviate significantly from a normal distribution. In the histogram of fig. IX.4A minima or maxima with less than 10 % chance of occurrence are found between 27-28, 38-39 ka and 41-42 ka.

To illustrate the environmental significance of such peaks, the histogram of fig. IX.4A should be compared with a histogram compiled from 212 randomly generated datings (fig. IX.4B; table IX.6). This histogram shows two peaks, one which even exceeds the 99 % probability level. Table IX.6 shows the range of distribution parameters derived from five simulated dating distributions (212 datings, time range 27-55 ka). The histogram of fig. IX.4B is selected from these because of close resemblance of its distribution parameters with those of the histogram of fig. IX.4A. The mean h_i of the histogram of the real datings is somewhat higher than the mean obtained from the simulations, due to the concentration of datings in the range of 30-45 ka of the real dating population. The standard deviations are comparable.

Non-random fluctuations in the production of datable material during the Middle Pleniglacial cannot be detected in the histogram of fig. IX.4A. Only a larger scale trend is visible (few datings <27 ka and >45). The strong decrease of datable material after ca. 27 ka should have been caused by generally unfavourable

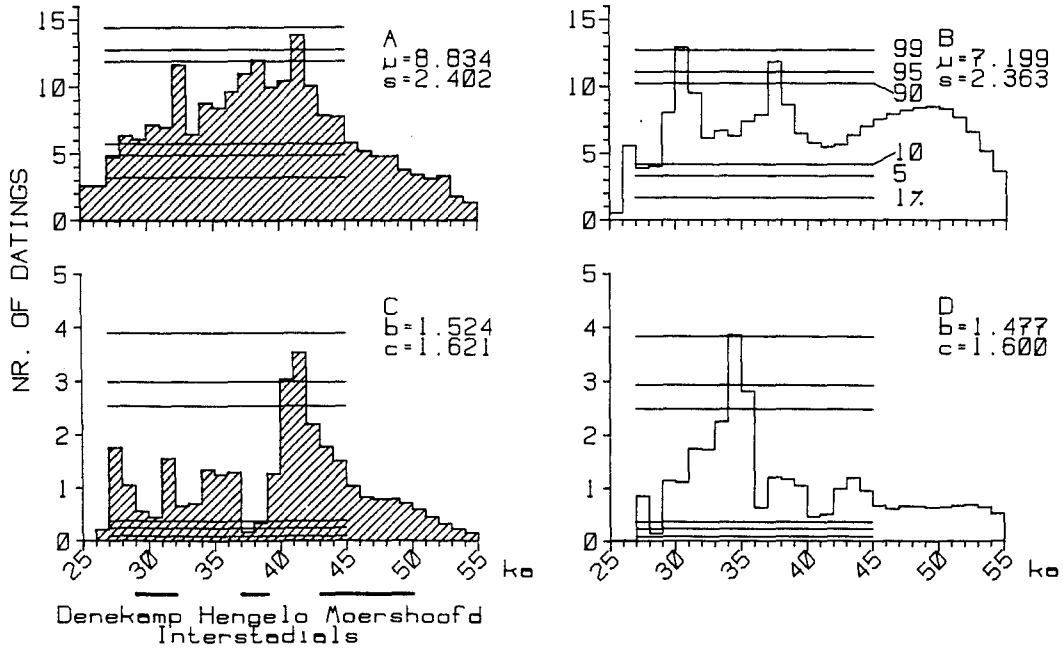

Figure IX.4. Dating distribution histograms. The time range of 27 to 45 ka has been subjected to further analysis. The hatched histograms (A, C) have been derived from real dating populations. Histogram A represents 212 datings on various Middle Pleniglacial sediments from Belgium, the Netherlands and NW Germany. Histogram C is a further selection from the datings of A (see text). The blank histograms (B, D) represent random simulations with the same numbers of datings as A and C. The horizontal lines in each histogram indicate 1, 5, 10, 90, 95 and 99 % probability levels as derived from the respective probability distributions of the nr. of datings/time interval for each histogram. μ and s are parameters of normal probability distribution, b and c parameters of Weibull distribution. For the A and C histograms the ages of Middle Pleniglacial interstadials according to Van der Hammen et al. (1967) have been indicated.

Nr. of datings	Distribution parameters				Distribution
	minimum μ or b	maximum μ or b	minimum σ or c	maximum σ or c	normal (μ,σ) Weibull (b,c)
212	6.891	7.552	1.652	2.363	normal
31	0.951	1.477	1.957	1.595	Weibull

Table IX.6. Probability distribution parameters of 5 random simulations of the real dating populations (212 resp. 31 datings, time range 27-55 ka). Compare with fig. IX.4A,C for the distribution parameters obtained from the real dating populations.

environmental conditions for the accumulation of organic sediment during the Late Pleniglacial (Van der Hammen et al., 1967; par. III.3.3.4). Also the number of datings in the time range of 27-32 ka (the Denekamp Interstadial) is rather low. This is probably caused by the erosion phase at the end of the Middle Pleniglacial (par. III.3.3.4). The low availability of datable material before

45 ka may be caused by under-sampling of the older, generally deeper levels, and the exclusion of infinite ages. Nevertheless, an environmental origin for this lack of older datings cannot be excluded, as the high sedimentation rates at the start of the Middle Pleniglacial (par. IX.3, V.3) will tend to reduce organic matter deposition by dominance of clastic deposition.

Part of the datings in the previous population may be erroneous, due to one of the error sources listed in table IX.2. Furthermore the type of sediment which has been dated varies, and, consequently, the relation of the dated events with environmental changes is not uniform. A further selection is necessary which is subjected to the following conditions:
- a uniform type of material, preferably peat, to ensure a consistent relation of sedimentary environment with climate;
- extract datings of the samples do not deviate substantially from the residue datings;
- further indications of erroneous dating results (based on evaluation in literature, or stratigraphical inconsistencies) are absent;
- datings on comparable depth levels in borings or exposures should be spaced at a certain distance from each other, to avoid over-representation of certain levels due to sampling schemes.

The latter criterion applies especially to a number of datings from the Tilligte area, where some layers have been sampled and dated with borehole distances of less than 100 m. In general peat beds in the borehole sections cannot be traced over distances longer than a few hundred meters. This suggests that a distance between samples of 500 m should be sufficient to avoid over-sampling of a single peat bed. The first criterion (material) proved untenable and yielded a too low number (22) of datings. In practice the Middle Pleniglacial organic deposits show all kinds of intergrades between different types (peat, gyttja or peaty/humic silts); furthermore, different sample collectors may give diverse descriptions of these materials. When besides peat samples reliable datings on other peaty deposits are included a number of 31 datings remains, located in the Netherlands and Belgium. Gyttjas have been excluded.

From these 31 datings the histogram of fig. IX.4C has been compiled. The interval values (h_i) of the range 27-45 ka follow a Weibull distribution with scale and shape parameter as indicated in fig. IX.4C, which is confirmed by a chi-square test. Also the shape parameter (c) of the Weibull distribution is comparable to those of distributions compiled from 31 random datings (table IX.6). An illustrative example of these simulated dating populations is fig. IX.4D. Analogous to the set of 212 datings, the scale parameter (b) of the real dating population deviates somewhat from the simulated datings, again due to concentration of the datings between 30-45 ka. Based on the distribution type the process by which the real population of 31 datings has been generated, cannot be distinguished from a random process.

Nevertheless, four extreme h_i values are present which have a low (<10%) chance of occurrence, while three of these have a probability of less than 5%. Strikingly, these extreme values occur in a time range where the subduing effect of large standard deviations of the datings is noticeable. The binomial probability for the occurrence of this number of extreme values in 18 intervals is less than 10%. Moreover, the arrangement of the extreme values is not very likely to be random. Maximum values

occur between 40 and 42 ka, closely followed by minimum values between 37 and 39 ka. Apparently, non-random fluctuations in the formation or preservation of peat occur between 37 and 42 ka.

As yet, evidence for atmospheric ^{14}C concentration variations during the Pleniglacial is fragmentary, and does not extend beyond 40 ka. Barbetti (1980) and Vogel (1983) present evidence for considerable fluctuations between 29 and 35 ka. The increase of atmospheric ^{14}C concentration between 29 and 35 ka assumed by Vogel (1983) should be capable of producing a cluster of radiocarbon datings around 29 ka. This is not detected in the histogram by a significantly high peak. The histogram minima/maxima between 37 and 39 ka are probably not caused by atmospheric ^{14}C fluctuations; on the other hand, the sedimentary sequence offers further evidence of an environmental origin.

The minimum between 37 and 39 ka conforms well with the age of erosion level II in the Dinkel valley and the thaw lake formation in the Hengelo A1 exposure, shortly after a period of ice wedge growth. Most likely the diminished peat formation indicates a period of floodplain instability and fluvial incision. Deposition of organic matter did occur during that time span, but has been restricted mainly to clastic or lacustrine environments (datings from humic silts and gyttjas mask the 37-39 ka minimum in fig. IX.4A). The occurrence of permafrost degradation at the same time shows that reduced peat growth has not necessarily been caused by cold climatic conditions.

The high number of datings between 40 and 42 ka also may be related to palaeo-hydrology. Higher temperatures, favouring organic matter deposition are less likely. Data compiled by Lieth (1975) suggest only a very minor increase of primary production of organic matter within the range of temperature variation which may be expected during the Middle Pleniglacial. On the contrary, presence of ice wedge casts closely above the 39-41 ka peat in the Hengelo A1 exposure suggest that the climate may have been colder than average. Indications of soil calcification closely above this peat (par. VI.2.1) and palaeobotanical data (Ran et el., 1990) also indicate fairly dry climatic conditions. A dryer climate, especially with lower winter precipitation, should have led to lower flood discharges. This may have promoted extension of semi-terrestrial areas with peat growth at the expense of regularly flooded sites with predominant clastic sedimentation. Establishment of a permafrost table with formation of ground ice, causing frost heave should have had a similar effect, which might have been most effective in northerly locations. The extension of peat formation appears to be restricted mainly to the northeastern Netherlands, with a concentration in the Twente area (Ran, 1990).

From the present data it appears that the classic Denekamp, Hengelo and Moershoofd stadials do not show a significantly high number of radiocarbon datings. The comparison of the extremes of the dating distribution with sedimentological data rather suggests a link of datable material formation with palaeo-hydrological changes, as could have been expected from a mainly fluvial environment. Furthermore, peat growth has been determined strongly by local edaphic factors.

X. The Dinkel Valley in the Middle Pleniglacial: dynamics of a tundra river system.

by Eva T.H. Ran and J. (Ko) Van Huissteden.

X.1. Synthesis of the palaeo-environment of the fluvial system during the Middle Pleniglacial in the Twente region.

In this section the results of the sedimentological, geomorphological, and palaeoecological studies (Van Huissteden, this volume; Ran, 1990) have been integrated. A palaeo-environmental model for the Middle Pleniglacial alluvial sequence is constructed for the Dinkel Valley. This sequence is compared with other European sequences to place the results of the Dinkel valley project in a wider context.

In the time interval from c. 60,000 to 26,000 B.P. alternating layers of sand, silt, peat and gyttja have been deposited in the Dinkel valley. The sands are predominantly of fluvial origin. Along the valley sides of the Dinkel valley upstream of Denekamp locally also a fluvio-aeolian facies has been found, which consists partly of (fluvially reworked) aeolian sand. In general however, the river system is characterized by extensive floodbasins with peat and silt deposition, alternating with sandy crevasse splay deposits. Especially in the glacial basins, these overbank deposits form most of the sedimentary sequence, while coarse-grained channel deposits are of comparatively small extent. The river system has been an anastomosing system within the glacial basins, while in higher gradient valley parts it may have tended towards meandering rivers in the sense of Rust (1978).

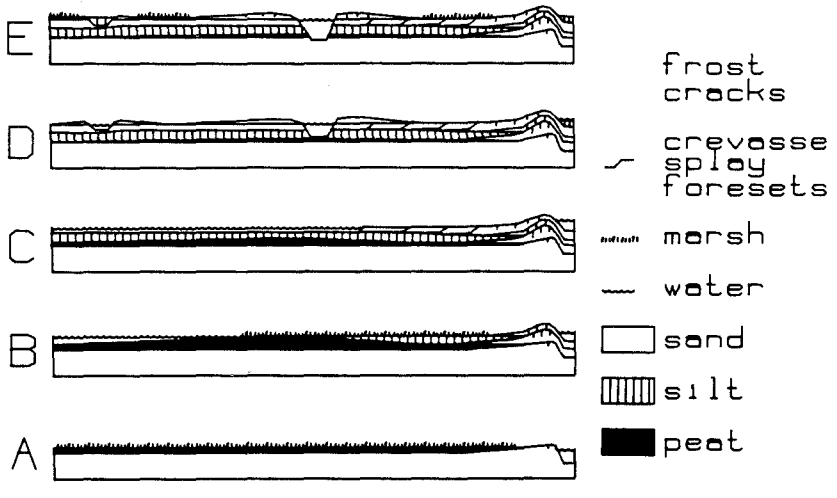

Figure X.1. A tentative reconstruction of floodbasin depositional cycles in the Middle Pleniglacial fluvial deposits. A. Initiation of floodbasin; peat growth starts on stabilized crevasse splay surface. B. Floodbasin drainage is restricted by levee development, extension of open water environments. C. Elevation difference between channel belt and floodbasin promotes crevasse splay development and clastic deposition. D. Crevasse splay development grades into avulsion. E. 'Reversion' stage of avulsion; multiple crevasse splay channels evolve into a single channel. Crevasse splay surfaces are stabilized and peat growth starts.

The river system tends to generate typical coarsening-upward sequences which may be stacked above each other (fig. X.1). These sequences consist at their base of peat, which grades upward into silts, overlain by crevasse splay deposits and eventually channel sands. A cyclic mechanism appears to be present within the system. Floodbasin formation starts as soon as sand supply in an area of the floodplain is reduced, for instance by channel displacement (avulsion) or channel stabilization ('reversion' stage after crevasse splay/avulsion development; Smith et al., 1989). Sedimentation starts with peat growth in a semi-terrestrial environment (fig. X.1A). Aggradation takes place preferably along and in the channels, restricting the drainage of the floodbasins. The floodbasins will show a tendency towards lake development (fig. X.1B). The balance between floodbasin and channel belt sedimentation is restored by crevasse splay expansion (fig. X.1C). The crevasse splays in the Middle Pleniglacial deposits may show typical delta-like foresets, indicating propagation into shallow floodplain lakes. Eventually, when crevasse splay channels evolve into a new channel belt the crevasse splay development may grade into an avulsion (Smith et al., 1989; fig. X.1D). When the floodbasin is filled in with crevasse splay sands, the sequence can start again (fig. X.1E).

This general cyclic mechanism, derived from sedimentological data and sequence analysis, is confirmed when palaeobotanical and sedimentological data are compared. Detailed grainsize and sedimentary structure analysis from the Lattroperstraat 1 palaeobotanical section shows a clear relation between sediment properties and vegetation in the floodbasin - crevasse splay environments (fig. X.2). In palaeobotanical zone I, the gradual transition from a moist terrestrial habitat towards a shallow pool coincides with an increase of the amount of sand. The fine and fairly well sorted sand is probably of a waterlaid origin, deposited by low energy currents. The site apparently has been protected from high energy flow, but not to the extent that silt-size material could settle during floods. When the sediment supply is cut off, the material changes from sand to peat. In the second zone indicators for running water (e.g. *Rheocricotopus*) occur together with coarser sand fractions, indicating that the site has been flooded regularly. Ponding has been sufficiently long to allow settling of fines together with coarser material. The return from peat towards clastic material corresponds to an increase of the sedimentation rate, confirmed by the lower pollen concentration values in this zone. In zone III thin sand beds are interbedded within the silty sediment. The coarse grainsize of the sand may point to rapid deposition, probably representing single flooding events. In these coarser layers moss remains are very rare. Moss remains are most abundant in layers with a higher silt content. Obviously, bryophytes thrive in relatively calm conditions with standing water, as is confirmed by the presence of aquatic elements in the vegetation. In the fourth and fifth zones more sand has been deposited and lamination is well preserved, pointing to an increased sedimentation rate of clastic material. The grainsize distributions show a significant increase in current velocity during flooding. Intercalated silt layers represent still-water phases between floods.

Altogether the sequence indicates an increasing clastic sedimentation rate and decreasing protection from rapid current flow during flooding of the site. This is reflected by the general

coarsening upward trend and by the organic matter content of the sediment, which decreases above zone I. During periods with a high clastic sedimentation rate most of the local vegetation growth has been inhibited. Especially mosses cannot establish themselves during these periods, but they return as soon as the sedimentary environment becomes less dynamic.

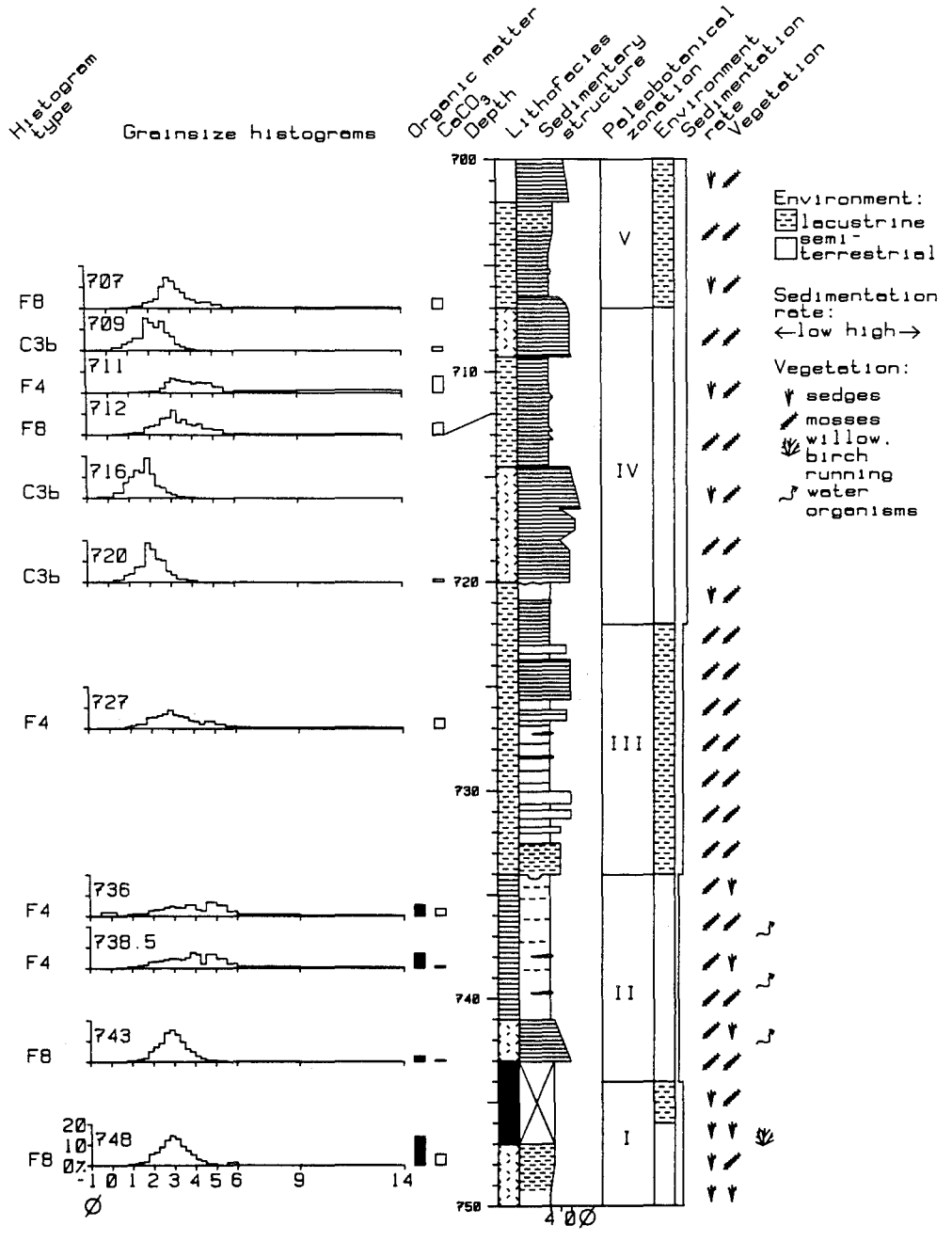

Figure X.2. Detailed log of Lattroperstraat core between 700 and 750 cm below surface. Legend for representation of sedimentary structures in fig. VI.2 (Van Huissteden, this volume). Grainsize histogram type cf. Van Huissteden (this volume), palaeobotanical zonation cf. Ran (this volume).

In all other palaeobotanical sections similar relations exist between vegetation and minerogenic sediment. In the Witstaartweg I section the site gradually becomes wetter throughout the depo-

sit. This corresponds with an increase in the silt content of the sediment. The length of the sequence points to an extraordinary prolonged absence of important clastic sediment influx. At the top of the section this influx is restored and local vegetation growth eventually is interrupted. The Vlierweg section represents a flood basin, which is colonized after its establishment by a sedge marsh vegetation. After a certain period with comparatively slow clastic sedimentation the water level rises and standing water dominates. Thereafter, clastic sedimentation rate increases and finally sand deposition takes over. In borings 526 and 527 (Tilligte detailed grid area) moist to aquatic habitats coincide with calcium-rich gyttja deposition. When the sedimentation rate slows down gyttja is deposited; with increasing sedimentation rate sand deposition dominates. When the amount of algae shows the presence of standing open water the silt content of the sediment increases.

Differences in lithology are not always accompanied by marked differences in vegetation, but are related to sedimentation rates, as derived from pollen concentrations. Concentration values are highest in the organic sediments, where the average is about 60 times as high as in the sandy sediments. This implies that sand sedimentation occurs much more rapidly than sedimentation of peat and gyttja.

The importance of the influence of the sand deposition on the local vegetation growth is also shown by the mathematical analyses of the palaeobotanical sequences. The amount of sand deposition is the first gradient along which the samples are subdivided. The second important gradient appears to be the groundwater level. Along that axis three positions become clear dependent on the level of the groundwater table: one with the groundwater table below the surface, the second with the groundwater table at the surface, and with the third, the groundwater table has been above the surface. When the groundwater table has been below the surface a dry variant of the order of Tofieldietalia with many Juncaceae occurs, when the groundwater table has been at the surface the optimum for the Tofieldietalia has been established and a diverse vegetation of Cyperaceae, Gramineae, and bryophytes occurs. In between these variants a third variant of the Tofieldietalia exists, intermediate in position between the mathematically distinguished extremes. In the phases where open water has been found Potametea communities thrive.

Generally, the floodbasin environment is to be characterized as semi-terrestrial to shallow lacustrine. Among the macro-remains indicators for running water have been recorded regularly. This is confirmed by the frequent occurrence of small amounts of sand in the fine-grained beds. The dominance of the silt and clay fractions, and absence of running water sedimentary structures implies that running water must have been episodic, related to high stage flooding. The fact that flooding is revealed by the local occurrence of faunal elements which depend for their life cycle on running water during summer periods, is a very important clue to river regime. It shows that inundations apparently could occur during the growing season, and have not been restricted to nival floods in early spring. This means that it has probably not been a strictly nival discharge regime. Summer rainstorms therefore, may have been common.

The vertical sequence in all cores agrees well with the model of floodbasin evolution outlined above. At the base of the se-

quence clastic sedimentation is reduced. The top of all organic levels is characterized by a well defined transition to open water, accompanied or followed by higher clastic influx. This is reflected by lithologic changes to silty sediment, usually followed by sand sedimentation. The vegetation appears to be inundated by a rise of the water level in the floodbasin, which marks the onset of renewed clastic sedimentation. The transition towards sand sedimentation usually is a gradual process. Even with a sharp transition towards overlying sand, the vegetation development in the floodbasin already announces the oncoming changes. Eventually, rapid clastic sedimentation may lead to a return towards a terrestrial environment.

Locally the vegetation does not seem to respond primarily to a change in temperature, but seems dependent on the water and sediment discharge of the nearby river system, which in turn may depend on climatic change. When flooding activity of the local river channel increases, sedimentation of sand also rises. This sand deposition, together with a rise in the water level often has brought an end to local marsh vegetation growth. When there has been only a temporary rise in water level or occasional flooding of the area, the vegetation changes from dry-marshy to marshy-aquatic.

Most of the plants identified grow in rosettes, as cushions, are creepers or have woody stems. Many plants keep their winter buds at or just below the ground surface. These adaptations point to the severity of the climate, as most of these plant forms at present occur in the shrub tundras, tundras, and polar deserts of the Arctic. Also the coleopteran community points to the presence of a relatively severe climate in an open environment. Thus, during the Middle Pleniglacial the landscape of river plains in The Netherlands consists of an arctic tundra to shrub tundra vegetation.

This vegetation consists only of herbs and shrubs, trees have not been present. Today the tree limit approximately follows the 10° C July isotherm. The mean summer temperature during the Middle Pleniglacial has been at or near 10° C. Kolstrup & Wijmstra (1977) explain the absence of trees in the Middle Pleniglacial deposits as effects of, 1. migration time (during stadials the forest refugia occur far to the south; it will take a long time for trees to migrate northwards), and 2. a too windy climate.

A vigorous wind regime is indicated by the presence of a fluvio-aeolian facies in some parts of the Dinkel valley, an important loessic component in the floodbasin silts, and other indications of frequent eolian reworking derived from grainsize analysis and grain surface texture. The wind regime might have been effective in higher parts outside the river plain, but probably the rapidly changing environment of the river system prevented the local establishment of trees on the floodplain as well. Migration however, is also an important limiting factor.

Figure X.3 (next page). Temperature and precipitation curves of Les Echets and Grande Pile (after Guiot et al., 1989); arboreal pollen/herbaceous pollen ratio of Grande Pile (after Woillard & Mook, 1982); temperature curves for the Netherlands (period 26-20,000 B.P. after Kolstrup, 1980, 60,000 B.P. after Zagwijn & Paepe, 1968); extension of peat/gyttja formation in the Netherlands (Ran, 1990).

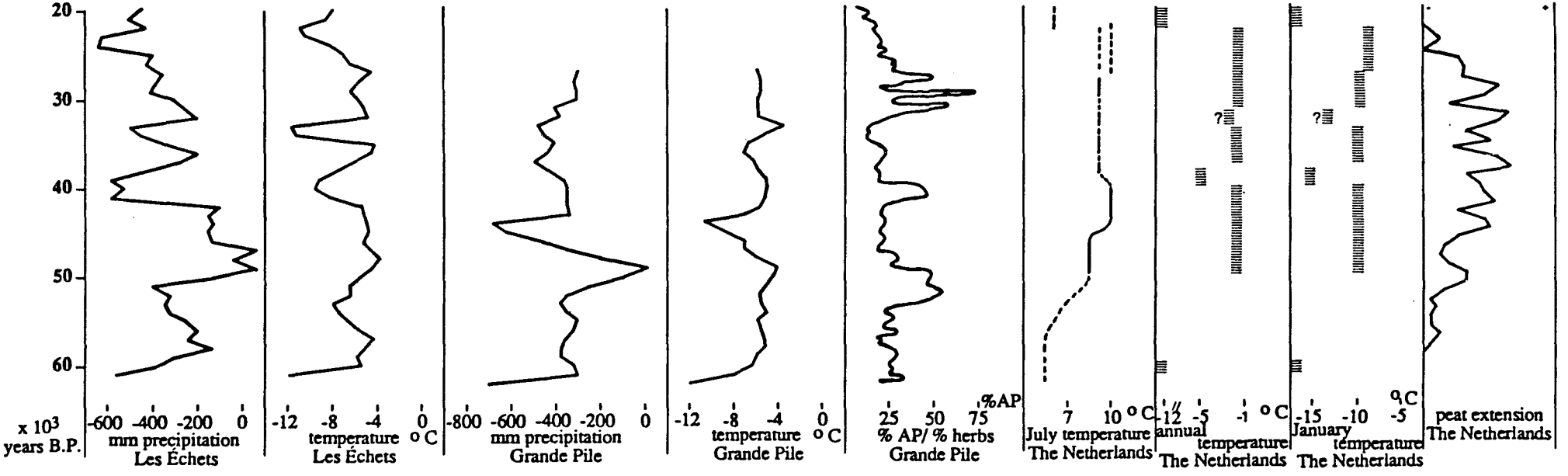
20
30
40
50
60
x 10³ years B.P.
-600 -400 -200 0
mm precipitation Les Échets
-12 -8 -4 0
temperature °C Les Échets
-800 -600 -400 -200 0
mm precipitation Grande Pile
-12 -8 -4 0
temperature °C Grande Pile
25 50 75 %AP
% AP/ % herbs Grande Pile
7 10 °C
July temperature The Netherlands
-12 -5 -1 °C
annual temperature The Netherlands
-15 -10 -5 °C
January temperature The Netherlands
peat extension The Netherlands

During the cold period preceding the Middle Pleniglacial, and during the coldest phases of the Middle Pleniglacial itself, the tree limit probably lay south of the Pyrenees. In the intervening warmer intervals the tree limit has moved north of the Alps and Vosges Mountains, but does not reach Belgium. Between c. 32,000 and 26,000 B.P. the tree limit obviously reaches northern France, as for Grande Pile a considerable expansion of the amount of tree pollen has been recorded (fig. X.3). From deposits in the Flemish valley a sparse tree cover has been recorded, thus indicating the tree limit has been shifted as far north as Belgium. However, the tree limit has remained south of the Netherlands.

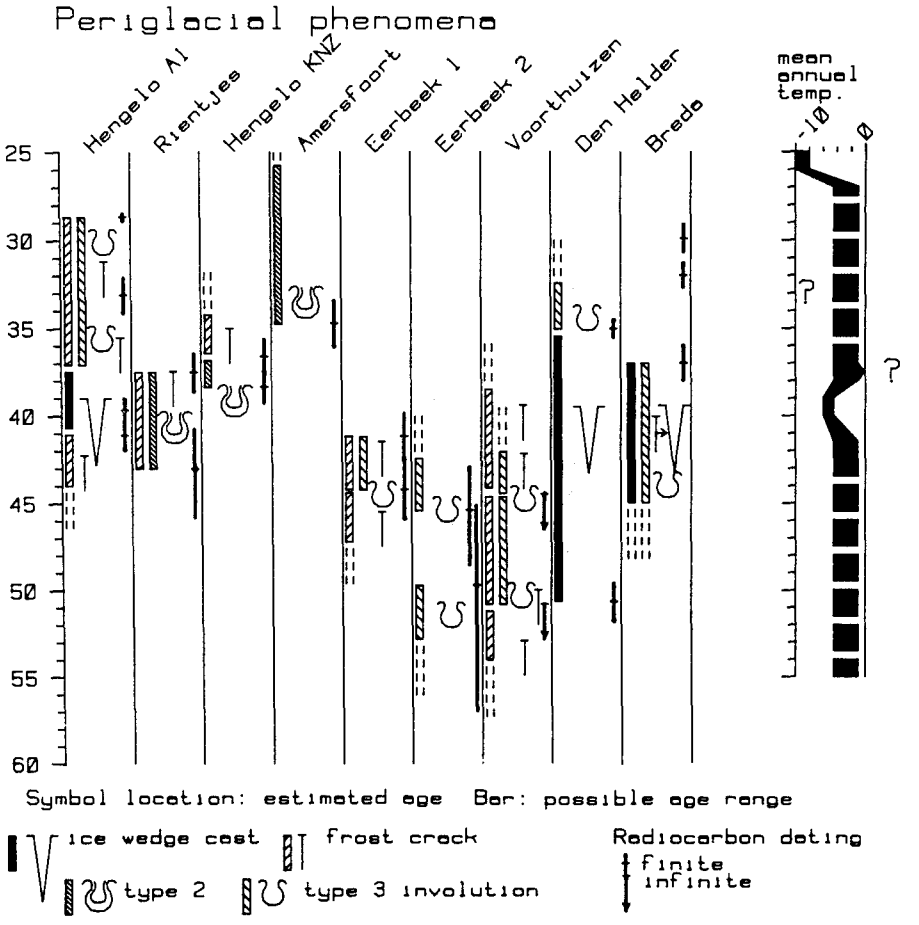

Figure X.4. Summary of dated Middle Pleniglacial periglacial phenomena in the Netherlands. The last column indicates estimate of mean annual temperature range derived from these phenomena. Classification of involutions cf. Vandenberghe (1988). Literature on the depicted sites: Hengelo A1 (This publication); Rientjes (Vermeij & Heukeshoven, 1973; Zagwijn,1974; De Jong, pers. comm.); Hengelo KNZ (Zagwijn, 1974); Amersfoort (Zagwijn, 1961); Eerbeek 1 (Van der Meer et al., 1984); Eerbeek 2 (Kolstrup & Wijmstra, 1977); Voorthuizen (Ruegg, 1971); Den Helder (De Mulder, undated; Ruegg, 1978); Breda (Van der Hammen et al., 1967; photos provided by Dr. Zagwijn).

Periglacial phenomena provide additional information on the climatic conditions in the Netherlands. Fig. X.4 summarizes dated Middle Pleniglacial periglacial phenomena from this study and several other publications. Two types of cryoturbatic involutions

have been distinguished, type 2 and 3 of Vandenberghe (1988). Type 2 are large involutions which probably form during degradation of continuous permafrost. Type 3 involutions are smaller features which do not require permafrost for their formation. Fissure structures have been subdivided into small fissures (< 10 cm wide) and ice wedge casts which show evidence of the former presence of an infilling with ice (see also par. VI.1, Van Huissteden, this volume). Only those phenomena have been displayed of which a Middle Pleniglacial age is likely.

The sedimentological data from the Hengelo A1 exposure indicate that frost cracks and type 3 involutions appear to occur preferably on higher parts of the Middle Pleniglacial alluvial plains (crevasse splay and levee surfaces). The common occurrence of well developed frost cracks in most Middle Pleniglacial sequences (fig. X.4) shows that at least frequently climatic conditions during the Middle Pleniglacial have not been marginal for thermal contraction cracking. Temperatures have been at least regularly well below the upper limit for their formation. It is assumed that mean annual temperatures between -1° and -4.5° C have been common during the Middle Pleniglacial. Temperature limits for the formation of the type 3 involutions cannot be given; their often flat-bottomed base suggests the common presence of a deeply frozen subsoil or a permafrost table during their formation. The present amount of data does not allow to delineate periods of more intense formation of frost cracks or involutions.

The ice wedge casts in the Hengelo basin appear to be restricted to silty deposits and indicate mean annual temperatures below -4.5 °C (par. VI.2.3, Van Huissteden, this volume; Ran et al., in press). Reports of well developed Middle Pleniglacial ice wedge casts in coarse sand are unknown. Ice wedge casts of similar age as those in the Hengelo basin possibly occur at Den Helder and Breda (fig. X.4). These casts have been developed in silty material as well. There is no proof that mean annual temperature has been lower than the -6° C required for ice wedge formation in sands.

The thaw lake formation and type 2 involutions in the Hengelo basin do not necessarily point to very strong climatic warming. The permafrost degradation may have been activated by fluvial erosion. Nevertheless, other consistent ice wedge cast levels appear to be absent immediately above the thaw lake deposit, therefore it is likely that the thaw lake development marks a return to a somewhat warmer climate. An upper temperature limit cannot be given. The occurrence of frost fissures closely above the associated erosion level in the Rientjes clay pit indicates that temperatures most likely remained below -1° C. Besides, from the cold climatic oscillation around 39,000 B.P., indisputable indications of permafrost are lacking. Only at Amersfoort type 2 involutions (younger than 34,000 B.P.) have been found of which a Middle Pleniglacial age cannot be excluded (fig. X.4).

The presence of ice wedge casts in one period and only frost cracks in other periods is not only an effect of precipitation variations. It must be attributed to changes in mean annual temperature as well. When the frost features have been only an effect of relatively low amounts of precipitation, the vegetation cover as a whole would have been more sparse and more taxa indicative of severe cold would have been recorded during the entire Middle Pleniglacial.

Clearly, important characteristics of the Middle Pleniglacial environment in the Netherlands are the common occurrence of frost crack polygons, episodic permafrost conditions, ample precipitation to maintain widespread lacustrine and marshy conditions on the river floodplains, and presence of a tundra/shrub tundra vegetation. These characteristics compare well with the subpolar-oceanic periglacial region as distinguished by Karte (1979) in his subdivision of the present-day periglacial zone. Comparable present-day areas occur in western Alaska, the Labrador peninsula, and tundra lowlands in the northern U.S.S.R. west of the Urals. During colder episodes a shift towards the polar tundra periglacial region (Karte, 1979) with a more continental and colder climate may have occurred.

Karte (1979) summarizes the climate of the subpolar-oceanic periglacial areas as a climate with short, cool and wet summers. Mean annual temperatures range between -1° and -6° C, mean temperature of the warmest month is below 10° C, mean temperature of the coldest month above -15° C. Mean annual precipitation exceeds 400 mm, most of which is snow. With respect to denudation processes, gelifluction and slopewash should have been prominent.

Despite the apparent occurrence of flooding during the growing season, most prominent and frequent overbank flooding should have been caused by the spring snowmelt discharge. Climatic parameters which determine its magnitude are the amount of winter precipitation and snowmelt rate (Church, 1988). Blocking of part of the floodplain channels by snowdrifts or ice further enhances the importance of overbank deposition. It is likely therefore, that the Middle Pleniglacial fluvial system has been most sensitive to changes in the amount of winter precipitation.

Large scale changes in fluvial facies are absent during the Middle Pleniglacial. Clearly, the changes have not been of sufficient magnitude to induce important changes in fluvial morphology. Responses of the fluvial system to external variables are complex, and geomorphological thresholds may have been present, which external forces must exceed before changes occur (Schumm, 1981). As shown above, the Middle Pleniglacial fluvial system itself is capable of producing a cyclical repeating series of sand, peat and silt without a clear relation to climate. Drastic variations in sediment yield or evapotranspiration are unlikely since only minor changes in vegetation types occur. The most secure indicators of a climatic event are phenomena observed in more than one valley system or basin. Features of the Middle Pleniglacial fluvial sequence which can be used for palaeohydrologic interpretation are indications of change in aggradation or erosion. These are:

- erosion levels (possibly pointing to an increase of discharge with respect to sediment yield);
- sedimentation rate as deduced from radiocarbon datings;
- sediment petrographical indications of more intense erosion of the drainage basin substratum;
- time distributions of fine-grained floodbasin deposits and peat (decrease of fine-grained floodbasin deposits indicates decrease of floodplain stability by either more frequent crevasse splay deposition and avulsion, or erosion).

Three erosion levels have been recorded in the Middle Pleniglacial sequence of the Dinkel valley (fig. X.5). Level II is also found in the Hengelo basin, which is therefore most likely of climatic origin. Sedimentation rate has been highest during

the early parts (> 40,000 B.P.) of the Middle Pleniglacial. Presence of detrital siderite in heavy mineral spectra of the Middle Pleniglacial deposits points to rapid substratum erosion. It occurs mainly in beds older than c. 40-50,000 B.P., both in the Dinkel valley and the Hengelo basin.

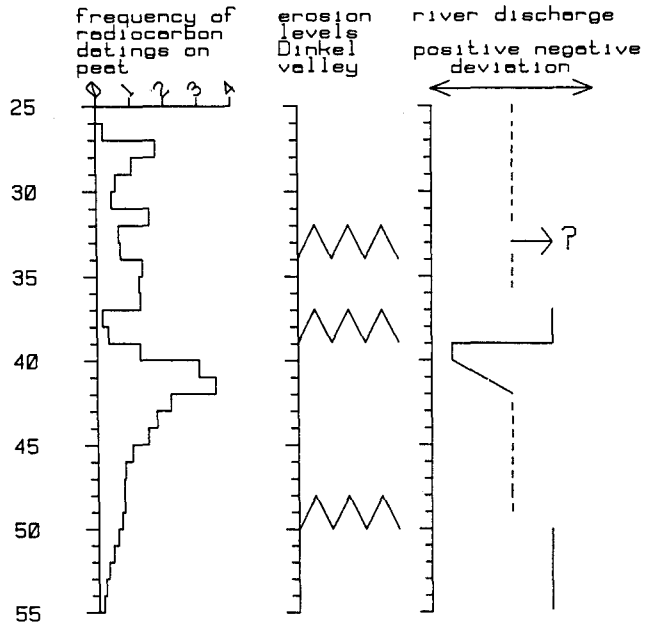

Figure X.5. Estimated changes of palaeo-discharge of the rivers in the Twente region, derived from erosion levels and peat growth maxima. Dashed lines in leftmost column indicate lack of data from fluvial sequence.

Combination of these data leads to the palaeohydrological sequence in fig. X.5. Only a qualitative indication of positive and negative deviations can be given. Before 50,000 B.P. indications of high substratum erosion and basin sedimentation rate coincide with a lake dominated low gradient river plain in the Dinkel valley (basal clays of the Middle Pleniglacial sequence). To maintain a low gradient river under conditions of high sediment yield, discharge should have been relatively high as well. Erosion level I is only known from the Dinkel valley, where it is associated with a shift of drainage direction within the basin; its relation to climate is possible, but uncertain. Next, a period of general floodplain stability can be deduced from a significant increase of peat formation between 42- and 40,000 B.P (fig. X.5). This is attributed to a decreasing discharge, which leads to less frequent flooding and clastic deposition in floodbasin environments. Indications of relatively dry climatic conditions have been found during the permafrost episode between 40,000 and 39,000 B.P. (Van Huissteden, this volume; Ran et al., in press). Erosion level II points to a general increase of discharge in the Twente area after 39,000 B.P. It has been confirmed by palaeobotanical data which indicate thicker snowcover in deposits overlying erosion level II (Ran et al., in press). The development of erosion level II may have been enhanced by permafrost degradation. Erosion level III has been found in the Dinkel valley only. However, it coincides with a (low significance) minimum in the distribution of radiocarbon datings. A clima-

tic change which influenced the discharge / sediment yield balance therefore cannot be excluded.

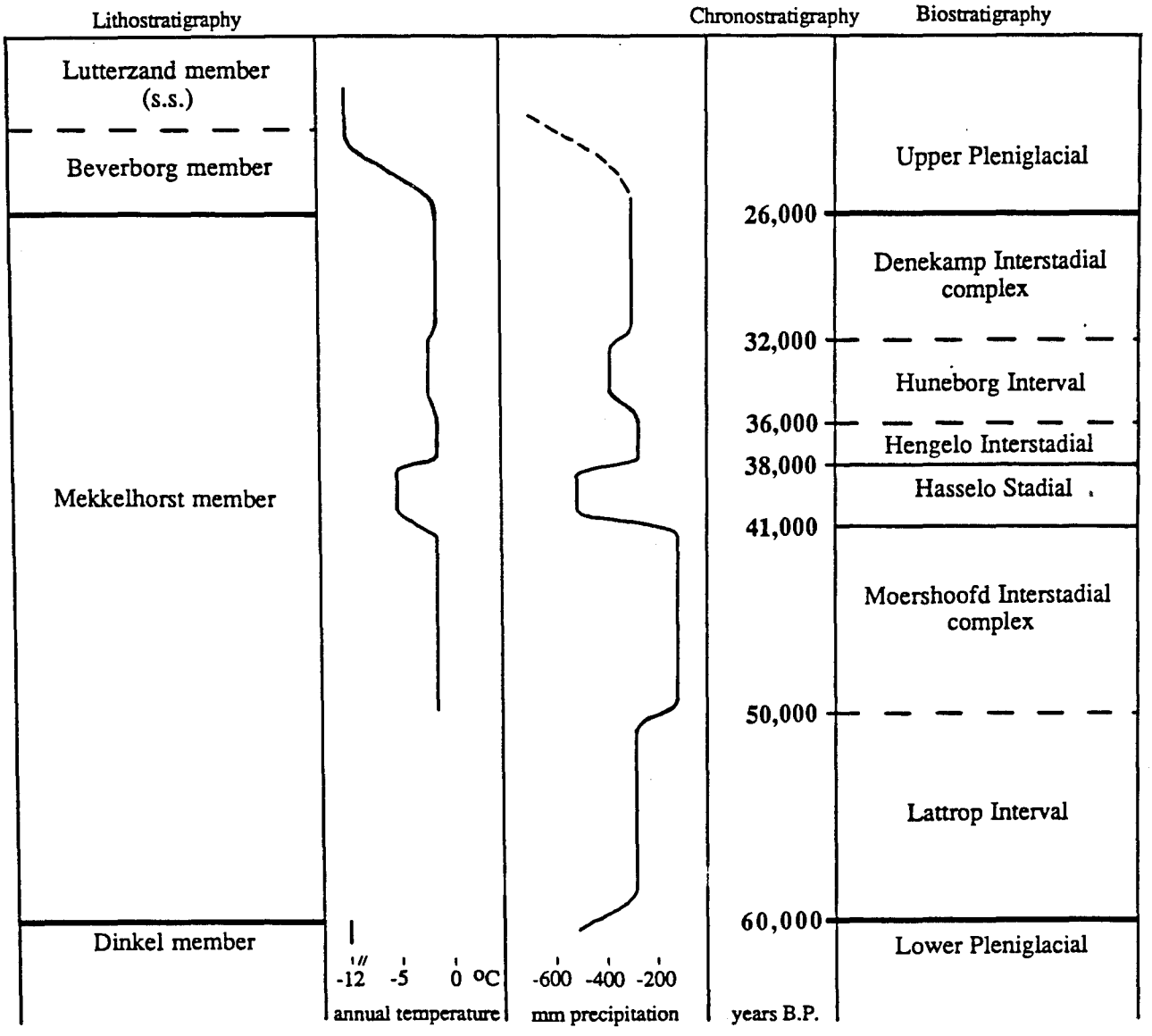

Figure X.6. Mean annual temperature, estimated precipitation and chronostratigraphy of the Middle Pleniglacial for the Netherlands.

To place the results obtained for the Dutch Middle Pleniglacial in a broader context the temperatures curves (chap. VIII.2, Ran) and the curve for the extension of peaty deposits in different sedimentation basins (chap. IV.3, Ran) have been compared with the temperature and precipitation curves of les Echets and Grande Pile (from Guiot et al., 1989) and with the arboreal pollen/herbaceous pollen ratio from Grande Pile (from Woillard & Mook, 1982). In Fig. X.3 these curves are combined. The climate during the Middle Pleniglacial has been relatively cold throughout Europe. In The Netherlands, July temperatures may have reached 10° C, but mean annual temperatures remained below 0° C. The present mean annual temperature of The Netherlands is around + 9° C indicating that compared with today the temperature had fallen at least 9°. Data on precipitation are difficult to collect from palaeobotanical studies. Deuterium analysis needs further investigation before it can be used as a temperature - precipitation

indicator, and at any event the data have been obtained from a fluvial system through which changes in precipitation are recorded indirectly. However, as fig. IV.7 (Ran, 1990) has shown the area frequency shows the same tendency as the frequency of ^{14}C numbers. This implies some overall ruling system, because the peat formation obviously is not only a local effect.

Although with lower precipitation than today, the climate does not seem to have been very dry. Precipitation probably has been considerably higher than during full glacial periods, and mostly lower than at present, but in combination with the lower temperatures the effective precipitation could have been relatively high. Guiot et al. (1989) reconstructed temperature and precipitation values for the French continental records of Grande Pile and Les Echets. At Les Echets two cold periods can be recognized within the Middle Pleniglacial, one around 40,000 B.P. and an even colder one dated around 33,000 B.P. At Grande Pile the first cold period is dated around 44,000 B.P. and a second but lesser colder period is dated around 36,000 B.P.It seems very likely that this first cold period at Grande Pile corresponds with that around 40,000 B.P. as recorded in Les Echets and The Netherlands, and that the second cold period corresponds with the cold interval of c. 33,000 B.P. The peak in the arboreal pollen/herbaceous pollen ratio around 42-41,000 B.P. has been correlated with the Hengelo Interstadial (Woillard & Mook, 1982). However, in that case this optimum should be placed in time around 38,000 B.P., which is very likely as also the cold periods seem to have been dated too old. At Les Echets and Grande Pile very cold stadial conditions appear to coincide with very dry conditions. Based on the changes in precipitation in Les Echets and Grande Pile, as calculated by Guiot et al. (1989), precipitation values for The Netherlands have been estimated. The tentative precipitation curve is given in Fig. X.6 together with the mean annual temperature and the chronostratigraphy. The precipitation values are expressed as differences to present-day precipitation values. The colder periods in western Europe around 40,000 - 39,000 B.P. and 34,000 - 33,000 B.P. also have been drier than the periods in between.

The precipitation and temperature estimates derived from the Les Echets and Grande Pile sequences match quite well with the climatic fluctuations which can be derived from the sequence in the Twente region. The cold and dry interval between 39,000 and 40,000 B.P. in the Netherlands is recognized also at Les Echets. A possible moist oscillation between 34,000 and 32,000 B.P. derived from erosion level III in the Dinkel valley possibly correlates with a high precipitation interval at Les Echets around 32,000 B.P. An extremely high precipitation interval between 50,000 and 47,000 B.P. at Les Echets may correlate with a probable high discharge period in the same time range, which has led to erosion in the Dinkel valley. The cold interval between 33,000 B.P. and 34,000 B.P. appears as yet to be less well represented in the Netherlands.

Time series analysis of the data on the peat extension in The Netherlands revealed a cycle of approximately 2,900 years, while the same analysis of the precipitation and temperature data of les Echets revealed a cycle of 3,000 years. With the uncertainty of 14C dates it is obvious that the recorded cycles are of the same magnitude of c. 3,000 years. This implies that the peat extension probably follows a climatic course. However, only a few

individual peaks or gaps in the dating distribution reach statistically significant levels which distinguishes them from random fluctuations. At a local level this climatic effect is obscured by dynamism of the river systems like in the Dinkel Valley. However, on a broader European scale, climate and vegetation appear to follow a cycle of 3,000 years.

The Lattroperstraat 2 section belongs to the Late Glacial period. The features recorded from micro- and macro-remains analysis show that deposition of organic material in the initial part of the Late Glacial (c. 12,885 B.P. see Chap.IV.3, Ran) has started in circumstances comparable to environmental conditions of the Middle Pleniglacial. However, after the start of the Late Glacial the climate improves further than in earlier phases and finally this has led to the formation of forests, and the transition to the Holocene.

X.2. Chronostratigraphy of the Middle Pleniglacial.

As shown above, climatic fluctuations appear to be expressed in the Middle Pleniglacial fluvial sequence in the Netherlands. In the vegetation the climatic fluctuations have resulted in small changes from tundra to shrub tundra vegetation types. These fluctuations have not been of sufficient magnitude to alter the fluvial system significantly. The fine-grained or organic beds represent common floodbasin deposits, which may have formed during colder as well as warmer episodes, although a statistical correlation between climate and peat formation appears to be present. Precipitation changes leading to increase of spring snowmelt discharge have left most imprint on the fluvial sequence. Next, a colder episode proves to be well recognizable in the fluvial sequence, as it has been registered by permafrost growth and decay features, and a decrease of shrub tundra vegetation in favour of more open tundra vegetation.

The episodes of higher temperature fluctuations and relatively high precipitation correspond in age to the previously defined interstadials Moershoofd, Hengelo, and Denekamp. However, the results presented here indicate that refinement of the subdivision is justified, especially with respect to the colder episodes. It appears that permafrost growth and decay have a relatively profound impact on the fluvial sequence. The chronostratigraphical subdivision of the Middle Pleniglacial as suggested here is presented in figure X.6.

At the base of the sequence the Lattrop interval has been distinguished. It starts at the beginning of the Middle Pleniglacial (c. 60,000 B.P.) and terminates at c. 50,000 B.P. Stratigraphically it coincides with the period of deposition of the basal clays in the Dinkel valley. It is uncertain whether this period should be characterized as stadial or interstadial. It has been generally warmer than the preceding Lower Pleniglacial, but cooler than the following Moershoofd Interstadial complex. It is even possible that within this period fluctuations of interstadial magnitude may have taken place (e.g. Riel Interstadial, Vandenberghe, 1985; Glinde Interstadial, Behre, 1989).

The Moershoofd Interstadial complex (49-41,000 B.P.) starts with an erosion phase in the Dinkel valley, which terminates deposition of the basal clays. The term 'complex' is necessary because of possible presence of several oscillations. Vegetation ranges between tundra and shrub tundra. The climate has become

warmer and much wetter than before. Mean annual temperature has remained below -1° C. Based on the Les Echets/Grande Pile data, it probably has been the period with the highest precipitation during the Middle Pleniglacial. In the last phase of this period a transition towards a colder and drier climate takes place.

The Hasselo Stadial (40-38,000 B.P.) is recorded as an ice wedge cast level in silty sediments, indicating mean annual temperatures between -4.5° and -6° C. Precipitation values have been very low, it appears to have been the driest period of the Middle Pleniglacial. Its definition is based on the Hengelo A1 exposure, near the village of Hasselo (Van Huissteden, this volume; Ran et al., in press).

The Hengelo Interstadial (38-36,000 B.P.) starts with a general erosion phase pointing to a return towards a moister climate. Mean annual temperature remains below 0° C. Precipitation values as derived from the French sequences have been lower than during the Moershoofd Interstadial complex. Vegetation ranges between tundra and shrub tundra.

The Huneborg interval (36-32,000 B.P.) has been distinguished for several reasons. At Les Echets this period has been very cold and dry, even colder than the Hasselo stadial.The period appears to be terminated by an erosion phase in the Dinkel valley, possibly analogous to the transition from the Hasselo Stadial to the Hengelo Interstadial. Precipitation values as derived from the French sequences indicate a relatively dry period. The term 'interval' is preferred, because some uncertainties still exist with regard to its climatic evolution. Further investigations should clarify if this period really is a 'stadial' phase or represents only a minor fluctuation. In the latter case it might be preferable to place it together with the Hengelo and Denekamp Interstadials into one interstadial complex. Its definition is based on the sections in the Tilligte basin (near the Huneborg site), where beds of this age and the overlying erosion level are found and dated.

The Denekamp Interstadial complex (32-26,000 B.P) starts after the erosion phase of the Huneborg interval. Mean annual temperature remains below 0°, precipitation values have been nearly as high as during the Hengelo Interstadial. Vegetation varies between tundra and shrub tundra. The term 'complex' is based on the presence of three fluctuations in peat extension, and increase of shrubs in the Netherlands (Zagwijn, 1974), and large oscillations in arboreal pollen/herbaceous pollen ratio in Grande Pile.

Despite its nature (climatically relatively insensitive fluvial deposits with hiatuses, in a tundra/shrub tundra environment) it is possible to use the fluvial sequence in the Dinkel valley as a model for chronostratigraphical subdivision of the Middle Pleniglacial within comparable environments. Especially the periglacial phenomena from the cold interval of the Hasselo Stadial, and the overlying erosion features and thaw lake deposits may prove to be fairly general features, also in sequences outside the Twente region. It should be stressed however, that the fluvial palaeo-environment in the Twente region has remained relatively similar during the Middle Pleniglacial. Further investigations in other sedimentary basins are necessary to support this subdivision. Especially investigations in more southern located areas with more marked vegetation changes might prove to be more profitable for this purpose.

References.

AELMANS, F.G. (1974): Grondwaterkaart van Nederland schaal 1:50.000. Geohydrologische toelichting bij kaartbladen 28 oost Almelo, 29 Denekamp, 34 oost Enschede en 35 Glanerbrug. Dienst Grondwaterverkenning T.N.O., Delft, 46 pp.

ALLEN, J.R.L. (1970): Studies in fluviatile sedimentation: a comparison of fining upwards cyclothems, with special reference to coarse member composition and interpretation. Journal of Sedimentary Petrology 40-1, p. 298-323.

ALLEN, G.P., P. CASTAING, A. KLINGEBIEL (1972): Distinction of elementary sand populations in the Gironde estuary (France) by R-mode factor analysis of grain-size data. Sedimentology 19, p. 21-35.

ANDERSEN, S.V., H.L. DE VRIES, W.H. ZAGWIJN (1960): Climatic change and radiocarbon dating in the Weichselian Glacial of Denmark and the Netherlands. Geologie en Mijnbouw 39, p. 38-42.

ANTONOV, V.S., V.V. IVANOV, Y.V. NALIMOV (1972): Types of breakup of rivers in Siberian arctic and subarctic zones. In: The role of snow and ice in Hydrology. Proc. of the Banff Symposia, Intern. Assoc. of the Hydrological Sci./W.M.O. Vol. I, p. 541-546.

ARNBORG, L., WALKER, H.J., PEIPPO, J. (1966): Water discharge in the Colville river. Geografiska Annaler 48A, p. 195-210.

AVERDIECK, F.R. (1967): Die Vegetationsentwicklung des Eem-Interglazials und der Früh-Würm-Interstadiale von Odderade, Schleswig-Holstein. Fundamenta (Monographien zur Urgeschichte), Reihe B 2, p. 101-125.

AXELSSON, V. (1967): The Laitaure delta - a study of deltaic morphology and processes. Geografiska Annaler 49A-1, 127 pp.

BAAK, J.A. (1936): Regional petrology of the southern North Sea. Ph. D. Thesis, State University Leiden, 127 pp.

BARBETTI, M. (1980): Geomagnetic strength over the last 50,000 years and changes in atmospheric ^{14}C concentration: emerging trends. Radiocarbon 22-2, p. 192-199.

BEHRE, K.E. (1989): Biostratigraphy of the Last Glacial period in Europe. Quaternary Science Reviews 8-1, p. 25-44.

BEHRE, K.E., U. LADE (1986): Ein Folge von Eem und 4 Weichsel-Interstadialen in Oerel / Niedersachsen und ihr Vegetationsablauf. Eiszeitalter und Gegenwart 36, p. 11-36.

BERENDSEN, H.J.A. (1984): Quantitative analysis of radiocarbon dates of the perimarine area of the Netherlands. Geologie en Mijnbouw 63-4, pp. 343-350.

BISSCHOPS, J.H. (1973): Toelichtingen bij de Geologische kaart van Nederland 1:50.000, blad Eindhoven Oost (51O). Rijks Geologische Dienst, Haarlem, 132 pp.

BLACK, R.F. (1969a): Thaw depressions and thaw lakes, a review. Biuletyn Peryglacjalny 19, p. 131-150.

BLACK, R.F. (1969b): Climatically significant fossil periglacial phenomena in northcentral United States. Biuletyn Peryglacjalny 20, p. 225-238.

BLACK, R.F. (1976): Periglacial features indicative of permafrost. Quaternary Research 6, p. 3-26.

BOENIGK, W. (1983): Schwermineralanalyse. Ferdinand Enke, Stuttgart, 158 pp.

BOIGK, H., C. DIETZ, H.O. GRAHLE, K. HOFFMANN, W. HOLLSTEIN, F. KÜHNE, W. RICHTER, H. SCHNEEKLOTH, R. WAGER (1960): Zur Geologie des Emslandes. Beihefte Geolisches Jahrbuch, Heft 37, 419 pp.

BOWEN, D.Q. (1978): Quaternary Geology. Pergamon Press, New York, 221 pp.
BRIDGE, J.S. (1981): Hydraulic interpretation of grainsize distributions using a physical model for bedload transport. Journal of Sedimentary Petrology 51-4, p. 1109-1124.
BRIDGE, J.S. (1984): Large-scale facies sequences in alluvial overbank environments. Journal of Sedimentary Petrology 54-2, p. 583-588.
BRIDGE, J.S., M.R. LEEDER (1979): A simulation model of alluvial stratigraphy. Sedimentology 26, p. 617-644.
BRINKKEMPER, O., B. VAN GEEL, J. WIEGERS (1987): Palaeoecological study of a Middle-Pleniglacial deposit from Tilligte, The Netherlands. Review of Palaeobotany and Palynology 51, p. 235-269.
BROWN, A.G. (1985): Traditional and multivariate techniques in the interpretation of floodplain sediment grainsize variations. Earth Surface Processes & Landforms 10-3, p. 281-292.
BROWN, J.E. (1973): Depositional histories of sand grains from surface textures. Nature 242, p. 396-398.
BRYANT, I.D. (1982): Periglacial river systems: ancient and modern. Unpublished Ph. D. thesis, University of Reading.
BRYANT, I.D. (1983): The utilization of arctic river analogue studies in the interpretation of periglacial river sediments from southern Britain. In: Gregory, K.J. (ed): Background to paleohydrology. Wiley, Chichester, p. 413-431.
BURGESS, T.M., R. WEBSTER (1984): Optimal sampling strategies for mapping soil types. I. Distribution of boundary spacings. Journal of Soil Science 35, p. 641-654.
BURLEIGH, R., K. MATTHEWS, M. LEESE (1984): Consensus $\delta^{13}C$ values. Radiocarbon 26-1, p. 46-53.
BURN, C.R., M.W. SMITH (1988): Thermokarst lakes at Mayo, Yukon Territory, Canada. Proc. Vth International Conf. on Permafrost, Trondheim, Norway, August 2-5, 1988, p. 700-705.
BUTRYM, J., J. CEGLA, S. DZULYNSKI, S. NAKONIECZNY (1964): New interpretation of 'periglacial structures'. Polska Acad. Nauk Oddzail in Krakowie, Folia Quaternaria 17, 34 pp.
CAMPBELL, C.V. (1967): Lamina, laminaset, bed and bedset. Sedimentology 8, p. 7-26.
CANT, D.J., R.G. WALKER (1976): Development of a braided fluvial facies model for the Devonian Battery Point sandstone, Quebec. Canadian Journal of Earth Sciences 13, p. 102-119.
CARR, T.R. (1982): Log-linear models, Markov chains and cyclic sedimentation. Journal of Sedimentary Petrology 52-3, p. 905-912.
CHAMBERS, R.L., S.B. UPCHURCH (1979): Multivariate analysis of sedimentary environments using grain-size frequency distributions. Mathematical Geology 11-1, p. 27-43.
CHURCH, M. (1974): Hydrology and permafrost with reference to North America. In: Permafrost Hydrology, Proceedings of Workshop Seminar, Canadian National Committee, p. 7-20.
CHURCH, M. (1977): River studies in Northern Canada: reading the record from river morphology. Geoscience Canada 4-1, p. 4-12.
CHURCH, M. (1988): Floods in cold climates. In: Baker, V.R., R.C. Kochel, P.C. Patton (eds): Flood Geomorphology. Wiley, New York, p. 205-231.
CLARK, M.J. (1988): Periglacial hydrology. In: M.J. Clark (ed.): Advances in periglacial geomorphology. Wiley, Chichester, p. 415-462.
CLARK, M.W. (1976): Some methods for statistical analysis of multimodal distributions and their application to grain-size data. Mathematical Geology 8-3, p. 267-282.

COLBY, B.R., C.H. SCOTT (1965): Effects of water temperature on the discharge of bed material. U.S. Geological Survey Professional Paper 462-G, 25 pp.
COLLINSON, J.D. (1978): Vertical sequence and sand body shape in alluvial sequences. In: Miall, A.D. (ed): Fluvial sedimentology. Canadian Society of Petroleum Geologists Memoir 5, Calgary, p. 85-89.
COLLINSON, J.D., D.B. THOMPSON (1982): Sedimentary structures. George Allen & Unwin, London, p. 194.
COOPER, R.H., A.B. HOLLINGSHEAD (1973): River banks erosion in regions of permafrost. In: Fluvial processes and sedimentation. Proc. Hydrology Symposium no. 9, University of Alberta, Edmonton, p. 272-283.
CRAIG, P.C., P.J. MCCART (1975): Classification of stream types in Beaufort Sea drainages between Prudhoe Bay, Alaska, and the Mackenzie delta, N.W.T., Canada. Arctic and Alpine Research 7-2, p. 183-198.
CROMMELIN, R.D. (1964): A contribution to the sedimentary petrology and provenance of Young Pleistocene coversand in The Netherlands. Geologie en Mijnbouw 43, p. 389-402.
CULVER, S.J., P.A. BULL, S. CAMPBELL, R.A. SHAKESBY, W.B. WHALLEY (1983): Environmental discrimination based on quartz grain surface textures: a statistical investigation. Sedimentology 30, p. 129-136.
DAHLSKOG, S. (1966): Sedimentation and vegetation in a Lappland mountain delta. Geografiska Annaler 48A-2, p. 86-101.
DAVIS, J.C. (1970): Information contained in sediment-size analyses. Journal Intern. Assoc. of Mathematical Geology 2-2, p. 105-112.
DAVIS, J.C. (1986): Statistics and data analysis in Geology. 2nd edition, Wiley, New York, 646 pp.
DE BEAULIEU, J.-L, M. REILLE (1984a): A long Upper Pleistocene pollen record from Les Echets, near Lyon, France. Boreas 13, p. 111-132.
DE BEAULIEU, J.-L, M. REILLE (1984b): The pollen sequence of Les Echets (France): A new element for the chronology of the Upper Pleistocene. Geographie Physique et Quaternaire 38, p. 3-9.
DE GANS, W. (1981): The Drentsche Aa valley system. Thesis, Free University, Amsterdam, 132 pp.
DE GANS, W. (1988): Pingo scars and their identification. In: M.J. Clark (ed.): Advances in periglacial geomorphology. Wiley, Chichester, p. 299-324.
DE MOOR, G. (1983): Cryogenic structures in the Weichselian deposits of Northern Belgium and their significance. Polarforschung 53-2, p. 79-86.
DE MULDER, E. (undated): Geologisch onderzoek in de bouwput te Den Helder. Intern Verslag 1, Rijks Geologische Dienst, District Noordwest, 23 pp.
DE PLOEY, J. (1961): Morfologie en Kwartair-stratigrafie van de Antwerpse Noorderkempen. Acta Geographica Lovaniensa 1, 130 pp.
DE PLOEY, J. (1972): Quelques expériences en rapport avec le rôle éventuel de l'érosion pluviale en milieu périglaciaire. Bulletin Centre de Géomorphologie, Caen, 13/14/15, p. 101-115.
DIONNE, J.C. (1987): Aspects morpho-sédimentologiques du glaciel. Abstract, INQUA XIIth International Congress, Ottawa, p. 157.
DOEGLAS, D.J. (1946): Interpretation of the results of mechanical analysis. Journal of Sedimentary Petrology 16, p. 19-40.
DONNER, J.J., H. JUNGNER, Y. VASARI (1971): The hard-water effect on radiocarbon datings from Säynäjälampi, north-east Finland. Comm. Physico-Mathem. 41, p 307-310.

DOPPERT, J.W.C., G.H.J. RUEGG, C.J. VAN STAALDUINEN, W.H. ZAGWIJN, J.G. ZANDSTRA (1975): Formaties van het Kwartair en Boven-Tertiair in Nederland. In: Zagwijn, W.H., C.J. van Staalduinen (eds): Toelichting bij geologische overzichtskaarten van Nederland. Rijks Geologische Dienst, Haarlem, p. 11-56.

DYLIK, J., G.C. MAARLEVELD (1967): Frost cracks, frost fissures and related polygons. Mededelingen Geologische Stichting N.S. 18, p. 7-21.

EDELMAN, C.H. (1933): Petrologische provincies in het Nederlandsche Quartair D.B. Centen's Uitgevers Maatschappij, Amsterdam, 104 pp.

EDELMAN, C.H., G.G.L. STEUR (1951): Over niveo-fluviale afzettingen op de westelijke Veluwe. Boor en Spade IV, p. 39-46.

EDEN, D.N. (1980): The loess of North-east Essex, England. Boreas 9, p. 165-177.

EDLUND, S.A. (1987): Plants: living weather stations. GEOS 16-2, p. 9-13.

ELLIOTT, T. (1974): Interdistributary bay seqeunces and their genesis. Sedimentology 21, p. 611-622.

ELZENGA, W., J. SCHWAN, Y.A. BAUMFALK, J. VANDENBERGHE, L. KROOK (1987): Grain surface characteristics of periglacial aeolian and fluvial sands. Geologie en Mijnbouw 65, p. 273-286.

EMILIANI, C., (1955): Pleistocene temperatures. Journal of Geology 63, p. 538-578.

ESCHNER, T.R., J.E. KIRCHER (1984): Interpretation of grain-size distributions from measured sediment data, Platte River, Nebraska. Sedimentology 31, p. 569-573.

FERRIANS, O.J., R. KACHADOORIAN, G.W. GREENE (1969): Permafrost and related engineering problems in Alaska. U.S. Geological Survey Professional Paper 678, 37 pp.

FOLK, R.L., W.C. WARD (1957): Braszo river bar: A study in the significance of grainsize parameters. Journal of Sedimentary Petrology 27-1, p. 3-26.

FORBES, D.L. (1983): Morphology and sedimentology of a sinuous gravel-bed channel system: lower Babbage river, Yukon coastal plain, Canada. In: Collinson, J.D., J. Lewin (eds): Modern and ancient fluvial systems. Special Publ. Nr. 6 Intern. Association of Sedimentologists, Blackwell, Oxford: p. 195-206.

FORD, J., B.L. BEDFORD (1987): The hydrology of Alaskan wetlands, U.S.A.: a review. Arctic and Alpine Research 19, p. 209-229.

FRENCH, H.M. (1976): The periglacial environment. Longman, London, 309 pp.

FRENCH, H.M. (1986): Periglacial involutions and mass displacement structures, Banks Island, Canada. Geografiska Annaler 68A-3, p. 167-174.

FRENCH, H.M., A. G. LEWKOWICZ (1981): Periglacial slopewash investigations, Banks Island, Western Arctic. Biuletyn Peryglacjalny 28, p. 33-45.

FRIEDMAN, G.M. (1961): Distinction between dune, beach and river sands from their textural characteristics. Journal of Sedimentary Petrology 31, p. 514-529.

FROEHLICH, W., J. SLØPIK (1982): River icings and fluvial activity in an extreme continental climate: Khangai Mountains, Mongolia. In: French, H.M. (ed): The Roger J.E. Brown Memorial Volume. Proc. 4th Canadian Permafrost Conf., National Research Council, Ottawa, p. 203-211.

GEYH, M.A. (1971): Die Anwendung der ^{14}C-Methode. Clausthaler Tektonische Hefte 11, 118 pp.

GEYH, M.A. (1980): Holocene sea-level history: Case study of the statistical evaluation of ^{14}C dates. Radiocarbon 22-3, P. 695-704.
GEYH, M.A., P.ROHDE (1972): Weichselian chronostratigraphy, ^{14}C dating, and statistics. XXIV International Geological Congress, Canada 1972, p. 765.
GILFILIAN, R.E., W.L. KLINE, T.E. OSTERKAMP, C.S. BENSON (1972): Ice formation in a small Alaskan stream. In: The role of snow and ice in hydrology. Proc. of the Banff Symposia, Int. Ass. of the Hydrogical Sci./W.M.O. Vol I, p. 505-513.
GREGORY, K.J. (ed.) (1983): Background to palaeohydrology. Wiley, Chichester, 486 pp.
GRIFFITHS, C.M. (1982): A proposed geologically consistent segmentation and reassignment algorithm for petrophysical borehole logs. In: J.M. Cubitt & R.A. Reyment (eds): Quantitative stratigraphic correlation. Wiley, New York, p. 287-298.
GRIMM, E.C. (1987): CONISS: a Fortran 77 program for stratigraphically constrained cluster analysis by the method of incremental sum of squares. Computers & Geosciences 13-1, p. 13-35.
GOOD, T.R., I.D. BRYANT (1985): Fluvio-eolian sedimentation - an example from Banks Island, N.W.T., Canada. Geografiska Annaler 67A-1/2, p. 33-46.
GUIOT, J., A. PONS, J.L. DE BEAULIEU, M. REILLE (1989): A 140,000-year continental climate reconstruction from two European pollen records. Nature, Vol. 338, p. 309-313.
HAESAERTS, P. (1985): Les loess du pleistocene superieur en Belgique; comparaisons avec les sequences d'Europe Centrale. Bull. de l'Association Française pour l'Etude Quaternaire 1985-2/3, p. 105-115.
HAEST, R. (1985): Invloed van het Weichsel-glaciaal op de geomorfologie van de Noorderkempen. Thesis, Leuven, 292 pp.
HARPER, C.W. (1984): Improved methods of facies sequence analysis. In: R.G. Walker (ed.): Facies models. Geoscience Canada Reprint Series No. 1 (2nd ed.), p. 11-13.
HARRY, D.G., J.S. GOZDZIK (1988): Ice wedges: growth, thaw transformation, and palaeoenvironmental significance. Journal of Quaternary Science 3-1, p. 39-55.
HARTZ, N., V. MILTHERS (1901): Det senglaciale Ler i Allerød Teglvaerskgrav. Med. Dansk Geol. Foren. 8, p. 31-60.
HATTORI, I. (1976): Entropy in Markov chains and discrimination of cyclic patterns in lithological successions. Mathematical Geology 8, p. 477-497.
HAYS, J.D., J. IMBRIE, N.J. SHACKLETON (1976): Variations in the earth's orbit: pacemaker of the ice ages. Science 194, p. 1121-1132.
HIGGS, R. (1979): Quartz grain surface features of Mesozoic-Cenozoic sands from the Labrador and Western Greenland continental margins. Journal of Sedimentary Petrology 49-2, p. 599-610.
HOPKINS, D.M. (1949): Thaw lakes and thaw sinks in the Imuruk Lake area, Seward Peninsula, Alaska. Journal of Geololgy 57, p. 119-131.
HOPKINS, D.M., J.G. KIDD (1988): Thaw lake sediments and sedimentary environments. Proc. Vth International Conf. on Permafrost, Trondheim, p. 790-795.
HUBBELL, D.W., KHALID AL-SHAIKH ALI (1961): Qualitative effects of temperature on flow phenomena in alluvial channels. U.S. Geological Survey Professional Paper 424-D, p. 21-33.
HUNTER, R.E. (1977): Basic types of stratification in small eolian dunes. Sedimentology 24, p. 361-387.

INQUA STRATIGRAPHIC COMMISSION (1981): Report on the activities of the Sub-Commission on Quaternary Stratigraphy of Europe for the intercongress period 1977-1982. Circulaire nr. 19, 4 pp.
INQUA STRATIGRAPHIC COMMISSION (1984): Final report on the meeting of the S.E.Q.S in Munich, 1983. Circulaire nr. 21, 3 pp.
IVERSEN, J. (1942): En pollenanalytisk tidsfuestelse of Ferks-vandslagene ved Nørre Lynby. Med. Danske Geol. Foren. 10, p. 130-151.
JESSEN, A. (1935): The composition of forest in Northern Europe in epipaleolithic time. Kgl. Danske Vidensk. Selsk. Biol. Med. 12-1, p. 1-69.
JELGERSMA, S., J.B. BREEUWER (1975): Toelichting bij de kaart glaciale verschijnselen gedurende het Saalien, 1:600.000. In: Zagwijn, W.H., C.J. van Staalduinen (eds): Toelichting bij geologische overzichtskaarten van Nederland. Rijks Geologische Dienst, Haarlem, p. 93-102.
JOHNSON, N.L., S. KOTZ (1970): Continuous univariate distributions - I. Wiley, New York, 300 pp.
KANE, D.L., L.D. HINZMAN (1988): Permafrost hydrology of a small arctic watershed. Proc. Vth International Conf. on Permafrost, Trondheim, Norway, August 2-5, 1988, p. 590-595.
KANE, D.L., C.W. SLAUGHTER (1972): Seasonal regime and hydrological significance of stream icings in central Alaska. In: The role of snow and ice in Hydrology. Proc. of the Banff Symposia, Int. Ass. of the Hydrological Sci./W.M.O. Vol. I, p. 528-540.
KARTE, J. (1979): Raumliche Abgrenzung und regionale Differenzierung des Periglaziars. Thesis, Bochum, 211 pp.
KARTE, J., H. LIEDTKE (1981): The theoretical and practical definition of the term "periglacial" in its geographical and geomorphological meaning. Biuletyn Peryglacjalny 28, p. 123-135.
KASSE, C. (1988): Early-Pleistocene tidal and fluviatile environments in the southern Netherlands and Northern Belgium. Thesis, Free University, Amsterdam, 190 pp.
KEMPER, E. (1968): Geologische Führer durch die Grafschaft Bentheim und die angrenzenden Gebiete. Verlag Heimatverein der Grafschaft Bentheim 3, Nordhorn, 172 pp.
KLEINSMAN, W.B., G.W. DE LANGE, G.C. MAARLEVELD, J.A.M. TEN CATE (1978): Geomorfologische kaart van Nederland, schaal 1:50.000, blad 28 en blad 29 Almelo/Denekamp. Stichting voor Bodemkartering, Wageningen / Rijks Geologische Dienst, Haarlem.
KLOVAN, J.E. (1966): The use of factor analysis in determining depositional environments from grain-size distributions. Journal of Sedimentary Petrology 36, p. 115-125.
KNOX, J.C. (1975): Concept of the graded stream. In: Melhorn, W.N., R.C. Flemal (eds.): Theories of Landform Development. George Allen & Unwin, London, p. 169-198.
KOLSTRUP, E. (1980): Climate and stratigraphy in Northwestern Europe between 30,000 B.P. and 13,000 B.P., with special reference to the Netherlands. Mededelingen Rijks Geologische Dienst 32-15, p. 181-253.
KOLSTRUP, E. (1985): Late Pleistocene periglacial conditions in Blaksmark near Varde (Denmark). Geologie en Mijnbouw 64-3, p. 263-270.
KOLSTRUP, E., T.A. WIJMSTRA (1977): A palynological investigation of the Moershoofd, Hengelo and Denekamp Interstadials in the Netherlands. Geologie en Mijnbouw 56-2, p. 85-102.
KOLSTRUP, E., V. MEJDAHL (1986): Three frost wedge casts from Jutland (Denmark) and TL-dating of their infill. Boreas 15, p. 311-321.

KONERT, M., J. VAN HUISSTEDEN (1987): Database boorstaten. Abstract, Symposium Handbook, "The use of personal computers in Earth-technology", Delft, p. 1.
KOROTAJ, M., E. MYCIELSKA-DOWGIAŁŁO (1982): Würmian periglacial processes on the Kolno plateau in the light of sedimentologic investigations with the use of the scanning electron microscope. Biuletyn Peryglacjalny 29, p. 53-76.
KOSTER, E.A. (1982): Terminology and lithostratigraphic division of (surficial) sandy eolian deposits in The Netherlands: an evaluation. Geologie en Mijnbouw 61, p. 121-129.
KOWALKOWSKI, A., Z. BROGOWSKI (1983): Features of cryogenic environment in soils of continental tundra and arid steppe on the southern Kangai slope under electron microscope. Catena 10, p. 199-205.
KOWALKOWSKI, A. E. MYCIELSKA-DOWGIAŁŁO (1983): The stratigraphy of fluvial and eolian deposits in the Kopanica river valley based on sedimentological and pedological investigations. Geologisches Jahrbuch A71, p. 119-148.
KRINSLEY, D., L. CAVALLERO (1970): Scanning electron microscopic examination of periglacial eolian sands from Long Island, New York. Journal of Sedimentary Petrology 40, p. 1345-1351.
KRINSLEY, D.H., J. DONAHUE (1968): Environmental interpretation of sand grain surface textures by electron microscopy. Geological Society of America Bull. 79, p. 743-748.
KRINSLEY, D.H., J.C. DOORNKAMP (1973): Atlas of quartz sand surface textures. Cambridge University Press, 91 pp.
KUENEN, P.H. (1960): Experimental abrasion, 4. Eolian action. Journal of Geology 68, p. 427-449.
LANE, E.W., M. ASCE, E.J. CARLSON, O.S. HANSON (1949): Low temperature increases sediment transportation in Colorado river. Civil Engineering 19-9, p. 45-46.
LANGBEIN, W.B., SCHUMM, S.A. (1958): Yield of sediment in relation to mean annual precipitation. Transactions of the American Geophysical Union 39, p. 1076-1084.
LIETH, H. (1975): Modelling the primary productivity of the world. In: H. Lieth, R.H. Whittaker (eds.): Primary productivity of the biosphere. Springer, New York, p. 237-264.
LETSCH, W.J., W. SISSINGH (1983): Tertiary stratigraphy of the Netherlands. Geologie en Mijnbouw 62-2, p. 305-318.
LEWKOWICZ, A.G. (1983): Erosion by overland flow, central Banks Island, Western Canadian Arctic. In: Proc. Fourth Intern. Permafrost Conf., Fairbanks, Alaska. National Academy Press, Washington D.C., p. 701-706.
LEWKOWICZ, A.G. (1987): Nature and importance of thermokarst processes, Sand Hills moraine, Banks Island, Canada. Geografiska Annaler 69A-2, p. 321-327.
LEWKOWICZ, A.G. (1988): Slope processes. In: M.J. Clark (ed.): Advances in periglacial geomorphology. Wiley, Chichester, p. 325-368.
LEWKOWICZ, A.G., T.J. DAY, H.M. FRENCH (1978): Observations on slopewash processes in an Arctic tundra environment, Banks Island, District of Franklin. Geological Survey of Canada Paper 78-1A, p. 516-520.
LIEDTKE, H. (1983): Periglacial slopewash and sedimentation in Northwestern Germany during the Würm (Weichsel-) Glaciation. Proc. Fourth Intern. Permafrost Conf., Fairbanks, Alaska, National Academy Press, Washington D.C., p. 715-718.
LINDÉ, K., E. MYCIELSKA-DOWGIAŁŁO (1980): Some experimentally produced microtextures on grain surfaces of quartz sand. Geografiska Annaler 62A-3/4, p. 171-184.

LOOTENS, M. (1987): Heavy minerals as a stratigraphical tool for the Eemian and Post-Eemian deposits in the Lower Lys valley (Belgium). Geologie en Mijnbouw 66-2, p. 139-146.
LOZINSKY, W. V. (1909): Über die mechanische Verwitterung der Sandsteine im gemäßigten Klima. Bulletin International de l'Académie des Sciences de Cracovie, Classe des Sciences Mathématiques et Naturelles, 1, Krakau, p. 1-25.
MAARLEVELD, G.C. (1949): Over de erosiedalen van de Veluwe. Tijdschrift Koninklijk Nederlands Aardrijkskundig Genootschap LXVI, p. 133.
MAARLEVELD, G.C. (1956): Grindhoudende Midden-Pleistocene sedimenten; het onderzoek van deze afzettingen in Nederland en aangrenzende gebieden. Mededelingen Geologische Stichting, Serie C, VI-6, 105 pp.
MAARLEVELD, G.C. (1960): Glacial and periglacial landscape forms in the central and northern Netherlands. Tijdschrift Koninklijk Nederlands Aardrijkskundig Genootschap, 2e reeks, LXXVII, p. 298-304.
MAARLEVELD, G.C. (1976): Periglacial phenomena and the mean annual temperature during the last glacial time in the Netherlands. Biuletyn Peryglacjalny 26, p. 57-78.
MAARLEVELD, G.C. (1981): Summer thaw depths in cold regions and fossil cryoturbation. Geologie en Mijnbouw 60-3, p. 289-464.
MACKAY, D.K., O.H. LØKEN (1974): Arctic hydrology. In: J.D. Ives, R.G. Barry (eds): Arctic and Alpine environments. Methuen & Co., London, p. 111-132.
MAK, C.E., P.E. VAN OLST, T.B. VAN DER WERF (1989): Veldwerkverslag Kwartairgeologisch veldwerk Twente 1985, omgeving Denekamp. Unpublished report, Instituut voor Aardwetenschappen, Vrije Universiteit, Amsterdam, 103 pp.
MANKER, J.P., R.D. PONDER (1978): Quartz grain surface features from fluvial environments of Northeastern Georgia. Journal of Sedimentary Petrology 48-4, p. 1227-1232.
MARGOLIS, S.V., D.H. KRINSLEY (1971): Submicroscopic frosting on eolian and subaqueous quartz sand grains. Geological Society of America Bull. 82, p. 3395-3406.
MARGOLIS, S.V., D.H. KRINSLEY (1973): Depositional histories of sand grains from surface textures. Nature 245, p. 30-31.
MARSH, P. (1988): Soil infiltration and snow-melt run-off in the Mackenzie delta, N.W.T. Proc. Vth International Conf. on Permafrost, Trondheim, Norway, August 2-5, 1988, p. 618-621.
MARSH, P., M.K. WOO (1981): Snowmelt, glacier melt and high arctic streamflow regimes. Canadian Journal of Earth Sciences 8, p. 1282-1301.
MATHER, P.M. (1976): Computational methods of multivariate analysis in Physical Geography. Wiley, London, 532 pp.
MCCANN, S.B., P.J. HOWARTH, J.G. COGLEY (1972): Fluvial processes in a periglacial environment. Transactions of the Institute of British Geographers 55, p. 69-82.
MCCLOY, J. (1970): Hydrometereological relationships and their effects on the levees of a small arctic delta. Geografiska Annaler 52A-3/4, p. 223-241.
MCKEE, E.D., G.W. WEIR (1953): Terminology for stratification and cross stratification in sedimentary rocks. Geological Society of America Bull. 64, p. 381-390.
MENKE, B. (1976): Neue Ergebnisse zur Stratigraphie und Landschaftsentwicklung im Jungpleistozän Westholsteins. Eiszeitalter und Gegenwart 27, p. 53-68.

MEYER, H.-H. (1986): Steinsohlen - ihre Genese und Altersstellung nach neueren Forschungsbefunden. Eiszeitalter und Gegenwart 36, p. 61-73.
MIALL, A.D. (1973): Markov chain analysis applied to an ancient alluvial plain succession. Sedimentology 20, p. 347-364.
MIALL, A.D. (1977): A review of the braided river depositional environment. Earth Science Reviews 13, p. 1-62.
MIALL, A.D. (ed.) (1978a): Fluvial Sedimentology. Canadian Society of Petroleum Geologists Memoir 5, Calgary, 859 pp.
MIALL, A.D. (1978b): Lithofacies type and vertical profile models in braided river deposits: a summary. In: A.D. Miall (ed): Fluvial Sedimentology. Canadian Society of Petroleum Geologists Memoir 5, Calgary, p. 597-604.
MIALL, A.D. (1980): Cyclicity and the facies model concept in fluvial deposits. Bull. of Canadian Petroleum Geology 28-1, p. 59-80.
MIALL, A.D. (1985): Architectural-element analysis: A new method of facies analysis applied to fluvial deposits. Earth-Science Reviews 22, p. 261-308.
MICHEL, B. (1972): Properties and processes of river and lake ice. In: The role of snow and ice in Hydrology. Proc. of the Banff Symposia, Int. Ass. of the Hydrological. Sci. / W.M.O. Vol. 1, p. 454-481.
MIDDLETON, G.V. (1976): Hydraulic interpretation of sand size distributions. Journal of Geology 84, p. 405-426.
MILES, M. (1976): An investigation of riverbank and coastal erosion, Banks Island, District of Franklin. Geological Survey of Canada, Paper 76-1A, p. 195-200.
MOOK, W.G., O. VAN DE PLASSCHE (1986): Radiocarbon dating. In: O. van de Plassche (ed.): Sea-level research: a manual for the collection and evaluation of data. Contibution to IGCP Projects 61 and 200, Geo Books, Norwich, p. 525-560.
MOOK, W.G., H.J. STREURMAN (1983): Physical and chemical aspects of radiocarbon dating. In: W.G. Mook & H. Tj. Waterbolk (eds): Proceedings of the Groningen Conference on 14C and Archaelogy. PACT Publication 8, p. 31-55.
MÜCHER, H.J. (1986): Aspects of loess and loess-derived slope deposits: An experimental and micromorphological approach. Thesis, University of Amsterdam, 267 pp.
MÜCHER, H.J., J. DE PLOEY (1977): Experimental and micromorphological investigation of erosion and redeposition of loess by water. Earth Surface Processes 2, p. 117-124.
MURRE, L.M. (1985): Hervereffening van de Tweede, Derde en Vierde Nauwkeurigheidswaterpassing van Nederland en vergelijking van de resultaten. Intern Rapport Technische Hogeschool (afd. Geodesie), Delft.
NIETER, W.M., D.H. KRINSLEY (1976): The production and recognition of aeolian features on sand grains by silt abrasion. Sedimentology 23, p. 713-720.
OLSSON, I.U. (1986): Radiometric dating. In: B.E. Berglund (ed): Handbook of Holocene paleoecology and paleohydrology. Wiley, London, p. 273-312.
OLSSON, I.U., F.A.N. OSADEBE (1974): Carbon isotope variations and fractionation corrections in ^{14}C dating. Boreas 3, p. 139-146.
PAEPE, R. (1972): Sedimentological parameters for a continuous climatic evolution throughout the Weichselian. Boreas 1, p. 173-183.
PASSEGA, R. (1964): Grainsize representation by CM patterns as a geological tool. Journal of Sedimentary Petrology 34, p. 830-847.

PÉWÉ, T.L. (1966): Ice wedges in Alaska: Classification, distribution, and climatic significance. Proc. Intern. Permafrost Conf., National Acad. Sci. - National Research Council Publ. No. 1287, p. 76-81.
PÉWÉ, T.L. (1969): The periglacial environment. In: Péwé, T.L. (ed.): The periglacial environment. McGill-Queens University Press, Montreal, p. 1-9.
PÉWÉ, T.L. (1975): Quaternary Geology of Alaska. U.S. Geological Survey Professional Paper 835: 145 pp.
PISSART, A. (1987): Weichselian periglacial structures and their environmental significance: Belgium, the Netherlands, and northern France. In: J. Boardman (ed.): Periglacial processes and landforms in Britain and Ireland. Cambridge University Press, Cambridge: p. 77-85
PISSART, A. (1988): Pingos: an overview of the present state of knowledge. In: M.J. Clark (ed.): Advances in periglacial geomorphology. Wiley, Chichester, p. 279-298.
PISSART, A., J.S. VINCENT, S.A. EDLUND (1977): Dépôts et phénomènes éoliens sur l'île de Banks, Territoires du Nord-Ouest, Canada. Canadian Journal of Earth Sciences 14, p. 2462-2480.
POWERS, D.W., R.G. EASTERLING (1982): Improved methodology for using embedded Markov chains to describe cyclical sediments. Journal of Sedimentary Petrology 52-3, p. 913-923.
PRESS, W.H., B.P. FLANNERY, S.A. TEUKOLSKY, W.T. VETTERLING (1986): Numerical recipes. Cambridge University Press, Cambridge, 818 pp.
RAN, E.T.H., (1990): Dynamics of vegetation and environment during the Middle Pleniglacial in the Dinkel valley. Thesis, University of Amsterdam, in press.
RAN, E.T.H., S.J.P. BOHNCKE, J. VAN HUISSTEDEN, J. VANDENBERGHE (1990): Evidence of episodic permafrost conditions during the Weichselian Middle Pleniglacial in the Hengelo basin (The Netherlands). Geologie en Mijbouw, in press.
RAPPOL, M. (1987): Saalian tills in The Netherlands: A review. In: Van der Meer, J.J.M. (ed.): Tills and glaciotectonics. Proceedings of an INQUA symposium on genesis and lithology of glacial deposits, Amsterdam, 1986. Balkema, Rotterdam, p.3-22.
RAPPOL, M., H.M.P. STOLTENBERG (1985): Compositional variability of Saalian till in the Netherlands. Boreas 14-1, p. 33-50.
REINECK, H.-E., I.B. SINGH (1975): Depositional sedimentary environments. Springer, Berlin, 439 pp.
RICHARDS, K. (1982): Rivers, form and process in alluvial channels. Methuen, London, 358 pp.
ROELEVELD, W. (1974): The Groningen coastal area. A study in Holocene geology and lowland physical geography. Thesis, Free University, Amsterdam, 252 pp.
ROMANOVSKY, N.H. (1976): The scheme of correlation of polygonal structures. Biuletyn Peryglacjalny 26, p. 287-294.
ROMANOVSKY, N.H. (1985): Distribution of recent active ice and soil wedges in the U.S.S.R. In: M. Church, S. Slaymaker (eds): Field and theory: Lectures in Geocryology. University of British Columbia, p. 154-165.
RUEGG, G.H.J. (1971): Sedimentologisch onderzoek van afzettingen van de Formatie van Twente, ontsloten in de E8-zandwinningsput bij Voorthuizen. Rijks Geologische Dienst, Sedimentologische Afdeling, Rapport no. 3, 9 pp.
RUEGG, G.H.J. (1975): Sedimentary structures and depositional environments of Middle- and Upper Pleistocene glacial time

deposits from an excavation at Peelo, near Assen, The Netherlands. Mededelingem Rijks Geologische Dienst N.S. 26-1, p. 17-37.
RUEGG, G.H.J. (1978): Bouwput fregatdok Den Helder: genese van een tot de Formatie van Twente behorend pakket van afzettingen op grond van korrelgrootte en strukturele opbouw. Rijks Geologische Dienst, Sedimentologische Afdeling, Rapport no. 42, 6 pp.
RUEGG, G.H.J. (1981): Sedimentary features and grainsize of glaciofluvial and periglacial Pleistocene deposits in the Netherlands and adjacent parts of Western Germany. Verhandlungen naturwissenschaftliche Verein Hamburg (N.F.) 24-2, p. 133-154.
RUST, B.R. (1978): A classification of alluvial channel systems. In: Miall, A.D. (ed): Fluvial sedimentology. Canadian Society of Petroleum Geologists Memoir 5, Calgary, p. 187-198.
SAGOE, K-M. O., G.S. VISHER (1977): Population breaks in grainsize distributions of sand - a theoretical model. Journal of Sedimentary Petrology 47-1, p. 285-310.
SANGLERAT, G. (1972): The penetrometer and soil exploration. Elsevier, Amsterdam, 464 pp.
SCHOUTE, J.F.TH., J.W. GRIEDE, W.G. MOOK, W. ROELEVELD (1981): Radiocarbon dating of vegetation horizons, illustrated by an example from the Holocene coastal plain in the Northern Netherlands. Geologie en Mijbouw 60, p. 453-459.
SCHOUTE, J.F.TH., W.G. MOOK & H.J. STREURMAN (1983): Radiocarbon dating of vegetation horizons: methods and preliminary results. In: W.G. Mook & H. Tj. Waterbolk (eds): Proceedings of the Groningen Conference on 14C and Archaelogy. PACT Publication 8, p. 295-311.
SCHUILING, R.D., R.J. DE MEIJER, H.J. RIEZEBOS, M.J. SCHOLTEN (1985): Grainsize distribution of different minerals in a sediment as a function of their specific density. Geologie en Mijnbouw 64-2, p. 199-204.
SCHUMM, S.A. (1977): The fluvial system. Wiley, New York, 338 pp.
Schumm, S.A. (1981): Evolution and response of the fluvial system, sedimentological implications. In: Ethridge, F.G., R.M. Flores (eds): Recent and ancient nonmarine depositional environments: Models for exploration. Special Publication 31, Society of Economic Paleontologists and Mineralogists, Tulsa, p. 19-30.
SCHWAN, J. (1986): The origin of horizontal alternating bedding in Weichselian aeolian sands in northwestern Europe. Sedimentary Geology 49, p. 73-108.
SCHWAN, J. (1987): Sedimentologic characteristics of a fluvial to aeolian succession in Weichselian Talsand in the Emsland (F.R.G.). Sedimentary Geology 52, p. 273-298.
SCHWAN, J. (1988a): Sedimentology of coversands in Northwestern Europe: a study on Weichselian to Early Holocene aeolian sand sheets in England, The Netherlands and the Federal Republic of Germany. Thesis, Free University, Amsterdam, 137 pp.
SCHWAN, J. (1988b): The structure and genesis of Weichselian to Early Holocene aeolian sand sheets in Western Europe. Sedimentary Geology 55, p. 197-232.
SCHWARZACHER, W. (1975): Sedimentation models and quantitative stratigraphy. Developments in Sedimentology 19, Elsevier, Amsterdam, 382 pp.
SCOTT, K.M. (1978): Effects of permafrost on stream channel behaviour in Arctic Alaska. U.S. Geological Survey Professional Paper 1068, 19 pp.
SELLEY, R.C. (1970): Ancient sedimentary environments. Chapman and Hall, London, 237 pp.

SEPPÄLÄ, M. (1971): Evolution of the eolian relief of the Kaamasjoki-Kiellajoki river basin in Finnish Lapland. Fennia 104, p. 1-88.
SEPPÄLÄ, M. (1972): Location, morphology and orientation of inland dunes in Northern Sweden. Geografiska Annaler 54, p. 85-104.
SEPPÄLÄ, M. (1988): Palsas and related forms. In: M.J. Clark (ed.): Advances in periglacial geomorphology. Wiley, Chichester, p. 247-278.
SHAW, B.R., J.M. CUBITT (1978): Stratigraphic correlation of well logs: an automated approach. In: D. Gill, D.F. Merriam (eds.): Geomathematical and petrophysical studies in sedimentology. Pergamom, Oxford, p. 127-148.
SHENNAN, I. (1979): Statistical evaluation of sea-level data. Sea-level 1, p. 6-11.
SHOTTON, F.W. (1972): An example of hard-water error in radiocarbon dating of vegetable matters. Nature 240, p. 460-461.
SLAUGHTER, C.W., C.M. COLLINS (1981): Sediment load and channel characteristics in subarctic upland catchments. Journal of Hydrology 20, p. 39-48.
SLAUGHTER, C.W., J.W. HILGERT, E.H. CULP (1983): Summer streamflow and sediment yield from discontinuous-permafrost headwater catchments. Proc. Fourth Intern. Permafrost Conf., Fairbanks, Alaska, National Academy Press, Washington D.C., p. 1172-1177.
SMART, P., N.K. TOVEY (1981): Electron microscopy of soils and sediments: Examples. Clarendon, Oxford, 177 pp.
SMITH, D.G. (1983): Anastomosed fluvial deposits: modern examples from Western Canada. In: Collinson, J.D., J. Lewin (eds): Modern and ancient fluvial systems. Special Publ. Nr. 6 International Association of Sedimentologists, Blackwell, Oxford, p. 155-168.
SMITH, D.G. (1986): Anatomosing river deposits, sedimentation rates and basin subsidence, Magdalena river, Northwestern Colombia, South America. Sedimentary Geology 46-3/4, p. 177-196.
SMITH, D.G., N.D. SMITH (1980): Sedimentation in anastomosed river systems: examples from alluvial valleys near Banff, Alberta Journal of Sedimentary Petrology 50, p. 157-164.
SMITH, N.D., T.A. CROSS, J.P. DUFFICY, S.R. CLOUGH (1989): Anatomy of an avulsion. Sedimentology 36, p. 1-23.
STARKEL, L. (1983): Climatic change and fluvial response. In: Gardiner, R., H. Scoging (eds): Mega-geomorphology. Clarendon Press, Oxford, p. 195-211.
STEUR, G.G.L., D.J. BRUS, M. VAN DEN BERG (1987): Atlas van Nederland, deel 14: Bodem. Stichting Wetenschappelijke Atlas van Nederland/ Staatsuitgeverij, 's-Gravenhage, 23 pp.
ST.-ONGE, D.A. (1965): La géomorphologie de l'île Ellef Ringnes, Territoires du Nord-Ouest, Canada. Direction de la Géographie, Ministère des Mines et des Relevés techniques, Ottawa, Etude Géographique 38, 46 pp.
TEDROW, J.C.F. (1969): Thaw lakes, thaw sinks and soils in Northern Alaska. Biuletyn Peryglacjalny 20, p. 337-344.
TEDROW, J.C.F. (1977): Soils of the polar landscapes. Rutgers University Press, New Jersey, 638 pp.
TER WEE, M.W. (1979): Toelichtingen bij de Geologische Kaart van Nederland 1:50.000 blad Emmen West (17W) en blad Emmen Oost (17O). Rijks Geologische Dienst, Haarlem, 218 pp.
TEUNISSEN, D., H. TEUNISSEN-VAN OORSCHOT (1974): Eine interstadiale Torfschicht bei Nijmegen (Niederlande) und deren Bedeutung fur die Erklarung der dortigen Landschaftsmorphologie. Geologie en Mijnbouw 53, p. 393-400.

THORNE, C.R., J. LEWIN (1979): Bank processes, bed material movement and planform development in a meandering river. In: Rhodes, D.D., G.P. Williams (eds): Adjustments of the fluvial system, Kendall-Hunt, Dubuque, Iowa, p. 117-37.
TRICART, J. (1970): Geomorphology of cold environments. The Macmillan Co., London, 320 pp.
TSANG, G., L. SZUCS (1972): Field experiments of winter flow in natural rivers. In: The role of snow and ice in Hydrology - Proc. of the Banff Symposia, Int. Ass. of the Hydrogical Sci. / W.M.O. Vol. I, p. 772-785.
TÜRK, G. (1979): Transition analysis of structural sequences: Discussion and reply. Geological Society of America Bull., Part I, 90, p. 989-992.
VAN DEN AKKER, A.M., M. KNIBBE (1963): Glaciale verschijnselen in de stuwwal van Ootmarsum. Boor en Spade XII, p. 12-20.
VAN DEN BERG, M.W., D.J. BEETS (1987): Saalian glacial deposits and morphology in The Netherlands. In: Van der Meer, J.J.M. (ed.): Tills and glaciotectonics. Proceedings of an INQUA symposium on genesis and lithology of glacial deposits, Amsterdam, 1986. Balkema, Rotterdam, p. 235-252.
VANDENBERGHE, J. (1981): Weichselian stratigraphy in the southern Netherlands and Northern Belgium. Quaternary Studies in Poland 3, p. 111-118.
VANDENBERGHE, J. (1983a): Some periglacial phenomena and their stratigraphical position in Weichselian deposits in the Netherlands. Polarforschung 53-2, p. 97-107.
VANDENBERGHE, J. (1983b): Ice-wedge casts and involutions as permafrost indicators and their stratigraphic position in the Weichselian. Proc. IVth International Conf. on Permafrost, Fairbanks, 1988, p. 1298-1302.
VANDENBERGHE, J. (1985): Paleoenvironment and stratigraphy during the Last Glacial in the Belgian-Dutch border region. Quaternary Research 24, p. 23-38.
VANDENBERGHE, J. (1987): Changing fluvial processes in a small lowland valley at the end of the Weichselian Pleniglacial and during the Late Glacial. In: V. Gardiner (ed): International Geomorphology 1986 Part I. Wiley, Chichester, p. 731-744.
VANDENBERGHE, J. (1988): Cryoturbations. In: M.J. Clark (ed.): Advances in periglacial geomorphology. Wiley, Chichester, p. 179-200.
VANDENBERGHE, J., N. VANDENBERGHE, F. GULLENTOPS, R. CLARYSSE (1974): Late Pleistocene and Holocene in the neighbourhood of Brugge. Mededelingen van de Koninklijke Academie voor Wetenschappen, Letteren en Schone Kunsten van Belgie. Klasse der Wetenschappen, Jaargang XXXVI, nr. 5, 77 p.
VANDENBERGHE, J., BOHNCKE, S.J.P., W. LAMMERS, L. ZILVERBERG (1987): Geomorphology and palaeocology of the Mark valley (southern Netherlands): geomorphological valley development during the Weichselian and Holocene. Boreas 16, p. 55-67.
VANDENBERGHE, J., F. GULLENTOPS (1977): Contribution to the stratigraphy of the Weichselian Pleniglacial in the Belgian coversand area. Geologie en Mijnbouw 56, p. 123-128
VANDENBERGHE, J., L. KROOK (1981): Stratigraphy and genesis of Pleistocene deposits at Alphen (southern Netherlands). Geologie en Mijnbouw 60, p. 417-426.
VANDENBERGHE, J., L. KROOK (1985): La stratigraphie et la genèse de depôts Pleistocènes a Goirle (Pays-Bas). Bulletin de l'Association Française pour l'Étude Quaternaire 1985-4, p. 239-247.

VANDENBERGHE, J., P. PARIS, C. KASSE, M. GOUMAN, L. BEYENS (1984): Paleomorphological and -botanical evolution of small lowland valleys - a case study of the Mark valley in Northern Belgium. Catena 11-2/3, p. 229-238.

VANDENBERGHE, J., J. VAN HUISSTEDEN (1988): Fluvio-eolian interaction in a region of continuous permafrost. Proc. Vth International Conf. on Permafrost, Trondheim, Norway, August 2-5, 1988, p. 876-881.

VANDENBERGHE, J., J. VAN HUISSTEDEN (1989): The Weichselian stratigraphy of the Twente Region, eastern Netherlands. In: J. Rose, C. Schlüchter (eds): Quaternary type sections: Imagination or reality? Balkema, Rotterdam, p. 93-100.

VANDENBERGHE, J., C. KASSE (1989): Periglacial environments during the Early Pleistocene in the southern Netherlands and northern Belgium. Palaeogeography, Palaeoclimatology, Palaeoecology 72, p. 133-139.

VANDENBERGHE, J., H.J. MÜCHER, W. ROEBROEKS, D. GEMKE (1985): Lithostratigraphy and palaeoenvironment of the Pleistocene deposits at Maastricht-Belvédère, Southern Limburg, The Netherlands. In: T. van Kolfschoten and W. Roebroeks (eds.): Maastricht-Belvédère: Stratigraphy, paleoenvironment and archeology of the Middle and Late Pleistocene deposits. Mededelingen Rijks Geologische Dienst 39-1, p. 7-18.

VANDENBERGHE, J., P. VAN DEN BROEK (1982): Weichselian convolution phenomena and processes in fine sediments. Boreas 11, p. 299-315.

VAN DER HAMMEN, T. (1951): Late-glacial flora and periglacial phenomena in the Netherlands. Leidse Geol. Meded. XVII, p. 71-183.

VAN DER HAMMEN, T. (1957): A new interpretation of the pleniglacial stratigraphical sequence in Middle and Western Europe. Geologie en Mijnbouw (N.S.) 14, p. 47-54.

VAN DER HAMMEN, T. (1971): The Upper Quaternary stratigraphy of the Dinkel valley. In: Van der Hammen, T., T.A. Wijmstra (eds): The Upper Quaternary of the Dinkel valley. Mededelingen Rijks Geologische Dienst, N.S. 22, p. 81-85.

VAN DER HAMMEN, T., J.A. BAKKER (1971): Former vegetation, landscape and man in the Dinkel valley. In: Van der Hammen, T., T.A. Wijmstra (eds): The Upper Quaternary of the Dinkel valley. Mededelingen Rijks Geologische Dienst, N.S. 22, p. 147-158.

VAN DER HAMMEN, T. G.C. MAARLEVELD, J.C. VOGEL, W.H. ZAGWIJN (1967): Stratigraphy, climatic succession and radiocarbon dating of the last glacial in the Netherlands. Geologie en Mijnbouw 46, p. 79-95.

VAN DER HAMMEN, T., J.C. VOGEL (1966): The Susacá interstadial and the subdivision of the Late Glacial. Geologie en Mijnbouw 45, p. 33-35.

VAN DER HAMMEN, T., T.A. WIJMSTRA (eds.) (1971): The Upper Quaternary of the Dinkel Valley. Meded. Rijks Geol. Dienst N.S. 22, p. 55-213.

VAN DER MEER, J.J.M., R.T. SLOTBOOM, I.M.E. DE VIRES-BRUYNSTEEN (1984): Lithology and palynology of Weichselian alluvial fan deposits near Eerbeek, The Netherlands. Boreas 13, p. 393-402.

VAN DER VLERK, I.M., F. FLORSCHÜTZ (1950): Nederland in het ijstijdvak. De Haan, Utrecht, 287 pp.

VAN DER VLERK, I.M., F. FLORSCHÜTZ (1953): The paleontological base of the subdivision of the Pleistocene in the Netherlands. Verhandelingen Koninklijke Nederlandse Akademie voor Wetenschappen, Afdeling Natuurkunde, Eerste reeks, deel XX, no.2, p. 3-58.

VAN DER WIJK, A. (1987): Radiometric dating by alpha spectrometry on uranium series nuclides. Thesis, Groningen, 168 pp.
VAN GEEL, B., A.G. KLINK, J.P. PALS, J. WIEGERS (1986): An Upper Eemian lake deposit from Twente, Eastern Netherlands. Review of Palaeobotany and palynology 47, p. 31-61.
VAN GEEL, B., G.R. COOPE, T. VAN DER HAMMEN (1989): Palaeocology and stratigraphy of the Lateglacial type section at Usselo (The Netherlands). Review of Palaeobotany and Palynology 60-1/2, p. 25-130.
VAN HUISSTEDEN, J. (1989): Geologisch onderzoek van natuurmonument "Het Hazelbekke", Twente, Overijssel. Unpublished report, Vereniging tot Behoud van Natuurmonumenten, 15 p.
VAN HUISSTEDEN, J., J. VANDENBERGHE, B. VAN GEEL (1986a): Late Pleistocene stratigraphy and fluvial history of the Dinkel basin (Twente, Eastern Netherlands). Eiszeitalter und Gegenwart 36, p. 43-59.
VAN HUISSTEDEN, J., L. VAN DER VALK, J. VANDENBERGHE (1986b): Geomorphological evolution of a lowland valley system during the Weichselian. Earth Surface Processes & Landforms 11, p. 207-216.
VAN HUISSTEDEN, J., J. VANDENBERGHE (1988): Changing fluvial style of periglacial lowland rivers during the Weichselian Pleniglacial in the eastern Netherlands. Zeitschrift für Geomorphologie N.F., Suppl.-Bd. 71, p. 131-146.
VAN VLIET-LANOE, B. (1985): Frost effects in soils. In: J. Boardman (ed.): Soils and Quaternary Landscape Evolution. John Wiley & Sons, Chichester, p. 118-158.
VERMEIJ, A., B. HEUKESHOVEN (1974): Verslag over een onderzoek gedaan in de groeve Rientjes te Hengelo (1972-1974). Unpublished report, Hugo de Vries Laboratorium, Universiteit van Amsterdam, 16 pp.
VINCENT, P.J. (1976): Some periglacial deposits near Aberystwyth, Wales, as seen with a scanning electron microscope. Biuletyn Peryglacjalny 25, p. 59-64.
VINK, A.P.A., J. SEVINK (1971): Soils and paleosoils in the Lutterzand. In: Van der Hammen, T., T.A. Wijmstra (eds): The Upper Quaternary of the Dinkel valley. Mededelingen Rijks Geologische Dienst, N.S. 22, p. 165-186.
VISHER, G.S. (1969): Grain size distributions and depositional processes. Journal Sedimentary Petrology 39-3, p. 1074-1106.
VOGEL, J.C., T. VAN DER HAMMEN (1967): The Denekamp and Paudorf Interstadials. Geologie en Mijnbouw 46, p. 188-194.
VOGEL, J.C. (1983): ^{14}C variations during the Upper Pleistocene. Radiocarbon 25-2, p.213-218.
WALKER, H.J. (1967): Some aspects of erosion and sedimentation in an arctic delta during breakup. In: Proc. of Symp. on Hydrology of Deltas, p. 209-219.
WALKER, H.J. (1973): Morphology of the North Slope. In: Britton, M.E. (ed): Alaskan arctic tundra. Arctic Institute of North America Technical Paper No. 25, p. 49-93.
WALKER, H.J. (1978): Lake-tapping in the Colville river delta, Alaska. Proc. 3d International Conf. on Permafrost, 1978, p. 232-238.
WALKER, H.J., L. ARNBORG (1966): Permafrost and ice-wedge effect on riverbank erosion. In: Proc. Permafrost International Conf., NRC Publication no. 1287, p. 164-171.
WALKER, J., L. ARNBORG, J. PEIPPO (1987): Riverbank erosion in the Colville delta, Alaska. Geografiska Annaler 69A-1, p. 61-70.
WALLACE, R.E. (1948): Cave-in lakes in the Nabesna, Chisana and Tanana river valleys, Eastern Alaska. Journal of Geology 56, p. 171-181.

WALLING, D.E., P.W. MOOREHEAD (1987): Spatial and temporal variation of the particle-size characteristics of fluvial suspended sediment. Geografiska Annaler 69A-1, p. 47-59.
WALLING, D.E., B.W. WEBB (1983): Patterns of sediment yield. In: Gregory, K.J. (ed.): Background to paleohydrology. Wiley, Chichester, p. 69-100.
WARD, J.H., Jr., (1963): Hierarchical grouping to optimize an objective function. Journal American Statist. Assoc. 58-301, p.236-244.
WALTHER, H., H. LIETH (1960): Klimadiagramm Weltatlas. VEB Gustav Fischer Verlag Jena.
WASHBURN, A.L. (1979): Geocryology. Edward Arnold, London, 406 pp.
WATERLEIDING MAATSCHAPPIJ "OVERIJSSEL" N.V. (1985): Nieuw waterwingebied Denekamp (inventarisatieonderzoek). Intern rapport Afdeling Onderzoek, 25 pp.
WEBSTER, R. (1973): Automatic soil-boundary location from transect data. Journal Intern. Assoc. Mathematical Geology 5-1, p. 27-37.
WELLS, N.A. (1989): A program in basic for facies-by-facies Markov chain analysis. Computers & Geosciences 15, p. 143-155.
WIJMSTRA, T.A., E. DE VIN (1971): The new Dinkel canal section. In: Van der Hammen, T., T.A. Wijmstra (eds): The Upper Quaternary of the Dinkel valley. Mededelingen Rijks Geologische Dienst, N.S. 22, p. 101-130.
WIJMSTRA, T.A., E.J. SCHREVE-BRINKMAN (1971): The Lutterzand section. In: Van der Hammen, T., T.A. Wijmstra (eds): The Upper Quaternary of the Dinkel valley. Mededelingen Rijks Geologische Dienst, N.S. 22, p. 87-100.
WIJMSTRA, T.A., E.J. SCHREVE-BRINKMAN, E. DE VIN (1971): Some data on the sedimentology of the Dinkel valley. In: Van der Hammen, T., T.A. Wijmstra (eds): The Upper Quaternary of the Dinkel valley. Mededelingen Rijks Geologische Dienst, N.S. 22, p. 141-146.
WIJMSTRA, T.A., E. DE VIN (1971): The new Dinkel canal section. In: Van der Hammen, T., T.A. Wijmstra (eds): The Upper Quaternary of the Dinkel valley. Mededelingen Rijks Geologische Dienst, N.S. 22, p. 101-130.
WILKINSON, T.J., B.T. BUNTING (1975): Overland transport of sediment by rill water in a periglacial environment in the Canadian high Arctic. Geografiska Annaler 57A-1,2, p. 105-116.
WILLIAMS, R.B.G. (1975): The British climate during the Last Glaciation; an interpretation based on periglacial phenomena. In: Wright, A.E., F. Moseley (eds): Ice Ages: Ancient and Modern. Geological Journal Special Issue 6, p. 95-120.
WINKELMOLEN, A.M. (1969): Experimental rollability and natural shape sorting of sand. Thesis, State University Groningen, 141 pp.
WOILLARD, G.M., W.G. MOOK (1982): Carbon-14 dates at Grande Pile: Correlation of land and sea chronologies. Science, Vol. 215, p. 159-161.
WOO, M.-K. (1988): Wetland and runoff regime in northern Canada. Proc. Vth International Conf. on Permafrost, Trondheim, Norway, August 2-5, 1988, p. 644-649.
WOO, M.-K., P. DICENZO (1989): Hydrology of small tributary streams in a subarctic wetland. Canadian Journal of Earth Sciences 26, p. 1557-1566.
ZAGWIJN, W.H. (1961): Vegetation, climate and radiocarbon datings in the Late Pleistocene of the Netherlands, Part I: Eemian and Early Weichselian. Mededelingen Geologische Stichting N.S. 14, p. 15-45.
ZAGWIJN, W.H. (1974) Vegetation, climate and radiocarbon datings in the Late Pleistocene of the Netherlands, Part II: Middle Weichselian. Mededelingen Rijks Geologische Dienst N.S. 25-3, p. 101-110.

ZAGWIJN, W.H. (1975): Indeling van het Kwartair op grond veranderingen in vegetatie en klimaat. In: Zagwijn, W.H., C.J. van Staalduinen (eds): Toelichting bij geologische overzichtskaarten van Nederland. Rijks Geologische Dienst, Haarlem, p. 109-113.

ZAGWIJN, W.H. (1983): Geological aspects of radiocarbon dating. In: W.G. Mook & H. Tj. Waterbolk (eds): Proceedings of the Groningen Conference on 14C and Archaelogy. PACT Publication 8, p. 71-90.

ZAGWIJN, W.H., R. PAEPE (1968): Die Stratigraphie der Weichsel-zeitlichen Ablagerungen der Niederlande und Belgiens. Eiszeitalter und Gegenwart 19, p. 129-146.

ZANDSTRA, J.G. (1978): Einfuhrung in die Feinkiesanalyse. Der Geschiebesammler 5-2/3, p. 21-38.

ZANDSTRA, J.G. (1983): Fine gravel, heavy mineral and grainsize analyses of Pleistocene, mainly glacigenic deposits in The Netherlands. In: J. Ehlers (ed.): Glacial deposits in North-West Europe. Balkema, Rotterdam, p. 361-377.

ZOLTAI, S.C., F.C. POLLETT (1983): Wetlands in Canada: Their classification, distribution and use. In: A.J.P. Gore (ed.): Ecosystems of the world. Vol. 4. Mires: Swamp, bog, fen and moor, B. Regional studies. Elsevier, Amsterdam, p. 245-268.

Appendix I.

List of radiocarbon datings, with evaluation of possibble errors.

Explanation of abbreviations in first column:
Till = Tilligte section; Bevb = Beverborg section; Lh-R = Laarhuis-Denekamp section; La-D = Lattrop-Denekamp section; De-D = detailed sections Denekamp; De-T = detailed sections Tilligte; O-NS = North-South overview section; DBr = De Braak exposure; Heng = Hengelo A1 exposure. Number in second column refer to sample numbers, mentioned in the text or figures.
Explanation of abbreviations in last column (indicates possible error source): c,ext = contaminated by younger extractable organic matter as indicated by too young extract dating; c,str = contaminated by younger organic matter, as concluded from stratigraphy; rew = dating too old due to presence of reworked older organic matter.
Material column: P = peat, G = gyttja, C = clay, S = silt, H = humic. Second character indicates additional material.
All datings have ondergone an alkali treatment, except those marked with '*'. Datings marked with '**' are accelerator datings on seeds, carried out at Svedberg Laboratory, Uppsala University.

Section exposure	boring number	Residue dating with standard deviation	Extract dating with standard deviation	Laboratory number, 2nd is extract dating GrN-	Material	Err. source
Till	9-1	35730 ±430	25450 ±500	8992, 12717	S,H	c,ext
Till	9-2	38350 ±600		8993	P	
Till	9-3	38200 ±600		8994	P	
Till	11-1	41300 ±1000	38200 ±1500	8995, 13440	P,S	
Till	11-2	40250 ±850	38200 ±1500	8996, 13440	P	
Till	13-1	40800 ±1000	38300 +1700 -1400	8997, 13439	P,S	
Till	15-1	40600 ±850	35600 +1700 -1400	8998, 12719	P	
Till	15-2	41250 ±800		8999	P,S	
Till	15-3	49800 +2700 -2600	45800 +4300 -2800	9000, 14190	P,S	
Till	15-4	47800 +2000 -1600	45800 +4300 -2800	10309, 14190	P,S	
Till	W1	40400 ±950		12198	P	c,str
Till	19A-1	43300 ±1000	38900 ±750	10836, 11533	P	rew
Till	19A-2	41550 ±900	38900 ±750	10837, 11533	P	
Till	19A-3	41700 ±900	38900 ±750	10838, 11533	P	
Till	19-4	44650 ±550		8985	P	c,str
Till	TV-1	51900 +4800 -3000		10839	P	
Till	TV-2	>5200		10840	P	
Till	21-1	46100 ±950		8988	P	
Till	22-1	37060 ±300		8986	P	
Till	22-2	47650 ±750		8987	P	
Till	24-1	36530 ±410	35100 ±1000	11534, 14186	P	
Till	26-1	40100 ±900	39400 +1700 -1400	11535, 14187	P	
Till	26-2	40800 ±750	39400 +1700 -1400	11536, 14187	P	
Lh-R	403-1	50300 +3900 -2600		12175	P	
Lh-R	403-2	47700 +2800 -2100		12176	P	
Lh-R	404-1	38350 ±950		12177	P	
Lh-R	409-1	36300 +3200 -2300		12178	S,P	
Lh-R	415-1	43300 +1900 -1500		12179	P	c,str
Lh-R	421-1	37900 ±750		12180	P	
Lh-R	410-1	35420 ±440		11537	P	
Lh-R	410-2	37500 ±600	43600 +3500 -2400	11538, 12718	P	

Section exposure	boring number	Residue dating with standard deviation	Extract dating with standard deviation	Laboratory number, 2nd is extract dating GrN-	Material	Err. source
Lh-R	423-1	29620 ±220	25550 ±500	11539, 14188	P	c,ext
Lh-R	424-1	36400 ±600	27050 ±600	11540, 12716	P	c,ext
Lh-R	427-1	11410 ±50	11080 ±120	11541, 14189	P	
Lh-R	429-1	45800 +2800 -2100		12192	P	
Lh-R	430-1	35700 ±550		12193	P	
Lh-R	433-1	37850 ±750		12194	P,S	
Lh-R	434-1	38150 ±850		11542	P,S	
Lh-R	436-1	34800 ±600		12195	P,S	
Lh-R	436-2	45000 +2000 -1600		12196	P	
Lh-R	436-3	47200 +3500 -2400		12197	P	
Lh-R	Sch-1	51000 +2000 -1900		11544	P	
Lh-R	VW-1	43200 +1300 -1100		13388	S,H	rew?
Lh-R	VW-2	>52000	45200 +2800 -2100	13390	G	
Lh-R	VW-3	54100 +3200 -2300		13391	G	
La-D	LA-3	13310 ±110 *		14214	S,H	
La-D	LA-3a	12885 ±185 **		Ua-924	SEED	
La-D	LA-3b	12315 ±125 **		Ua-925	SEED	
La-D	LA-1	41750 ±900	38400 +1700 -1400	13392, 13393	G	
La-D	LA-2	>52000		13394	P	
La-D	NIC-1	34270 ±380		13395	P	
La-D	685-1	11285 ±25	10470 ±190	13403, 13404	P	
La-D	685-2	47400 +1500 -1200		13405	P	rew
La-D	674-1	43850 ±1000	>41000	13416, 13417	G	
La-D	605-1	30360 ±410	27390 ±210	13408, 13409	P	c,ext
La-D	607-1	36010 ±350	35750 ±550	13406, 13407	P	
La-D	611-1	36470 ±480		13410	S,H	c,str
La-D	652-1	33300 ±500		13420	S,H	
La-D	615-1	33000 ±500		13397	G	
La-D	615-3	36740 ±340		14192	P	
La-D	615-2	40150 ±700	34300 +1900 -1500	13399, 14220	S,P	
La-D	621-1	39600 ±900	39100 +1900 -1600	13412, 13413	P	
Bevb	33-1	35100 ±700	35600 +1800 -1500	11521, 8989	S,P	
Bevb	35-1	34820 ±440	32300 +1200 -1000	11522, 8990	S,P	
Bevb	39-1	27500 ±250 *		11523	S,P	
De-T	506-1	41100 ±900		12181	P	rew
De-T	508-1	39300 ±850		12182	G	
De-T	509-1	41500 ±1400		12183	P	rew
De-T	512-1	30390 ±370		12184	S,P	
De-T	513-1	32050 ±500		12185	P,S	
De-T	514-1	39600 ±1100		12186	G	
De-T	518-1	41300 ±1000		12187	P	rew
De-T	537-1	28850 ±470		12188	S,H	
De-T	537-2	38000 ±850		12189	P	
De-T	542-1	40350 ±950		12190	P	
De-T	558-1	32500 ±380		12191	P	c,str
De-D	644-1	35540 ±370	27430 ±200	13400, 13401	S,P	c,ext
De-D	644-2	42200 +1600 -1300		13402	P	
De-D	688-1	34810 ±480	34050 ±750	13422, 13423	G	
De-D	689-1	39050 ±650		13418	P	rew
De-D	627-1	28600 ±750		13414	C,H	
O-NS	LOS-1	42000 +1300 -1100		11544	P	
DBr	I	12310 ±70	14050 ±180	13430, 13431	S,H	
Heng	80	28670 ±110	27780 ±230	13428, 13429	S,H	

Section exposure	boring number	Residue dating with standard deviation	Extract dating with standard deviation	Laboratory number, 2nd is extract dating GrN-	Material	Err. source
Heng	3	32860 ±270	27350 ±210	13424, 13425	P	c,ext
Heng	50	32490 ±160	30040 ±450	13426, 15146	P	c,ext
Heng	P7	31250 ±600		15124	P,S	c,ext
Heng	P4	33100 ±600		15123	S,H	?
Heng	70	41110 ±480	39200 +1800 -1500	13427, 14221	P	
Heng	P6	39640 ±370		14215	P	

Appendix 2.

Grain size samples of which histograms have been displayed in figures of section VI.

Fig.	nr. in fig.	sample location (section or exposure)	nr (exposure samples) or boring name (hydr. borings) or boring number (hand borings)	depth below surface (borings)
3	1	Laarhuis-Rammelbeek	423	715-725
3	2	Gildehaus	571	970-980
3	3	Hengelo A1	6	
3	4	Laarhuis-Rammelbeek	402	585-590
3	5	Tilligte detailed grid	548	280-285
3	6	Tilligte detailed grid	503	440-447
3	7	Hengelo A1	25	
3	8	Hengelo A1	28	
3	9	Gildehaus	573	770-780
3	10	Laarhuis-Rammelbeek	413	670-682
3	11	Tilligte	Tilligte Vlierweg	710-715
3	12	Laarhuis-Rammelbeek	412	820-830
3	13	Gildehaus	573	730-736
3	14	Gildehaus	573	694-700
3	15	Hengelo A1	27	
3	16	De Poppe	IV.5	
3	17	Laarhuis-Rammelbeek	Noord Deurningen	720-725
3	18	Laarhuis-Rammelbeek	412	615-625
3	19	Laarhuis-Rammelbeek	Venweg	1007
4	20	Laarhuis-Rammelbeek	407	748-756
4	21	Laarhius-Rammelbeek	413	335-345
4	22	Laarhuis-Rammelbeek	Noord Deurningen	846-850
4	23	Tilligte detailed grid	556	422-428
4	24	Hengelo A1	83	
4	25	Hengelo A1	84	
4	26	Tilligte detailed grid	530	290-298
4	27	Laarhuis-Rammelbeek	Noord Deurningen	1041-1046
4	28	Hengelo A1	31	
4	29	Lattrop-Denekamp	Lattroperstraat	1070-1073
4	30	Laarhuis-Rammelbeek	411	750-757
4	31	Beverborg	127	728-738
4	32	Laarhuis-Rammelbeek	437	771-783
4	33	Laarhuis-Rammelbeek	417	390-400
4	34	Tilligte detailed grid	503	370-373
4	35	Tilligte detailed grid	small exposure	Singraven Fm.?
4	36	Tilligte detailed grid	512	520-525
4	37	Tilligte detailed grid	537	285-290
4	38	Laarhuis-Rammelbeek	414	495-500
4	39	Tilligte detailed grid	550	444-450
4	40	Lattrop-Denekamp	Lattroperstraat	743